

**PHOTODYNAMIC THERAPY OF SKIN
USING PORPHYRIN PRECURSORS**
*optical monitoring, vascular effects
and personalized medicine*

Tom Middelburg

**Photodynamic Therapy of Skin using Porphyrin Precursors:
Optical Monitoring, Vascular Effects and Personalized Medicine**

Tom Middelburg

Financial support for the printing of this thesis was generously provided by:

La Roche-Posay

Waldmann BV

Oldekamp Medisch

Galderma Benelux BV

Pfizer BV

Astellas Pharma BV

Abbvie BV

Medizorg

Eucerin

Fagron BV

Shimadzu Benelux BV.



ISBN: 978-94-6169-508-6

Layout & Printing: Optima Grafische Communicatie, Rotterdam, The Netherlands

**Photodynamic Therapy of Skin using Porphyrin Precursors:
Optical Monitoring, Vascular Effects and Personalized Medicine**

*Fotodynamische therapie van de huid met porfyrine precursors:
optisch monitoren, vaateffecten en gepersonaliseerde geneeskunde*

Proefschrift

ter verkrijging van de graad van doctor aan de
Erasmus Universiteit Rotterdam
op gezag van de
rector magnificus
Prof. dr. H.G. Schmidt
en volgens besluit van het College voor Promoties.
De openbare verdediging zal plaatsvinden op

woensdag 11 juni 2014 om 9:30 uur

door

Tom Alexander Middelburg
Geboren 13 augustus 1980 te Rotterdam



Promotiecommissie

Promotor: Prof. dr. H.A.M. Neumann
Overige leden: Prof. dr. R.J. Baatenburg de Jong
Prof. dr. ir. M.J.C. van Gemert
Prof. dr. T.E.C. Nijsten
Copromotor: Dr. D.J. Robinson

Contents

Chapter 1.	Introduction	7
Chapter 2.	Red light ALA-PDT for large areas of actinic keratosis is limited by severe pain and patient dissatisfaction <i>Photodermatol Photoimmunol Photomed. 2013;29(5):276-8.</i>	35
Chapter 3.	Fractionated illumination at low fluence rate photodynamic therapy in mice <i>Photochem Photobiol. 2010;86(5):1140-6.</i>	43
Chapter 4.	Topical hexylaminolevulinate and aminolevulinic acid photodynamic therapy: complete arteriole vasoconstriction occurs frequently and depends on protoporphyrin IX concentration in vessel wall <i>J Photochem Photobiol B. 2013;126:26-32.</i>	63
Chapter 5.	Topical Photodynamic Therapy Using Different Porphyrin Precursors Leads to Differences in Vascular Photosensitization and Vascular Damage in Normal Mouse Skin <i>Photochem Photobiol. 2013. Accepted for publication.</i>	83
Chapter 6.	The effect of light fractionation with a 2-h dark interval on the efficacy of topical hexyl-aminolevulinate photodynamic therapy in normal mouse skin <i>Photodiagn and Photodyn ther. 2013(10);703-709.</i>	101
Chapter 7.	Monitoring blood volume and saturation using superficial fibre optic reflectance spectroscopy during PDT of actinic keratosis <i>J Biophotonics. 2011;4(10):721-30.</i>	131
Chapter 8.	Correction for tissue optical properties enables quantitative skin fluorescence measurement using single fiber optic spectroscopy <i>Lasers Surg Med. Submitted.</i>	133
Chapter 9.	Discussion	159
Chapter 10.	Summary	175
Chapter 11.	Samenvatting	183
Chapter 12.	Addendum	191
	<i>Dankwoord</i>	193
	<i>List of publications</i>	195
	<i>Curriculum vitae</i>	199
	<i>PhD portfolio</i>	201
	<i>List of abbreviations</i>	203

1

General introduction

1. WHAT IS PHOTODYNAMIC THERAPY?

Photodynamic therapy (PDT) is based on a photochemical reaction that involves three basic components: (1) a photosensitizer, which is a light-sensitive molecule that mediates transfer of light energy to molecular oxygen; (2) light of the appropriate wavelength that is absorbed by the photosensitizer, and (3) molecular oxygen. These components interact with each other and with the surrounding tissue, creating the photodynamic effect. The photodynamic processes are based on quantum mechanical principles that are described below and schematically illustrated in figure 1.

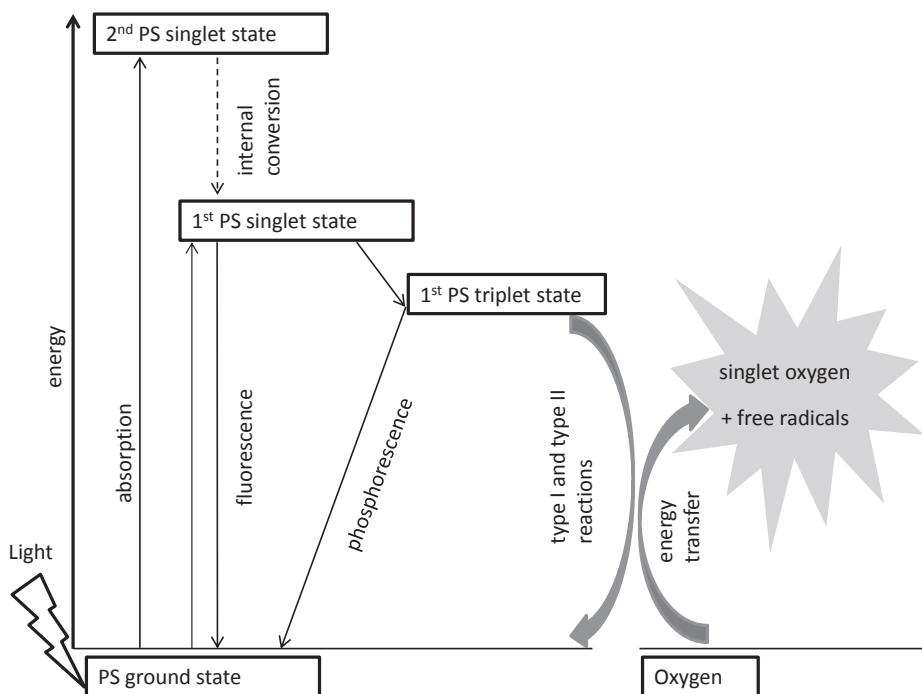


Figure 1. Quantum mechanical principles of PDT. The photosensitizer (PS) is excited by absorption of light energy. The excess energy is then released in various ways that include emission of fluorescent light and energy transfer to oxygen. This results predominantly in formation of the highly reactive singlet oxygen.

1.1. Quantum mechanics of PDT

Light is part of the electromagnetic spectrum and can be considered both as an electromagnetic wave and as consisting of separate particles of energy, called photons. The interaction between photons and molecules such as photosensitizers depends on the energy of the photon and the specific light absorption characteristics of the photosen-

sitizer. A photon can interact with the electronic structure of the photosensitizer and transfer its energy to the photosensitizer. The photosensitizer is transformed from its stable, low-energy ground state to a higher energy singlet state. This singlet state is unstable and the photosensitizer transfers its excess energy back to the environment. Some of the energy is released as heat in a process termed internal conversion. Two other de-excitation pathways are possible: an electron returns to its ground state accompanied by the emission of a lower energy photon, termed fluorescence. Or energy is transferred in a process that involves electronic spin conversion, leading to formation of a triplet state photosensitizer. This triplet state is more stable than the singlet state, and has a longer lifetime but still loses its energy to the environment. This can occur in a similar way to fluorescence via the emission of a phosphorescent photon. This is an unfavourable spin forbidden transition and means that the triplet state is able to interact with other molecules in the environment of the photosensitizer. Two triplet state interactions predominate and are termed type I and type II reactions. Type I reactions involve direct electron or hydrogen transfers with surrounding molecules, resulting in formation of free radicals or radical ions, which subsequently can react with oxygen to form several reactive oxygen species. Type II reactions are more likely to happen than type I reactions, and involve energy transfer between the photosensitizer triplet state and nearby oxygen to form singlet oxygen, which is highly reactive and causes damage to surrounding biomolecules.

Type I and II reactions result in photodynamic damage to cellular structures that can be used to destroy specific cells such as tumour cells. An important aspect of PDT is that singlet oxygen has a short lifetime ($\sim 30\text{-}180\text{ ns}^{-1}$) and thus only damages molecules that are very close to the photosensitizer (within a distance of $10\text{-}55\text{ nm}^2$). One of the molecules that is very close to site of the generation of singlet oxygen is the photosensitizer itself which, as a result, is also destroyed. This process termed photobleaching is important because it means that the amount of fluorescence from the photosensitizer can be used as an indirect measure for singlet oxygen formation and thus for PDT effect. The cellular distribution of photosensitizers and their distribution in tissue are critical factors related to the effectiveness of PDT. The topics of distribution of the photosensitizer in tissue and the use of fluorescence measurements to monitor the PDT process are important topics that will be explained in more detail. First the potential usefulness of PDT in general are introduced, followed by its specific use in dermatology.

2. APPLICATIONS OF PDT

The possible applications for PDT are widespread within and outside of medicine. For instance it can be used to kill micro-organisms without inducing resistance³, which is an increasing problem with the widespread use of antibiotics. Contrary to antibiotics, PDT incorporates a physical way of inducing cell death: singlet oxygen formation that cannot be circumvented by a biological mechanism. Such a PDT application could be very interesting for sterilization purposes such as water sterilisation⁴ or to destroy bacterial biofilms⁵. There are also attempts to use PDT to kill arthropods that pose a considerable health problem in certain areas of the world⁶.

The main application of PDT is as a medical treatment. A general positive feature of PDT is its selectivity to the site where the light is applied, limiting systemic side effects. It can theoretically be used in any organ and for any cell type in the body, as long as they are accessible for light delivery. Since the dominant effect of PDT is photodynamic damage, its primary use is focused on destruction of diseased tissues. The typical case for this is cancer and examples that are being treated using PDT are cancers in the head and neck⁷, brain⁸, gastrointestinal tract⁹, urological tract,¹⁰ and in the skin¹¹. Also non-malignant tissues can be targeted such as for instance the vasculature in age related macular degeneration or choroidal neovascularisation¹². This thesis will only focus on the use of PDT in the skin, the organ in which there is the most and highest level of evidence for its effectiveness¹³.

3. PDT IN DERMATOLOGY USING PORPHYRIN PRECURSORS

3.1. PDT applications

In dermatology, PDT is primarily used to treat actinic keratosis, superficial basal cell carcinoma and Bowen's disease. Although PDT is one of several possible treatment options for these conditions, this thesis will only focus on PDT and does not concern comparing these different treatment options. Other, off-label applications for PDT are Paget's disease, mycosis fungoides acne, psoriasis, lichen sclerosus, common warts and more^{11, 14-16}.

3.2. Porphyrin precursors and PpIX synthesis

In the vast majority of cases skin PDT involves topical application of a vehicle (i.e. a cream, gel or ointment) that contains porphyrin precursor molecules. Aminolevulinic acid (ALA), its methyl ester methylaminolevulinate (MAL) and its hexyl ester hexylaminolevulinate (HAL) are all three precursor drugs of the photosensitizer PpIX. ALA and

MAL are registered for the indications mentioned above, but HAL is not. It is registered for photodiagnosis of bladder cancer but there is on-going research to use HAL-PDT as a therapeutic agent for several indications in dermatology, gynaecology and urology.

After topical application the porphyrin precursors penetrate into the skin through diffusion and active transport. After uptake, MAL and HAL are first cleaved into ALA and an alcohol after which a multi-step enzymatic cascade follows. This cascade is part of the heme biosynthesis pathway that starts in the cytosol and continues in the mitochondria. The last step in this pathway is iron chelation of PpIX to form heme. This step is relatively slow, which results in a temporary accumulation of PpIX within in the mitochondria. The process of penetration through the skin followed by uptake and PpIX synthesis is illustrated for ALA in figure 2. Typically, it takes 3-4 hours to reach maximum PpIX concentrations, at which time-point illumination takes place.

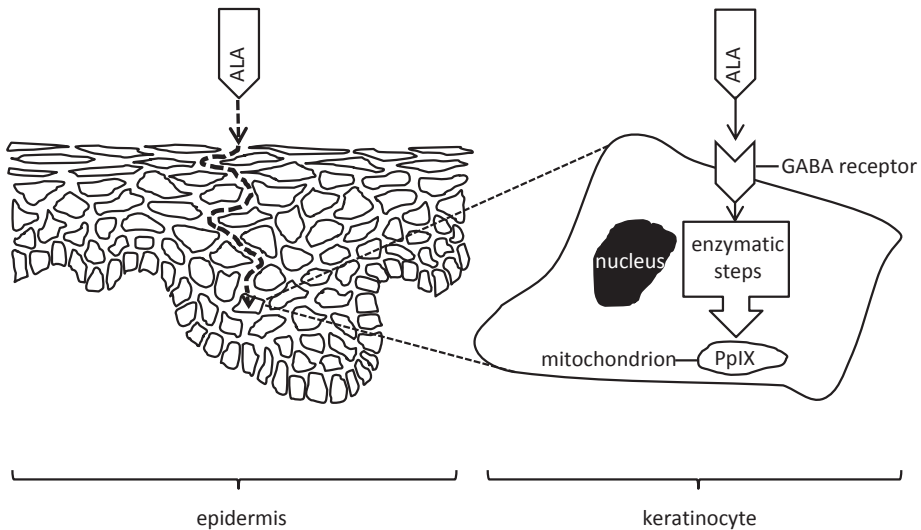


Figure 2. Aminolevulinic acid (ALA) penetrates through the epidermis and is transported into the keratinocyte cytosol via the gamma-aminobutyric acid (GABA) transporter. Multiple enzymatic steps within the heme synthesis pathway lead to protoporphyrin IX (PpIX) accumulation in the mitochondrion.

3.3. Illumination

Depending on the indication and on geographic differences in treatment protocols either blue or red light is used, which are both based on peaks in the absorption spectrum of PpIX (figure 3). In this figure it can be seen that it is possible to choose a variety of wavelengths of light to excite PpIX, because PpIX has its major absorption peak around 400nm (blue) and several smaller ones between 500 (green) and 630 nm (red). However,

blue and green light are also very much more strongly absorbed by other chromophores such as haemoglobin and melanin in skin (figure 4). Because of this and also because shorter wavelengths of light are scattered more, the bioavailability of blue and green light decreases with increasing depth compared with red light. For this reason in basal cell carcinoma red light is the preferred choice. Both red and blue light are used for actinic keratosis.

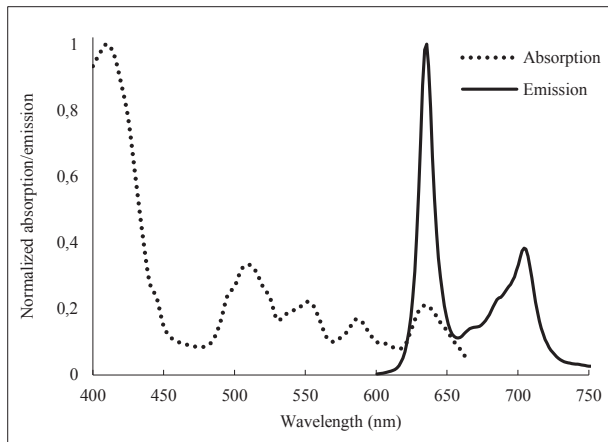


Figure 3. The normalized absorption and emission spectra of protoporphyrin IX. Absorption is highest around 405 nm, with several smaller peaks at longer wavelengths. The emission peak is centred around 635 nm.

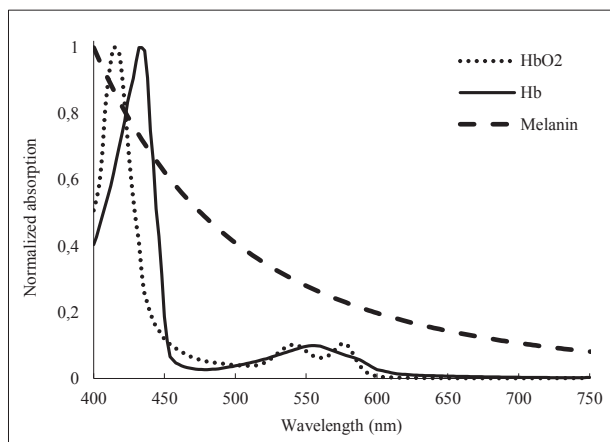


Figure 4. Normalized absorption spectra of three common chromophores in the skin: melanin, haemoglobin (HbO₂) and deoxygenized haemoglobin (Hb). Absorption of light of these chromophores is higher in the blue region (around 400 nm) than in the red (around 600nm).

3.4. Responses to PDT

PDT occurs as soon as light, photosensitizer and oxygen are simultaneously present. Thus, illumination several hours after topical application of a porphyrin precursor initiates the photodynamic process that leads to formation of singlet oxygen and ultimately cell death. However, cell death by singlet oxygen formation is a somewhat simplified representation of events. The response of tissue to PDT is more complex and can be divided in three main categories: cellular, immunological and vascular responses. A combination of these three ultimately results in an overall response to PDT that includes destruction of the target (e.g. tumor) tissue.

3.4.1. Cellular response to PDT

After PDT cells may either die by necrosis or the more controlled apoptosis, or by other pathways such as autophagy¹⁷⁻²⁰. Necrosis is the least controlled mechanism leading to cellular debris, whereas apoptosis is an ordered way for a cell beyond repair to dispose of itself. The process of autophagy involves phagocytosis and lysosomal breakdown of dysfunctional cellular components and it can act both as a death and survival mechanism. The specifics of these cellular mechanisms are complex and beyond the scope of this thesis but the cellular response to PDT using porphyrin pre-cursors is dominated by apoptosis. This is because PpIX is predominately localised in the mitochondria at the time PDT is normally applied. Direct damage to mitochondrial proteins leads to the destruction of the mitochondrial membranes, the release of cytochrome c and caspase induction.

3.4.2. Immunological response to PDT

The absence of immunity has been shown to reduce PDT outcome, indicating an important role for the immune system^{21, 22}. After PDT a quick influx of neutrophils is observed, followed by mast cell and macrophage invasion to the treated site²³. Both this type of acute innate anti-tumor response and also adaptive immune responses are recognized to contribute to the overall PDT success²⁴. Although the complexity of the immune response to PDT is an interesting topic, its specifics are also beyond the scope of this thesis.

3.4.3. Vascular response to PDT

It is known that blood vessels can respond to PDT, primarily from what is known about PDT using systemic porphyrins in the late 1980s when constriction and destruction of the microvasculature have been reported²⁵⁻³⁰. These vascular effects can work in both ways in terms of PDT effect. If vessels constrict too much during PDT, this will hamper the influx of blood, and thus of oxygen to the PDT site. This type of response will reduce the PDT effect. On the other hand, if vasoconstriction happens late (during or after PDT),

or if vessels are damaged, it can be beneficial because local ischemia may help destroy remaining cancer cells that would otherwise survive^{31,32}. This in turn means that the ischemia cannot be too extensive or long-lasting because the normal tissue may die too, resulting in an inferior cosmetic or functional outcome. These effects suggest that there may be a delicate balance between causing too much and too little vascular damage, illustrating the potential importance of such vascular effects on PDT response³³.

For topical PDT such as is used in dermatology, it is however generally assumed that vascular effects either do not take place in human skin or are irrelevant, despite the fact that there is preclinical evidence to the contrary in the literature³⁴⁻³⁶. It has also been reported that vessels can constrict during PDT due to release of vasoactive substances such as nitric oxide³⁷ or cyclooxygenase products²⁹. Despite the results of these studies the clinical effects and the extent of vascular responses of topical ALA-PDT remain unclear. In this thesis the study of these vascular processes during and after PDT is a recurring theme. To understand these vascular effects, one of the relevant factors is the distribution of PpIX within the vasculature. I will go into the details of the PpIX distribution below, but will first I will explain why further PDT research is necessary.

3.5. Limitations of PDT

PDT in the skin is generally quite effective with 3 month complete response rates reported in meta-analyses varying from 69-96% for actinic keratosis³⁸ and 71-87% for superficial basal cell carcinoma³⁹. However, long term follow up is often not reported but will likely be lower, yet better reflect the real cure rate. For example 69% and 76% 5 year response rates have been described for nodular bcc after debulking^{40,41} and the highest reported 5 year complete response is 88% for superficial basal cell carcinoma⁴². Moreover, considering the patient selection bias in clinical trials the complete response in everyday practice is probably lower than reported in such studies.

Despite these -for cancer treatment- relatively high complete response rates there remain significant limitations to PDT. First, still about 1 in 4 or 5 patients ultimately does not respond to the treatment and it is not understood why particular patients fail to respond. A second important current limitation of PDT is that it can be extremely painful, which is considered the most important potential side effect of PDT⁴³. However, despite pain being a frequently studied subject⁴⁴, it is also not well understood why this is variable for individual patients. It is essential to understand such underlying mechanisms for further improvement of PDT.

3.5.1. Personalized medicine

To try and understand individual treatment failures or side effects is where the concept of personalized medicine becomes an interesting subject. It is based on the observation that individual patients can respond quite different to any medical treatment. Potential reasons for these differences may vary from large scale (e.g. gender) to very small scale differences (e.g. genetic base) or anything in between. The concept of personalized medicine has gained attention over the past years mainly because of advances in genetics. However, the main idea behind personalized medicine is to identify the causative factors for differences in response to optimize treatment on an individual basis.

For PDT, there is much to gain by applying this concept of personalized medicine. Currently, in everyday practice all patients receive the same treatment. However, we are unsure of the exact parameters that are responsible for treatment success on an individual basis. In order to be able to fine-tune PDT to the individual patient's needs it is important to define characteristics that may be important for treatment outcome, measure them and evaluate their relevance. Knowledge derived in such a way can next be used to optimize and personalize treatment to achieve best therapeutic efficacy and least side effects. The consequential logical question that arises then is: what are the relevant measurable or controllable parameters that are related to PDT effectiveness and how do we gain insight in them?

3.6. Relevant parameters for PDT outcome

Obviously the most important factors for PDT success are either related to: the PpIX concentration and its localisation in the skin; the oxygen supply to the target site; or the local amount of light that is available for the photodynamic process. As we will see, things are significantly more complicated but this is a useful starting point. Many parameters that may influence PDT outcome can be measured or controlled in the PDT process and this can be done at various time-points. Three important time periods that can be defined are either before, during or after the illumination. These three time periods will be discussed separately, and I will focus on the parameters that can be measured or controlled *during* PDT for reasons that will become clear.

3.6.1. Before PDT

Before PDT starts, the obvious measurement is the clinical evaluation which can be followed by histological examination to determine the tumour type, its growth pattern and sometimes its thickness in order to decide if the lesion is eligible for PDT in the first place⁴⁵. The thickness can be relevant because the availability of both PpIX and light are depth-dependent. Another thing that may be relevant is the status of the patient's immune system. Considering the role of the immune system in the PDT response, immu-

nosuppression is expected to decrease PDT efficacy. A significant effect was not found however in one study of PDT for basal cell carcinoma ⁴⁶, but long term responses were lower for PDT of actinic keratosis in immunosuppressed patients ⁴⁷. In practice however, the lesion type and growth pattern are generally all that is being measured before PDT. The main difficulty here is to identify which parameters may be relevant to predict PDT effectiveness and side effects.

It is interesting to philosophise on what other parameters can theoretically be measured before PDT that provide information on the likelihood of treatment success. Some lesions may contain cells that are particularly capable of surviving oxidative damage by some enhanced repair mechanism such as autophagy. Certain uptake transporters of ALA may be down-regulated in tumour cells; there may be small alterations in the heme synthesis pathway, or there may be an active pump mechanism that inhibits PpIX accumulation. Another possibility is that some tumour cells are living in hypoxic conditions that leads to them being better protected against PDT, which requires oxygen. Mechanisms such as these potentially enhance tumour cell survival chances during or after PDT. They may have a genetic basis to them, or they may be related to endocrine or paracrine functions. It could be useful if they can be measured in the skin biopsy prior to PDT. Similarly, there may be predispositions for experiencing increased pain which may vary from psychological to genetic factors. Be sure to note that these are just hypothetical examples of why some patients may respond differently to therapy than other and which could theoretically be taken into account before deciding upon PDT. The hypothetical and speculative nature of this paragraph shows that there is much more to explore.

3.6.2. During PDT

Currently the most interesting moment to perform measurement is during PDT. This monitoring of PDT is a prominent feature throughout this thesis, which is why I will discuss this in most detail here. Because the local photosensitizer, oxygen and light concentrations are the key ingredients for effective PDT, these parameters and their interactions are the most obvious ones to measure. In addition to measuring effectiveness, side effects can also be measured of which pain is the most important parameter.

3.6.2.1. Photosensitizer

An obvious but crucial aspect for PDT success is the availability of sufficient amounts of PpIX at the correct locations in the skin. This makes the distribution of PpIX in the skin critical. It depends on both the ability of the precursor molecule to penetrate the skin and to be taken up by the target cells. The ability to penetrate the skin is related to the lipophilicity, which is different for the precursors and related to the ester groups of MAL

and HAL. The cellular uptake of ALA, MAL and HAL is regulated by different transporter molecules⁴⁸⁻⁵³. Because of these differences between ALA, MAL and HAL there is an on-going debate about which one is the "best" PpIX precursor. Part of this debate is also concerned with potential differences in selectivity for cancerous tissue between them. Both the increased metabolic rate of neoplastic cells and the enhanced penetration through a disrupted stratum corneum in (pre)cancerous skin conditions have been attributed to such differences⁵⁴.

Because ALA, MAL and HAL are very small molecules they are very hard to detect and when detectable markers are added to them, their biochemical behaviour will change. An interesting solution for this problem would be to use radioactive ¹⁴C isotopes of them, but this has not been extensively employed. Instead, the resulting PpIX concentration is normally determined. PpIX is easily detectable because it fluoresces and the fluorescence intensity can potentially be used as a measure for the PpIX concentration. Hence, optical measurements of PpIX fluorescence provide valuable insight into the PDT process. Indeed, it has been shown that the PpIX fluorescence intensity before start of PDT and the photobleaching percentages during PDT are valuable tools to predict treatment outcome⁵⁵⁻⁶⁰. For this reason we also measured PpIX fluorescence in the majority of the studies in this thesis. It is however important to realize that there are limitations to such measurements. Because of the very useful nature of measuring PpIX fluorescence I will explain more on the limitations of measurement techniques and the physics involved in separate sections later in this introduction.

3.6.2.2. Oxygen

Not only the photosensitizer is photobleached, oxygen is also consumed during PDT. This means that oxygen needs to be constantly supplied and that lack of oxygen will inhibit the PDT process⁶¹. A consequence of this is that when sufficient light and photosensitizer are present, the availability of oxygen can be deduced from the efficiency of PpIX photobleaching³⁷. This again highlights the importance of monitoring PpIX fluorescence during PDT. Another way to measure oxygen consumption and monitor the PDT process would be to measure the singlet oxygen luminescence¹. This is possible but is technologically challenging and is far from being applied in routine clinical treatments. Yet another method to study the oxygen availability at the site of PDT is to study the blood supply from nearby blood vessels. Blood flow, constriction of blood vessels, blood oxygenation and microvascular damage are important measurable parameters here.

3.6.2.3. Light

Light has a somewhat different character in that it is not routinely measured during PDT in the skin, but it is one of the most obvious controllable parameters. It is possible to vary the wavelength, the dose and intensity as well as the light delivery scheme. Each of these will be discussed in detail below.

3.6.2.3.1. Light - wavelength

As described above, the wavelength needs to match the absorption spectrum of PpIX: Both blue and red light are used, depending on the indication and geographic differences in treatment protocols. Another factor to consider is whether the PpIX fluorescence can be monitored during PDT. When red excitation light is used, it is difficult to measure PpIX fluorescence because the main red emission peak of PpIX, is centred at 635 nm (figure 3). Therefore, when PpIX fluorescence measurements are concerned, blue excitation light allows for the easy separation of excitation and emission light. Finally, when choosing the wavelength of the excitation light it should be noted that the most controllable light source in terms of effective light dose is a laser. Laser light has a single wavelength, which enables to calculate how much light is effective at exciting the photosensitizer. Broad light sources have the drawback that each wavelength has different ability to excite the photosensitizer, making it difficult to define the deposited effective light dose with depth.

3.6.2.3.2. Light – dose and intensity

When the amount of light delivery is concerned, both the total light dose and the rate at which this dose is delivered are relevant. The light dose is usually given as the total fluence, expressed in J cm^{-2} . The rate of light delivery is given by the fluence rate (defined inside the tissue being illuminated) or by the irradiance (defined at the tissue surface). Both fluence rate and irradiance are expressed in W cm^{-2} , which equals $\text{Jcm}^{-2} \text{ s}^{-1}$. These two parameters have very different impacts on the PDT process but the distinction between them can be confusing. The total dose is related to the total singlet oxygen production, which can be chosen to be as high so that all available PpIX is photobleached. The fluence rate determines how fast singlet oxygen is produced and oxygen is consumed, which can be detected by measuring the rate of photobleaching. An interesting consideration is that a high fluence rate ($>100 \text{ mW cm}^{-2}$) can exceed the ability of the tissue to supply oxygen, resulting in an inefficient overall PDT process. A lower fluence rate on the other hand improves PDT efficiency by better utilizing available oxygen^{57, 62-65}. When the fluence rate is chosen too low however, it may be that not enough singlet oxygen is formed per time unit to cause lethal cellular damage because the cell repair mechanisms are faster. Again there seems to be a delicate balance between choosing too high or too low

a fluence rate. Fluence and fluence rate combined also determine the total illumination time, which can have considerable practical consequences.

3.6.2.3.3. Light - delivery scheme

A final controllable parameter related to light delivery is whether to deliver the light continuously or fractionated. A quick on-off fractionated regime can be chosen to avoid depleting oxygen supply, which essentially has a comparable effect as delivery of a lower fluence rate. Particular attention within our research group has been paid to investigating the use of a completely different light fractionated scheme. In this scheme two (continuous) light fractions are delivered separated by a dark interval of two hours. This was based on the observation that after PDT again PpIX was resynthesized, which could be utilized again in a second light fraction increasing efficacy^{66,67}. In several pre-clinical mouse models it was concluded that the first light fraction needs to be relatively small and the dark interval relatively long (> 2 hours) for optimal results^{68,69}. This series of preclinical studies has led to a clinical ALA-PDT treatment protocol that has proven to be beneficial^{42,70}. It turned out that the total amount of PpIX that was photobleached was not the mechanism of action that explained the increase in efficacy, which led to additional studies to elucidate this mechanism. It was shown that, contrary to ALA, light fractionation did not increase the effect of MAL-PDT in mouse skin⁷¹. Differences in local PpIX concentration and distribution were hypothesized to account for this, because of the different lipophilicity and uptake mechanisms. Subsequent studies confirmed that the distribution of PpIX in endothelial cells *in vitro*, in the vasculature and the vascular response are different for ALA and MAL^{53,72}. From these studies it was concluded that the vasculature plays an important role in the mechanism behind light fractionation. An *in-vitro* study further showed that light fractionation was especially effective under low concentrations of PpIX⁷³. Such low concentrations are expected to be present in for example the vasculature, but also potentially in some areas of a tumour that would not respond to a single (but would to a fractionated) illumination. Using the knowledge from these previous studies we have continued to investigate the vascular effects of topical PDT in some chapters in this thesis. We focused on such effects of HAL-PDT and compared this with ALA and MAL to help optimize HAL-PDT before it is regularly applied in the clinic.

3.6.2.4. Pain

A final clinically important parameter to measure during PDT is pain. The pain typically starts shortly after start of illumination and either disappears quickly when the light is switched off, but it can also last for several hours afterwards. Pain can be measured during PDT simply by asking the patient how intense the pain is, which is generally scored using a Visual Analogue Scale (VAS). In addition to scoring the intensity of the

pain, both the temporal aspect of pain and the quality of the pain sensation (i.e. burning, stinging etc.) are interesting parameters to measure. This type of information may help understand the underlying mechanism of pain during PDT which is currently not well understood. Because ALA is taken up by GABA receptors^{74,75} it has been suggested that the pain is caused by direct PDT damage to nerve cell endings, but this would not explain why MAL-PDT is also painful. Pain may be caused by stimulation of specialized c-fibre nerve receptors, because patients experience intense burning heat although during PDT although the temperature hardly increases. So called transient receptor potential vanilloid (TRPV) receptors are a family of receptors that generate a heat sensation upon stimulation. An example of such a receptor is the TRPV1 channel which is activated by capsaicin (the substance that makes chilli peppers hot), causing a warm, burning sensation. However, in a small pilot study there was no decrease in pain perception after desensitization using capsaicin cream during the week prior to PDT⁷⁶. It could therefore be interesting to measure the release of other substances during PDT that may activate any of the TRPV channels. A possible benefit of conducting such research is that it may be possible to selectively block the receptors responsible for PDT pain perception.

3.6.3. After PDT

When measuring anything after PDT it is of course already too late to use these measurements to modify that particular treatment in the clinic. Such measurement can however be valuable for research purposes. For example, therapeutic effect can be used in combination with other parameters (measured during or before PDT) to help understand mechanisms such as biological pathways that contribute to the ultimate PDT response. Therapeutic effect can be determined over the short and long term by measuring complete disappearance of the lesion. Proxy measures of this may also be used such as tumour volume decrease, visual skin damage or histological evaluation of PDT damage. Visual skin damage of normal mouse skin is used in two studies in this thesis, because in the past this proved to a good translational model for clinical PDT response. On histology necrosis and apoptosis may be directly visible, while it may be helpful to measure biochemical markers to improve sensitivity or study other cellular pathways such as autophagy. Use of such immunohistochemistry can also be helpful to determine vascular damage and immunological response to PDT. In addition to measurements that inform on treatment efficacy, it can be valuable to score side effects such as swelling, redness, pain, cosmetic or functional outcome and patient satisfaction.

3.7. Optical measurements

Having defined the potential relevant parameters to measure and/or control I will focus on PpIX fluorescence measurements, because this is major theme throughout this thesis. To better understand the techniques used in the studies of this thesis I will

introduce how optical techniques can be used. Several optical fluorescence measurement techniques exist that make use of light to excite the fluorophore after which the fluorescent light is detected. As simple as this may sound, it gets complicated when the light interacts with other components in the tissue. This is not a significant problem when for example relatively flat tissues such as histological sections are analysed. However, when tissue is optically sampled these interactions between excitation and emission light with tissue components become very important. The way in which PpIX fluorescence measurements are influenced by these interactions and how this problem can be overcome will become clear later. First it is helpful to introduce the dominant tissue light interactions: absorption, scattering and fluorescence. Then, the different optical measurement techniques are explained that involve optical imaging and optical reflectance and fluorescence spectroscopy.

3.7.1. Absorption

Photons that propagate through tissue can collide with tissue constituents whereafter light energy is transferred (mostly to electrons) and quickly released as heat. This process is called absorption. The molecules that absorb the light are called chromophores. The major chromophores in skin that absorb light in the visible wavelength region are haemoglobin, deoxy-haemoglobin and melanin (figure 4). Bilirubin and beta-carotene are other chromophores that, under normal circumstances, are also present in the skin but at much lower concentrations. Each chromophore has a specific absorption spectrum, indicating which wavelengths are best absorbed. Because of this, the wavelength-specific fraction of light that returns to a collector (when a wide range of wavelengths is used to illuminate the skin) can provide information on the type and amount of chromophores that are present. This is the basic principle for any reflectance spectroscopy technique. In addition to this absorption of light, another tissue-light interaction is scattering.

3.7.2. Scattering

Light scattering can be described in simple terms as the interaction of light with matter that results in a change of direction in which the light travels. The easiest way to think about this phenomenon is to visualize looking at a red laser beam from the side that is only visible when the light is scattered towards the retina by smoke or steam. In tissue such as the skin similar interactions occur. Macromolecules such as proteins and lipids have a higher molecular density than the cytosol. As a result, they have a different refractive index, indicating their capacity to scatter light in several directions⁷⁷. Therefore, cellular structures with lipid membranes (e.g. nucleus, Golgi apparatus and mitochondria) or with high protein content (e.g. lysosomes) behave as strong scattering centres⁷⁸. When the light is scattered, the direction in which this happens depends -amongst others- on the relative size and distance between scattering particles and on

the angle and the wavelength of the incident light (shorter wavelengths scatter more). These scattering events in the skin also play an important role for optical measurements because light may or may not have returned to the collector due to it being scattered towards or away from it.

3.7.3. Fluorescence

Special types of chromophores called fluorophores absorb light energy and re-emit part of that energy as fluorescence. The quantum mechanics of this process have already been explained in the beginning of this introduction. As also mentioned earlier, the most important fluorophore for PDT in the skin is PpIX which is synthesized after the application of a precursor. There are however other fluorophores that are present in the skin also under normal conditions. Common fluorophores are collagen, NAD(H), FAD, flavins, and advanced glycation end-products^{79,80}. The combined emission from all of these constitute the skin autofluorescence, which exhibits a characteristic bell-shaped emission peak centred around 480 nm after blue light excitation (the wavelength region that is commonly used to excite PpIX).

A critical aspect for fluorescence measurements of the skin is that both the excitation wavelength and the emission wavelength of the fluorophore are also absorbed and scattered before they can either excite the fluorophore or be collected by a detector. This means that the measured fluorescence intensity by any optical method will over or underestimate the intrinsic fluorophore concentration depending on the optical properties. Therefore it is necessary to correct for these absorption and scattering effects when quantitative measurements of fluorophore content are desired. Because PpIX fluorescence kinetics during PDT are helpful to predict PDT outcome, such accurate and quantitative PpIX fluorescence measurement are indeed desirable in PDT. Furthermore, optical properties are likely to change during the course of PDT, which will affect the temporal accuracy of PpIX fluorescence measurement when they are not corrected for optical properties. To perform adequate correction of any fluorescence measurement, the optical properties of the skin must first be measured. This is where reflectance spectroscopy comes into play.

4. REFLECTANCE SPECTROSCOPY

Reflectance spectroscopy involves the use of a broad wavelength light source that illuminates the tissue and a spectrometer that detects the reflected light over this wavelength range. Fiber optic reflectance spectroscopy uses optical fibers for light delivery from the light source to the tissue and light collection from the tissue to the

spectrometer. The reflectance spectrum is next analysed to extract the optical properties of the tissue. Reflectance spectroscopy can be very useful in itself because the optical properties provide information on the absorption and scattering characteristics of the tissue. The absorption properties can be used to calculate chromophore concentrations and blood oxygenation. The scattering properties may be used to detect nanoscale morphological and architectural changes that occur during early carcinogenesis^{81,82}. Several reflectance spectroscopic methods have been used and differences between them are generally dependent on the distribution and geometry of the delivery and collecting fibers. The most important consequence of various geometries are the differences in optically sampled volumes, which are determined by the photon path length.

4.1. Photon path length – isotropic and anisotropic light scattering

Both the amount of absorption and scattering events depend in the first place on the distance that the light has travelled in the tissue. This photon path-length determines the sampling volume –and depth– of a spectroscopic measurement. As mentioned above, it is mainly dependent on the geometry of the delivery and collection optical fibers. The further apart they are, the longer the photon path length. A longer photon path-length will result in more photons being absorbed and scattered. This in turn has important consequences for the average direction of light scattering. When the photon path length is relatively long (>0.5 mm sampling depth), the number of scattering events is very high. As a consequence, it can be assumed that the light does not have a preferred direction of scattering, but rather diffuses down a concentration gradient. This is termed diffuse or isotropic scattering⁸³. Conversely when the photon path length is short, light scattering becomes anisotropic. This means that the direction in which the light is scattered becomes critical for the amount of photons returning to the spectrometer⁸⁴⁻⁸⁶. The probability distribution of these scattering angles is determined by a parameter called the phase function which can take complicated (in some cases unknown) forms, depending on the scattering constituents of the tissue. Unfortunately, reflectance spectroscopic measurements do not allow a complete determination of the phase function and assumptions have to be made. As will be explained soon, mathematical models have been developed to describe this phase function. Before we go there let's first consider again the purpose for which we would like to utilise optical spectroscopy in this thesis: PDT.

4.2. Optimal sampling depth in PDT

When using reflectance spectroscopy in the skin for PDT purposes the optical sampling depth is a crucial factor. Because PpIX fluorescence comes mainly from the epidermis and because the oxygen necessary for PDT is supplied by blood vessels in the superficial dermis, the desired sampling depth is just into the superficial dermis. This has conse-

quences for the choice of geometry used for spectroscopic measurements in the skin. A common technique such as diffuse reflectance spectroscopy samples both superficial and deep layers of the skin. As a result the sensitivity of measuring the optical properties of the superficial part of the skin decreases. This is why for PDT it is important to use reflectance spectroscopic techniques with a geometry that allow superficial sampling depths.

However, because of the anisotropic nature of light scattering in such superficial spectroscopic measurements it is not easy to account for these effects. During the course in which the studies in this thesis were carried out, methods to accurately quantify the optical properties of this superficial part of the skin were developed. We initially used diffuse reflectance spectroscopy (sampling deep into the skin). Later we used a technique termed differential pathlength spectroscopy (DPS) that allows determination of superficial absorption properties. The latest technique is termed multi-diameter single fibre reflectance (MDSFR) spectroscopy that allows a complete description of the optical properties in the superficially sampled volume.

4.3. Differential path length spectroscopy

DPS involves taking a reflectance spectrum using two adjacent optical fibers with different diameters. that can be varied to accommodate the desired sampling depth^{87, 88}. Because one fiber collects and delivers light while the other only collects light, one fiber samples from both deep and superficial volumes while the other samples predominantly from deeper in the skin. Subtracting the signals yields information on the absorption characteristics of only the superficial layer. The influence of (differences) in scattering of the tissue have a small effect on the path-length of light in this superficial volume and DPS allows for the measurement of the blood volume fraction, the saturation, and the melanin, bilirubin and beta carotene content. We used this technique to monitor the superficial blood volume and saturation during PDT of human skin in one study in this thesis. The primary drawback of DPS is that it does not allow for a determination of the scattering properties of tissue. This is problematic since (1) the scattering properties are known to be diagnostically relevant and (2) without knowledge of the scattering properties of tissue it is impossible to correct the raw fluorescence for the influence of differences in optical properties.

4.4. Single fiber reflectance (SFR) spectroscopy

In SFR spectroscopy a single fiber is used for both delivery and collection of light⁸⁹⁻⁹¹. The sampling depth is shallow and depends on the diameter of the fiber. From the measured reflectance spectrum the tissue absorption coefficient μ_a can be quantified (without prior knowledge of the scattering properties)⁹². Decomposition of μ_a into the

constituent spectra of the chromophores present in the skin yields measurements of the blood volume, saturation, and melanin, bilirubin and beta-carotene concentrations. When more than one fiber with different diameters are used simultaneously it is possible to determine the scattering phase function parameter γ , which allows quantification of the tissue scattering properties that are given as the reduced scattering coefficient μ_s' . This use of more than one single fiber measurement is termed multi diameter single fiber (MDSFR) spectroscopy⁹³⁻⁹⁵. In addition to measuring γ and μ_s' , the slope of μ_s' as a function of wavelength is also measured in MDSFR. This parameter is termed a_2 , or the scattering power. Where μ_s' can be considered a measure of the density of scattering particles, a_2 can be considered a measure of the relative size of these particles. Both these measures may be relevant if MDSFR spectroscopy is used for diagnostic purposes, for example to detect morphological changes in cellular architecture that may be altered in early carcinogenesis. In addition to the possible use of MDSFR as a diagnostic tool, its primary use for PDT is that the optical properties derived from MDSFR spectra can be used to correct fluorescence measurements⁹⁶.

5. SINGLE FIBER FLUORESCENCE (SFF) SPECTROSCOPY

In fluorescence spectroscopy light with a defined wavelength is used to excite a fluorophore (e.g. PpIX) and a spectrometer collects light above this wavelength emitted by the fluorophore. As explained, the optical properties of the sampled volume are important for the probability of both the excitation light to excite the fluorophore and for emission light to reach the spectrometer. In single fiber fluorescence (SFF) spectroscopy one of the fibers of the MDSFR spectroscopy measurement is used to acquire a fluorescence spectrum. Combining the information of the MDSFR and the SFF measurements enables to correct fluorescence spectra for the optical properties of the same sampling volume⁹⁷⁻⁹⁹. This is the topic of the last study in this thesis.

6. THIS THESIS OUTLINE

In short, the major topics that are included in this thesis are focused on monitoring relevant parameters during PDT and to use this information to improve our understanding of PDT. Ultimately this type of information will be necessary in order to understand and predict individual treatment failures and to optimize and personalize treatment in terms of maximizing effectiveness and minimizing side effects. One of the main parameters that is being monitored in this thesis is the PpIX fluorescence. Different fluorescence measurement methods are used to investigate PpIX concentration and localisation

within the tissue, with a focus on the distribution of PpIX in the vasculature in some chapters. In addition, PpIX photobleaching kinetics are monitored during PDT that inform on oxygen consumption, which is also related to the vascular response to PDT. Because PpIX fluorescence is so informative for monitoring PDT, it is essential that accurate fluorescence measurements are performed. As explained above it is necessary to measure the optical properties of the sampled skin volume first, so this information can be used to correct fluorescence measurements. Measuring the optical properties can also be useful to monitor changes in blood volume and saturation during PDT which in turn are related to vascular responses. Furthermore, quantifying optical properties may also be valuable for diagnostic purposes.

In chapter 2 a major limitation of PDT is introduced: pain. In a clinical investigation, characteristics that may predict severe pain during PDT are measured and their influence is evaluated. This knowledge may add to a more personalized approach to PDT. A potential solution to decrease pain during PDT is described in Chapter 3. In a mouse model the effect of low fluence rate PDT on photobleaching kinetics and PDT efficacy is studied.

Chapters 4 and 5 focus on the vascular distribution of PpIX and the vascular effects of topical PDT in mouse models using different porphyrin precursors. PpIX fluorescence is measured in histological sections and in subcutaneous blood vessels in a skin fold chamber model in which these vessels are directly visible. The distribution of PpIX in the vasculature and the vascular response to PDT are measured which may be relevant for the oxygen supply during PDT and ultimately for the success or failure of individual treatments. In chapter 6 the knowledge from chapters 4 and 5 is used to investigate the effect of light fractionation on PDT efficacy for HAL. The rationale is that the vasculature is believed to play a role in the mechanism behind light fractionation. In this study the relation between PpIX fluorescence kinetics and PDT efficacy is again investigated .

In chapter 7 the clinical importance of monitoring optical properties of the skin during PDT for individual patients is introduced. DPS is introduced as a new optical technique that allows superficial measurements of absorption parameters during PDT such as the blood content and saturation. In chapter 8 the clinical use of MDSFR spectroscopy is introduced in human skin which measures not only the absorption but also the scattering characteristics. It is described how this complete determination of optical properties can be used in combination with single fiber fluorescence spectroscopy to correct the measured fluorescence. The importance to do this for individual patients undergoing PDT is described. Chapter 9 provides a general discussion of the results of the studies presented in this thesis, and how they contribute to the optimization of photodynamic therapy. It concludes with a brief discussion of future perspectives.

REFERENCES

1. Niedre M, Patterson MS, Wilson BC. Direct near-infrared luminescence detection of singlet oxygen generated by photodynamic therapy in cells in vitro and tissues in vivo. *Photochem Photobiol.* 2002;75(4):382-91.
2. Moan J. On the diffusion length of singlet oxygen in cells and tissues. *J Photochem Photobiol B.* 1990;6:343-4.
3. Tavares A, Carvalho CM, Faustino MA, Neves MG, Tome JP, Tome AC, et al. Antimicrobial photodynamic therapy: study of bacterial recovery viability and potential development of resistance after treatment. *Mar Drugs.* 2010;8(1):91-105. doi: 10.3390/md8010091.
4. Jori G, Magaraggia M, Fabris C, Soncin M, Camerin M, Tallandini L, et al. Photodynamic inactivation of microbial pathogens: disinfection of water and prevention of water-borne diseases. *J Environ Pathol Toxicol Oncol.* 2011;30(3):261-71.
5. Mang TS, Tayal DP, Baier R. Photodynamic therapy as an alternative treatment for disinfection of bacteria in oral biofilms. *Lasers Surg Med.* 2012;44(7):588-96. doi: 10.1002/lsm.22050. Epub 2012 Jul 27.
6. Baptista MS, Wainwright M. Photodynamic antimicrobial chemotherapy (PACT) for the treatment of malaria, leishmaniasis and trypanosomiasis. *Braz J Med Biol Res.* 2011;44(1):1-10. Epub 2010 Dec 10.
7. de Visscher SA, Dijkstra PU, Tan IB, Roodenburg JL, Witjes MJ. mTHPC mediated photodynamic therapy (PDT) of squamous cell carcinoma in the head and neck: a systematic review. *Oral Oncol.* 2013;49(3):192-210. doi: 10.1016/j.oraloncology.2012.09.011. Epub Oct 13.
8. Eljamel S. Photodynamic applications in brain tumors: a comprehensive review of the literature. *Photodiagnosis Photodyn Ther.* 2010;7(2):76-85. doi: 10.1016/j.pdpdt.2010.02.002. Epub Mar 20.
9. Wolfsen HC. Uses of photodynamic therapy in premalignant and malignant lesions of the gastrointestinal tract beyond the esophagus. *J Clin Gastroenterol.* 2005;39(8):653-64.
10. Bozzini G, Colin P, Betrouni N, Nevoux P, Ouzzane A, Puech P, et al. Photodynamic therapy in urology: what can we do now and where are we heading? *Photodiagnosis Photodyn Ther.* 2012;9(3):261-73. doi: 10.1016/j.pdpdt.2012.01.005. Epub Feb 22.
11. Kostovic K, Pastar Z, Ceovic R, Mokos ZB, Buzina DS, Stanimirovic A. Photodynamic therapy in dermatology: current treatments and implications. *Coll Antropol.* 2012;36(4):1477-81.
12. Lang GE, Mennel S, Spital G, Wachtlin J, Jurklics B, Heimann H, et al. [Different indications of photodynamic therapy in ophthalmology]. *Klin Monbl Augenheilkd.* 2009;226(9):725-39. doi: 10.1055/s-0028-1109514. Epub 2009 Jul 14.
13. Fayter D, Corbett M, Heirs M, Fox D, Eastwood A. A systematic review of photodynamic therapy in the treatment of pre-cancerous skin conditions, Barrett's oesophagus and cancers of the biliary tract, brain, head and neck, lung, oesophagus and skin. *Health Technol Assess.* 2010;14(37):1-288. doi: 10.3310/hta14370.

14. Nardelli AA, Stafinski T, Menon D. Effectiveness of photodynamic therapy for mammary and extra-mammary Paget's disease: a state of the science review. *BMC Dermatol.* 2011;11:13. (doi):10.1186/471-5945-11-13.
15. Fernandez-Guarino M, Jaen P. Photodynamic therapy and plaque phase mycosis fungoides. *G Ital Dermatol Venereol.* 2011;146(6):457-61.
16. Lee Y, Baron ED. Photodynamic therapy: current evidence and applications in dermatology. *Semin Cutan Med Surg.* 2011;30(4):199-209. doi: 10.1016/j.sder.2011.08.001.
17. Kushibiki T, Hirasawa T, Okawa S, Ishihara M. Responses of cancer cells induced by photodynamic therapy. *J Healthc Eng.* 2013;4(1):87-108. doi: 10.1260/2040-295.4.1.87.
18. Reiners JJ, Jr., Agostinis P, Berg K, Oleinick NL, Kessel D. Assessing autophagy in the context of photodynamic therapy. *Autophagy.* 2010;6(1):7-18. Epub 2010 Jan 1.
19. Buytaert E, Dewaele M, Agostinis P. Molecular effectors of multiple cell death pathways initiated by photodynamic therapy. *Biochim Biophys Acta.* 2007;1776(1):86-107. Epub 2007 Jul 6.
20. Yoo JO, Ha KS. New insights into the mechanisms for photodynamic therapy-induced cancer cell death. *Int Rev Cell Mol Biol.* 2012;295:139-74.(doi):10.1016/B978-0-12-394306-4.00010-1.
21. Korbely M, Krosi G, Krosi J, Dougherty GJ. The role of host lymphoid populations in the response of mouse EMT6 tumor to photodynamic therapy. *Cancer Res.* 1996;56(24):5647-52.
22. Korbely M, Dougherty GJ. Photodynamic therapy-mediated immune response against subcutaneous mouse tumors. *Cancer Res.* 1999;59(8):1941-6.
23. Krosi G, Korbely M, Dougherty GJ. Induction of immune cell infiltration into murine SCCVII tumour by photofrin-based photodynamic therapy. *Br J Cancer.* 1995;71(3):549-55.
24. Castano AP, Mroz P, Hamblin MR. Photodynamic therapy and anti-tumour immunity. *Nat Rev Cancer.* 2006;6(7):535-45.
25. Chaudhuri K, Keck RW, Selman SH. Morphological changes of tumor microvasculature following hematoporphyrin derivative sensitized photodynamic therapy. *Photochem Photobiol.* 1987;46(5):823-7.
26. Wieman TJ, Mang TS, Fingar VH, Hill TG, Reed MW, Corey TS, et al. Effect of photodynamic therapy on blood flow in normal and tumor vessels. *Surgery.* 1988;104(3):512-7.
27. Reed MW, Wieman TJ, Schuschke DA, Tseng MT, Miller FN. A comparison of the effects of photodynamic therapy on normal and tumor blood vessels in the rat microcirculation. *Radiat Res.* 1989;119(3):542-52.
28. Feyh J, Goetz A, Heimann A, Konigsberger R, Kastenbauer E. [Microcirculatory effects of photodynamic therapy with hematoporphyrin derivative]. *Laryngorhinootologie.* 1991;70(2):99-101.
29. Fingar VH, Wieman TJ, Wiehle SA, Cerrito PB. The role of microvascular damage in photodynamic therapy: the effect of treatment on vessel constriction, permeability, and leukocyte adhesion. *Cancer Res.* 1992;52(18):4914-21.
30. Herman MA, Fromm D, Kessel D. Tumor blood-flow changes following protoporphyrin IX-based photodynamic therapy in mice and humans. *J Photochem Photobiol B.* 1999;52(1-3):99-104.

31. Henderson BW, Fingar VH. Oxygen limitation of direct tumor cell kill during photodynamic treatment of a murine tumor model. *Photochem Photobiol.* 1989;49(3):299-304.
32. Henderson BW, Waldow SM, Mang TS, Potter WR, Malone PB, Dougherty TJ. Tumor destruction and kinetics of tumor cell death in two experimental mouse tumors following photodynamic therapy. *Cancer Res.* 1985;45(2):572-6.
33. Wang HW, Putt ME, Emanuele MJ, Shin DB, Glatstein E, Yodh AG, et al. Treatment-induced changes in tumor oxygenation predict photodynamic therapy outcome. *Cancer Res.* 2004;64(20):7553-61.
34. Becker TL, Paquette AD, Keymel KR, Henderson BW, Sunar U. Monitoring blood flow responses during topical ALA-PDT. *Biomed Opt Express.* 2010;2(1):123-30.
35. Wang I, Andersson-Engels S, Nilsson GE, Wardell K, Svanberg K. Superficial blood flow following photodynamic therapy of malignant non-melanoma skin tumours measured by laser Doppler perfusion imaging. *Br J Dermatol.* 1997;136(2):184-9.
36. van der Veen N, Hebeda KM, de Bruijn HS, Star WM. Photodynamic effectiveness and vasoconstriction in hairless mouse skin after topical 5-aminolevulinic acid and single- or two-fold illumination. *Photochem Photobiol.* 1999;70(6):921-9.
37. Wang KK, Cottrell WJ, Mitra S, Oseroff AR, Foster TH. Simulations of measured photobleaching kinetics in human basal cell carcinomas suggest blood flow reductions during ALA-PDT. *Lasers Surg Med.* 2009;41(9):686-96. doi: 10.1002/lsm.20847.
38. Nashed D, Meiss F, Muller M. Therapeutic strategies for actinic keratoses—a systematic review. *Eur J Dermatol.* 2013;23(1):14-32. doi: 10.1684/ejd.2013.1923.
39. Roozeboom MH, Arits AH, Nelemans PJ, Kelleners-Smeets NW. Overall treatment success after treatment of primary superficial basal cell carcinoma: a systematic review and meta-analysis of randomized and nonrandomized trials. *Br J Dermatol.* 2012;167(4):733-56. doi: 10.1111/j.1365-2133.012.11061.x. Epub 2012 Sep 7.
40. Roozeboom MH, Aardoom MA, Nelemans PJ, Thissen MR, Kelleners-Smeets NW, Kuijpers DI, et al. Fractionated 5-aminolevulinic acid photodynamic therapy after partial debulking versus surgical excision for nodular basal cell carcinoma: a randomized controlled trial with at least 5-year follow-up. *J Am Acad Dermatol.* 2013;69(2):280-7. doi: 10.1016/j.jaad.2013.02.014. Epub Apr 6.
41. Rhodes LE, de Rie MA, Leifsdottir R, Yu RC, Bachmann I, Goulden V, et al. Five-year follow-up of a randomized, prospective trial of topical methyl aminolevulinic acid photodynamic therapy vs surgery for nodular basal cell carcinoma. *Arch Dermatol.* 2007;143(9):1131-6.
42. de Vijlder HC, Sterenborg HJ, Neumann HA, Robinson DJ, de Haas ER. Light fractionation significantly improves the response of superficial basal cell carcinoma to aminolevulinic acid photodynamic therapy: five-year follow-up of a randomized, prospective trial. *Acta Derm Venereol.* 2012;92(6):641-7. doi: 10.2340/00015555-1448.
43. Ibbotson SH. Adverse effects of topical photodynamic therapy. *Photodermatol Photoimmunol Photomed.* 2011;27(3):116-30. doi: 10.1111/j.1600-0781.2010.00560.x.
44. Mikolajewska P. Pain during topical photodynamic therapy [www document]. 2011;https://www.duo.uio.no/handle/10852/11075?locale-attribute=en [accessed on 12 March 2013].

45. Christensen E, Mjones P, Foss OA, Rordam OM, Skogvoll E. Pre-treatment evaluation of basal cell carcinoma for photodynamic therapy: comparative measurement of tumour thickness in punch biopsy and excision specimens. *Acta Derm Venereol.* 2011;91(6):651-4. doi: 10.2340/00015555-1127.
46. Collier NJ, Ali FR, Lear JT. Efficacy of photodynamic therapy for treatment of basal cell carcinoma in organ transplant recipients. *Lasers Med Sci.* 2013;15:15.
47. Dragieva G, Hafner J, Dummer R, Schmid-Grendelmeier P, Roos M, Prinz BM, et al. Topical photodynamic therapy in the treatment of actinic keratoses and Bowen's disease in transplant recipients. *Transplantation.* 2004;77(1):115-21.
48. Rud E, Gederaas O, Hogset A, Berg K. 5-aminolevulinic acid, but not 5-aminolevulinic acid esters, is transported into adenocarcinoma cells by system BETA transporters. *Photochem Photobiol.* 2000;71(5):640-7.
49. Rodriguez L, Batlle A, Di Venosa G, MacRobert AJ, Battah S, Daniel H, et al. Study of the mechanisms of uptake of 5-aminolevulinic acid derivatives by PEPT1 and PEPT2 transporters as a tool to improve photodynamic therapy of tumours. *Int J Biochem Cell Biol.* 2006;38(9):1530-9. Epub 2006 Mar 18.
50. Rodriguez L, Batlle A, Di Venosa G, Battah S, Dobbin P, MacRobert AJ, et al. Mechanisms of 5-aminolevulinic acid ester uptake in mammalian cells. *Br J Pharmacol.* 2006;147(7):825-33.
51. Schulten R, Novak B, Schmitz B, Lubbert H. Comparison of the uptake of 5-aminolevulinic acid and its methyl ester in keratinocytes and skin. *Naunyn Schmiedebergs Arch Pharmacol.* 2012;385(10):969-79. doi: 10.1007/s00210-012-0777-4. Epub 2012 Jul 17.
52. Uehlinger P, Zellweger M, Wagnieres G, Juillerat-Jeanneret L, van den Bergh H, Lange N. 5-Aminolevulinic acid and its derivatives: physical chemical properties and protoporphyrin IX formation in cultured cells. *J Photochem Photobiol B.* 2000;54(1):72-80.
53. Rodriguez L, de Bruijn HS, Di Venosa G, Mamone L, Robinson DJ, Juarranz A, et al. Porphyrin synthesis from aminolevulinic acid esters in endothelial cells and its role in photodynamic therapy. *J Photochem Photobiol B.* 2009;96(3):249-54. Epub 2009 Jul 5.
54. Collaud S, Juzeniene A, Moan J, Lange N. On the selectivity of 5-aminolevulinic acid-induced protoporphyrin IX formation. *Curr Med Chem Anticancer Agents.* 2004;4(3):301-16.
55. Zeng H, Korbelik M, McLean DI, MacAulay C, Lui H. Monitoring photoproduct formation and photobleaching by fluorescence spectroscopy has the potential to improve PDT dosimetry with a verteporfin-like photosensitizer. *Photochem Photobiol.* 2002;75(4):398-405.
56. Yu G, Durduran T, Zhou C, Zhu TC, Finlay JC, Busch TM, et al. Real-time in situ monitoring of human prostate photodynamic therapy with diffuse light. *Photochem Photobiol.* 2006;82(5):1279-84.
57. Sitnik TM, Henderson BW. The effect of fluence rate on tumor and normal tissue responses to photodynamic therapy. *Photochem Photobiol.* 1998;67(4):462-6.
58. Dysart JS, Patterson MS, Farrell TJ, Singh G. Relationship between mTHPC fluorescence photobleaching and cell viability during in vitro photodynamic treatment of DP16 cells. *Photochem Photobiol.* 2002;75(3):289-95.

59. Dysart JS, Patterson MS. Photobleaching kinetics, photoproduct formation, and dose estimation during ALA induced PpIX PDT of MLL cells under well oxygenated and hypoxic conditions. *Photochem Photobiol Sci.* 2006;5(1):73-81. Epub 2005 Nov 15.
60. Boere IA, Robinson DJ, de Bruijn HS, Kluin J, Tilanus HW, Sterenborg HJ, et al. Protoporphyrin IX fluorescence photobleaching and the response of rat Barrett's esophagus following 5-aminolevulinic acid photodynamic therapy. *Photochem Photobiol.* 2006;82(6):1638-44.
61. Henderson BW, Fingar VH. Relationship of tumor hypoxia and response to photodynamic treatment in an experimental mouse tumor. *Cancer Res.* 1987;47(12):3110-4.
62. Langmack K, Mehta R, Twyman P, Norris P. Topical photodynamic therapy at low fluence rates— theory and practice. *J Photochem Photobiol B.* 2001;60(1):37-43.
63. Finlay JC, Conover DL, Hull EL, Foster TH. Porphyrin bleaching and PDT-induced spectral changes are irradiance dependent in ALA-sensitized normal rat skin in vivo. *Photochem Photobiol.* 2001;73(1):54-63.
64. Foster TH, Murant RS, Bryant RG, Knox RS, Gibson SL, Hilf R. Oxygen consumption and diffusion effects in photodynamic therapy. *Radiat Res.* 1991;126(3):296-303.
65. Robinson DJ, de Bruijn HS, van der Veen N, Stringer MR, Brown SB, Star WM. Fluorescence photobleaching of ALA-induced protoporphyrin IX during photodynamic therapy of normal hairless mouse skin: the effect of light dose and irradiance and the resulting biological effect. *Photochem Photobiol.* 1998;67(1):140-9.
66. van der Veen N, van Leengoed HL, Star WM. In vivo fluorescence kinetics and photodynamic therapy using 5-aminolaevulinic acid-induced porphyrin: increased damage after multiple irradiations. *Br J Cancer.* 1994;70(5):867-72.
67. Robinson DJ, de Bruijn HS, de Wolf WJ, Sterenborg HJ, Star WM. Topical 5-aminolevulinic acid-photodynamic therapy of hairless mouse skin using two-fold illumination schemes: PpIX fluorescence kinetics, photobleaching and biological effect. *Photochem Photobiol.* 2000;72(6):794-802.
68. Robinson DJ, de Bruijn HS, Star WM, Sterenborg HJ. Dose and timing of the first light fraction in two-fold illumination schemes for topical ALA-mediated photodynamic therapy of hairless mouse skin. *Photochem Photobiol.* 2003;77(3):319-23.
69. de Bruijn HS, van der Ploeg-van den Heuvel A, Sterenborg HJ, Robinson DJ. Fractionated illumination after topical application of 5-aminolevulinic acid on normal skin of hairless mice: the influence of the dark interval. *J Photochem Photobiol B.* 2006;85(3):184-90. Epub 2006 Sep 1.
70. de Haas ER, Kruijt B, Sterenborg HJ, Martino Neumann HA, Robinson DJ. Fractionated illumination significantly improves the response of superficial basal cell carcinoma to aminolevulinic acid photodynamic therapy. *J Invest Dermatol.* 2006;126(12):2679-86. Epub 006 Jul 13.
71. de Bruijn HS, de Haas ER, Hebeda KM, van der Ploeg-van den Heuvel A, Sterenborg HJ, Neumann HA, et al. Light fractionation does not enhance the efficacy of methyl 5-aminolevulinic acid mediated photodynamic therapy in normal mouse skin. *Photochem Photobiol Sci.* 2007;6(12):1325-31. Epub 2007 Aug 28.

72. de Vijlder H, de Bruijn H, van der Ploeg-van den Heuvel A, van Zaane F, Schipper D, ten Hagen T, et al. Acute vascular responses during photodynamic therapy using topically administered porphyrin precursors. *Photochem Photobiol Sci* 2013 in press. 2013.
73. de Bruijn HS, Casas AG, Di Venosa G, Gandara L, Sterenborg HJ, Batlle A, et al. Light fractionated ALA-PDT enhances therapeutic efficacy in vitro; the influence of PpIX concentration and illumination parameters. *Photochem Photobiol Sci*. 2013;12(2):241-5. doi: 10.1039/c2pp25287b. Epub 2012 Oct 29.
74. Brennan MJ, Cantrill RC. Delta-aminolaevulinic acid is a potent agonist for GABA autoreceptors. *Nature*. 1979;280(5722):514-5.
75. Muller WE, Snyder SH. delta-Aminolevulinic acid: influences on synaptic GABA receptor binding may explain CNS symptoms of porphyria. *Ann Neurol*. 1977;2(4):340-2.
76. Sandberg C, Stenquist B, Rosdahl I, Ros AM, Synnerstad I, Karlsson M, et al. Important factors for pain during photodynamic therapy for actinic keratosis. *Acta Derm Venereol*. 2006;86(5):404-8.
77. Wax A, Backman V. *Biomedical Applications of Light Scattering*: McGraw-Hill Professional; 2009.
78. Mourant JR, Canpolat M, Brocker C, Esponda-Ramos O, Johnson TM, Matanock A, et al. Light scattering from cells: the contribution of the nucleus and the effects of proliferative status. *J Biomed Opt*. 2000;5(2):131-7.
79. Fereidouni F, Bader AN, Colonna A, Gerritsen HC. Phasor analysis of multiphoton spectral images distinguishes autofluorescence components of in vivo human skin. *J Biophotonics*. 2013;11(10):201200244.
80. Na R, Stender IM, Ma L, Wulf HC. Autofluorescence spectrum of skin: component bands and body site variations. *Skin Res Technol*. 2000;6(3):112-7.
81. Pradhan P, Damania D, Joshi HM, Turzhitsky V, Subramanian H, Roy HK, et al. Quantification of nanoscale density fluctuations by electron microscopy: probing cellular alterations in early carcinogenesis. *Phys Biol*. 2011;8(2):026012. doi: 10.1088/1478-3975/8/2/. Epub 2011 Mar 25.
82. Subramanian H, Pradhan P, Liu Y, Capoglu IR, Li X, Rogers JD, et al. Optical methodology for detecting histologically unapparent nanoscale consequences of genetic alterations in biological cells. *Proc Natl Acad Sci U S A*. 2008;105(51):20118-23. doi: 10.1073/pnas.0804723105. Epub 2008 Dec 10.
83. Jacques SL, Pogue BW. Tutorial on diffuse light transport. *J Biomed Opt*. 2008;13(4):041302. doi: 10.1117/1.2967535.
84. Cihan C, Arifler D. Influence of phase function on modeled optical response of nanoparticle-labeled epithelial tissues. *J Biomed Opt*. 2011;16(8):085002. doi: 10.1117/1.3608999.
85. Yaroslavsky AN, Yaroslavsky IV, Goldbach T, Schwarzmaier HJ. Influence of the scattering phase function approximation on the optical properties of blood determined from the integrating sphere measurements. *J Biomed Opt*. 1999;4(1):47-53.
86. Mourant JR, Boyer J, Hielscher AH, Bigio IJ. Influence of the scattering phase function on light transport measurements in turbid media performed with small source-detector separations. *Opt Lett*. 1996;21(7):546-8.

87. Kanick SC, Sterenborg HJ, Amelink A. Empirical model description of photon path length for differential path length spectroscopy: combined effect of scattering and absorption. *J Biomed Opt.* 2008;13(6):064042.
88. Kaspers OP, Sterenborg HJ, Amelink A. Controlling the optical path length in turbid media using differential path-length spectroscopy: fiber diameter dependence. *Appl Opt.* 2008;47(3):365-71.
89. Amelink A, van der Ploeg van den Heuvel A, de Wolf WJ, Robinson DJ, Sterenborg HJ. Monitoring PDT by means of superficial reflectance spectroscopy. *J Photochem Photobiol B.* 2005;79(3):243-51. Epub 2005 Mar 23.
90. Amelink A, Bard MP, Burgers SA, Sterenborg HJ. Single-scattering spectroscopy for the endoscopic analysis of particle size in superficial layers of turbid media. *Appl Opt.* 2003;42(19):4095-101.
91. Kanick SC, Gamm UA, Schouten M, Sterenborg HJ, Robinson DJ, Amelink A. Measurement of the reduced scattering coefficient of turbid media using single fiber reflectance spectroscopy: fiber diameter and phase function dependence. *Biomed Opt Express.* 2011;2(6):1687-702. doi: 10.364/BOE.2.001687. Epub 2011 May 25.
92. Kanick SC, Robinson DJ, Sterenborg HJ, Amelink A. Method to quantitate absorption coefficients from single fiber reflectance spectra without knowledge of the scattering properties. *Opt Lett.* 2011;36(15):2791-3. doi: 10.1364/OL.36.002791.
93. Gamm UA, Kanick SC, Sterenborg HJ, Robinson DJ, Amelink A. Measurement of tissue scattering properties using multi-diameter single fiber reflectance spectroscopy: in silico sensitivity analysis. *Biomed Opt Express.* 2011;2(11):3150-66. doi: 10.1364/BOE.2.003150. Epub 2011 Oct 26.
94. Gamm UA, Kanick SC, Sterenborg HJ, Robinson DJ, Amelink A. Quantification of the reduced scattering coefficient and phase-function-dependent parameter gamma of turbid media using multidiameter single fiber reflectance spectroscopy: experimental validation. *Opt Lett.* 2012;37(11):1838-40. doi: 10.364/OL.37.001838.
95. Kanick SC, Gamm UA, Sterenborg HJ, Robinson DJ, Amelink A. Method to quantitatively estimate wavelength-dependent scattering properties from multidiameter single fiber reflectance spectra measured in a turbid medium. *Opt Lett.* 2011;36(15):2997-9. doi: 10.1364/OL.36.002997.
96. Kanick SC, Robinson DJ, Sterenborg HJ, Amelink A. Extraction of intrinsic fluorescence from single fiber fluorescence measurements on a turbid medium. *Opt Lett.* 2012;37(5):948-50. doi: 10.1364/OL.37.000948.
97. van Leeuwen-van Zaane F, Gamm UA, van Driel PB, Snoeks TJ, de Bruijn HS, van der Ploeg-van den Heuvel A, et al. In vivo quantification of the scattering properties of tissue using multi-diameter single fiber reflectance spectroscopy. *Biomed Opt Express.* 2013;4(5):696-708. doi: 10.1364/BOE.4.000696. Print 2013 May 1.
98. Hoy CL, Gamm UA, Sterenborg HJ, Robinson DJ, Amelink A. Use of a coherent fiber bundle for multi-diameter single fiber reflectance spectroscopy. *Biomed Opt Express.* 2012;3(10):2452-64. doi: 10.1364/BOE.3.002452. Epub 2012 Sep 12.
99. Hoy CL, Gamm UA, Sterenborg HJ, Robinson DJ, Amelink A. Method for rapid multidiameter single-fiber reflectance and fluorescence spectroscopy through a fiber bundle. *J Biomed Opt.* 2013;18(10):107005.

2

Red light ALA-PDT for large areas of actinic keratosis is limited by severe pain and patient dissatisfaction

Tom Middelburg
Tamar Nijsten
Martino Neumann
Ellen de Haas
Dominic Robinson

Photodermatol Photoimmunol Photomed. 2013;29(5):276-8.

ABSTRACT

In PDT the clinical relevance of predictors for increased pain is unclear and the effect on patient satisfaction unknown. We identified risk factors associated with severe pain and patient dissatisfaction in ALA-PDT for actinic keratosis field cancerisation using multivariate binary logistic regression. Treatment area size was the only significant predictor for severe pain and patient dissatisfaction. In our largest treatment area group (85-190 cm²) severe pain was reported by 81% of patients, clearly illustrating the need for adequate pain control. A way to decrease pain is low fluence rate PDT, of which daylight PDT is a popular recent example.

TEXT (LETTER TO THE EDITOR)

Treatment of actinic keratosis field cancerization poses an increasing challenge to the dermatologist. Photodynamic therapy (PDT) using aminolevulinic acid (ALA) or its methyl ester is an attractive treatment modality for this indication because it is an effective, single day procedure with excellent cosmetic results. The main disadvantage of PDT is that it can be painful, limiting its applicability. Many factors influencing pain have been described in the literature: PpIX concentration; fluence rate; wavelength; treatment area size; localization; use of ALA or its methyl ester; sex; skin type; lesion redness; age; and lesion type¹⁻⁶, but results are inconsistent.

Moreover, an important consideration is that the outcomes are often difficult to interpret clinically. Pain is typically measured using a visual analogue scale. One approach has been to identify risk factors for pain using linear regression, resulting in beta coefficients that predict higher VAS scores. Another approach has been to compare the mean VAS score between two randomized groups. Both the beta coefficients and the magnitude of the mean difference can be difficult to interpret, due to the non-linear nature of the VAS score, and may not represent a clinically relevant association or difference.

Therefore, in this prospective study we chose severe versus non-severe pain as binary outcome, which is clinically relevant and easy to understand. In addition, patient satisfaction was studied, which is becoming an increasingly important endpoint of clinical studies but which is not well studied in PDT. Our aim was to identify risk factors for severe pain, measure patient satisfaction and investigate the influence of severe pain on satisfaction. The study was approved by the local ethical committee, is in accordance with the declaration of Helsinki and all patients gave written informed consent prior to inclusion.

We included 48 patients that were treated with fractionated ALA-PDT for actinic field cancerization of at least 25 cm² in the face, scalp or back of hands. The light fractionated treatment protocol is the standard treatment in our university hospital. It involves delivery of 20 J cm⁻² in the first illumination after 4 hours of 20% ALA gel application under occlusion, followed by a dark interval of two hours and delivery of an additional 80 J cm⁻² in a second illumination. We used a Waldmann PDT 1200L lamp, with an emission peak around 635 nm and a spectrum of 600-730 nm. The following characteristics were collected: age (older or younger than the mean), sex (m/f), hair color (red/other), skin type (I-III) and the size of the treatment area (divided into three equal categories based on the data's tertiles). Pain was scored immediately after the first and after the second illumination using a VAS score (scale 0-10) with 0 representing no pain and 10 the worst

pain imaginable. Severe pain was defined as a VAS score ≥ 7 . If necessary, patients received local infiltrative or nerve block anesthesia. Treatment satisfaction was scored after three months using the Dutch version of the Treatment Satisfaction Questionnaire for Medication (TSQM)⁷. This questionnaire has four domains: effectiveness, side effects, convenience, and global satisfaction (scale 0-100). A score ≥ 70 was considered "satisfied" and lower scores as "dissatisfied". Predicting variables associated with severe pain and those associated with dissatisfaction were analyzed using univariate and multivariate binary logistic regression.

In total 58% (28/48) of patients reported severe pain at any time point during the treatment (i.e. either during the first or second illumination). All patients that experienced severe pain requested and received anesthesia, which reduced the reported median VAS from 9 to 5 in those patients. However, 7 of them still considered their pain as severe

Table 1. Predicting variables for reporting severe pain at any time-point during PDT, using a univariate and multivariate binary logistic regression model (n=48). The odds ratios presented are relative to their baseline, indicated by the number 1.

	Univariate analysis		Multivariate analysis *	
	OR (95% CI)	P-value	OR (95% CI)	P-value
Sex				
female	1		1	
male	2.48 (0.65-9.40)	0.18	0.57 (0.10-3.15)	0.52
Hair color				
red	1		n.a.	
other	1.47 (0.27-8.17)	0.66	n.a.	
Fitzpatrick skin type				
1	1		1	
2 or 3	3.57 (0.77-16.54)	0.13	3.35 (0.54-20.72)	0.19
Treatment area size (cm²)				
25-54	1		1	
55-85	2.12 (0.52-8.81)	0.29	4.3 (0.73-25.40)	0.11
85-190	7.22 (1.44-36.22)	0.02	9.70 (1.43-65.58)	0.02
Pain medication use				
no	1		n.a.	
yes	1.30 (0.38-4.43)	0.68	n.a.	
Location				
hand	1		1	
face/scalp	2.57 (0.62-10.71)	0.19	3.15 (0.55-17.91)	0.20

Abbreviations: OR, Odds Ratio; CI, Confidence Interval; n.a. not applicable

* P-values < 0.20 were added to the multivariate analysis

after anesthesia, and two of these patients did not complete treatment due to pain severity. The only significant predictor for severe pain was treatment area size (Table 1). Severe pain was reported by 38%, 56% and 81% of patients in respectively the smallest, middle and largest size categories (the total treatment area range was 25-190 cm²). The TSQM questionnaire was completed by 44 patients. Most patients that did not experience severe pain were satisfied for all domains, whereas most patients that experienced severe pain were dissatisfied for the domains effectiveness, convenience and global satisfaction (Table 2). Severe pain was a significant predictor for dissatisfaction on the TSQM convenience domain after adjusting for size (OR 6.8, 95% CI 1.4-33, P=0.02). Treatment area size was a significant predictor for dissatisfaction on the TSQM effectiveness domain after adjusting for pain (OR 8.1, 95% CI 1.4-50, P=0.02).

Table 2. Treatment satisfaction: TSQM domain scores for all patients (Total) and stratified for severe pain (VAS \geq 7) versus non-severe pain (VAS<7).

TSQM domain	Total	VAS<7 group	VAS \geq 7 group	P-value
	n=44	n=18	n=26	(Mann-Whitney test)
effectiveness (median, IQR)	67 (56-78)	72 (61-83)	67 (50-72)	0.12
side effects (median, IQR)	100 (90-100)	100 (98-100)	100 (69-100)	0.32
convenience (median, IQR)	53 (39-72)	72 (50-79)	47 (33-56)	0.01
global satisfaction (median, IQR)	61 (38-79)	71 (57-79)	50 (29-71)	0.02

Abbreviations: TSQM, Treatment Satisfaction Questionnaire for Medication; VAS, Visual Analogue Scale; IQR, InterQuartile Range

This study shows that PDT for large areas of actinic field cancerization is limited due to severe pain. This is a clinically relevant short term complication that also reduces long term patient satisfaction. Our finding that only size of the treatment area is a predictor for severe pain differs from other studies that have found other pain predictors, but match the conclusions from a review on this topic ⁶. Our limited sample size may have resulted in insufficient power to detect weaker predictors for severe pain. However, it is uncertain if these weaker predictors will have any clinical relevance. The results indicate that there is need for adequate pain control when treating large fields. Infiltrative lidocain and nerve block anesthesia are considered effective in reducing pain⁸, but have their own side effects. Moreover, in our study a considerable number of patients still reported severe pain after local or nerve block anesthesia. Therefore, future studies that focus on other solutions to decrease pain are needed. Data from the literature suggest that lowering the fluence rate may be the most interesting option to decrease pain ^{2,9}. The mechanism behind this is not clear, but possibly the lower rate at which singlet oxygen is produced plays a role. Lowering the fluence rate utilizes oxygen more efficiently, so a lower total light dose can be sufficient to deliver the same effective PDT dose (which can be measured by monitoring protoporphyrin IX fluorescence). Fluence

rate, length of illumination, pain and clinical efficacy may need to be carefully weighed against each other. An increasingly popular example of low-dose, very low fluence rate PDT is daylight PDT which is indeed less painful but still effective ¹⁰.

REFERENCES

1. Arits AH, van de Weert MM, Nelemans PJ, Kelleners-Smeets NW. Pain during topical photodynamic therapy: uncomfortable and unpredictable. *J Eur Acad Dermatol Venereol*. 2010;24(12):1452-7. doi: 10.1111/j.168-3083.2010.03670.x.
2. Wiegell SR, Skiveren J, Philipsen PA, Wulf HC. Pain during photodynamic therapy is associated with protoporphyrin IX fluorescence and fluence rate. *Br J Dermatol*. 2008;158(4):727-33. Epub 2008 Feb 16.
3. Sandberg C, Stenquist B, Rosdahl I, Ros AM, Synnerstad I, Karlsson M, et al. Important factors for pain during photodynamic therapy for actinic keratosis. *Acta Derm Venereol*. 2006;86(5):404-8.
4. Gholam P, Denk K, Sehr T, Enk A, Hartmann M. Factors influencing pain intensity during topical photodynamic therapy of complete cosmetic units for actinic keratoses. *J Am Acad Dermatol*. 2010;63(2):213-8. Epub 2010 Jun 9.
5. Mikolajewska P. Pain during topical photodynamic therapy [www document]. 2011; <https://www.duo.uio.no/handle/10852/11075?locale-attribute=en> [accessed on 12 March 2013].
6. Warren CB, Karai LJ, Vidimos A, Maytin EV. Pain associated with aminolevulinic acid-photodynamic therapy of skin disease. *J Am Acad Dermatol*. 2009;61(6):1033-43.
7. Atkinson MJ, Sinha A, Hass SL, Colman SS, Kumar RN, Brod M, et al. Validation of a general measure of treatment satisfaction, the Treatment Satisfaction Questionnaire for Medication (TSQM), using a national panel study of chronic disease. *Health Qual Life Outcomes*. 2004;2:12.
8. Halldin CB, Paoli J, Sandberg C, Gonzalez H, Wennberg AM. Nerve blocks enable adequate pain relief during topical photodynamic therapy of field cancerization on the forehead and scalp. *Br J Dermatol*. 2009;160(4):795-800. Epub 2009 Feb 4.
9. Cottrell WJ, Paquette AD, Keymel KR, Foster TH, Oseroff AR. Irradiance-dependent photobleaching and pain in delta-aminolevulinic acid-photodynamic therapy of superficial basal cell carcinomas. *Clin Cancer Res*. 2008;14(14):4475-83.
10. Wiegell SR, Fabricius S, Stender IM, Berne B, Kroon S, Andersen BL, et al. A randomized, multicentre study of directed daylight exposure times of 1(1/2) vs. 2(1/2) h in daylight-mediated photodynamic therapy with methyl aminolaevulinate in patients with multiple thin actinic keratoses of the face and scalp. *Br J Dermatol*. 2011;164(5):1083-90. doi: 10.1111/j.1365-2133.011.10209.x. Epub 2011 Apr 5.

3

Fractionated illumination at low fluence rate photodynamic therapy in mice

Tom Middelburg

Floor van Zaane

Riëtte de Bruijn

Angelique van der Ploeg-van den Heuvel

Dick Sterenberg

Martino Neumann

Ellen de Haas

Dominic Robinson

Photochem Photobiol. 2010;86(5):1140-6.

ABSTRACT

Photodynamic therapy (PDT) for actinic field cancerization is effective but painful. Pain mechanisms remain unclear but fluence rate has been shown to be a critical factor. Lower fluence rates also utilize available oxygen more efficiently. We investigated PDT effect in normal SKH1-HR mice using low and high fluence rate aminolevulinic acid (ALA) PDT and a fractionated illumination scheme. Six groups of six mice with different light treatment parameters were studied. Visual skin damage was assessed up to 7 days post PDT. Fluorescence and reflectance spectroscopy during illuminations provided us with real time information about PpIX photobleaching. A novel dosing approach was introduced in that we used a photobleaching percentage instead of a pre-set fluence. Data show similar total and maximum damage scores in high and low fluence rate groups. Photobleaching of PpIX in the low fluence rate groups shows a trend towards more efficient photobleaching. Results indicate that low fluence rate PDT is as effective as, and more efficient than high fluence rate PDT in normal mouse skin. Low fluence rate PDT light protocols need to be explored in human studies in search for an effective and well tolerated treatment for actinic field cancerization.

INTRODUCTION

Non-melanoma skin cancer and precursor lesions are a steadily increasing health care problem¹⁻⁵. Especially extensive field cancerization necessitates the use of full field treatment options, such as photodynamic therapy (PDT). PDT using topical aminolevulinic acid (ALA) or its ester derivatives, such as methyl-ALA (Metvix[®]) is now well accepted and used for treating actinic keratosis (AK), Bowen's disease (BD) and superficial basal cell carcinoma (sBCC). There is a consensus on the use of PDT for these indications, as presented in recent European guidelines^{6,7}. Topically applied ALA is converted via the heme synthesis pathway resulting in the accumulation of the photosensitizer protoporphyrin IX (PpIX). Illumination with light of the appropriate wavelength leads to the generation of reactive oxygen species, notably singlet oxygen. This results in a range of tissue effects that include cell apoptosis, necrosis, vascular and immunological responses. The effectiveness of ALA-PDT is influenced by many variables such as fluence, fluence rate, light source, illumination scheme, the application time, the use of iron chelators and the use of penetration enhancers^{8,9}.

Our group observed new formation of PpIX in time after single illumination in the past and subsequently investigated this in various animal models¹⁰⁻¹². A two-fold illumination scheme, separated by a substantial dark interval and a small first light fraction, increased response to PDT. We tested this light fractionated scheme in a clinical setting in sBCC's and found a significant improvement in response compared to single illumination. One year response rates in fractionated ALA PDT were 97%¹³ and in another study with different light treatment parameters, 5 year response rate was 84%¹⁴. This approach appears to compare favourably with the results for methyl aminolevulinic acid (Metvix[®]), where two-year response rates for primary 'difficult to treat' BCC are 76%¹⁵ and 78% for patients prone to complications and poor cosmetic outcome with conventional treatment¹⁶.

The main disadvantage of PDT is that it is often a painful treatment¹⁷, limiting the suitability of PDT as a treatment of first choice. Patients report a burning or tingling sensation that sometimes leads to need for local anaesthesia or termination of therapy. Especially treating extensive field cancerization with actinic keratosis in the face and scalp region is painful for the patient^{17,18}. The exact mechanism underlying the pain is unclear. Some authors suggested that pain increases with higher PpIX concentrations, although results are conflicting^{17,19,20}. It has also been proposed that the methyl ester (Metvix[®]) produces less pain than ALA²¹. Recently a number of authors have reported significantly less pain during PDT using lower fluence rates²²⁻²⁴ with low VAS scores at

20 mW cm⁻². Besides the advantage in pain perception, it is well documented that using lower fluence rates results in more efficient usage of the available oxygen in tissue ²⁵⁻³⁰.

We would like to incorporate the use of low fluence rate to light fractionated ALA-PDT to maintain effectiveness while minimizing pain. Therefore we designed the present study comparing high and low fluence rate PDT and several illumination schemes in hairless mouse skin. These schemes were in part the same as used in previous studies from our group at 50 mW cm⁻² and new groups were introduced using 20 mW cm⁻². We delivered a cumulative total fluence (first + second light fraction) of 100 J cm⁻² and lowered this to 50 J cm⁻² since this is the range of fluence that was studied previously and to minimize treatment time.

There are some obstacles that must be overcome when using lower fluence rate PDT. At 20 mW cm⁻² treatment time will be 2.5 times longer compared to 50 mW cm⁻² when the total fluence is kept constant. For clinical purposes short treatment times are strived for. As mentioned before, low fluence rate PDT leads to more efficient use of available oxygen. This indicates that less fluence is needed at 20 mW cm⁻², which as a result may keep treatment times constant ¹⁹. Here a question arises as to how much less fluence needs to be delivered to achieve the same effect. This is an issue for both the first and second illumination. Especially dosing of the relatively small first light fraction is critical for maintaining PDT efficacy, as we showed previously ¹¹, necessitating us to employ more accurate dosing than using a predetermined fluence.

Therefore, a novel dosing method for the first light fraction was adopted, making use of PpIX fluorescence measurements. During the photodynamic process, PpIX is destroyed by singlet oxygen, in a process termed photobleaching. In ALA-PDT the rate of PpIX photobleaching is directly related to the amount of singlet oxygen produced and can potentially be used as a predictor of PDT induced response. In normal mouse skin, in which the variations in the amount of PpIX are relatively small, the normalised extent of photobleaching can be used as a predictor of the PDT dose deposited ^{27,31}. In the present study we have used a fixed photobleaching percentage to determine when to stop the first illumination.

Our goal was to investigate if the animals that were illuminated at 20 mW cm⁻² would react in a similar way to fractionated ALA-PDT as the animals that were illuminated at 50 mW cm⁻² with respect to PpIX fluorescence kinetics and damage response. Visual damage to normal hairless mouse skin was used as a measure for efficacy. We hypothesized that 20 mW cm⁻² is as effective as 50 mW cm⁻² in inducing visually assessed skin damage.

MATERIALS AND METHODS

Animals

Thirty-six female albino hairless mice (SKH1 HR) were included in this experiment, divided into 6 groups that received different treatment parameters as described below. Animals were put on a chlorophyll-free diet two weeks prior to treatment to remove autofluorescence from pheophorbide-a. The study was approved by the animal experimental committee of the Erasmus University Medical Centre.

ALA application

Animals were anesthetized with ketamine and valium before the application of 20% 5-aminolevulinic acid (ALA, Medac, Hamburg, Germany), dissolved in 3% carboxymethylcellulose and NaOH in water (pH =4) to the skin using a 7mm round gauze, and occluded with a semi occlusive dressing (Tegaderm[®]). A spot on the left thigh of the mice was chosen as the illumination area. There was a four hour interval between ALA application and the delivery of the first light fraction. Prior to and during illumination animals were again anesthetized using 2-3% Isoflurane in 100% oxygen.

Groups of animals and light treatment parameters

We used six different illumination schemes (n=6 animals in each group). For delivered fluences per group see also table 1. Groups 1-3 served as control groups for comparison with experiments performed previously at 50 mW cm⁻², while groups 4-6 were illuminated at 20 mW cm⁻². Group 1 received 100 J cm⁻² in a single illumination at 50 mW cm⁻². All other groups received two light fractions, separated by a dark interval of two hours. The exact duration of the illuminations in the first light fraction in groups 2-6 was based on the extent of PpIX fluorescence photobleaching measured during PDT in individual

Table 1. Delivered fluences and treatment times per group for both light fractions.

Group	mW cm ⁻²	Delivered fluence ± SD (J cm ⁻²)		Expected fluence (J cm ⁻²)		Total time
		1 st fraction	2 nd fraction	1 st fraction	2 nd fraction	
1	50	100.00		100		33 min. 20 sec.
2	50	4.44 ± 0.45	95.56	5	95	33 min. 20 sec.
3	50	5.20 ± 1.06	44.80	5	45	16 min. 40 sec.
4	20	3.67 ± 0.34	96.33	2	98	83 min. 20 sec.
5	20	3.74 ± 0.42	46.26	4	48	41 min. 40 sec.
6	20 + 50	4.28 ± 0.86	45.72 +50	2	48+50	58 min. 20 sec.

Fluence values represent means ± standard deviation (SD). For the first light fraction less fluence was needed to bleach 52% of PpIX in the 20 mW cm⁻² groups compared to the 50 mW cm⁻² groups. Illumination times for the first illumination were approximately two times longer in the low fluence rate groups.

animals. This individualisation of the first light fraction is described in more detail in the data analysis section below. Each animal received a fluence that was needed to bleach 52% of initial PpIX in the first light fraction, with an additional fluence during the second light fraction to reach various total fluences. Groups 2 and 3 were illuminated at 50 mW cm^{-2} to a total dose of 100 and 50 J cm^{-2} respectively. Groups 4 and 5 were illuminated at 20 mW cm^{-2} to a total dose of 100 and 50 J cm^{-2} respectively. Group 6 received the same treatment scheme as group 5 immediately followed by 50 J cm^{-2} at 50 mW cm^{-2} . This was based on a recent study, investigating the use of low fluence rates for the treatment of sBCC where PpIX photobleaching measurements were used as a method of determining the point during therapy where the fluence rate could be increased without inducing pain²³.

PDT light delivery

The experimental set-up was adapted from that which we used previously³², to maximize the amount of fluorescence light collected from the tissue and facilitate spectral fitting of the data. Figure 1 shows a schematic overview of the setup. During PDT, an Argon ion laser (514 nm) was used as the treatment light source with fluences of either

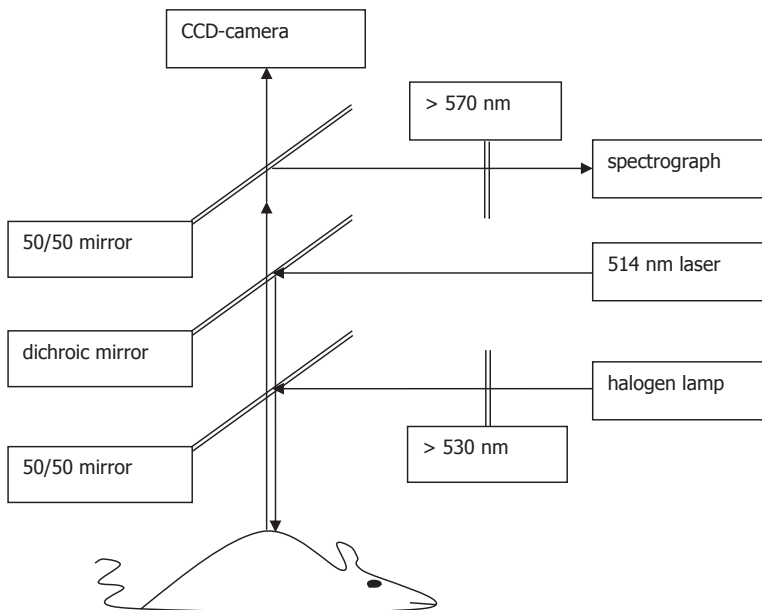


Figure 1. Experimental setup. During PDT, laser light was focused on the mouse skin treatment area and fluorescence emission, induced by the treatment light, was collected using a spectrograph. Reflectance was measured using a halogen lamp light source and the same spectrograph. A CCD camera was used for focusing and relocation purposes.

20 or 50 mW cm⁻². Light was delivered via a 400 micrometer optic fibre and focused to a homogenous 7 mm treatment area on the mouse skin via a dichroic mirror using a micro lens (QLT, Vancouver, BC, Canada) and a single biconvex lens. A charged coupled device (CCD) camera (ORCA-ER, Hamamatsu, Japan) was used for taking fluorescence images, to relocate the area of interrogation and maintain a constant distance between the mouse skin and the head of the spectrograph.

Fluorescence measurements

Fluorescence intensity was used as a measure of the PpIX concentration in the tissue. Fluorescence emission was collected from the illuminated area and focused into a 1 mm optical fibre coupled to a spectrograph (USB4000, Ocean Optics, Duiven, The Netherlands) via a 50/50 beam-splitter. Fluorescence spectra were taken continuously during the first and second illumination with integration times of 1000 ms and 2000 ms for 50 mW cm⁻² and 20 mW cm⁻² respectively, without interrupting PDT light delivery. Scattered excitation light was blocked using a long-pass filter (570 nm, Melles Griot, Zevenaar, The Netherlands), placed in the optical path.

During the first light fraction, spectra were analyzed in real-time as described below to calculate the percentage of photobleaching and the illumination was terminated automatically when the extent of PpIX fluorescence photobleaching had reach 52% of its initial value. This value was based on highest damage scores with this bleaching percentage in previous experiments ¹⁰.

Reflectance spectroscopy

Reflectance spectra were obtained before and immediately after illumination for correcting the fluorescence spectra for changes in tissue optical properties in the fluorescence emission band. Light from a halogen lamp (0.15 mW cm⁻², Stortz, Tutlingen, Germany) was filtered with a long-pass filter (OG 530, Melles Griot, Zevenaar, the Netherlands) to minimize fluorescence excitation of the tissue during reflectance measurements, and delivered via another optical fibre and focussed on the same 7 mm treatment area using a second 50/50 beam splitter. Reflected light was collected using the same system as the fluorescence emission. This enables fluorescence and reflection measurements being acquired using the same source-detection geometry. A white plastic reference card (Vink, Didam, The Netherlands) was used to correct spectra for small changes in light intensity and spectral output.

Data analysis

The reflectance spectra before and after illumination were corrected for changes in light intensity, spectral lamp output and background with the use of the reference card. These

spectra can be used to detect changes in tissue optical properties during illumination and correct the PpIX fluorescence intensity for this with a method first suggested by Wu et al.³³. Fluorescence spectra were analyzed in real-time during the first illumination. Spectra were analyzed as a linear combination of the basis fluorescence spectra of normal mouse skin, autofluorescence and hydroxyaldehyde chlorin photoproduct of PpIX, using a single value decomposition (SVD) algorithm. The output of this analysis yields information on the PpIX fluorescence intensity. The decrease of PpIX fluorescence intensity over time was used to determine the rate and the extent of PpIX photobleaching. The first illumination was terminated when the PpIX fluorescence was decreased by 52% of its original value. The spectra acquired during the first and second illumination were analyzed more extensively after the end of therapy. The fitted PpIX intensity values were corrected for different integration times and laser light intensities for accurate comparison and if necessary corrected for changes in tissue optical properties. These fluorescence intensities were normalized to 100% at the start of the first illumination using a second-order-decay fit²⁷. The fluorescence intensity at the start of the second light fraction was either again normalized to 100%, or presented as a percentage of the fluorescence intensity at the start of the first illumination.

Damage score

Damage scoring was performed daily up to 7 days post PDT by 2 investigators blinded from the treatment schemes (by HdeB and AvdP). We used a visual scoring system, that we have described previously²⁷, with a zero to five-point scale: grade 0 means no damage; 1 = minimal erythema; 2 = moderate erythema; 3 = severe edema or a white blister; 4 = thin crust and 5 = thick crust. The severity and extent of PDT response was measured and scored where different levels of severity were considered within each treatment field. The overall damage score was calculated according to the damage and the relative contribution of each region. Means were calculated per group of mice and plotted against time. The distribution of maximum damage score per group over time was evaluated using daily photographs.

Statistics

In a previous experiment¹¹ we measured a cumulative damage score (see section 2.7) of $17 \pm 4SD$ ($n=19$) for control group 1 and $25 \pm 4SD$ ($n=15$) for control group 2. Since we expect 20 mW cm^{-2} to be as effective in inducing skin damage as 50 mW cm^{-2} , the expected skin damage for group 4 would be equal to group 2. A power analysis with $\alpha = 0.05$ and $\beta = 0.80$ results in 6 animals needed per group. For calculating differences in total damage scores between groups Student-Newman-Keuls multiple comparisons testing was performed, after calculating the total area under the curve (AUC) for subsequent daily damage scores.

RESULTS

Reflectance measurements

Figure 2 shows the average reflectance spectra measured immediately before and after the first light fraction for animals treated in groups 2 and 3 (at 50 mW cm^{-2}). Both spectra show the absorption features that are expected from tissue in this region of the spectrum (560-860 nm). Mice from all other groups showed the same response. There is very little change in the absorption of mouse skin before and after illumination when reflectance is measured in this geometry. Therefore, the PpIX fluorescence intensities shown in this study are not corrected for changes in tissue optical properties.

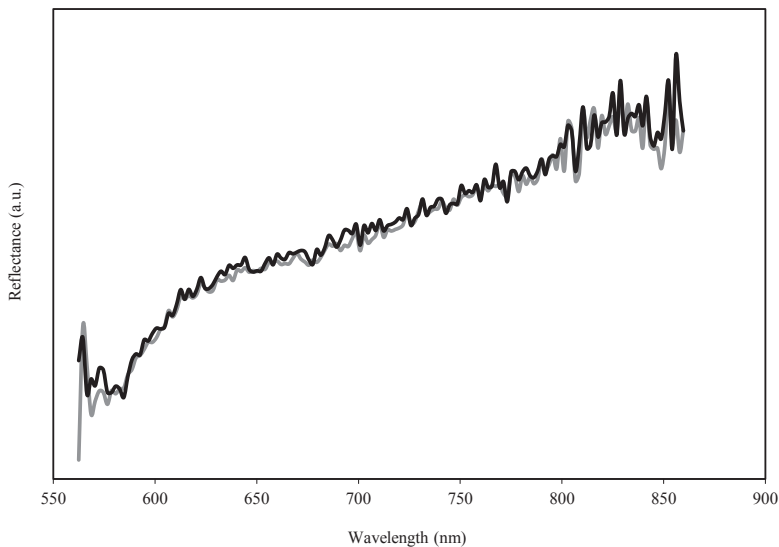


Figure 2. Reflectance intensity before and after PDT in the range of 560-860 nm. Reflectance is shown as arbitrary units. The grey line represents measurement before and the black line after PDT.

Delivered fluence in first light fraction

Delivered fluences in the first and second illumination and treatment times per group are shown in Table 1. Less fluence was needed in the low fluence rate groups and treatment times were longer.

PpIX fluorescence during illumination

Figure 3 shows the mean normalized PpIX fluorescence intensity during a two fold illumination in which a total dose of 100 J cm^{-2} was delivered 4 and 6 hours after ALA application at a fluence rate of 50 mW cm^{-2} (group 2). Data from the first light fraction (panel a) and second light fraction (panel b) are separated by a two hour dark interval.

The first illumination was terminated when the intensity of PpIX fluorescence had bleached by 52%. In the 2-hour dark interval PpIX fluorescence increased to over 80% of the initial value. This increase was subject to large variation, as indicated by large error bars. For both illuminations the first 6 J cm⁻² is shown for clarity: the second light fraction continued on to a total of 100 J cm⁻², after which approximately 3,2% of the initial PpIX intensity at the start of the first light fraction remained.

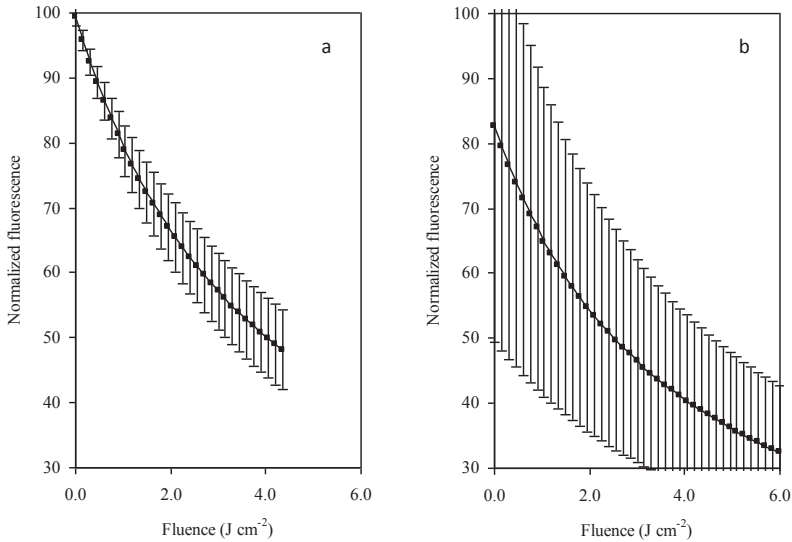


Figure 3. Mean normalized PpIX photobleaching in the first (panel a) and second (panel b) illumination in groups 2 and 3 (50 mW cm⁻²), separated by a dark interval of 2 hours. Error bars indicate one standard deviation.

Figure 4 shows the mean normalized PpIX photobleaching for the first illumination to illustrate differences with respect to fluence rate. The 20 mW cm⁻² groups (4, 5 and 6) showed more efficient photobleaching than the 50 mW cm⁻² groups (2 and 3). At lower fluence rates, less fluence was needed to bleach 52% of available PpIX ($P=0.002$). For clarity only the first 6 J cm⁻² is shown.

Figure 5 shows the mean normalized PpIX photobleaching for the second illumination for different fluence rates. The 20 mW cm⁻² groups again showed a non-significant trend towards faster bleaching than the 50 mW cm⁻² groups. In group 6, (50 J cm⁻² at 20 mW cm⁻² using a fractionated illumination, followed by 50 J cm⁻² at 50 mW cm⁻²), no change in bleaching rate was observed when the fluence rate was increased from 20 to 50 mW cm⁻² (data not shown).

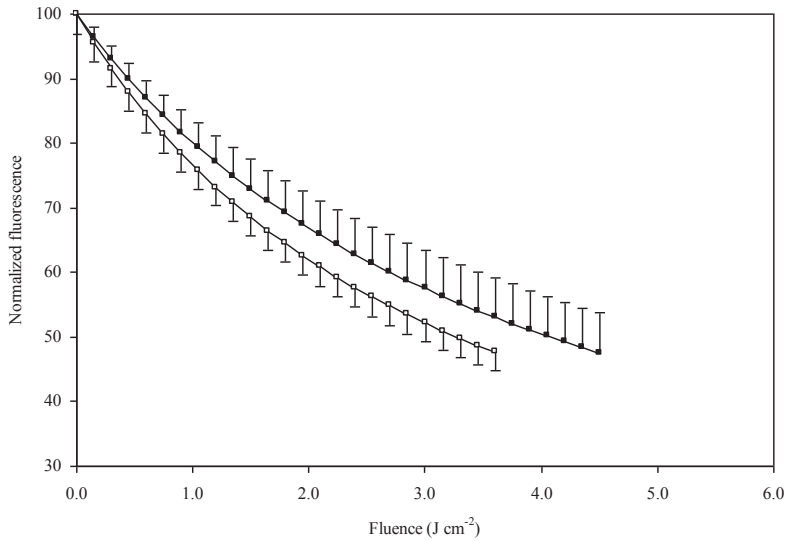


Figure 4. Mean normalized PpIX photobleaching for the first illumination for different fluence rates. The full squares indicate averages at 50 mW cm⁻² (groups 2 and 3). The open squares indicate averages at 20 mW cm⁻² (groups 4, 5 and 6). At 20 mW cm⁻² less fluence was needed to bleach 52% of available PpIX (P=0.002). Error bars indicate one standard deviation.

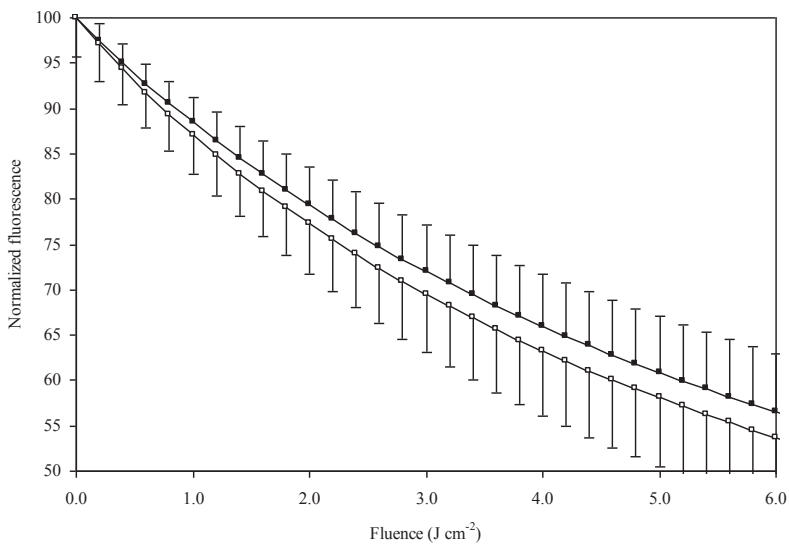


Figure 5. Mean normalized PpIX photobleaching for the second illumination for different fluence rates. The open squares represent averages of the 20 mW cm⁻² groups and full squares averages of the 50 mW cm⁻² groups.

Damage score

One day after PDT severe edema or white blister formation was visible, while damage increased over time up to day 4 when highest damage scores were observed.

Figure 6 shows the mean damage scores for each group of animals, calculated as the area under the curve (AUC) for subsequent daily damage scores.

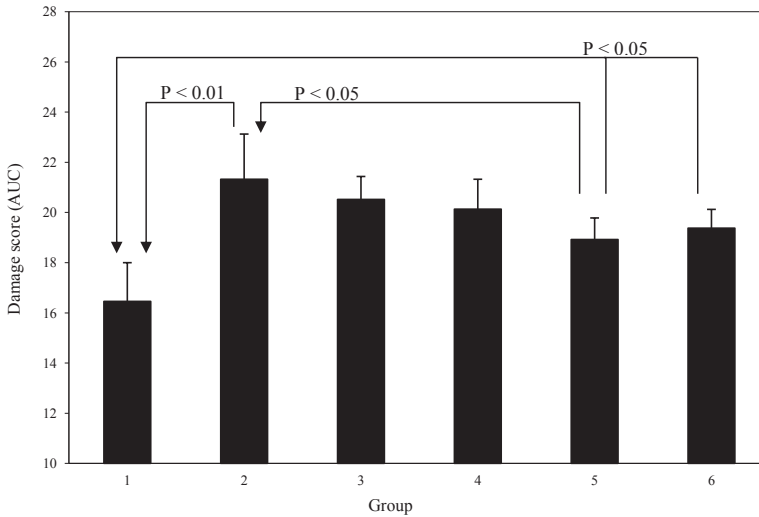


Figure 6. Mean damage score for 7 days after PDT for each group of animals, calculated as the area under the curve for subsequent daily damage scores. Group 1: 100 J cm⁻² at 50 mW cm⁻² (this is the only group with a single illumination, groups 2-6 received a fractionated illumination). Group 2: 100 J cm⁻² at 50 mW cm⁻². Group 3: 50 J cm⁻² at 50 mW cm⁻². Group 4: 100 J cm⁻² at 20 mW cm⁻². Group 5: 50 J cm⁻² at 20 mW cm⁻². Group 6: 50 J cm⁻² at 20 mW cm⁻² followed by 50 J cm⁻² at 50 mW cm⁻². Differences between groups are illustrated by arrows and P-values (Student-Newman-Keuls test).

All fractionated groups had higher total damage scores than the single illumination group and statistical differences are indicated by arrows with their P-values (ANOVA, Student-Newman-Keuls test).

In figure 7 the maximum score reached at any time point within the treated area is shown per group of 6 mice. Only in group 1, where a single illumination to 100 J cm⁻² at 50 mW cm⁻² is delivered, 3 mice had maximum scores of only 3, representing severe edema or a white blister. In all other groups all mice reached maximum scores of either 4 or 5, representing a thin or thick crust respectively.

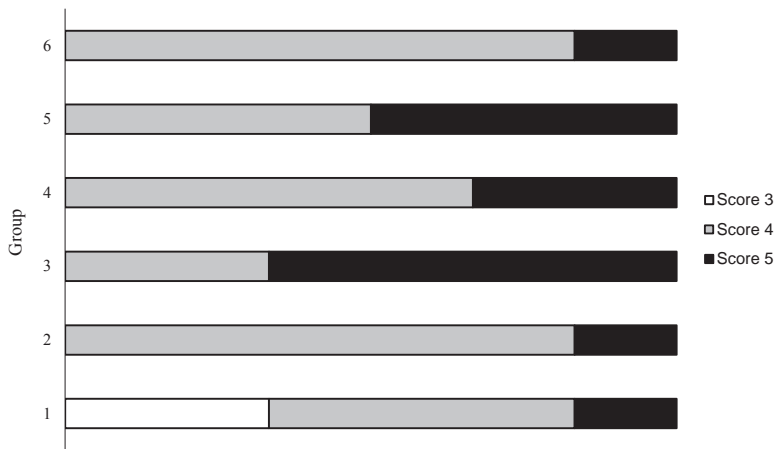


Figure 7. The maximum score reached (regardless of day or size) per group of mice. Only in group 1 (single illumination group) no higher damage score than 3 was observed. Groups 2-6 appear to be similar to each other with minimum scores of either 4 or 5 (5=maximum possible score).

DISCUSSION

This study was designed to investigate the efficacy of low fluence rate ALA-PDT in normal mouse skin. Our primary outcome was visual skin damage and this model has previously successfully been used as an indicator for clinical PDT efficacy. Our results show that low fluence rate ALA-PDT is as effective as high fluence rate PDT in inducing skin damage in normal mouse skin. We used real-time PpIX fluorescence spectroscopy to provide us with more insight into the complex mechanisms and interactions of light, PpIX formation and depletion, oxygen consumption, and photoproduct formation during PDT. Results are in line with the concept that low fluence rate ALA-PDT results in more efficient use of available oxygen. An important and novel modification in the present study was the use of a fixed PpIX photobleaching percentage for the first illumination, instead of using a fixed fluence. In normal mouse skin using the light treatment parameters we have chosen in the present study, the percentage photobleaching is likely to be well correlated to the amount of singlet oxygen formed, and therefore to the PDT dose delivered in a single light fraction. When using a fixed fluence scheme there is risk of delivering too much or too little fluence during the first light fraction due to inter-individual variations in photobleaching rate. Previously we have shown that this results in less PDT damage¹¹. For this reason we used real-time fluorescence measurements to determine PpIX photobleaching as a way of standardizing the effective PDT dose for the first illumination in both high and low fluence rate groups. We stress the importance of monitoring PpIX photobleaching during illumination since it makes comparing the different illumination

schemes more reliable. We chose to deliver as much fluence as needed to bleach 52% of available PpIX for the first illumination, based on previous experiments in normal mouse skin. It is important to note that the normalization step should be made with care. The fluorescence intensity variations in the skin of normal hairless mice are relatively small and on the order of 25% of the average initial PpIX intensity before the first light fraction. To accommodate large variations in the initial PpIX concentration in skin that may be present in other (clinical) lesions would require a more thorough analysis of PDT dose deposition so that the treatment parameters could be changed accordingly. It is probable that the 'optimal' bleaching dose may be different or variable for individual patients and lesions and for different dermatological conditions, which could differ in intrinsic response to PDT, blood supply and thickness of the lesion. It should also be noted that this photobleaching method is only valid for photosensitizers that undergo photobleaching mediated by singlet oxygen alone. For instance, the hematoporphyrin derivative Photofrin[®] can also be bleached by other mechanisms.³⁴

We also measured reflectance spectra before and after PDT. Previously, we always corrected the PpIX fluorescence measurements for possible changes in optical properties of the tissue layer the emitted PpIX fluorescence has to travel through. It is reasonable to assume that the tissue absorption will change, due to PDT-induced changes in blood flow and saturation. Any change in absorption of this tissue layer will bias the PpIX fluorescence intensity measurements at the skin surface. The results from our reflectance measurements, as illustrated in figure 2, indicate that correcting is not necessary when using our measurement method. This does not necessarily mean that the tissue optical properties in the superficial skin layer do not change; it is possible that other measurement methods could reveal such changes. The measurement volume over which the reflectance measurements are taken is much deeper than the superficial treatment effect of PDT. The influence of this dimension mismatch will be the scope of future investigation.

We were able to reproduce the results that we have found previously. The PpIX photobleaching kinetics for the two-fold illumination schemes at 50 mW cm^{-2} , as illustrated in figure 3, show a similar photobleaching rate as previous studies^{10, 11, 27} during the first and second illumination as well as a comparable increase in PpIX fluorescence to around 80% of the initial value during the dark interval and subsequent bleaching to under 5% at the end of the second illumination. These groups of animals (groups 2 and 3) and their results therefore serve as controls for the 20 mW cm^{-2} groups.

In accordance to several previous studies, we found that illuminating at lower fluence rates (20 mW cm^{-2}) results in more efficient PDT than at higher fluence rates (50 mW cm^{-2}),

as is illustrated in figure 4 and table 1. Using higher fluence rates causes depletion of available oxygen during PDT, interrupting the continuous PpIX photobleaching process. The treatment time for the first illumination is approximately two times longer in the 20 mW cm⁻² groups than in the 50 mW cm⁻² groups, instead of $50/20 = 2.5$ times as would be the case if the photobleaching rate were the same. However, the amount of fluence needed (and as a result also treatment time) does not decrease proportionally with decreasing fluence rate. The consequence of this is that treatment times remain longer at lower fluence rates if the same amount of total photobleaching is desired. Our choice of low fluence rate in the present study was based on our wish to minimize pain in clinical PDT. Since it may be possible to further reduce the pain associated with the illumination by further reducing the fluence rate, it is interesting to consider the relationship between fluence rate and the fluence needed to achieve a fixed photobleaching percentage. In previous studies, we and others^{26,27} have shown that the efficiency of PpIX photobleaching was even higher when the fluence rate is reduced to 5 mW cm⁻² and lower for fluence rates above 50 mW cm⁻². Finlay et al²⁶ have shown that the efficiency of photobleaching increases even further for lower fluence rates in rat skin. Theoretically there will be a maximum efficiency of photobleaching below 1 mW cm⁻², where PDT efficiency is optimal. The practical value of delivering PDT at these very low fluence rates remains unclear, since treatment times will likely be very long at very low fluence rates.

For the second illumination we also observed a trend to faster photobleaching in the 20 mW cm⁻² groups compared to the 50 mW cm⁻² groups, as is shown in figure 6. This indicates that also for the second illumination, which is longer than the first, low fluence rate photobleaching occurs somewhat more efficiently. In the first illumination the difference is much more obvious however. This may be explained by vasodilatation after the first illumination, increasing oxygen availability during the second illumination.

When comparing damage scores between groups, figures 6 and 7 illustrate different methods of damage scoring. Groups 1-3 are illumination schemes that we have used in previous experiments and skin damage scores are consistent to the results from these previous experiments, while groups 4-6 were the low fluence rate groups. As is shown in figure 6, the single illumination group 1 has the lowest total damage score. All the other groups have higher scores with the highest in group 2 (100 J cm⁻² at 50 mW cm⁻²). Our special interest was whether the low fluence rate groups (4, 5 and 6) would score significantly better than the single group and not significantly worse than the control group 2. All low fluence rate groups have a significant higher total damage score compared to the single illumination group. Groups 4 and 6 (100 J cm⁻² total) are not statistically different from group 2, but only group 5 (50 J cm⁻² in total) is borderline statistically worse than

group 2. Total differences between all fractionated groups are small however. A small, but statistical difference may not necessarily represent a clinically relevant difference.

We used damage to normal mouse skin as a substitute for clinical effect, because this model previously proved to be a good translational model^{10,11,13,27}. In the present study we extended the previously used model by measuring maximum damage, which is likely to be also indicative of PDT effect. It is important however to realize that in a clinical setting, PDT effect is based on destruction of dysplastic tissue instead of normal tissue and in human skin instead of mouse skin.

From figure 7 it is clear that in the single illumination (group 1) maximum scores were more shifted towards lower scores than in the fractionated groups 2-6, while there is no apparent difference in score between these fractionated groups. A difference in the results in this scoring method and the one illustrated in figure 6 is that group 5 (50 J cm^{-2}) has three animals with highest maximum damage scores and doesn't appear to be worse than any other group. Combining the different damage scoring methods, there appears to be no difference between high and low fluence rate groups in terms of inducing visual skin damage.

Taking the results from this study into account when designing a clinical trial comparing low and high fluence rate light fractionated PDT, there are additional considerations. As is clear from our results there is no proportional relationship between fluence and fluence rate for a fixed bleaching percentage. This means that treatment times will remain longer at lower fluence rates when the same amount of PpIX bleaching is used as a treatment metric.

The clinical implications of this are important because treatment times for the second illumination could be substantially longer using lower fluence rates. The duration of the first illumination is in the order of a few minutes so differences will be small and clinically irrelevant. In group 2 (100 J cm^{-2} at 50 mW cm^{-2}) the second illumination takes 31 minutes and at the end on average 3,2% (SD 1,5) of initial PpIX is left. For group 5 (50 J cm^{-2} at 20 mW cm^{-2}) the second illumination takes 40 minutes, leaving 7,7% (SD 2,7) of PpIX. In group 6 (50 J cm^{-2} at 50 mW cm^{-2} followed by 50 J cm^{-2} at 50 mW cm^{-2}) the second illumination takes 56 minutes and 2,9% (SD 1,0) of PpIX is left. Interestingly, the bleaching rate does not change at the point when fluence rate is increased. Probably the amount of oxygen is no longer the limiting factor for PpIX photobleaching but the concentration of PpIX is. It is unclear however what the biological advantage is of illuminating tissues with very little PpIX content. An interesting extension of the present study would be to

use a fixed remaining PpIX percentage to stop the second illumination, but it will be difficult to determine this percentage.

It is also important to recognize that mouse skin is considerably thinner compared to human skin. Theoretically, deeper layers of skin may need higher total fluences since fluence rate decreases exponentially in tissue with increasing depth. Especially in the deeper bases of sBCC the fluence at depth may be an important consideration. Also the variation in vascularisation of tumor tissue results in variable light absorption and oxygen supply. Therefore it theoretically makes sense to have a clinical illumination scheme based on the illumination scheme of group 6 (50 J cm^{-2} at 20 mW cm^{-2} followed by 50 J cm^{-2} at 50 mW cm^{-2}). Effectiveness is expected to be maintained, pain is expected to be minimal and treatment times remain relatively short.

In conclusion the present study shows that low fluence rate, light fractionated ALA-PDT appears to be as effective in inducing visual skin damage in mouse skin, while PpIX photobleaching occurs more efficiently. This in part limits the duration of therapy, although lower fluence rate PDT does result in longer illuminations when the same amount of photobleaching is desired. There is need for further investigations that should include a clinical trial investigating pain and clinical efficacy using low and high fluence rate fractionated PDT, while performing PpIX fluorescence measurements. Maintaining high efficacy of therapy should be the most important consideration, while pain and treatment time must be carefully weighed against each other. Thickness of lesions must be taken into account when interpreting the results from the present study because of differences in thickness between mouse and human skin.

REFERENCES

1. Marks R. An overview of skin cancers. Incidence and causation. *Cancer*. 1995;75(2 Suppl):607-12.
2. Salasche SJ. Epidemiology of actinic keratoses and squamous cell carcinoma. *J Am Acad Dermatol*. 2000;42(1 Pt 2):4-7.
3. Diepgen TL, Mahler V. The epidemiology of skin cancer. *Br J Dermatol*. 2002;146(Suppl 61):1-6.
4. de Vries E, van de Poll-Franse LV, Louwman WJ, de Gruijl FR, Coebergh JW. Predictions of skin cancer incidence in the Netherlands up to 2015. *Br J Dermatol*. 2005;152(3):481-8.
5. Trakatelli M, Ulrich C, del Marmol V, Euvrard S, Stockfleth E, Abeni D. Epidemiology of nonmelanoma skin cancer (NMSC) in Europe: accurate and comparable data are needed for effective public health monitoring and interventions. *Br J Dermatol*. 2007;156(Suppl 3):1-7.
6. Morton CA, McKenna KE, Rhodes LE. Guidelines for topical photodynamic therapy: update. *Br J Dermatol*. 2008;159(6):1245-66. Epub 2008 Oct 13.
7. Braathen LR, Szeimies RM, Basset-Seguín N, Bissonnette R, Foley P, Pariser D, et al. Guidelines on the use of photodynamic therapy for nonmelanoma skin cancer: an international consensus. International Society for Photodynamic Therapy in Dermatology, 2005. *J Am Acad Dermatol*. 2007;56(1):125-43.
8. Wilson BC, Patterson MS. The physics, biophysics and technology of photodynamic therapy. *Phys Med Biol*. 2008;53(9):R61-109. Epub 2008 Apr 9.
9. Gerritsen MJ, Smits T, Kleinpenning MM, van de Kerkhof PC, van Erp PE. Pretreatment to Enhance Protoporphyrin IX Accumulation in Photodynamic Therapy. *Dermatology*. 2008;11:11.
10. de Bruijn HS, van der Ploeg-van den Heuvel A, Sterenborg HJ, Robinson DJ. Fractionated illumination after topical application of 5-aminolevulinic acid on normal skin of hairless mice: the influence of the dark interval. *J Photochem Photobiol B*. 2006;85(3):184-90. Epub 2006 Sep 1.
11. Robinson DJ, de Bruijn HS, Star WM, Sterenborg HJ. Dose and timing of the first light fraction in two-fold illumination schemes for topical ALA-mediated photodynamic therapy of hairless mouse skin. *Photochem Photobiol*. 2003;77(3):319-23.
12. van der Veen N, van Leengoed HL, Star WM. In vivo fluorescence kinetics and photodynamic therapy using 5-aminolaevulinic acid-induced porphyrin: increased damage after multiple irradiations. *Br J Cancer*. 1994;70(5):867-72.
13. de Haas ER, Kruijt B, Sterenborg HJ, Martino Neumann HA, Robinson DJ. Fractionated illumination significantly improves the response of superficial basal cell carcinoma to aminolevulinic acid photodynamic therapy. *J Invest Dermatol*. 2006;126(12):2679-86. Epub 006 Jul 13.
14. Star WM, van't Veen AJ, Robinson DJ, Munte K, de Haas ER, Sterenborg HJ. Topical 5-aminolevulinic acid mediated photodynamic therapy of superficial basal cell carcinoma using two light fractions with a two-hour interval: long-term follow-up. *Acta Derm Venereol*. 2006;86(5):412-7.
15. Vinciullo C, Elliott T, Francis D, Gebauer K, Spelman L, Nguyen R, et al. Photodynamic therapy with topical methyl aminolaevulinate for 'difficult-to-treat' basal cell carcinoma. *Br J Dermatol*. 2005;152(4):765-72.

16. Horn M, Wolf P, Wulf HC, Warloe T, Fritsch C, Rhodes LE, et al. Topical methyl aminolaevulinate photodynamic therapy in patients with basal cell carcinoma prone to complications and poor cosmetic outcome with conventional treatment. *Br J Dermatol*. 2003;149(6):1242-9.
17. Grapengiesser S, Ericson M, Gudmundsson F, Larko O, Rosen A, Wennberg AM. Pain caused by photodynamic therapy of skin cancer. *Clin Exp Dermatol*. 2002;27(6):493-7.
18. Sandberg C, Stenquist B, Rosdahl I, Ros AM, Synnerstad I, Karlsson M, et al. Important factors for pain during photodynamic therapy for actinic keratosis. *Acta Derm Venereol*. 2006;86(5):404-8.
19. Ericson MB, Sandberg C, Stenquist B, Gudmundson F, Karlsson M, Ros AM, et al. Photodynamic therapy of actinic keratosis at varying fluence rates: assessment of photobleaching, pain and primary clinical outcome. *Br J Dermatol*. 2004;151(6):1204-12.
20. Wiegell SR, Skiveren J, Philipsen PA, Wulf HC. Pain during photodynamic therapy is associated with protoporphyrin IX fluorescence and fluence rate. *Br J Dermatol*. 2008;158(4):727-33. Epub 2008 Feb 16.
21. Moloney FJ, Collins P. Randomized, double-blind, prospective study to compare topical 5-aminolaevulinic acid methylester with topical 5-aminolaevulinic acid photodynamic therapy for extensive scalp actinic keratosis. *Br J Dermatol*. 2007;157(1):87-91. Epub 2007 May 14.
22. Clark C, Bryden A, Dawe R, Moseley H, Ferguson J, Ibbotson SH. Topical 5-aminolaevulinic acid photodynamic therapy for cutaneous lesions: outcome and comparison of light sources. *Photodermatol Photoimmunol Photomed*. 2003;19(3):134-41.
23. Cottrell WJ, Paquette AD, Keymel KR, Foster TH, Oseroff AR. Irradiance-dependent photobleaching and pain in delta-aminolevulinic acid-photodynamic therapy of superficial basal cell carcinomas. *Clin Cancer Res*. 2008;14(14):4475-83.
24. Wiegell SR, Haedersdal M, Philipsen PA, Eriksen P, Enk CD, Wulf HC. Continuous activation of PpIX by daylight is as effective as and less painful than conventional photodynamic therapy for actinic keratoses; a randomized, controlled, single-blinded study. *Br J Dermatol*. 2008;158(4):740-6. Epub 2008 Feb 19.
25. Langmack K, Mehta R, Twyman P, Norris P. Topical photodynamic therapy at low fluence rates— theory and practice. *J Photochem Photobiol B*. 2001;60(1):37-43.
26. Finlay JC, Conover DL, Hull EL, Foster TH. Porphyrin bleaching and PDT-induced spectral changes are irradiance dependent in ALA-sensitized normal rat skin in vivo. *Photochem Photobiol*. 2001;73(1):54-63.
27. Robinson DJ, de Bruijn HS, van der Veen N, Stringer MR, Brown SB, Star WM. Fluorescence photobleaching of ALA-induced protoporphyrin IX during photodynamic therapy of normal hairless mouse skin: the effect of light dose and irradiance and the resulting biological effect. *Photochem Photobiol*. 1998;67(1):140-9.
28. Foster TH, Murant RS, Bryant RG, Knox RS, Gibson SL, Hilf R. Oxygen consumption and diffusion effects in photodynamic therapy. *Radiat Res*. 1991;126(3):296-303.
29. Sitnik TM, Henderson BW. The effect of fluence rate on tumor and normal tissue responses to photodynamic therapy. *Photochem Photobiol*. 1998;67(4):462-6.

30. Henderson BW, Busch TM, Vaughan LA, Frawley NP, Babich D, Sosa TA, et al. Photofrin photodynamic therapy can significantly deplete or preserve oxygenation in human basal cell carcinomas during treatment, depending on fluence rate. *Cancer Res.* 2000;60(3):525-9.
31. Robinson DJ, de Bruijn HS, de Wolf WJ, Sterenberg HJ, Star WM. Topical 5-aminolevulinic acid-photodynamic therapy of hairless mouse skin using two-fold illumination schemes: PpIX fluorescence kinetics, photobleaching and biological effect. *Photochem Photobiol.* 2000;72(6):794-802.
32. de Bruijn HS, de Haas ER, Hebeda KM, van der Ploeg-van den Heuvel A, Sterenberg HJ, Neumann HA, et al. Light fractionation does not enhance the efficacy of methyl 5-aminolevulinate mediated photodynamic therapy in normal mouse skin. *Photochem Photobiol Sci.* 2007;6(12):1325-31. Epub 2007 Aug 28.
33. Wu J, Feld M, Rava R. Analytical model for extracting intrinsic fluorescence in turbid media. *Applies Optics.* 1993;32(19):3585-95.
34. Finlay JC, Mitra S, Patterson MS, Foster TH. Photobleaching kinetics of Photofrin in vivo and in multicell tumour spheroids indicate two simultaneous bleaching mechanisms. *Phys Med Biol.* 2004;49(21):4837-60.

4

Topical hexylaminolevulinate and aminolevulinic acid photodynamic therapy: complete arteriole vasoconstriction occurs frequently and depends on protoporphyrin IX concentration in vessel wall

Tom Middelburg

Riëtte de Bruijn

Lisanne Tettero

Angelique van der Ploeg-van den Heuvel

Martino Neumann

Ellen de Haas

Dominic Robinson

J Photochem Photobiol B. 2013;126:26-32

ABSTRACT

Vascular responses to photodynamic therapy (PDT) may influence the availability of oxygen during PDT and the extent of tumor destruction after PDT. However, for topical PDT vascular effects are largely unknown. Arteriole and venule diameters were measured before and after hexylaminolevulinatate (HAL) and aminolevulinic acid (ALA) PDT and related to the protoporphyrin IX (PpIX) concentration in the vessel wall. A mouse skin fold chamber model and an intravital confocal microscope allowed direct imaging of the subcutaneous vessels underlying the treated area. In both HAL and ALA groups over 60% of arterioles constricted completely, while venules generally did not respond, except for two larger veins that constricted partially. Arteriole vasoconstriction strongly correlated with PpIX fluorescence intensity in the arteriole wall. Total PpIX fluorescence intensity was significantly higher for HAL than ALA for the whole area that was imaged but not for the arteriole walls. In conclusion, complete arteriole vasoconstriction occurs frequently in both HAL and ALA based topical PDT, especially when relatively high PpIX concentrations in arteriole walls are reached. Vasoconstriction will likely influence PDT effect and should be considered in studies on topical HAL and ALA-PDT. Also, our results may redefine the vasculature as a potential secondary target for topical PDT.

INTRODUCTION

In photodynamic therapy (PDT) sufficient amounts of photosensitizer, oxygen and light in tumor tissue lead to the generation of reactive oxygen species, notably singlet oxygen, and subsequent destruction of the tumor¹⁻³. The effectiveness of tumor destruction also depends on biological factors such as immunological responses and vascular effects^{4,5}. The availability of oxygen during PDT as well as the oxygen supply to surviving tumor cells after PDT may be influenced by vascular effects⁶. Previous in-vivo studies have shown that reduced oxygenation during PDT can lead to less efficient and less effective PDT⁷⁻¹⁰. Vascular effects therefore may be very relevant to the efficiency of the PDT process. For this reason research has focused in the late 80's and early 90's on vascular effects of PDT. For systemic hematoporphyrin and aminolevulinic acid (ALA)-PDT vascular effects such as arteriole vasoconstriction, endothelial damage and reduced blood flow have been well documented¹¹⁻¹⁸.

For topical PDT with porphyrin precursors however, there is a limited amount of publications on vascular effects. Since topical PDT is used frequently (particularly in dermatology), it is important to also investigate and understand the vascular mechanisms. In dermatology, ALA is used for treating non melanoma skin cancers, while HAL is currently registered for photodiagnosis of bladder cancer, but might also be used for therapeutic applications in the future. For topical ALA-PDT, some studies have focused on trans epidermal spectroscopic measurements and found reduced blood flow^{19,20} and a decrease of intravasal fluorescein fluorescence, indicating vasoconstriction²¹. In other studies, blood vessels were measured microscopically in a similar animal model as we have used for ALA in which vasoconstriction²² and loss of functional vessels²³ were found. Only two studies describe the vascular effects of topical hexyaminolevulinate (HAL)-PDT. In both, a spectroscopic approach was used; in one to measure fluorescein fluorescence decrease in mouse skin vessels²⁴ and in the other to measure blood concentration in human skin, which increased after PDT²⁵.

An important underlying question is to try and understand why and in particular over what timescale vessels respond during and following PDT. It is logical to assume that constriction of blood vessels is related to the ability of the vessel wall to accumulate PpIX. In this respect it is important to consider the differences between the photosensitizer precursors that we investigated. Both HAL and ALA lead to the intracellular formation and accumulation of the photosensitizer protoporphyrin IX (PpIX). Because ALA is a hydrophilic molecule it does not penetrate well through the lipophilic upper layers of skin, especially the stratum corneum²⁶. To overcome this, more lipophilic esters of ALA became commercially available, claiming deeper penetration and possibly higher

affinity for tumor cells. These esters, of which HAL is one example, enter cells by different uptake mechanisms than ALA. The uptake of ALA depends largely on active transport into cells through BETA transporters^{27,28}, whereas ALA esters have been described to depend on PEPT1 or PEPT2 transporters²⁹. It was also concluded that for neither ALA or ALA esters, diffusion is responsible for cellular uptake, a conclusion based on oil-water distribution coefficients^{30,31}. For the ability of the vessel wall to accumulate PpIX, these uptake mechanisms may be relevant with respect to the vascular response after HAL or ALA-PDT. Vascular endothelial cells have been demonstrated to accumulate PpIX after both HAL and ALA application *in vitro*³² and for ALA it was demonstrated that vessel walls accumulate PpIX *in vivo*³³.

In summary the vascular effects of topical PDT, in particular of HAL-PDT are not well known, as well as the relation between the ability of the vessel wall to accumulate PpIX and the vascular response. Therefore we investigated the *in vivo* PpIX distribution in tissue including the vessel walls after topical HAL application in mice, the effect of PDT on the venule and arteriole diameters and compared this with ALA. We used a skin fold chamber model and intravital confocal microscopy. This geometry allowed us to interrogate the vasculature directly without being hampered by overlying epidermis. This is different from previous studies that imaged through the epidermis as described above. Primary outcomes were vascular response, measured as change in vessel diameter and PpIX fluorescence intensity.

MATERIALS AND METHODS

Experimental setup

A dorsal skin fold mouse model was prepared as described in another study²². The setup is schematically illustrated in Figure 1. On one side of the fold, the skin was completely removed up to the cutaneous muscular layer of the opposed skin. The fold was then fixed with light metal bolts and sutures and closed with a glass cover slide. The intact side was used to apply ALA or HAL to the skin and for PDT light delivery. The non-intact side was used to take transmission and fluorescence images using a confocal microscope before and after PDT. Window chamber preparation, drug and light delivery, and image recording were all performed under general anaesthesia.

Treatment groups and drug delivery

Ten female albino hairless mice (SKH1 HR, Charles River, Someren, The Netherlands) were included in this experiment, divided in two groups of five mice. The mice were put on a chlorophyll-free diet two weeks prior to treatment to remove autofluorescence

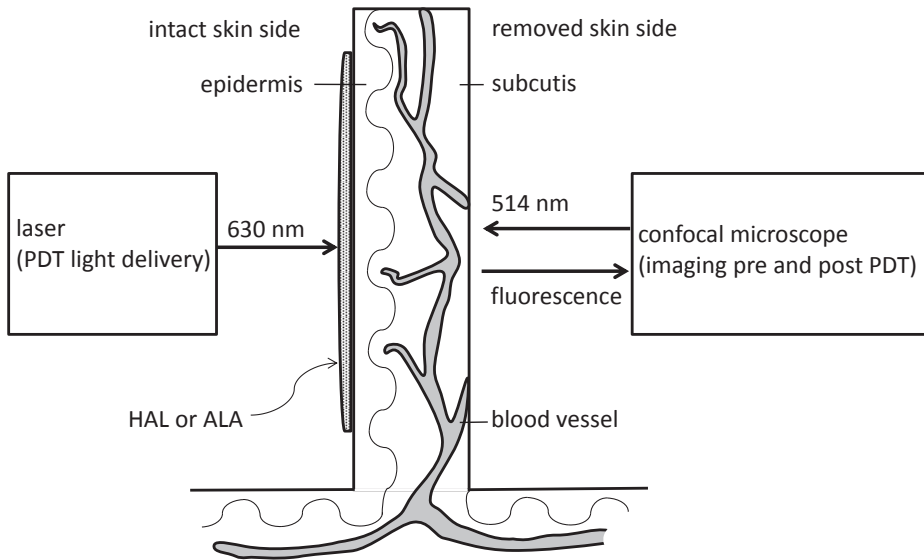


Figure 1. Experimental setup. Schematic representation of the mouse skin fold model. Removing the skin on one side allowed detailed confocal imaging of the subcutaneous blood vessels and PpIX fluorescence before and after topical HAL or ALA based PDT.

from pheophorbide-a. The study was approved by the animal experimental committee of the Erasmus University Medical Center.

In one group of five mice 20% ALA (Fagron, Oud Beijerland, The Netherlands) in carboxymethylcellulose in water and NaOH (pH=4) and in the other group of five mice 5% HAL ointment (Photocure, Oslo, Norway) was applied to the skin. ALA and HAL were occluded in the dark for 4 hours before light delivery. In 3 mice from the ALA group and 5 mice from the HAL group, 0.2 mg fluorescein (FITC-BSA, Sigma) was injected intravenously directly after illuminations, to visualize delayed vascular response in a different way. In the remaining two ALA animals the fluorescein injection failed so for these animals no data for the fluorescein time-point were obtained.

Confocal imaging

Prior to ALA or HAL application autofluorescence spectra were obtained using an intravital confocal microscope (Zeiss LSM510META, Carl Zeiss B.V., Sliedrecht, The Netherlands). Four hours after ALA or HAL application PpIX was excited using 514 nm laser light and fluorescence was recorded in lambda mode (695-681 nm) using a 10x objective and an optical slice thickness of 40 μm . Immediately hereafter transmission images of the same location were taken. For each mouse images were obtained from two or three

different representative locations at 100x magnification for all images, plus an overview image at 20x that was not included in later analysis. After PDT light delivery transmission images were taken again from the same location. Twenty minutes later transmission and fluorescein fluorescence images were recorded in some mice using 488 nm excitation light and a 505-515 nm band pass filter for detection.

PDT light delivery

All mice received a single dose of 100 J cm^{-2} at 65 mW cm^{-2} , using a 630 nm laser (Visuals 630, Carls Zeiss B.V., Sliedrecht, The Netherlands). Light was focused on a 7 mm diameter area using a microlens. A fluence rate of 65 mW cm^{-2} was chosen to allow for the comparison of PDT performed previously at 50 mW cm^{-2} using 514 nm illumination. The rationale for this choice is discussed in a previous study from our group ²².

Image analysis

The PpIX fluorescence intensity was corrected for autofluorescence as described previously ³⁴.

A sequence of images taken from the same location was imported and analysed using ImageJ software (ImageJ 1.46, National Institute of Health, USA). Each sequence consisted of a transmission image before PDT, a PpIX fluorescence image, a transmission image directly after PDT and transmission and fluorescein fluorescence images twenty minutes after PDT.

Two types of analysis were made: one to measure the vascular response to PDT and another to measure the distribution of PpIX fluorescence intensity in the tissue. The investigator was blinded for the treatment groups.

To measure the vascular response to PDT, venule and arteriole diameters were measured in the transmission images before and after PDT, and in the transmission image twenty minutes after PDT. Vasoconstriction was defined as: $(1 - \text{vessel diameter after PDT} / \text{vessel diameter before PDT}) * 100\%$.

To measure the PpIX distribution, regions of interest (ROIs) were drawn in the transmission image before PDT in different tissue types: adipose tissue, venule wall, venule centre and arteriole wall. For all tissue types ROIs from different locations were drawn. The PpIX fluorescence intensity of the ROIs was subsequently measured in the corresponding fluorescence image.

Data were exported to Excel, Office Professional Plus 2010 and to IBM SPSS statistics 21 and subsequently analysed.

Statistics

Vasoconstriction was descriptively analysed by means of medians and interquartile ranges. Each vessel measurement was considered as an independent variable, resulting in $n=14$ measurements in the HAL group and $n=15$ measurement in the ALA group. Non-parametric tests were used to compare differences within and between groups. PpIX distribution in tissue was analysed by means of descriptive statistics presented as means and standard deviations and a two-sided student's *t*-test to test for statistical significance. A two-sided *P*-value of 0.05 was considered statistically significant.

RESULTS

Vascular response to PDT

The arteriole vascular response was similar for HAL and ALA. Complete vasoconstriction -i.e. no arteriole could be seen in the transmission image immediately after PDT- occurred in 64% (9 out of 14) of arterioles for HAL and in 60% (9 out of 15) for ALA. Other arterioles constricted partially, except for two in the ALA group that dilated instead. Overall, the arteriole diameter after PDT was significantly lower than before PDT in both HAL and ALA groups ($P=0.001$ and $P=0.003$ respectively, Wilcoxon signed rank test).

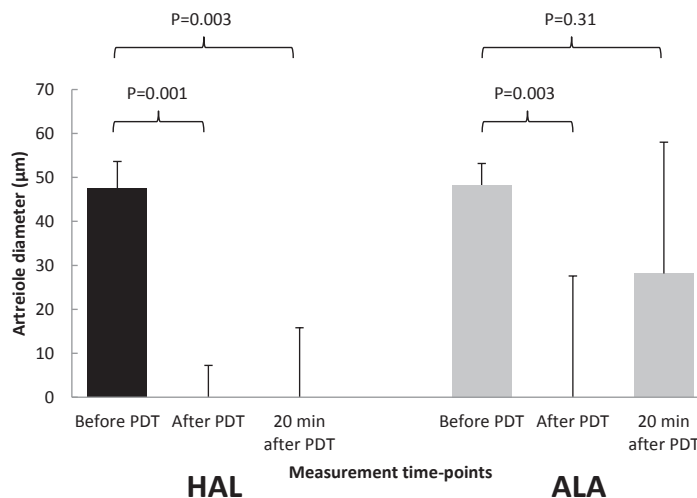


Figure 2. Vascular response of arterioles at different time-points. For both HAL (black) and ALA (grey) median arteriole diameter decreased to zero immediately after PDT, indicating complete vasoconstriction. Twenty minutes after PDT arterioles remained partly constricted. Error bars indicate the 75th percentile.

Between the HAL and ALA groups there was no significant difference in vasoconstriction after PDT ($P=0.91$, Mann-Whitney U test). In the subset of arterioles that received fluorescein and were imaged twenty minutes after PDT ($n=11$ for HAL and $n=6$ for ALA), arterioles frequently remained constricted, and this was still significantly different from before PDT in the HAL group. The fluorescein injection and subsequent proper imaging failed in a number of cases, which explains the lower numbers of arterioles included in this analysis. Figure 2 illustrates the vascular response of the arterioles at different time-points.

In contrast, the venules that were imaged at 100x magnification did not show constriction after PDT. Only in the HAL group two larger ($> 150 \mu\text{m}$) feeder veins imaged at 20x magnification showed partial constriction at several sites along the vein.

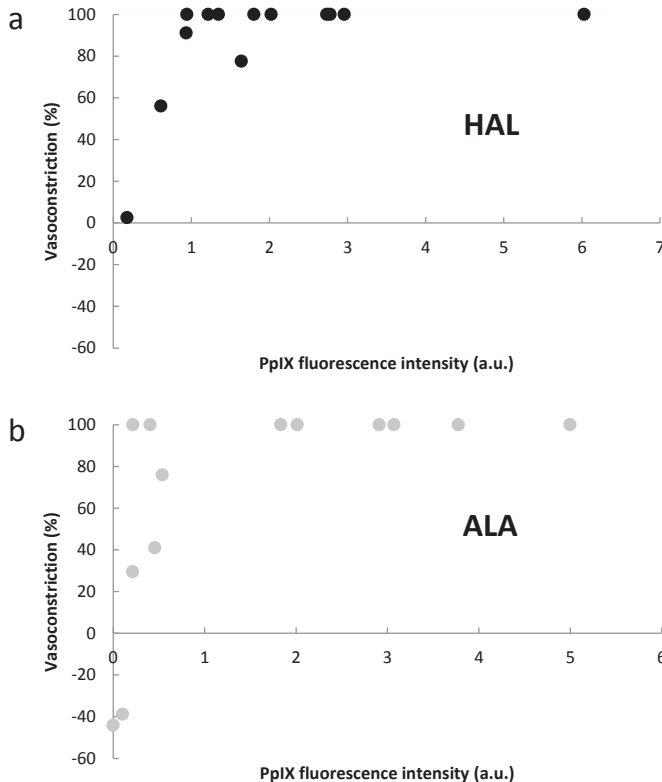


Figure 3. Relationship between PpIX fluorescence intensity and vasoconstriction. The relation between PpIX fluorescence intensity of individual arteriole walls and the arteriole vasoconstriction immediately after PDT for HAL (a) and ALA (b). Relatively high PpIX fluorescence intensities resulted in 100% vasoconstriction, while relatively low PpIX fluorescence intensities resulted in various degrees of vasoconstriction. This relation is similar for HAL and ALA.

Relation between vascular response and PpIX fluorescence intensity

The amount of arteriole vasoconstriction immediately after PDT strongly correlated with the PpIX fluorescence intensity in the arteriole wall for both HAL (Figure 3a) and ALA (Figure 3b). Spearman's correlation coefficient was 0.75 ($P=0.002$) for HAL and 0.73 for ALA ($P=0.002$). In the arterioles that had relatively high PpIX fluorescence intensity in the vessel wall, vasoconstriction frequently was 100%. Lower PpIX fluorescence intensities correlated with various degrees of vasoconstriction. The two arterioles that dilated -indicated by the negative vasoconstriction values in figure 3b- were from one particular ALA mouse and in this mouse there was a very low PpIX fluorescence intensity in all ROIs (adipose tissue, vessel walls and vessel centres).

Spatial distribution of PpIX

PpIX fluorescence intensity for all regions of interest combined was higher for HAL than ALA ($P=0.00083$, two-sided student's t-test). For the individual ROIs this difference was significant for the venule wall ($P=0.0252$) and venule centre ($P=0.0029$), but not for the arteriole wall ($P=0.259$) or adipose tissue ($P=0.153$). The PpIX fluorescence intensity for HAL and ALA in the different regions of interest is illustrated in figure 4.

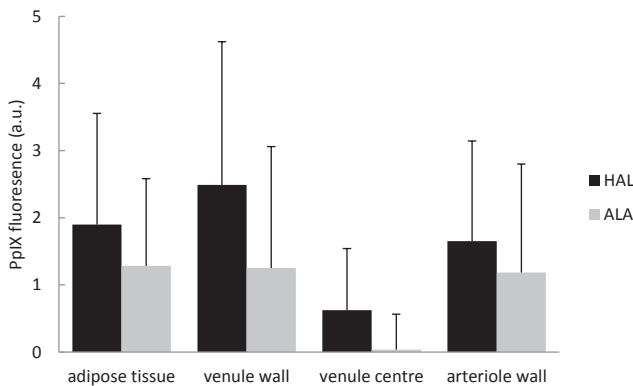


Figure 4. Mean PpIX fluorescence intensity in various tissue regions: HAL versus ALA. In the HAL group overall mean PpIX fluorescence intensity was higher than in the ALA group ($P=0.00083$). For the individual regions, PpIX fluorescence intensity was significantly higher in the venule wall ($P=0.0252$) and venule centre ($P=0.0029$) but the difference was not significant for the arteriole wall ($P=0.259$) and adipose tissue ($P=0.153$). Error bars indicate one standard deviation.

Confocal image example

Figure 5 shows a representative example of the images obtained using the confocal microscope. Figure 5a is a transmission image before PDT; figure 5b is the transmission image taken immediately after PDT; figure 5c is the transmission and 5d the fluorescein fluorescence image 20 minutes after PDT. These images illustrate that the arteriole (black

arrow in figure 5a) is completely constricted immediately and twenty minutes after PDT. The contour of the arteriole can still be seen in the fluorescein image indicating the presence of FITC-labelled albumin. This type of response was seen in most measurements.

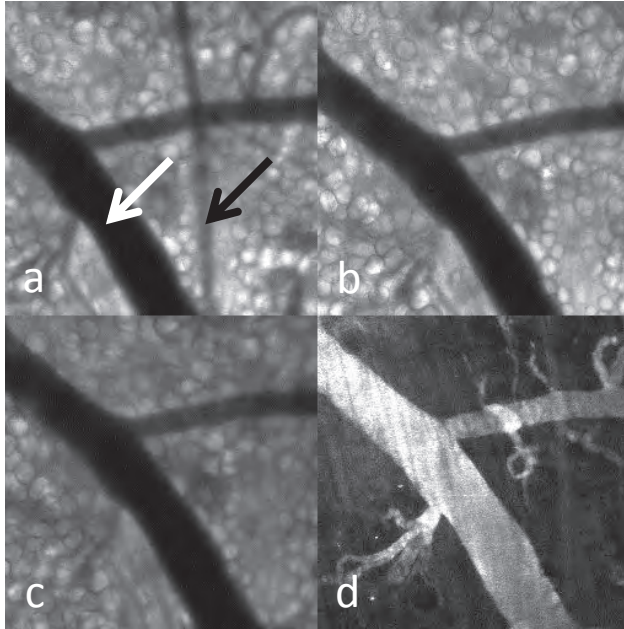


Figure 5. Typical confocal images taken at different time points illustrating arteriole response. The transmission images before (a) and immediately after (b) PDT show complete vasoconstriction of the arteriole (black arrow) while the venule (white arrow) does not show any response. Twenty minutes after PDT (c) the arteriole is still constricted but vaguely visible in the fluorescein fluorescence image (d). Each image measures 0.9*0.9 mm, magnification 100x.

DISCUSSION

This study was designed to investigate the effects of topical HAL and ALA-PDT on the underlying vasculature in a mouse skin fold chamber, and to investigate the ability of the vessel wall to accumulate PpIX. Interestingly, HAL and ALA had similar effects in terms of both vascular response and PpIX distribution in the vessel wall. The vascular effect was very clear for the arterioles as nearly all of them showed vasoconstriction after PDT and in most cases this constriction was 100% and lasted at least 20 minutes. The extent of vasoconstriction strongly correlated with the PpIX fluorescence intensity in the arteriole wall. In contrast to the arterioles, the venules did not respond to PDT but two larger veins did. This may be explained by the relative inability of venules to constrict, whereas larger veins have some constrictive ability. Our findings are important

because they reveal so far unknown pharmacokinetic characteristics of PpIX after the topical administration of HAL. In contrast to what is commonly believed, the depth of penetration was no limitation in this mouse skin model for both HAL and ALA as these molecules penetrated the skin well into the subcutis. They were also capable of actually entering the subcutaneous vessel wall, leading to biologically relevant PpIX accumulation. This has not been demonstrated *in vivo* for HAL, and is in accordance with a study that demonstrated PpIX formation in endothelial cells after HAL application *in vitro*³². For ALA the results are comparable to a previous study from our group in which a similar mouse chamber model was used. ALA resulted in higher endothelial PpIX accumulation and more extensive vascular effects than methylaminolevulinate (MAL)²². Our results also show that when the PpIX concentration in the endothelial cells is high enough, the arterioles will show complete vasoconstriction. As figure 4 shows, high PpIX fluorescence intensities resulted in 100% vasoconstriction, whereas low PpIX fluorescence intensities resulted in no or partial vasoconstriction. This suggests a PpIX concentration threshold in the vessel wall that results in complete vasoconstriction.

The finding that arterioles show PpIX-dose dependent vasoconstriction is important for our understanding of topical PDT mechanisms and, as a result, possibly for the optimization of future HAL or ALA-PDT protocols. Complete vasoconstriction especially can be of great relevance for PDT outcome. For instance when this happens early during the illumination, oxygen supply to the PDT site may be insufficient, resulting in an inefficient photodynamic effect. On the other hand, complete vasoconstriction could also be beneficial to PDT outcome, especially when it occurs late or after PDT when most PpIX has already been bleached. Our findings indicate that in many cases, the constriction lasted at least 20 minutes after PDT. Such longer duration of ischemia could further damage and help destroy (tumor) cells that survived the oxidative damage of the PDT. Complete vasoconstriction may also be relevant to other uses for topical HAL or ALA PDT where the vasculature can be a potential target, such as port wine stains. One animal study clearly showed that tumor vasculature could be destroyed¹⁸ using topical ALA-PDT. However, tumour cell photosensitization was a more important factor for tumor destruction than vascular photosensitization. This suggests that vascular effects are not primarily responsible for tumor cell destruction but may be an important secondary factor.

When comparing our results with those from other investigators it is important to note that a relevant comparison cannot be made between topical and systemic administration of porphyrin pre-cursors. The bio-distribution of PpIX after the systemic administration of ALA and HAL are known to be significantly different than after topical administration³⁵. We have therefore only compared our findings to others that have investigated vascular responses after topical HAL or ALA-PDT. The only study conducted

so far that investigated vascular effects after topical HAL-PDT in mice found no vasoconstriction after 3 hours of HAL application, while 17 hours of HAL application resulted in complete vasoconstriction²⁴. The results of this study are in general agreement with our proposed dose dependent threshold mechanism, but their findings after 3 hours are different from ours. As these investigators used fluorescein angiography using a camera that imaged the skin from above, their experimental design was not sensitive enough to detect small arteriole constriction. It may well be that larger, deeper arteries were also imaged that constricted under very high PpIX circumstances, which occurred only after 17 hours of HAL application. It is likely that after such a long application time HAL is distributed throughout the entire thickness of the skin, as longer application times lead to deeper penetration³⁶. In contrast, we measured only superficial arterioles directly and on a microscopic rather than a macroscopic scale, which allows for more detailed measurements.

Interestingly, the same group of investigators have also investigated the PDT response after topical HAL application in human skin, and found increased blood volume immediately after PDT²⁵. That study used reflectance spectroscopy to assess the response over a time-period of two weeks in five healthy volunteers. Possible explanations for this could lie in the differences in structure between mouse and human skin. Maybe the HAL did not penetrate deep enough to result in high enough PpIX accumulation in the vessels. Another plausible explanation is that the diffuse reflectance spectroscopy used was measuring vasodilatation in deeper blood vessels. These deeper vessels may respond differently to PDT than superficial ones. This distinction between deep and superficial blood vessels is relevant, because the superficial blood vessels directly supply the oxygen that is necessary for PDT. Larger, deeper blood vessels on the other hand may deliver blood to the surrounding skin area, and not to the skin that is immediately above it. Furthermore, techniques such as diffuse reflectance spectroscopy measure combined information from both arterioles and venules, which we have shown to respond completely different to PDT. The depth at which vessels are measured and the difference between macroscopic versus microscopic measurements are also important considerations when viewing our results against the background of studies that investigated vascular effects of topical ALA-PDT.

One approach that has been used to measure vascular response after topical ALA-PDT is measuring the depletion of fluorescein fluorescence using a camera that is some distance away from the skin²¹. A decrease in fluorescein signal is indicative of vasoconstriction. Another approach is to measure blood flow using laser Doppler imaging^{20,37} or diffuse correlation spectroscopy¹⁹. As mentioned above, these type of approaches measure on a much larger scale and will be greatly influenced by signals from deeper

blood vessels. Two studies used a similar chamber model to investigate blood vessel response after topical ALA-PDT and concluded that topical ALA-PDT leads to distinct vasoconstriction responses^{22,23}. In the first, a study performed by our own group²², the vascular effects of high versus low fluence PDT was investigated for ALA and another ester of ALA, methylaminolevulinate (MAL). In addition to imaging the subcutaneous vessels directly, trans-epidermal images were also obtained which yielded less sensitive results. The extent of vascular damage for the high fluence ALA-PDT group was very similar to our results for ALA. In the second study,²³ a decrease in functional vessels and reduced blood flow for ALA was found using a hamster dorsal skin fold model. In the current study we investigated not only ALA, but also HAL. Furthermore, we also included the relationship between vascular response and PpIX concentration in the vessel wall.

There are of course some limitations to the present study. First, the results are based on a limited number of mice (5 in each group). To increase accuracy we measured 3 arterioles in each mice and performed statistics on these numbers, resulting in 15 arterioles in the HAL and 14 arterioles in the ALA group (in one mouse we could only image two arterioles instead of three explaining the difference). It may be argued whether or not the averaged results per mouse would be a better way to analyse the data, although this results in loss of information. Our choice is further supported by finding no different distribution of arteriole responses between individual mice for HAL, our primary group of interest ($P=0.261$, Kruskal Wallis independent samples test) and also for ALA ($P=0.06$) if the one mouse that hardly accumulated PpIX is excluded. A second drawback is that we did not measure tissue oxygenation during, or skin damage after PDT. Then it would have been possible to correlate vasoconstriction with tissue ischemia and with treatment effect. Also, our setup only allowed us to measure vascular response after, but not during PDT. This means that we were unable to measure dynamic vascular responses during illumination that could help explain blood flow dynamics such as found by Becker et al¹⁹. Temporal dynamics of vasoconstriction may be important because very high PpIX concentrations in the arteriole wall may lead to vasoconstriction very early in the PDT process, leading to insufficient oxygen availability and therefore inefficient or ineffective PDT. Therefore prolonged application times may not be the way to increase response, as vascular effects start to play an important limiting role.

Assuming that the extent of vasoconstriction depends on the PpIX concentration in the vessel wall it is not surprising that complete arteriole vasoconstriction occurred about as frequent for HAL (64%) as for ALA (60%) since there was no difference in PpIX concentration in the arteriole wall between the two. However, considering all our outcome measures it seems that HAL may be more potent than ALA in inducing vascular effects, even though we found no statistical differences between them. The HAL concentration

we used was lower than that of ALA, but the resulting PpIX concentration in tissue was generally higher. Also, the two larger veins that constricted partially were from the HAL group. Finally, more arterioles remained constricted twenty minutes after PDT in the HAL group than the ALA group. This last finding should be interpreted with caution since these measurements were only performed in a subset of arterioles. In this subset the measurements in the ALA group were greatly influenced by the one mouse in which PpIX concentration was very low and the arterioles actually dilated. Despite the differences between HAL and ALA, our results suggest a similar biological behaviour of HAL and ALA in terms of vascular response and distribution of PpIX in vessel walls.

This similarity in biological behaviour between HAL and ALA is especially interesting when compared with MAL. Several studies have shown that lower concentrations of HAL than of ALA and lower concentrations of ALA than of MAL are needed to reach the same PpIX concentrations in different models³⁸⁻⁴², although some investigators found contradictory results⁴³⁻⁴⁵. The same holds true for PpIX concentration in the vascular endothelium, which was investigated *in vitro*³² and *in vivo*^{33,46}, resulting in more vasoconstriction using ALA than MAL²². These biological behavioural differences between ALA and MAL have also been suggested to play a role in the mechanism behind light fractionated PDT. A two hour dark interval followed by a second light fraction resulted in increased PDT effect for ALA⁴⁷ but not for MAL in normal mouse skin⁴⁸. Using this type of light fractionation for HAL has not been investigated yet. Our results indicate a similar behaviour of HAL and ALA, so it can be speculated that light fractionation may be valuable to increase effect of HAL PDT as well. In accordance with this speculation, a short light fractionation protocol was investigated for HAL-PDT in one animal study, increasing the response⁴⁹.

It should be noted that the translational step towards clinical use of HAL in relation to our results should be taken carefully (for both skin and other epithelial surfaces). Besides obvious general differences between mouse and human biology, there are other specific considerations. Normal human skin is considerably thicker than mouse skin. This is of great relevance for the ability of HAL and ALA to penetrate into the dermis and into vessel walls. This may result in less PpIX accumulation in the vessel walls in thick human skin. If our proposed dose-dependent mechanism works for humans too, we would then expect less vasoconstriction in human skin. In addition to differences in thickness, the anatomy of normal mouse skin vasculature also differs from normal human skin, which has a superficial and a deep plexus. Furthermore, for skin lesions that are typically treated with PDT such as superficial basal cell carcinoma (BCC), the vasculature is in turn different from normal skin. Not only is the amount and diameter of blood vessels increased in BCC, they also tend to grow in a disorganized pattern and

may not have the same muscular power to constrict^{50,51}. Finally, individual patients and lesions may vary in their vascular response to PDT, as was found for both BCC¹⁹ and actinic keratosis⁵². The vasodilatation found in HAL-PDT of normal human skin²⁵ versus the vasoconstriction that was found in ALA and MAL-PDT of BCC³⁷ illustrates that the vascular responses of PDT in human skin need further study.

In conclusion, arteriole vasoconstriction occurred frequently in both HAL and ALA based topical PDT in our mouse model, especially when relatively high PpIX concentrations in arteriole walls were reached. Venules in general did not respond. However, larger veins that have more constrictive ability may also constrict after PDT, since two of them did in this study. Overall PpIX concentration was higher in the HAL group than in the ALA group, but this difference was not significant for the arteriole walls. Vasoconstriction will likely influence PDT effect and should also be considered in studies on topical HAL and ALA-PDT in humans. Also, our results may redefine the vasculature as a potential secondary target for topical HAL and ALA based PDT.

REFERENCES

1. Henderson BW, Dougherty TJ. How does photodynamic therapy work? *Photochem Photobiol.* 1992;55(1):145-57.
2. Dougherty TJ, Gomer CJ, Henderson BW, Jori G, Kessel D, Korbelik M, et al. Photodynamic therapy. *J Natl Cancer Inst.* 1998;90(12):889-905.
3. Weishaupt KR, Gomer CJ, Dougherty TJ. Identification of singlet oxygen as the cytotoxic agent in photoinactivation of a murine tumor. *Cancer Res.* 1976;36(7 PT 1):2326-9.
4. van Duijnhoven FH, Aalbers RI, Rovers JP, Terpstra OT, Kuppen PJ. The immunological consequences of photodynamic treatment of cancer, a literature review. *Immunobiology.* 2003;207(2):105-13.
5. Juarranz A, Jaen P, Sanz-Rodriguez F, Cuevas J, Gonzalez S. Photodynamic therapy of cancer. Basic principles and applications. *Clin Transl Oncol.* 2008;10(3):148-54.
6. Krammer B. Vascular effects of photodynamic therapy. *Anticancer Res.* 2001;21(6B):4271-7.
7. Robinson DJ, de Bruijn HS, van der Veen N, Stringer MR, Brown SB, Star WM. Fluorescence photobleaching of ALA-induced protoporphyrin IX during photodynamic therapy of normal hairless mouse skin: the effect of light dose and irradiance and the resulting biological effect. *Photochem Photobiol.* 1998;67(1):140-9.
8. Middelburg TA, Van Zaane F, De Bruijn HS, Van Der Ploeg-van den Heuvel A, Sterenborg HJ, Neumann HA, et al. Fractionated illumination at low fluence rate photodynamic therapy in mice. *Photochem Photobiol.* 2010;86(5):1140-6. doi: 10.111/j.751-097.2010.00760.x.
9. Ascencio M, Collinet P, Farine MO, Mordon S. Protoporphyrin IX fluorescence photobleaching is a useful tool to predict the response of rat ovarian cancer following hexaminolevulinate photodynamic therapy. *Lasers Surg Med.* 2008;40(5):332-41.
10. Tyrrell JS, Campbell SM, Curnow A. The relationship between protoporphyrin IX photobleaching during real-time dermatological methyl-aminolevulinate photodynamic therapy (MAL-PDT) and subsequent clinical outcome. *Lasers Surg Med.* 2010;42(7):613-9.
11. Chaudhuri K, Keck RW, Selman SH. Morphological changes of tumor microvasculature following hematoporphyrin derivative sensitized photodynamic therapy. *Photochem Photobiol.* 1987;46(5):823-7.
12. Wieman TJ, Mang TS, Fingar VH, Hill TG, Reed MW, Corey TS, et al. Effect of photodynamic therapy on blood flow in normal and tumor vessels. *Surgery.* 1988;104(3):512-7.
13. Reed MW, Wieman TJ, Schuschke DA, Tseng MT, Miller FN. A comparison of the effects of photodynamic therapy on normal and tumor blood vessels in the rat microcirculation. *Radiat Res.* 1989;119(3):542-52.
14. Feyh J, Goetz A, Heimann A, Konigsberger R, Kastenbauer E. [Microcirculatory effects of photodynamic therapy with hematoporphyrin derivative]. *Laryngorhinotologie.* 1991;70(2):99-101.
15. Fingar VH, Wieman TJ, Wiehle SA, Cerrito PB. The role of microvascular damage in photodynamic therapy: the effect of treatment on vessel constriction, permeability, and leukocyte adhesion. *Cancer Res.* 1992;52(18):4914-21.

16. Herman MA, Fromm D, Kessel D. Tumor blood-flow changes following protoporphyrin IX-based photodynamic therapy in mice and humans. *J Photochem Photobiol B*. 1999;52(1-3):99-104.
17. Leveckis J, Brown NJ, Reed MW. The effect of aminolevulinic acid-induced, protoporphyrin IX-mediated photodynamic therapy on the cremaster muscle microcirculation in vivo. *Br J Cancer*. 1995;72(5):1113-9.
18. Henderson BW, Vaughan L, Bellnier DA, van Leengoed H, Johnson PG, Oseroff AR. Photosensitization of murine tumor, vasculature and skin by 5-aminolevulinic acid-induced porphyrin. *Photochem Photobiol*. 1995;62(4):780-9.
19. Becker TL, Paquette AD, Keymel KR, Henderson BW, Sunar U. Monitoring blood flow responses during topical ALA-PDT. *Biomed Opt Express*. 2010;2(1):123-30.
20. Wang I, Andersson-Engels S, Nilsson GE, Wardell K, Svanberg K. Superficial blood flow following photodynamic therapy of malignant non-melanoma skin tumours measured by laser Doppler perfusion imaging. *Br J Dermatol*. 1997;136(2):184-9.
21. van der Veen N, Hebeda KM, de Bruijn HS, Star WM. Photodynamic effectiveness and vasoconstriction in hairless mouse skin after topical 5-aminolevulinic acid and single- or two-fold illumination. *Photochem Photobiol*. 1999;70(6):921-9.
22. de Vijlder H, de Bruijn H, van der Ploeg-van den Heuvel A, van Zaane F, Schipper D, ten Hagen T, et al. Acute vascular responses during photodynamic therapy using topically administered porphyrin precursors. *Photochem Photobiol Sci* 2013 in press. 2013.
23. Schacht V, Szeimies RM, Abels C. Photodynamic therapy with 5-aminolevulinic acid induces distinct microcirculatory effects following systemic or topical application. *Photochem Photobiol Sci*. 2006;5(5):452-8. Epub 2006 Mar 30.
24. Juzeniene A, Juzenas P, Iani V, Moan J. Reflectance spectroscopy and fluorescein angiography applied to assess photodynamic response in healthy mouse skin treated with topical hexylaminolevulinic acid. *Photodiagnosis Photodyn Ther*. 2010;7(4):239-45. Epub 2010 Jul 31.
25. Juzeniene A, Nielsen KP, Zhao L, Ryzhikov GA, Biryulina MS, Stamnes JJ, et al. Changes in human skin after topical PDT with hexyl aminolevulinic acid. *Photodiagnosis Photodyn Ther*. 2008;5(3):176-81. Epub 2008 Aug 28.
26. Smits T, Kleinpenning MM, Blokx WA, van de Kerkhof PC, van Erp PE, Gerritsen MJ. Fluorescence diagnosis in keratinocytic intraepidermal neoplasias. *J Am Acad Dermatol*. 2007;57(5):824-31. Epub 2007 Jul 31.
27. Rud E, Gederaas O, Hogset A, Berg K. 5-aminolevulinic acid, but not 5-aminolevulinic acid esters, is transported into adenocarcinoma cells by system BETA transporters. *Photochem Photobiol*. 2000;71(5):640-7.
28. Rodriguez L, Batlle A, Di Venosa G, Battah S, Dobbin P, MacRobert AJ, et al. Mechanisms of 5-aminolevulinic acid ester uptake in mammalian cells. *Br J Pharmacol*. 2006;147(7):825-33.
29. Rodriguez L, Batlle A, Di Venosa G, MacRobert AJ, Battah S, Daniel H, et al. Study of the mechanisms of uptake of 5-aminolevulinic acid derivatives by PEPT1 and PEPT2 transporters as a tool to improve photodynamic therapy of tumours. *Int J Biochem Cell Biol*. 2006;38(9):1530-9. Epub 2006 Mar 18.

30. Schulten R, Novak B, Schmitz B, Lubbert H. Comparison of the uptake of 5-aminolevulinic acid and its methyl ester in keratinocytes and skin. *Naunyn Schmiedebergs Arch Pharmacol.* 2012;385(10):969-79. doi: 10.1007/s00210-012-0777-4. Epub 2012 Jul 17.
31. Uehlinger P, Zellweger M, Wagnieres G, Juillerat-Jeanneret L, van den Bergh H, Lange N. 5-Aminolevulinic acid and its derivatives: physical chemical properties and protoporphyrin IX formation in cultured cells. *J Photochem Photobiol B.* 2000;54(1):72-80.
32. Rodriguez L, de Bruijn HS, Di Venosa G, Mamone L, Robinson DJ, Juarranz A, et al. Porphyrin synthesis from aminolevulinic acid esters in endothelial cells and its role in photodynamic therapy. *J Photochem Photobiol B.* 2009;96(3):249-54. Epub 2009 Jul 5.
33. de Vijlder H, de Bruijn H, van der Ploeg-van den Heuvel A, Sterenborg H, Neumann H, de Haas E, et al. Differences in protoporphyrin IX localisation in dermal vasculature after topical application of 5-aminolevulinic acid and methyl-5 aminolevulinate. Submitted to: *Journal of photochemistry and photobiology.* 2013.
34. Kacakova S, de Visscher S, Kruijt B, de Bruijn HS, van der Ploeg-van den Heuvel A, Sterenborg HJ, et al. In vivo quantification of photosensitizer fluorescence in the skin-fold observation chamber using dual-wavelength excitation and NIR imaging. *Lasers Med Sci.* 2011;26(6):789-801. doi: 10.1007/s10103-011-0888-z. Epub 2011 Jan 29.
35. Di Venosa G, Batlle A, Fukuda H, Macrobert A, Casas A. Distribution of 5-aminolevulinic acid derivatives and induced porphyrin kinetics in mice tissues. *Cancer Chemother Pharmacol.* 2006;58(4):478-86. Epub 2006 Feb 17.
36. Zhao L, Nielsen KP, Juzeniene A, Juzenas P, Lani V, Ma LW, et al. Spectroscopic measurements of photoinduced processes in human skin after topical application of the hexyl ester of 5-aminolevulinic acid. *J Environ Pathol Toxicol Oncol.* 2006;25(1-2):307-20.
37. Palsson S, Gustafsson L, Bendsoe N, Soto Thompson M, Andersson-Engels S, Svanberg K. Kinetics of the superficial perfusion and temperature in connection with photodynamic therapy of basal cell carcinomas using esterified and non-esterified 5-aminolaevulinic acid. *Br J Dermatol.* 2003;148(6):1179-88.
38. Casas A, Perotti C, Fukuda H, Rogers L, Butler AR, Batlle A. ALA and ALA hexyl ester-induced porphyrin synthesis in chemically induced skin tumours: the role of different vehicles on improving photosensitization. *Br J Cancer.* 2001;85(11):1794-800.
39. Dognitz N, Salomon D, Zellweger M, Ballini JP, Gabrecht T, Lange N, et al. Comparison of ALA- and ALA hexyl-ester-induced PpIX depth distribution in human skin carcinoma. *J Photochem Photobiol B.* 2008;93(3):140-8. Epub 2008 Aug 17.
40. Endlicher E, Rummele P, Hausmann F, Krieg R, Knuchel R, Rath HC, et al. Protoporphyrin IX distribution following local application of 5-aminolevulinic acid and its esterified derivatives in the tissue layers of the normal rat colon. *Br J Cancer.* 2001;85(10):1572-6.
41. Juzeniene A, Juzenas P, Ma LW, Lani V, Moan J. Topical application of 5-aminolaevulinic acid, methyl 5-aminolaevulinate and hexyl 5-aminolaevulinate on normal human skin. *Br J Dermatol.* 2006;155(4):791-9.

42. Marti A, Jichlinski P, Lange N, Ballini JP, Guillou L, Leisinger HJ, et al. Comparison of aminolevulinic acid and hexylester aminolevulinate induced protoporphyrin IX distribution in human bladder cancer. *J Urol.* 2003;170(2 Pt 1):428-32.
43. van den Akker JT, Holroyd JA, Vernon DI, Sterenberg HJ, Brown SB. Comparative in vitro percutaneous penetration of 5-aminolevulinic acid and two of its esters through excised hairless mouse skin. *Lasers Surg Med.* 2003;33(3):173-81.
44. Moan J, Ma LW, Juzeniene A, Iani V, Juzenas P, Apricena F, et al. Pharmacology of protoporphyrin IX in nude mice after application of ALA and ALA esters. *Int J Cancer.* 2003;103(1):132-5.
45. Perotti C, Casas A, Fukuda H, Sacca P, Batlle A. Topical application of ALA and ALA hexyl ester on a subcutaneous murine mammary adenocarcinoma: tissue distribution. *Br J Cancer.* 2003;88(3):432-7.
46. de Bruijn HS, H. C. de Vijlder, E. R. M. de Haas, van der Ploeg-van den Heuvel, F. van Zaane, D. Schipper, H. J. C. M. Sterenberg, T. L. M. ten Hagen. Endothelial cells are involved in the response to topical PpIX-PDT. Submitted to *Photodiagnosis and Photodynamic Therapy* 2011(8).
47. de Haas ER, Kruijt B, Sterenberg HJ, Martino Neumann HA, Robinson DJ. Fractionated illumination significantly improves the response of superficial basal cell carcinoma to aminolevulinic acid photodynamic therapy. *J Invest Dermatol.* 2006;126(12):2679-86. Epub 006 Jul 13.
48. de Bruijn HS, de Haas ER, Hebeda KM, van der Ploeg-van den Heuvel A, Sterenberg HJ, Neumann HA, et al. Light fractionation does not enhance the efficacy of methyl 5-aminolevulinate mediated photodynamic therapy in normal mouse skin. *Photochem Photobiol Sci.* 2007;6(12):1325-31. Epub 2007 Aug 28.
49. Ascencio M, Estevez JP, Delemer M, Farine MO, Collinet P, Mordon S. Comparison of continuous and fractionated illumination during hexaminolaevulinate-photodynamic therapy. *Photodiagnosis Photodyn Ther.* 2008;5(3):210-6. Epub 2008 Oct 19.
50. Bedlow AJ, Stanton AW, Cliff S, Mortimer PS. Basal cell carcinoma—an in-vivo model of human tumour microcirculation? *Exp Dermatol.* 1999;8(3):222-6.
51. Grunt TW, Lametschwandtner A, Staindl O. The vascular pattern of basal cell tumors: light microscopy and scanning electron microscopic study on vascular corrosion casts. *Microvasc Res.* 1985;29(3):371-86.
52. Middelburg TA, Kanick SC, de Haas ER, Sterenberg HJ, Amelink A, Neumann MH, et al. Monitoring blood volume and saturation using superficial fibre optic reflectance spectroscopy during PDT of actinic keratosis. *J Biophotonics.* 2011;4(10):721-30. doi: 10.1002/jbio.201100053. Epub 2011 Aug 15.

5

Topical Photodynamic Therapy Using Different Porphyrin Precursors Leads to Differences in Vascular Photosensitization and Vascular Damage in Normal Mouse Skin

Tom Middelburg

Hanke de Vijlder

Riëtte de Bruijn

Angelique van der Ploeg-van den Heuvel

Martino Neumann

Ellen de Haas

Dominic Robinson

Photochem Photobiol. 2013. Accepted for publication.

ABSTRACT

Different distributions of hexyl-aminolevulinat (HAL), aminolevulinic acid (ALA) and methyl-aminolevulinat (MAL) in the superficial vasculature are not well studied but they are hypothesised to play an important role in topical photodynamic therapy (PDT). The colocalisation of fluorescent CD31 and protoporphyrin IX (PpIX) was calculated using confocal microscopy of mouse skin sections to investigate the vascular distribution after topical application. Vascular damage leads to disruption of the normal endothelial adherens junction complex, of which CD144 is an integral component. Therefore normal CD31 combined with loss of normal fluorescent CD144 staining was visually scored to assess vascular damage. Both the vascular PpIX concentration and the vascular damage were highest for HAL, then ALA and then MAL. Vascular damage in MAL was not different from normal contralateral control skin. This pattern is consistent with literature data on vasoconstriction after PDT, and with the hypothesis that the vasculature plays a role in light fractionation that increases efficacy for HAL and ALA-PDT but not for MAL. These findings indicate that endothelial cells of superficial blood vessels synthesize biologically relevant PpIX concentrations, leading to vascular damage. Such vascular effects are expected to influence the oxygenation of tissue after PDT which can be important for treatment efficacy.

INTRODUCTION

In skin photodynamic therapy (PDT) both aminolevulinic acid (ALA) and its methyl ester methylaminolevulinate (MAL) are being used worldwide for treating malignant and premalignant skin disease. Another ester derivative of ALA is hexylaminolevulinate (HAL). HAL ointment is registered for photodiagnosis of, and for margin establishment during surgery of bladder cancer but research is ongoing investigating its therapeutic use in the skin, cervix and bladder¹⁻⁶. HAL, ALA and MAL are porphyrin precursors that lead to intramitochondrial accumulation of protoporphyrin IX, but they have different pharmacokinetic properties. These properties are in part related to the more lipophilic character of HAL and MAL compared to ALA, but are also related to known differences in cellular uptake mechanisms⁷⁻⁹. This will lead to differences in penetration and bio-distribution between them after topical application, which may account for otherwise unexplained differences in biological behaviour. In particular the biodistribution in the superficial vasculature could be important to account for these differences. It is known that prolonged topical ALA application results in systemic distribution of PpIX, whereas PpIX is restricted to the site of MAL application in mice^{10,11}. Furthermore, subcutaneous arterioles completely constricted directly after topical HAL and ALA-PDT of mouse skin¹², while this was less frequent for MAL-PDT¹³. Related to this, *in vitro* data show that HAL is more potent than ALA, which in turn is more potent than MAL in photosensitising human endothelial cells¹⁴. Also, there is more dermal oedema after light fractionated PDT in ALA than MAL: an indirect indication that leakage through the dermal vessel walls is an acute response to light fractionated ALA-PDT¹⁵. These and other studies¹⁵⁻¹⁷ have led our group to hypothesize that the vasculature also plays a critical role in the mechanism behind the response to light fractionation. Light fractionation involves delivery of a small first light fraction, followed by a dark interval of two hours and a larger second light fraction. It improves the preclinical and clinical response of ALA-PDT, but not of MAL-PDT in mouse skin^{16,18}. Recent data suggest that light fractionation is also beneficial for HAL-PDT¹⁹. We postulate that these differences in response to light fractionation are related to differences in vascular sensitization between the three porphyrin precursors.

However, there remain areas of ambiguity. First, it has not been studied if and to what extent the blood vessels in the superficial dermis accumulate PpIX. Second, it is unknown if PDT using porphyrin precursors damages these vessels, as opposed to causing transitory vasoconstriction which subsequently recovers. For these reasons we conducted the present study, performed on normal mouse skin. The study has two parts: a study of the vascular distribution of PpIX in dermal blood vessels after topical HAL, ALA or MAL application (part A), and a study of the vascular damage for each porphyrin precursor after PDT (part B). For both part A and B the vasculature was visualized in frozen sections

of skin biopsies using fluorescent CD31 (platelet endothelial cell adhesion molecule) antibodies, a commonly used marker for this purpose. Confocal microscopy images were subsequently analysed to calculate the co-localisation of PpIX and CD31 as a measure for the distribution of PpIX in endothelial cells (part A). To study the presence and the extent of vascular damage to these superficial blood vessels after light fractionated PDT (part B), a combination of fluorescent-labelled CD31 and CD144 antibodies were used. The integrity of the vasculature was imaged and scored using a confocal microscope. CD144 -vascular endothelial cadherin- is an integral component of the endothelial adherens junction complex. Endothelial damage results in a disruption of the normal endothelial complex so that CD144 can no longer be stained along the plasma membrane. This effect is maximal after 24 hours, after which CD144 is slowly restored^{20,21}.

MATERIALS AND METHODS

A: The vascular distribution of PpIX, 4 hours after the application of HAL, ALA or MAL (the time-point at which light fractionated PDT is performed as described in B).

Animals and drug delivery

A total of 20 SKH1-hr mice (Charles River, Someren, The Netherlands) were divided in 4 groups of 5 mice. In the first 3 groups different porphyrin precursors were applied on a 7mm skin area: 5% HAL ointment, 16% MAL cream or 20% ALA gel. The 4th group was the control group in which only the gel was applied. The HAL ointment and MAL cream were the standard commercially available products from Photocure (Oslo, Norway) and Galderma (Freiburg Germany) respectively. The ALA gels were freshly prepared by dissolving ALA (Fagron, Oud Beijerland, The Netherlands) in 3% carboxymethylcellulose in water with NaOH added to reach pH4.

Tissue sampling and imaging

After 4 hours occlusion a 5 mm punch biopsy was taken from the center of the application area and snap frozen in liquid nitrogen. On the day before fluorescence imaging 3 frozen sections (10 µm) from each biopsy were cut under subdued light conditions to prevent PpIX photobleaching. In order not to wash out the PpIX fluorescence we chose to minimize the staining procedure and to omit the fixation step. Sections were carefully washed with a few drops of PBS and incubated with rat anti-mouse CD31 conjugated with Alexa Fluor® 488 (BioLegend, Uithoorn, The Netherlands) diluted 1:200 in PBS overnight at 4°C. Sections were re-washed carefully with PBS and covered with glycerol (1:3 in PBS).

The distributions of PpIX and AlexaFluor (CD31) in the dermis were imaged at a resolution of 512x512 pixels using a confocal microscope (Zeiss, LSM 510 Meta) in lambda mode at 400x magnification. PpIX was imaged first utilizing 405 nm excitation light and spectral detection between 582 and 753 nm. Immediately thereafter Alexa Fluor[®] 488 was imaged under 488 nm excitation and a band pass filter (BP 530/600) or spectral detection between 493 and 753 nm. From each section 3 areas were imaged in which blood vessels were clearly visible, using a slice thickness of 5 µm. The images were exported and analyzed using ImageJ software (version 1.46, National Institute of Health, USA).

An important consideration in this type of approach is artefacts, normally termed bleed-through/overlap, caused by a significant background contribution of each fluorophore in the emission band of the other fluorophore. Preliminary experiments using control samples and singularly stained sections showed that there is no influence from PpIX fluorescence in the detected emission band of AlexaFluor[®]488 (BP 530-600 nm) and a negligible influence of the tail of AlexFluor[®]488 fluorescence in the detected emission band of PpIX (620–710 nm) under 405 nm excitation. The contribution of autofluorescence in both emission bands was accounted for by performing a background subtraction based on an average uniform autofluorescence collected from control sections containing only PpIX or AlexFluor[®]488 from the region of interest within which colocalisation analyses were performed.

Colocalisation analysis

Our primary outcome was the colocalisation between PpIX and AlexaFluor in the vessel wall. To calculate the extent of colocalisation, regions of interest were drawn following all visible vessel walls. In these regions of interest the fluorescence intensities of PpIX and Alexa Fluor were measured. The colocalisation was calculated in two ways. First, the degree of correlation between the CD31 and PpIX fluorescence intensities for each pixel in the region of interest were calculated and expressed as the intensity Pearson's correlation coefficient. Second, Mander's coefficients were calculated over the same region of interest, which are another measure for the degree of colocalisation²². This analysis yields two outcomes: M1 and M2. M1 is the proportion of PpIX positive pixels that also contain a CD31 signal intensity larger than zero. M2 is the proportion of CD31 positive pixels that also contain a PpIX signal intensity larger than zero.

B: Vascular damage after light fractionated HAL, ALA or MAL-PDT.*Animals, drug delivery and light fractionated PDT*

A total of 12 SKH1 HR mice were divided into three groups of four animals. Either HAL ointment, MAL cream or ALA gel was applied to a 7 mm skin area and occluded for four hours. Then the area was illuminated using 532 nm laser light at a fluence rate of 89 mWcm⁻² to a dose at which 50% of PpIX was bleached (on average this was approximately 3 J cm⁻²). The 89 mWcm⁻² was calculated to be equivalent to delivery of 50 mWcm⁻² at 514 nm, which is what we used in most previous experiments. This calculation is based on the PpIX absorption and photon energy for these wavelengths. The rationale for the 50% photobleaching dose is explained in more detail elsewhere^{23,24}. After a dark interval of two hours a second illumination was delivered to reach a total dose of 100 J cm⁻².

Tissue sampling and imaging

At 24 hours after PDT, a 7 mm biopsy was taken from the treated area and from contralateral control skin, sectioned, stained, imaged and analyzed. Both the staining method and the imaging analysis were different from the methods described in A. Frozen sections were fixated with acetone (20 min), cellular permeability was increased using 0.5% triton in 1% BSA in PBS (30 min) and non-specific staining was reduced using 5% BSA in PBS (60 min). The vessel wall was visualized by staining with anti CD31 conjugated with AlexaFluor®647 (BioLegend, San Diego, CA, USA) in 1% BSA in PBS. To determine damage to the vessel wall the sections were also stained with anti-CD144 conjugated with biotin in 1% BSA in PBS. Both CD31 and CD144 stainings were performed simultaneously at 4°C overnight, followed by biotin-specific staining with streptavidin efluor 570 in 1% BSA in PBS (both from eBioscience, Vienna, Austria) the next morning.

Scoring of vascular damage

In each section three 400x images were scored for the presence of vascular damage which was our primary outcome for this part of the study. Vascular damage was defined as the absence of an identifiable blood vessel in the CD144 staining while there was a blood vessel visible in the CD31 staining. This scoring method was applied to both the PDT treated skin and the contralateral control skin. This resulted in 9 scores of vascular damage (yes/no) per mouse for the PDT skin sections and another 9 for the control skin. The investigator was blinded from the treatment groups.

Drug application, taking the biopsies and performing PDT were all performed under general anesthesia. The experiments were approved by the local animal experiments committee.

RESULTS

Part A: PpIX colocalisation with CD31

There was clear PpIX fluorescence in the epidermis and in hair follicles for all three groups (HAL, ALA, MAL). In the dermis there was much less PpIX signal. Some of the dermal PpIX was visible as spindle shaped fluorescence throughout the interstitial upper dermis, corresponding to dermal fibroblasts. In many cases the PpIX fluorescence was visibly located in the wall of a superficial blood vessel, which was also positively stained with CD31 (Figure 1).

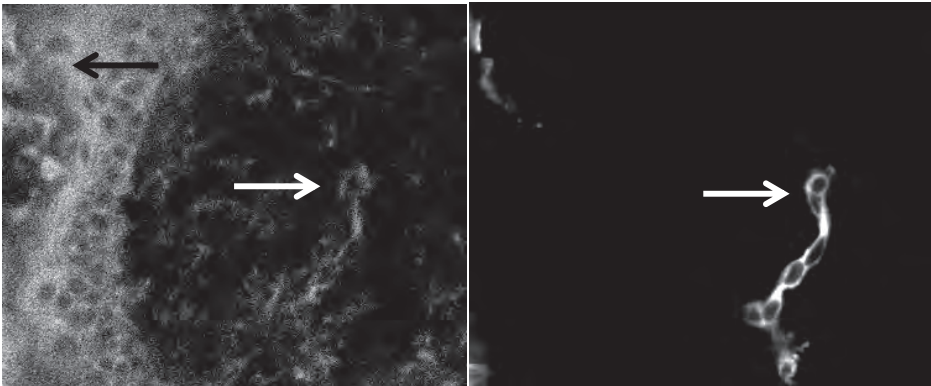


Figure 1. Illustrative example of a PpIX fluorescence image (upper) and the corresponding Alexafluor[®]488-conjugated CD31 fluorescence image (lower). Note the presence of PpIX in the epidermis (black arrow) and in the endothelium of a dermal blood vessel (white arrows). There was also some non-specific CD31 staining in the epidermis. Magnification 400x.

Such colocalisation of PpIX with CD31 was variable per mouse in all groups. On average the highest colocalisation was observed in the HAL group, less in the ALA and MAL groups and the lowest in the control skin (Figure 2). Both the average correlation and M2 coefficients per mouse in the three groups (HAL, ALA and MAL) were significantly different from the control group (correlation coefficient: $P=0.005$; M2: $P=0.002$), but not different from each other (correlation coefficient: $P=0.19$; M2: $P=0.29$, Kruskal-Wallis test). The colocalisation was significantly higher in the HAL, ALA and MAL when individually compared with the control group ($P=0.008$ for all comparisons except for the M2 coefficient of MAL versus control, $P=0.16$ Mann-Whitney U-test). The M1 coefficient was high (>0.95) for all groups.

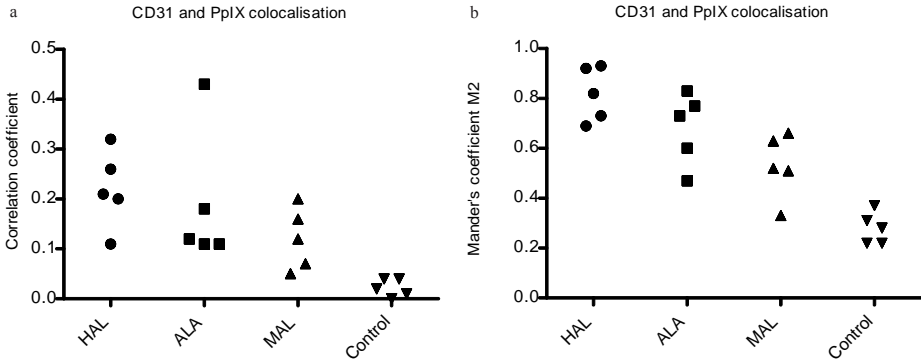


Figure 2. The extent of colocalisation between PpIX fluorescence and CD31 conjugated with AlexaFluor®488, represented as (a) the Pearson's correlation coefficient between individual pixels; and (b) Mander's M2 coefficient, which indicates the proportion of CD31 positive pixels that also contain PpIX fluorescence. Data shown are average values per mouse (n=5) for each group. The value for each mouse was calculated from a total of 9 images taken in 3 microscopic tissue sections.

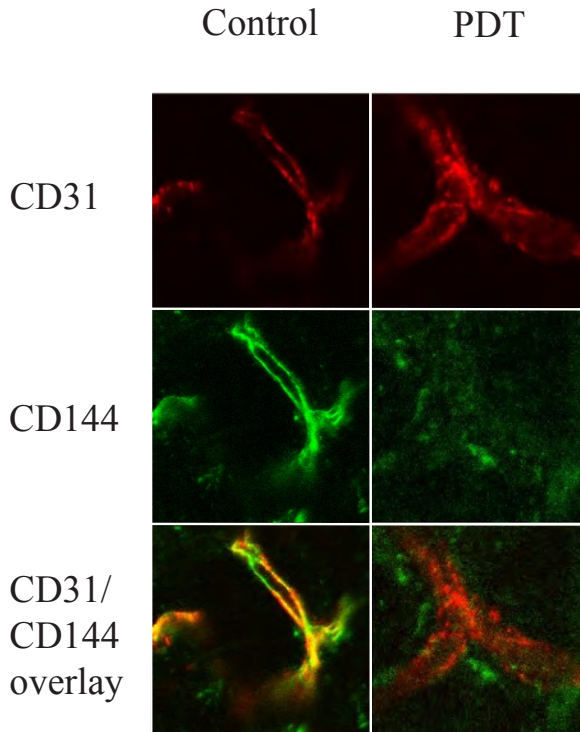


Figure 3. Confocal fluorescence images example of control skin (left) and HAL-PDT-treated skin (right) of the same mouse. The upper images are the CD31 and the corresponding CD144 stainings. The lower image is the overlay of the upper images, showing overlap of CD31/CD144 in the control skin, but not in the PDT skin. In the PDT-treated skin the CD144 no longer stained along the plasma membrane, indicating vascular damage. Magnification 400x, zoom 5.3x.

Part B: vascular damage.

In all three groups (HAL, ALA and MAL) focal loss of normal fluorescent CD144 located along the vascular endothelium was observed. Instead, the CD144 was relocated into the immediate surroundings of the vessel, indicating disruption of the endothelium. Such a response was scored as vascular damage and an example of this is shown in Figure 3.

This type of loss of identifiable vessel in the CD144 staining was also observed in 400x images of normal skin (in 12/99 of total images), but much more often in the PDT-treated skin (in 33/99 of total images). The number of total images that was scored as vascular damage was highest in the HAL-PDT group (14/36), then in the ALA-PDT group (10/27) and lowest in the MAL-PDT group (9/36). When the data per mouse (instead of per image) are considered, 3 of 4 mice in the HAL group showed more vascular damage in the PDT treated skin than in normal skin, which was 2 of 3 mice in the ALA group and 2 of 4 mice in the MAL group.

The percentage of 400x images that was scored as vascular damage is illustrated in figure 4 for all three groups, including PDT treated and normal skin. One mouse in the ALA group died which is why there are fewer data in this group. In both the HAL and ALA-PDT treated skin the percentage in which vascular damage was scored in 400x images was statistically significantly higher than the combined data of all 99 control skin images ($P=0.0005$ and $P=0.003$ respectively). In the MAL group there was no significant difference between PDT treated skin and control skin ($P=0.068$, chi-square test). The number of vascular damage scores per 400x image was not different between the HAL, ALA and MAL groups ($P=0.408$ chi square test).

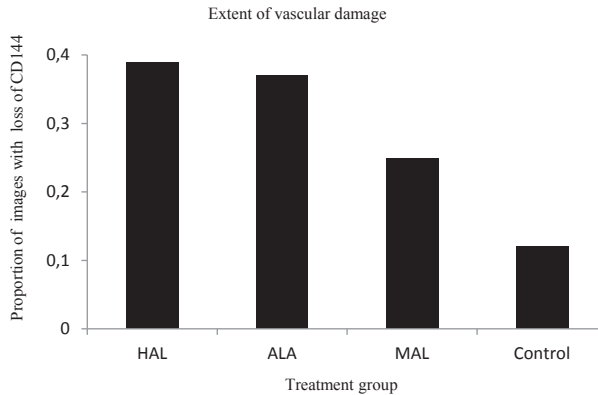


Figure 4. Proportion of 400x images in which vascular damage was scored for the three PDT-treated groups (n=36 for HAL, n=27 for ALA, n=36 for MAL and n=99 for control). HAL and ALA groups were significantly different from control skin (P=0.0005 and 0.003 respectively, but MAL was not (P=0.068, Chi-squared test).

DISCUSSION

In this study the distribution of PpIX in dermal blood vessels was investigated after either HAL, ALA or MAL application. In addition, we studied if fractionated PDT using HAL, ALA or MAL damages the vascular integrity of these vessels. We found that after application of all three porphyrin precursors, endothelial cells in the vessel walls synthesized PpIX. However, these PpIX concentrations (represented by the degree of colocalisation between PpIX and CD31) were highest in the HAL group, next in the ALA group and lowest in the MAL group. The same trend was seen for the vascular damage after PDT: highest vascular damage scores for HAL, followed by ALA and then MAL.

These combined findings indicate that the amount of PpIX synthesis in the vessel wall actually causes vascular damage and that this effect is the strongest for HAL. We previously reported more extensive constriction of subcutaneous arterioles for HAL than for ALA-PDT, which was correlated with PpIX concentration in the vessel wall¹² and more extensive arteriole constriction after PDT using ALA than MAL¹³. In another study we observed more acute edema after ALA than MAL-PDT¹⁵. From these studies and our current findings we can conclude that 5% HAL ointment leads to higher PpIX concentrations in dermal and subcutaneous vessel walls than 20% ALA gel, which leads to higher PpIX concentrations than 16% MAL cream. As a logical result, the vascular constriction and vascular damage is increasingly extensive with this increasing potential to accumulate PpIX in vessel walls.

From our current findings, which were performed on normal skin, it can be assumed that the vasculature is also damaged after topical HAL and ALA-PDT of cancer tissue. Obviously the aim here is to destroy all cancer cells while preserving normal tissue. This ratio may be dependent on the vascular response. When vessels constrict too much during PDT, this limits the oxygen supply to the PDT treated site. This type of response will decrease the potency of PDT to destroy tumor cells. On the other hand, if vasoconstriction happens late during or after PDT or if vessels are damaged, local ischemia may help destroy cancer cells that would otherwise survive. However, when the ischemia becomes too extensive or long-lasting, normal tissue will die too which may result in an inferior cosmetic or functional outcome. This suggests that there may be a delicate balance between too much or too little vascular photosensitization to achieve optimal PDT effect. The phenomenon that the PDT outcome is related in a complex manner to vascular responses and oxygen supply has already been described for PDT using systemic porphyrins in the 1980s²⁵⁻²⁷. Our current results indicate that the extent of vascular constriction or damage may be important for the overall effect of topical PDT too.

In addition to enhanced tumor cell kill due to hypoxia from vascular damage, the vascular responses may also be part of the mechanism behind the success of light fractionated PDT. For ALA-PDT, light fractionation has proven beneficial in both preclinical^{23, 28-30} and clinical studies^{18, 31}. We hypothesize that the vascular endothelium synthesizes a small but relevant amount of PpIX which makes it vulnerable to a second illumination. Because the effect of light fractionation is stronger for relatively low PpIX concentrations¹⁷ the vascular endothelium is a potential target for fractionated PDT. In both in-vitro and in-vivo studies it has been shown that vascular endothelial cells can be photosensitized using ALA^{14, 32}. It could very well be however that a minimum PpIX concentration is necessary to cause vascular damage. Because light fractionation does not increase efficacy of MAL-PDT in normal mouse skin¹⁶, it may be that the endothelial PpIX concentration is too low which is in accordance with our current findings. Our current data are also in line with the expectation and recent evidence that light fractionation may also be beneficial for HAL-PDT¹⁹, which could be relevant for clinical trials.

Before translating our findings to clinical implications however, we should bear in mind that such a step needs to be taken carefully. Apart from the obvious biological differences between humans and mice, a considerable difference lies in the increased thickness of human skin (and other epithelial surfaces such as those of the bladder and cervix). This is relevant with respect to penetration. Also, tumor tissue such as basal cell carcinoma is known to have a different vasculature than normal skin^{33, 34} which potentially influences the ability of the endothelial cells to accumulate PpIX.

Despite these differences between human and mouse tissues, our findings may be useful when designing clinical trials. It could very well be that vascular responses also play a role in clinical PDT, for which there is some evidence in the literature. Simulations of PpIX photobleaching kinetics and subsequent measurements have confirmed blood flow changes during ALA-PDT of basal cell carcinoma^{35,36} and blood volume and saturation changes were observed in ALA-PDT of actinic keratosis³⁷. Also, after PDT for skin rejuvenation the number of telangiectasias in the face decreased after ALA-PDT³⁸, but not after MAL-PDT³⁹. This could reflect the increased ability to sensitize endothelial cells of ALA compared with MAL. ALA-PDT is also used off-label to treat port wine stains⁴⁰. It is questionable however if the vascular accumulation of PpIX in port wine stains will be sufficient to cause direct vascular damage, or that other mechanisms after PDT may play a role. The effect of ALA-PDT on port wine stains can however be considered an indication that the vasculature can also be a primary target of PDT, which suggests that other vascular tumors may theoretically also benefit from topical HAL or ALA-PDT.

There are some limitations to the current study which must be addressed. Most importantly we observed a loss of CD144 staining along the vessel wall also in the normal skin sections. Since the normal skin was taken from contralateral site is it extremely unlikely that this finding represents actual vascular damage. It may instead be associated with a background level of loss of CD144 staining that is also observed in other cellular studies^{41,42}. It can then be logically assumed that such a background level is also present in the PDT treated sections. Although this decreases the specificity of our scoring system, we did find a significantly larger loss of CD144 staining in the PDT treated skin than in normal skin using unpaired statistical testing. We are therefore confident in our conclusion that our findings reflect the presence of vascular damage.

Another potential concern is the relatively low Pearson's correlation coefficient, which can be explained by its sensitivity to background noise and to variable fluorescence intensities²². The M2 coefficient however provides additional information on the degree of colocalisation that is less sensitive to noise and uneven PpIX intensity distributions in this case. Because our region of interest contains only the vessel wall, it is saturated with CD31 positive pixels. The high value of M2 (especially high for HAL) indicates that a large proportion of these CD31 positive pixels also contain PpIX signal, even if this signal is low. The level of noise is represented by the average M2 value in the control sections (0.28). This high noise level originates from the PpIX images. It explains why the M1 coefficient is almost 1 for all groups as nearly all of the PpIX/noise pixels will colocalise with CD31 pixels in our region of interest. A way to reduce the signal to noise ratio in the future may be to increase the integration times during the PpIX image acquisition.

However, it should be noted that the rapid photobleaching rate of PpIX will limit the signal to noise ratio that is achievable.

It must also be noted that we did not include a functional test to study the functional consequences of the vascular damage, which would provide additional evidence for vascular damage. We previously observed more oedema after light fractionated ALA-PDT than after MAL-PDT¹⁵, which indicates increased permeability after PDT. To support the results of the present study we have performed additional in-vivo intra-vital microscopy investigating the distribution of fluorescein after fractionated ALA-PDT. In an extension of the mouse dorsal skin fold chamber model that we have previously used to investigate the vascular response during PDT with porphyrin pre-cursors¹² 514 nm light from the confocal microscope (ca 12 J cm⁻²) was used both for light delivery and for imaging through the epidermis. Immediately after PDT, fluorescein (FITC-BSA, Sigma) was injected intravenously at a dose of 0.2 mg/mouse. Trans-epidermal images were obtained and showed focal leakage of fluorescein into the perivascular space. An example image of this is shown in figure 5.

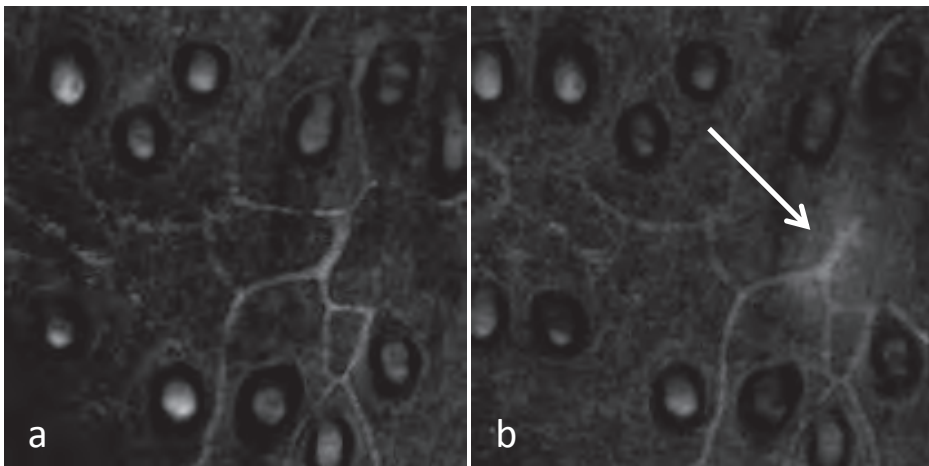


Figure 5. Trans-epidermal confocal images in a mouse skin fold chamber model. Immediately after fractionated ALA-PDT fluorescein was injected intravenously. On the left (a) is a transmission image before PDT and on the right (b) a fluorescence image after PDT showing leakage of fluorescein into the perivascular space (white arrow). The round dots in both images are hair follicle units. Image adapted from the thesis "New insights into photodynamic therapy using porphyrin precursors" by de Vijlder in 2013 with permission.

Such focal fluorescein leakage is in accordance with our current finding of focal loss of CD144 staining. Increased permeability leads to stress fiber formation, followed by phosphorylation of RhoA, inhibiting CD144 formation⁴³. So the direct increase in

permeability is a functional measure of vascular dysfunction, which results in structural changes that can be detected as loss of normal CD144 staining 24 hours later.

A possible limitation could also be that we compared the ability of HAL, ALA and MAL to penetrate through the epidermis and synthesize PpIX in the vascular endothelium, but we used different concentrations and formulations. In several studies it has been shown that lower concentrations of HAL than ALA and lower concentrations of ALA than MAL are needed to reach the same PpIX concentration in different models^{6, 44-46}. Also, the vehicle can influence the penetration of the molecules^{47, 48}. To translate the relevance of our findings for clinical applications we considered it more useful to compare the standard available products which is why we chose to use these in the current study.

For future research it may be interesting to investigate if there are any differences in vascular damage after single versus light fractionated PDT. If our hypotheses are correct we can expect to see less vascular damage after a single illumination, but considering the presence of CD144 staining artifacts, the number of animals and/or sections needs to be larger to detect statistical differences. Another interesting future step would be to further investigate the benefit of light fractionated for HAL-PDT *in vivo*.

In conclusion we have now shown for the first time that there is vascular damage of dermal blood vessels after topical light fractionated HAL and ALA-PDT, which is related to the ability of the vessel wall to synthesize PpIX. In this and previous work we find a consistent trend that shows the highest vascular PpIX synthesis, vascular constriction and vascular damage for HAL, followed by ALA and then MAL. While the vascular constriction that we found in previous studies may be relevant for the oxygen supply *during* PDT, the vascular damage that we found in this study could also be relevant for the oxygen supply *after* light fractionated PDT. This potentially plays a role as an enhanced kill mechanism of light fractionated PDT for cancer cells that would otherwise survive. In addition, our findings suggest that topical fractionated HAL and ALA-PDT can be used to primarily target the vasculature. This could be an important aspect of PDT for cosmetic purposes, port wine stains and possibly other vascular tumors.

REFERENCES

1. Soergel P, Wang X, Stepp H, Hertel H, Hillemanns P. Photodynamic therapy of cervical intraepithelial neoplasia with hexaminolevulinate. *Lasers Surg Med.* 2008;40(9):611-5. doi: 10.1002/lsm.20686.
2. Soergel P, Makowski L, Makowski E, Schippert C, Hertel H, Hillemanns P. Treatment of high grade cervical intraepithelial neoplasia by photodynamic therapy using hexylaminolevulinate may be costeffective compared to conisation procedures due to decreased pregnancy-related morbidity. *Lasers Surg Med.* 2011;43(7):713-20. doi: 10.1002/lsm.21072.
3. Soergel P, Dahl GF, Onsrud M, Hillemanns P. Photodynamic therapy of cervical intraepithelial neoplasia 1-3 and human papilloma virus (HMV) infection with methylaminolevulinate and hexaminolevulinate—a double-blind, dose-finding study. *Lasers Surg Med.* 2012;44(6):468-74. doi: 10.1002/lsm.22041. Epub 2012 Jun 12.
4. Juzeniene A, Nielsen KP, Zhao L, Ryzhikov GA, Biryulina MS, Stamnes JJ, et al. Changes in human skin after topical PDT with hexyl aminolevulinate. *Photodiagnosis Photodyn Ther.* 2008;5(3):176-81. Epub 2008 Aug 28.
5. Bader MJ, Stepp H, Beyer W, Pongratz T, Sroka R, Kriegmair M, et al. Photodynamic Therapy of Bladder Cancer - A Phase I Study Using Hexaminolevulinate (HAL). *Urol Oncol.* 2012;20:20.
6. Dognitz N, Salomon D, Zellweger M, Ballini JP, Gabrecht T, Lange N, et al. Comparison of ALA- and ALA hexyl-ester-induced PpIX depth distribution in human skin carcinoma. *J Photochem Photobiol B.* 2008;93(3):140-8. Epub 2008 Aug 17.
7. Rodriguez L, Batlle A, Di Venosa G, Battah S, Dobbin P, Macrobert AJ, et al. Mechanisms of 5-aminolevulinic acid ester uptake in mammalian cells. *Br J Pharmacol.* 2006;147(7):825-33.
8. Rud E, Gederaas O, Hogset A, Berg K. 5-aminolevulinic acid, but not 5-aminolevulinic acid esters, is transported into adenocarcinoma cells by system BETA transporters. *Photochem Photobiol.* 2000;71(5):640-7.
9. Schulten R, Novak B, Schmitz B, Lubbert H. Comparison of the uptake of 5-aminolevulinic acid and its methyl ester in keratinocytes and skin. *Naunyn Schmiedebergs Arch Pharmacol.* 2012;385(10):969-79. doi: 10.1007/s00210-012-0777-4. Epub 2012 Jul 17.
10. Juzeniene A, Juzenas P, Iani V, Moan J. Topical application of 5-aminolevulinic acid and its methyl ester, hexylester and octylester derivatives: considerations for dosimetry in mouse skin model. *Photochem Photobiol.* 2002;76(3):329-34.
11. Moan J, Ma LW, Juzeniene A, Iani V, Juzenas P, Apricena F, et al. Pharmacology of protoporphyrin IX in nude mice after application of ALA and ALA esters. *Int J Cancer.* 2003;103(1):132-5.
12. Middelburg TA, de Bruijn HS, Tettero L, van der Ploeg van den Heuvel A, Neumann HA, de Haas ER, et al. Topical hexylaminolevulinate and aminolevulinic acid photodynamic therapy: complete arteriole vasoconstriction occurs frequently and depends on protoporphyrin IX concentration in vessel wall. *J Photochem Photobiol B.* 2013;126:26-32.(doi):10.1016/j.jphotobiol.2013.06.014. Epub Jul 11.

13. de Vijlder H, de Bruijn H, van der Ploeg-van den Heuvel A, van Zaane F, Schipper D, ten Hagen T, et al. Acute vascular responses during photodynamic therapy using topically administered porphyrin precursors. *Photochem Photobiol Sci* 2013 in press. 2013.
14. Rodriguez L, de Bruijn HS, Di Venosa G, Mamone L, Robinson DJ, Juarranz A, et al. Porphyrin synthesis from aminolevulinic acid esters in endothelial cells and its role in photodynamic therapy. *J Photochem Photobiol B*. 2009;96(3):249-54. Epub 2009 Jul 5.
15. de Bruijn HS, Meijers C, van der Ploeg-van den Heuvel A, Sterenborg HJ, Robinson DJ. Microscopic localisation of protoporphyrin IX in normal mouse skin after topical application of 5-aminolevulinic acid or methyl 5-aminolevulinate. *J Photochem Photobiol B*. 2008;92(2):91-7. doi: 10.1016/j.jphotobiol.2008.05.005. Epub May 15.
16. de Bruijn HS, de Haas ER, Hebeda KM, van der Ploeg-van den Heuvel A, Sterenborg HJ, Neumann HA, et al. Light fractionation does not enhance the efficacy of methyl 5-aminolevulinate mediated photodynamic therapy in normal mouse skin. *Photochem Photobiol Sci*. 2007;6(12):1325-31. Epub 2007 Aug 28.
17. de Bruijn HS, Casas AG, Di Venosa G, Gandara L, Sterenborg HJ, Batlle A, et al. Light fractionated ALA-PDT enhances therapeutic efficacy in vitro; the influence of PpIX concentration and illumination parameters. *Photochem Photobiol Sci*. 2013;12(2):241-5. doi: 10.1039/c2pp25287b. Epub 2012 Oct 29.
18. de Haas ER, Kruijt B, Sterenborg HJ, Martino Neumann HA, Robinson DJ. Fractionated illumination significantly improves the response of superficial basal cell carcinoma to aminolevulinic acid photodynamic therapy. *J Invest Dermatol*. 2006;126(12):2679-86. Epub 006 Jul 13.
19. Middelburg T, De Bruijn H, Van der Ploeg van den Heuvel A, Neumann H, Robinson D. The effect of light fractionation with a two-hour dark interval on the efficacy of topical hexyl-aminolevulinate photodynamic therapy in normal mouse skin. Submitted to *Photodiagnosis and Photodynamic Therapy*. 2013.
20. Sutton TA, Mang HE, Campos SB, Sandoval RM, Yoder MC, Molitoris BA. Injury of the renal microvascular endothelium alters barrier function after ischemia. *Am J Physiol Renal Physiol*. 2003;285(2):F191-8. Epub 2003 Apr 8.
21. Corada M, Mariotti M, Thurston G, Smith K, Kunkel R, Brockhaus M, et al. Vascular endothelial-cadherin is an important determinant of microvascular integrity in vivo. *Proc Natl Acad Sci U S A*. 1999;96(17):9815-20.
22. Bolte S, Cordelieres FP. A guided tour into subcellular colocalization analysis in light microscopy. *J Microsc*. 2006;224(Pt 3):213-32.
23. de Bruijn HS, van der Ploeg-van den Heuvel A, Sterenborg HJ, Robinson DJ. Fractionated illumination after topical application of 5-aminolevulinic acid on normal skin of hairless mice: the influence of the dark interval. *J Photochem Photobiol B*. 2006;85(3):184-90. Epub 2006 Sep 1.
24. Middelburg TA, Van Zaane F, De Bruijn HS, Van Der Ploeg-van den Heuvel A, Sterenborg HJ, Neumann HA, et al. Fractionated illumination at low fluence rate photodynamic therapy in mice. *Photochem Photobiol*. 2010;86(5):1140-6. doi: 10.1111/j.751-097.2010.00760.x.

25. Henderson BW, Fingar VH. Relationship of tumor hypoxia and response to photodynamic treatment in an experimental mouse tumor. *Cancer Res.* 1987;47(12):3110-4.
26. Henderson BW, Waldow SM, Mang TS, Potter WR, Malone PB, Dougherty TJ. Tumor destruction and kinetics of tumor cell death in two experimental mouse tumors following photodynamic therapy. *Cancer Res.* 1985;45(2):572-6.
27. Henderson BW, Fingar VH. Oxygen limitation of direct tumor cell kill during photodynamic treatment of a murine tumor model. *Photochem Photobiol.* 1989;49(3):299-304.
28. Robinson DJ, de Bruijn HS, van der Veen N, Stringer MR, Brown SB, Star WM. Fluorescence photobleaching of ALA-induced protoporphyrin IX during photodynamic therapy of normal hairless mouse skin: the effect of light dose and irradiance and the resulting biological effect. *Photochem Photobiol.* 1998;67(1):140-9.
29. Robinson DJ, de Bruijn HS, de Wolf WJ, Sterenberg HJ, Star WM. Topical 5-aminolevulinic acid-photodynamic therapy of hairless mouse skin using two-fold illumination schemes: PpIX fluorescence kinetics, photobleaching and biological effect. *Photochem Photobiol.* 2000;72(6):794-802.
30. Robinson DJ, de Bruijn HS, Star WM, Sterenberg HJ. Dose and timing of the first light fraction in two-fold illumination schemes for topical ALA-mediated photodynamic therapy of hairless mouse skin. *Photochem Photobiol.* 2003;77(3):319-23.
31. de Vijlder HC, Sterenberg HJ, Neumann HA, Robinson DJ, de Haas ER. Light fractionation significantly improves the response of superficial basal cell carcinoma to aminolaevulinic acid photodynamic therapy: five-year follow-up of a randomized, prospective trial. *Acta Derm Venereol.* 2012;92(6):641-7. doi: 10.2340/00015555-1448.
32. Chang CJ, Ma SF, Wei FC. In vitro and in vivo photosensitizing capabilities of 5-ALA in vascular endothelial cells. *Changgeng Yi Xue Za Zhi.* 1999;22(2):181-8.
33. Bedlow AJ, Stanton AW, Cliff S, Mortimer PS. Basal cell carcinoma—an in-vivo model of human tumour microcirculation? *Exp Dermatol.* 1999;8(3):222-6.
34. Grunt TW, Lametschwandtner A, Staindl O. The vascular pattern of basal cell tumors: light microscopy and scanning electron microscopic study on vascular corrosion casts. *Microvasc Res.* 1985;29(3):371-86.
35. Wang KK, Cottrell WJ, Mitra S, Oseroff AR, Foster TH. Simulations of measured photobleaching kinetics in human basal cell carcinomas suggest blood flow reductions during ALA-PDT. *Lasers Surg Med.* 2009;41(9):686-96. doi: 10.1002/lsm.20847.
36. Becker TL, Paquette AD, Keymel KR, Henderson BW, Sunar U. Monitoring blood flow responses during topical ALA-PDT. *Biomed Opt Express.* 2010;2(1):123-30.
37. Middelburg TA, Kanick SC, de Haas ER, Sterenberg HJ, Amelink A, Neumann MH, et al. Monitoring blood volume and saturation using superficial fibre optic reflectance spectroscopy during PDT of actinic keratosis. *J Biophotonics.* 2011;4(10):721-30. doi: 10.1002/jbpo.201100053. Epub 2011 Aug 15.
38. Gold MH, Bradshaw VL, Boring MM, Bridges TM, Biron JA. Split-face comparison of photodynamic therapy with 5-aminolevulinic acid and intense pulsed light versus intense pulsed light alone for photodamage. *Dermatol Surg.* 2006;32(6):795-801; discussion -3.

39. Sanclemente G, Medina L, Villa JF, Barrera LM, Garcia HI. A prospective split-face double-blind randomized placebo-controlled trial to assess the efficacy of methyl aminolevulinate + red-light in patients with facial photodamage. *J Eur Acad Dermatol Venereol*. 2011;25(1):49-58. doi: 10.1111/j.1468-3083.2010.03687.x.
40. Li W, Yamada I, Masumoto K, Ueda Y, Hashimoto K. Photodynamic therapy with intradermal administration of 5-aminolevulinic acid for port-wine stains. *J Dermatolog Treat*. 2010;21(4):232-9. doi: 10.3109/09546630903159099.
41. Eiselein L, Wilson DW, Lame MW, Rutledge JC. Lipolysis products from triglyceride-rich lipoproteins increase endothelial permeability, perturb zonula occludens-1 and F-actin, and induce apoptosis. *Am J Physiol Heart Circ Physiol*. 2007;292(6):H2745-53. Epub 007 Jan 26.
42. Kidoya H, Naito H, Takakura N. Apelin induces enlarged and nonleaky blood vessels for functional recovery from ischemia. *Blood*. 2010;115(15):3166-74. doi: 10.1182/blood-2009-07-232306. Epub 2010 Feb 25.
43. Ota H, Matsumura M, Miki N, Minamitami H. Photochemically induced increase in endothelial permeability regulated by RhoA activation. *Photochem Photobiol Sci*. 2009;8(10):1401-7. doi: 10.039/b906028f. Epub 2009 Jul 29.
44. Endlicher E, Rummele P, Hausmann F, Krieg R, Knuchel R, Rath HC, et al. Protoporphyrin IX distribution following local application of 5-aminolevulinic acid and its esterified derivatives in the tissue layers of the normal rat colon. *Br J Cancer*. 2001;85(10):1572-6.
45. Juzeniene A, Juzenas P, Ma LW, Iani V, Moan J. Topical application of 5-aminolaevulinic acid, methyl 5-aminolaevulinate and hexyl 5-aminolaevulinate on normal human skin. *Br J Dermatol*. 2006;155(4):791-9.
46. Marti A, Jichlinski P, Lange N, Ballini JP, Guillou L, Leisinger HJ, et al. Comparison of aminolevulinic acid and hexylester aminolevulinate induced protoporphyrin IX distribution in human bladder cancer. *J Urol*. 2003;170(2 Pt 1):428-32.
47. Casas A, Fukuda H, Di Venosa G, Batlle AM. The influence of the vehicle on the synthesis of porphyrins after topical application of 5-aminolaevulinic acid. Implications in cutaneous photodynamic sensitization. *Br J Dermatol*. 2000;143(3):564-72.
48. Casas A, Perotti C, Fukuda H, Rogers L, Butler AR, Batlle A. ALA and ALA hexyl ester-induced porphyrin synthesis in chemically induced skin tumours: the role of different vehicles on improving photosensitization. *Br J Cancer*. 2001;85(11):1794-800.

6

The effect of light fractionation with a 2-h dark interval on the efficacy of topical hexyl-aminolevulinate photodynamic therapy in normal mouse skin.

Tom Middelburg
Riëtte de Bruijn
Angelique van der Ploeg-van den Heuvel
Martino Neumann
Dominic Robinson

Photodiagn and Photodyn ther. 2013(10);703-709

ABSTRACT

Background: Light fractionation with a two-hour dark interval increases the efficacy of topical aminolevulinic acid (ALA) photodynamic therapy (PDT). Hexyl-aminolevulinic acid (HAL) is the hexyl ester of ALA. Both HAL and ALA lead to protoporphyrin IX (PpIX) accumulation in endothelial cells and to vascular effects, which are important for light fractionation. We investigated light fractionation for HAL-PDT in a mouse skin model and compared this with ALA.

Methods: Three illumination schemes were studied: a) 100 Jcm⁻² in a single illumination; b) 50+50 Jcm⁻² in a two-fold illumination; c) a small first light fraction until 50% of PpIX was photobleached (ca. 3 Jcm⁻²), followed by 97 Jcm⁻² two hours later. PpIX fluorescence was measured continuously during illumination. Efficacy was evaluated by daily visual skin damage scoring up to 7 days after PDT.

Results: Light fractionation showed a trend towards increased efficacy for HAL-PDT. Both the initial PpIX synthesis and the PpIX resynthesis during the dark interval were higher for ALA, but these were not correlated with efficacy. Single HAL-PDT was more effective than single ALA-PDT. Photobleaching rates of HAL and ALA were similar indicating similar biodistributions at depth.

Conclusion: Our results provide evidence to support that light fractionation may be beneficial for HAL-PDT. We are cautious because we found only a non-significant increase in response. However, combining our results with literature data suggest that the illumination scheme may be further optimized for HAL-PDT to potentially enhance the effect of light fractionation.

INTRODUCTION

Since 1990 aminolevulinic acid (ALA) is being used topically for photodynamic therapy (PDT)¹. Later more lipophilic ALA-esters have been developed such as methyl-aminolevulinate (MAL) and hexyl-aminolevulinate (HAL). All three lead to protoporphyrin IX (PpIX) accumulation in mitochondria. Our group has previously focused primarily on ALA and we have developed and optimized a protocol for light fractionated ALA-PDT. Fractionated ALA-PDT involves delivery of a small light fraction followed by a large light fraction, separated by a two-hour dark interval. This protocol improves clinical efficacy in ALA-PDT for human basal cell carcinoma^{2,3}. It is based on a number of mouse studies in which, for different illumination schemes, the fluorescence kinetics and visual skin damage in normal skin were measured⁴⁻⁷. This mouse model has proven to provide information on the subtleties of PpIX synthesis and PpIX photobleaching that has aided our understanding of underlying mechanisms.

Interestingly, light fractionation did not increase response for MAL-PDT using the same illumination scheme and mouse model⁸. It was hypothesized that differences in vessel wall distribution and vascular response between ALA and MAL explain this difference in response. Further studies supported this hypothesis and showed that ALA application indeed leads to higher PpIX levels in the vessel wall than MAL^{9,10}, and that ALA-PDT leads to more vascular constriction than MAL-PDT¹¹.

Contrary to ALA and MAL, HAL is not used in dermatology. HAL ointment is registered for photodiagnosis of, and for margin establishment during surgery of bladder cancer but research is ongoing investigating its therapeutic use in the skin, cervix and bladder¹²⁻¹⁷. It is therefore useful to investigate if light fractionation also enhances the efficacy of HAL-PDT. There are similarities between HAL and ALA that suggest that this approach would be beneficial. First, HAL also penetrates into endothelial cells *in-vitro*¹⁸ and in vessel walls *in-vivo*¹⁹. Second, HAL-PDT leads to a comparable vascular response as ALA-PDT¹⁹.

For these reasons our goal was to investigate if our light fractionated protocol also increases HAL-PDT efficacy, measured as visual skin damage in the same mouse model as previously used for ALA and MAL. Three illumination schemes were studied for HAL and for ALA, which served as a control group. Furthermore, we measured PpIX fluorescence kinetics during PDT. It is well documented that the rate of PpIX photobleaching is related to the efficiency of the PDT process²⁰⁻²² and this information has also been used successfully to predict differences in (sub)cellular PpIX distribution⁸.

MATERIALS AND METHODS

Animal model and porphyrin precursor application

The experiment was approved by the local animal ethical committee. We used 45 albino hairless mice (SKH1 HR), that had been on a chlorophyll free diet for two weeks and divided them in three groups of 15 animals. We applied either HAL ointment, or ALA gel on a 7 mm skin area under occlusion for 4 hours. The ALA gel was freshly prepared as follows: 20% ALA (Fagron, Oud Beijerland, The Netherlands) in 3% carboxymethylcellulose in water with NaOH added to reach pH=4. HAL, 5% (100mg ointment: Cevira™, Photocure Oslo, Norway) is the standard available product for the treatment of cervical intraepithelial neoplasia.

PDT light delivery and setup

The setup we used for PDT light delivery and fluorescence measurements (see section below) was similar as described earlier²² (Figure 1). A relevant difference was that we now had to use a different laser. To deliver the same effective fluence rate as in previous experiments (50 mW cm^{-2} at 514 nm) we now delivered a measured fluence rate of 89 mW cm^{-2} at 532 nm. Using the same calculation as in a previous study¹¹ this was considered as the equivalent effective fluence rate, based on the PpIX absorption and photon energy for these wavelengths.

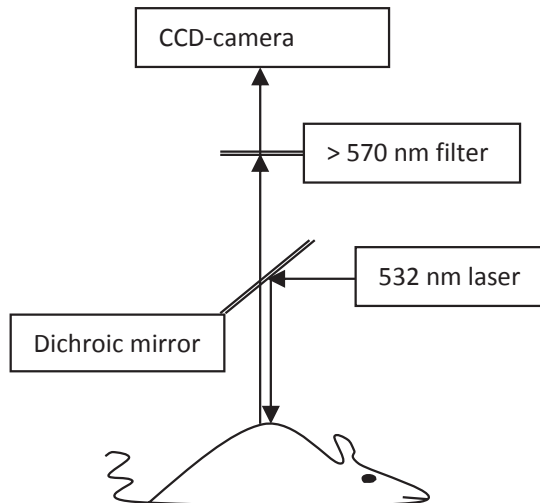


Figure 1. Setup. Laser light is delivered on the treatment area on mouse skin, while the fluorescence images are collected by a CCD camera.

In both groups (n=15 per group) all animals received a total light dose of 100 J cm^{-2} , but we used three different illumination schemes (n=5 animals per scheme). In one scheme 100 J cm^{-2} was delivered in a single illumination. In the second scheme an initial dose of 50 J cm^{-2} was delivered, followed by a dark interval of two hours and delivery of an additional 50 J cm^{-2} . In the third scheme the duration of the first light fraction was based on the extent of PpIX fluorescence photobleaching measured during PDT in individual animals (see fluorescence measurements section below). In this scheme the first illumination was stopped when approximately 50% of initial PpIX was photobleached. This was considered as the optimal photobleaching percentage for ALA in a previous experiment using the same mouse model and 50 mW cm^{-2} at 514 nm^7 . The dose of this first light fractions was on average in the order of 3 J cm^{-2} . The remaining fluence was delivered in the second light fraction to reach 100 J cm^{-2} in total.

Fluorescence measurements

Light from the 532 nm laser was focused on a 7mm treatment area and fluorescence images were taken using a CCD camera (ORCA-ER, Hamamatsu, Japan) which was also used to focus and to relocate the treatment area. Scattered excitation light was blocked from the spectrograph using a 570 nm long-pass filter. Fluorescence images were taken at regular time-intervals during illumination, without interrupting PDT light delivery. Protoporphyrin IX (PpIX) fluorescence intensity was used as a measure for the PpIX concentration and the extent of PpIX photobleaching. The images were corrected for the dark background signal and for a factor to account for the contribution from skin autofluorescence, which was measured in each animal before the administration of ALA or HAL.

Damage score

Damage scoring was performed daily up to seven days after PDT. A previously described visual scoring system was used with a scale from zero to five: 0 = no damage; 1 = minimal erythema; 2 = moderate erythema; 3 = severe erythema or a blister; 4 = thin crust and 5 = thick haemorrhagic crust²². Within the total treated area the damage score of smaller areas contributed to the total damage score based on their size relative to the total area.

Data analysis and statistics

To compare damages between groups and illumination schemes the cumulative damage score was calculated as the area under the curve (AUC) of the daily damage scores seven days after PDT. An ANOVA was used to test for differences in AUC between the illumination schemes within each group (HAL or ALA) using 0.05 as a significance level. To compare differences in rate of photobleaching and PpIX resynthesis during the dark interval the fluorescence was normalized by dividing the PpIX fluorescence intensity by its initial value before the first illumination. This normalisation step was performed to correct

for variations in these starting intensities. Differences in PpIX resynthesis and initial PpIX fluorescence intensity between the three groups were tested by means of independent samples T-test. Correlations between initial fluorescence intensity or PpIX resynthesis and cumulative skin damage (AUC) were calculated as Pearson's correlation coefficient.

RESULTS

Visual skin damage score

The daily visual skin damage in the days after PDT typically showed blister formation, followed by crust formation and healing of the treated skin. The general pattern was

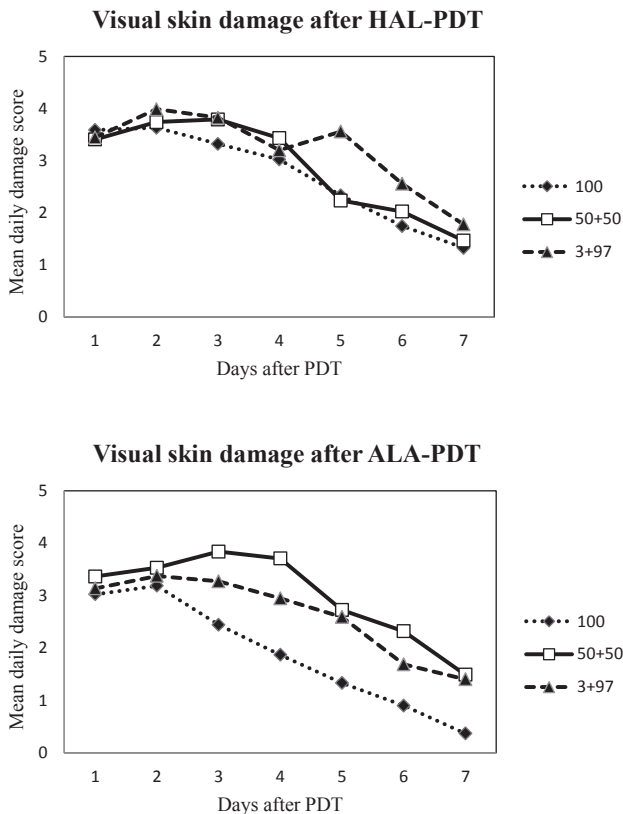


Figure 2. Visual skin damage score after PDT. The mean daily damage scores up to 7 days after PDT for each illumination scheme in the HAL(a) and ALA(b) groups. Scheme "100" refers to delivery of a 100 J cm^{-2} in a single illumination; "50+50" to delivery of 50 and 50 J cm^{-2} ; and "3+97" to delivery of a small first light fraction in the order of 3 J cm^{-2} , followed by a second light fraction to deliver 100 J cm^{-2} in total. For clarity standard deviations are not shown, but they average at 0.53 (range 0.04-1.19) and are similar for ALA and HAL.

similar for HAL and ALA (Figure 2). The three lines in this figure represent the three different illumination schemes, which overlap in the HAL group. In both the HAL and ALA groups the single illumination line (100 J cm^{-2}) is generally lower than the fractionated group lines ($50+50$ and $3+97 \text{ J cm}^{-2}$), but this is much more clearly visible in the ALA group. Also, only in the ALA group there was a significant difference in the calculated AUC between the illumination schemes (Figure 3, ANOVA, $P=0.039$). In the HAL ointment group however there was a trend towards increased damage for light fractionation (highest damage in the $3+97$ group and lowest in the single illumination group), but this trend was not significant ($P=0.157$, linear regression).

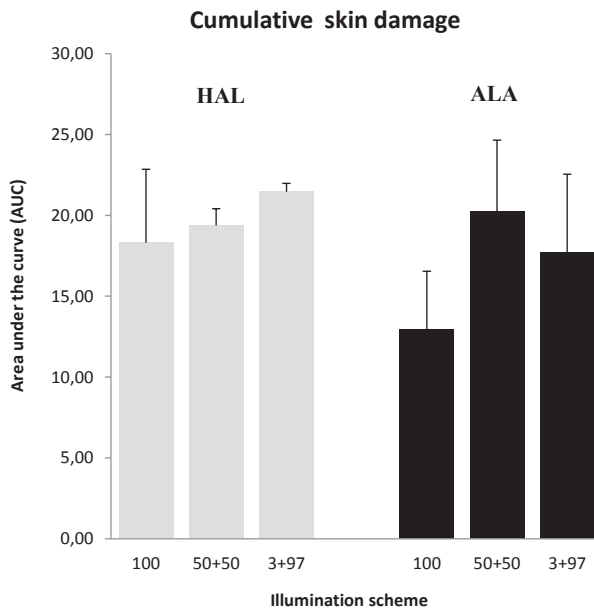


Figure 3. Cumulative visual skin damage per group and illumination scheme, presented as the area under the curve (AUC) of daily damage score up to 7 days after PDT. Scheme “100” refers to delivery of a 100 J cm^{-2} in a single illumination; “50+50” to delivery of 50 and 50 J cm^{-2} ; and “3+97” to delivery of a small first light fraction in the order of 3 J cm^{-2} , followed by a second light fraction to deliver 100 J cm^{-2} in total. Error bars indicate one standard deviation.

Protoporphyrin IX fluorescence measurements

There was large variation in starting PpIX fluorescence intensity (i.e. just before the first illumination) for both ALA and HAL. The starting fluorescence was significantly higher in the ALA group than in the HAL group (respectively mean 1760 a.u. , SD 628 and mean 1125 a.u. , SD 564 , $P=0.006$). This starting fluorescence intensity was not correlated with the cumulative skin damage (Pearson’s correlation coefficient = -0.16).

The PpIX resynthesis during the dark interval, which was defined as the increase in normalized PpIX fluorescence was also higher for ALA than for HAL, but this difference was not significant (respectively mean 66%, SD 24% and mean 44%, SD 25%, $P=0.06$). This PpIX resynthesis percentage was also not correlated with the cumulative skin damage (Pearson's correlation coefficient $=-0.08$). The variability in starting fluorescence, PpIX resynthesis and photobleaching is illustrated for the 50+50 illumination schemes in figure 4.

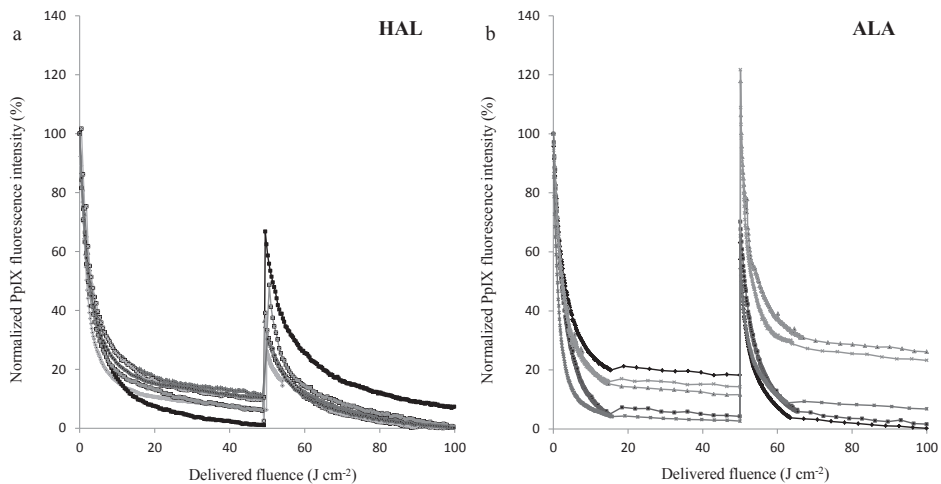


Figure 4. Examples of PpIX kinetics during illumination in the 50+50 $J\ cm^{-2}$ illumination scheme for (a): HAL and (b) ALA. Shown are PpIX fluorescence intensities normalized to the starting intensity for individual mice. Note the variability in photobleaching rate (slope of the curve) between individual animals, and in PpIX resynthesis percentage between HAL and ALA during the two-hour dark interval at 50 $J\ cm^{-2}$.

The rate of PpIX photobleaching (the slope of the curve) varied between individual animals. For each animal this rate was fastest in the beginning of the illumination and decreased with increasing fluence. Although individual animals showed variation in photobleaching rate, there was no systematic difference between ALA and HAL. This photobleaching rate for HAL and ALA is illustrated in figure 5 for the first 2 $J\ cm^{-2}$.

DISCUSSION

This study provides evidence to support that light fractionation may increase efficacy of HAL-PDT. For HAL the skin damage was highest in the scheme that received a low first dose of approximately 3 $J\ cm^{-2}$, which is exactly the scheme in which we expected

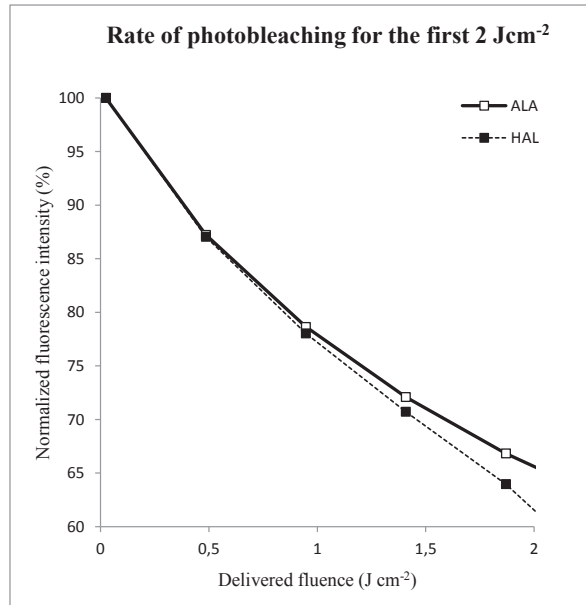


Figure 5. Photobleaching rate during first 2 J cm⁻² for HAL ALA. For each group the data represent the averages of the normalized PpIX fluorescence intensity in all mice of all illumination schemes (n=15 per group). Standard deviations were 8% on average, but are not presented for graphical clarity.

the highest efficacy, based on results from previous dose-finding studies with ALA^{6,7,22}. However, the difference in skin damage between the illumination schemes was not significant and a single illumination was already more effective for HAL than ALA. As briefly mentioned in the introduction it is important to keep in mind the mechanism behind increased efficacy for light fractionated ALA-PDT. Previous studies showed that for ALA the biodistribution in the vasculature is an important factor behind the increased PDT effect of light fractionation^{8-10,23}. Because the vascular distribution and vascular effects are similar for HAL and ALA¹⁹, we expected light fractionation to also significantly increase efficacy for HAL-PDT, but we found only a trend towards this result.

Before fully considering this finding it is interesting to first consider the higher initial PpIX synthesis for ALA than HAL. Note that the different PpIX concentrations should be interpreted carefully, because we used different concentrations of HAL than ALA (5% versus 20% respectively), which are both standard concentrations. Previous studies found that similar to up to 18 times lower concentrations of HAL than ALA are needed to yield similar PpIX concentrations^{17,19,24-26}. Taken into account the variability of tissue types and measurement methods used in these studies, our ratio of HAL/ALA concentration related to the PpIX concentration is somewhere in the middle of what is described in the literature. When interpreting our PpIX fluorescence findings it is crucial to realize that

we used a surface fluorescence measurement. Since the epidermal PpIX dominates the signal from surface fluorescence measurements, the method we used now is insensitive to differences in PpIX distributions or concentrations at depth. From our findings it can therefore be concluded that 20% ALA leads to higher epidermal PpIX concentrations than 5% HAL, but that deeper PpIX concentrations could not be measured.

The higher epidermal PpIX concentration for ALA is interesting because more PpIX leads to more singlet oxygen formation during PDT. It would therefore be logical to also expect higher damage scores in the ALA groups. However, we found no correlation between the initial PpIX synthesis and the skin damage, and also not between the amount of PpIX resynthesis and the skin damage. This indicates that the total amount of epidermal PpIX is not important for the effect of light fractionation. Instead, differences in PpIX distribution at depth such as in endothelial cells - resulting in different site of PDT damage- apparently play a more important role in the response to single and fractionated PDT for both HAL and ALA. This conclusion is in accordance with the conclusions from a previous study⁸.

When considering the effect of light fractionation on HAL-PDT, we found highest damage in the 3+97 group (mean AUC=21.5) and lowest in the single illumination group (mean AUC=18.3), which is as expected. This difference is relatively small however compared to what we found previously for ALA^{7,8,22}, and is also not statistically different. Whether or not this may still be a biologically relevant difference is not immediately clear. In figure 3 can be seen that the main reason that the additional effect of light fractionation was relatively small for HAL, is that a single illumination was already quite effective in inducing skin damage. Despite this, it is arguable that light fractionation may still provide additional benefit for HAL-PDT. The reasons for this are as follows.

First, for light fractionation to be most effective, the PDT dose of the first illumination needs to be low^{7,23}. Because we found that the effect of a single illumination lead to more damage for HAL than for ALA, it can be assumed that the first light fraction of a fractionated HAL scheme also does more damage. This in turn decreases the effect of light fractionation. Delivery of a smaller effective PDT dose in the first illumination may therefore be a logical and possible valuable improvement for light fractionated HAL-PDT.

Second, the other and possibly more important aspect in the mechanism behind light fractionation is the site of PDT damage. Even though our current PpIX fluorescence measurement method is insensitive to differences in PpIX distribution at depth, we did find a similar rate of photobleaching for HAL and ALA. In a comparable study that investigated the use of light fractionated MAL, it was found that the rate of photobleaching was

significantly slower for MAL than for ALA. It was hypothesized that this was due to a different distribution at depth, resulting in a different site of PDT damage. This hypothesis was further tested and confirmed in follow-up studies^{10,11}. Our current findings that the rate of photobleaching was the same for HAL and ALA may also indicate a similar distribution at depth of HAL and ALA. This is in accordance with previous findings that HAL and ALA share an ability to accumulate in endothelial cells, unlike MAL. This similarity in localisation and rate of photobleaching probably accounts for the tendency towards increased response for light fractionated HAL-PDT.

Third, our visual skin damage model may not be sensitive enough to measure a statistical increase when the efficacy is already high for a single illumination. The maximum score in our model is limited so every step towards higher PDT damage will tend to result in smaller increases in measured total cumulative skin damage. Eventually a maximum damage score plateau will be reached. The decreasing standard deviation with increasing cumulative skin damage for HAL could be an indication of the onset of this effect. To detect a statistically significant effect for smaller differences in efficacy may require more animals than the numbers that we have used in the present study. This may explain why we found a trend towards increased efficacy for light fractionation of HAL-PDT but no statistically significant difference. Although the scoring system can be considered a limitation of the current study, our model previously proved to be a good translational model, ultimately leading to increased clinical effect³.

Finally, it is important to realize that the light fractionation scheme we used in this study was extensively investigated and optimized for ALA, but not for HAL. It may well be that for HAL the optimal illumination scheme is somewhat different. As mentioned above, an interesting option would be to lower the effective PDT dose of the first illumination. This can be achieved by delivering the first illumination sooner (e.g. after two instead of four hours application) or by lowering the dose (e.g. 30% photobleaching instead of 50%) to decrease the amount of damage in this first light fraction. Possibly other illumination schemes, light doses or fluence rates may be better suitable for HAL.

Since the biodistribution of HAL, ALA and MAL plays an important role for the effect of light fractionation it is useful to realize that these molecules are similar to each other but differ in some important biological properties. The two main factors are differences in lipophilicity and in cellular uptake mechanisms. The lipophilicity is mainly relevant for the potential to penetrate through epithelial tissues. The uptake of ALA uptake depends on BETA transporters^{27,28}, whereas the ALA esters are taken up through PEPT1 or PEPT2 transporters²⁹ although other differences and also similarities in uptake mechanisms have been described³⁰. Different uptake mechanisms may result in differences in spatial

distribution of ALA, HAL, MAL and PpIX, which could play a role in the light fractionation process. However, our current setup was not designed and therefore not very sensitive to detect such differences.

Before coming to conclusions we need to address some limitations of the current study. One limitation is that our findings for our control group ALA were slightly different from what was expected. Although we could again show increased effect of light fractionation for ALA-PDT, we expected the damage to be highest in the 3+97 group instead of the 50+50 group. This expectation is based on previous study results in which slightly higher AUC scores (of around 22) were found in the 3+97 group using the same scoring model^{6,7,22}. Since no abnormalities occurred and PpIX photobleaching kinetics and the shape of daily damage response curves were as expected, we do not have an adequate explanation for this.

Another limitation is that our normal mouse skin model does not measure the effect of light fractionation in tumor tissue, but in healthy tissue only. Because tumor tissue is known to have a different vasculature and because the vasculature is believed to play a role in light fractionation we cannot exclude a potentially increased benefit of fractionation for HAL-PDT in tumor tissue. Similarly, other tissue types such as bladder or cervix may respond differently to light fractionation than skin. It would therefore be interesting to also study the effect of fractionated HAL-PDT in these tissues and in tumor models.

Unfortunately, to our knowledge there are no further studies on the effect of light fractionation on topical HAL-PDT in any tissue. It is therefore not easy to see our results against the background of existing literature. In this respect it should be noted that the rationale for a short light fractionated scheme such as used in two other studies^{31,32} is completely different from our light fractionation scheme. A repeated on/off cycle of light delivery in short light fractionation utilises available oxygen more efficiently, similar to lowering the fluence rate. Instead, our light fractionation scheme makes cells sensitive to a large second illumination after delivery of a short first illumination and a dark interval of at least two hours. Such short light fractionation schemes can therefore not be compared with our results. Nevertheless, use of short light fractionation schemes or low fluence rate PDT may be a very interesting option to decrease pain, which is a common problem in human skin³³.

In summary we have evidence to support that light fractionation may be beneficial for HAL-PDT. Since we did not see a statistically significant benefit we need to be cautious with this conclusion. We found that initial epidermal PpIX concentration and resynthesis

during the dark interval are irrelevant for the effect of light fractionation. Rather, the PpIX distribution at depth plays an important role. The same PpIX photobleaching rate of HAL and ALA may indicate a similar distribution which is in accordance with findings of similar PpIX distributions in previous studies. The light fractionated protocol for HAL can potentially be further optimized by delivery of a lower first light dose or by shortening the application time. The main rationale behind this option is to decrease the PDT damage of the first illumination. Also, the important role of the vasculature for light fractionation makes it interesting to also investigate fractionated HAL-PDT in tumour tissue which in general have more blood vessels. Such possibilities combined with the trend towards increased efficacy suggest that light fractionated HAL-PDT continues to be an interesting research topic to optimize PDT effect.

REFERENCES

1. Kennedy JC, Pottier RH, Pross DC. Photodynamic therapy with endogenous protoporphyrin IX: basic principles and present clinical experience. *J Photochem Photobiol B.* 1990;6(1-2):143-8.
2. de Haas ER, Kruijt B, Sterenborg HJ, Martino Neumann HA, Robinson DJ. Fractionated illumination significantly improves the response of superficial basal cell carcinoma to aminolevulinic acid photodynamic therapy. *J Invest Dermatol.* 2006;126(12):2679-86. Epub 006 Jul 13.
3. de Vijlder HC, Sterenborg HJ, Neumann HA, Robinson DJ, de Haas ER. Light fractionation significantly improves the response of superficial basal cell carcinoma to aminolevulinic acid photodynamic therapy: five-year follow-up of a randomized, prospective trial. *Acta Derm Venereol.* 2012;92(6):641-7. doi: 10.2340/00015555-1448.
4. Robinson DJ, de Bruijn HS, van der Veen N, Stringer MR, Brown SB, Star WM. Fluorescence photobleaching of ALA-induced protoporphyrin IX during photodynamic therapy of normal hairless mouse skin: the effect of light dose and irradiance and the resulting biological effect. *Photochem Photobiol.* 1998;67(1):140-9.
5. Robinson DJ, de Bruijn HS, de Wolf WJ, Sterenborg HJ, Star WM. Topical 5-aminolevulinic acid-photodynamic therapy of hairless mouse skin using two-fold illumination schemes: PpIX fluorescence kinetics, photobleaching and biological effect. *Photochem Photobiol.* 2000;72(6):794-802.
6. Robinson DJ, de Bruijn HS, Star WM, Sterenborg HJ. Dose and timing of the first light fraction in two-fold illumination schemes for topical ALA-mediated photodynamic therapy of hairless mouse skin. *Photochem Photobiol.* 2003;77(3):319-23.
7. de Bruijn HS, van der Ploeg-van den Heuvel A, Sterenborg HJ, Robinson DJ. Fractionated illumination after topical application of 5-aminolevulinic acid on normal skin of hairless mice: the influence of the dark interval. *J Photochem Photobiol B.* 2006;85(3):184-90. Epub 2006 Sep 1.
8. de Bruijn HS, de Haas ER, Hebeda KM, van der Ploeg-van den Heuvel A, Sterenborg HJ, Neumann HA, et al. Light fractionation does not enhance the efficacy of methyl 5-aminolevulinate mediated photodynamic therapy in normal mouse skin. *Photochem Photobiol Sci.* 2007;6(12):1325-31. Epub 2007 Aug 28.
9. de Bruijn HS, Meijers C, van der Ploeg-van den Heuvel A, Sterenborg HJ, Robinson DJ. Microscopic localisation of protoporphyrin IX in normal mouse skin after topical application of 5-aminolevulinic acid or methyl 5-aminolevulinate. *J Photochem Photobiol B.* 2008;92(2):91-7. doi: 10.1016/j.jphotobiol.2008.05.005. Epub May 15.
10. de Vijlder H, de Bruijn H, van der Ploeg-van den Heuvel A, Sterenborg H, Neumann H, de Haas E, et al. Differences in protoporphyrin IX localisation in dermal vasculature after topical application of 5-aminolevulinic acid and methyl-5 aminolevulinate. Submitted to: *Journal of photochemistry and photobiology.* 2013.
11. de Vijlder H, de Bruijn H, van der Ploeg-van den Heuvel A, van Zaane F, Schipper D, ten Hagen T, et al. Acute vascular responses during photodynamic therapy using topically administered porphyrin precursors. *Photochem Photobiol Sci* 2013 in press. 2013.

12. Soergel P, Wang X, Stepp H, Hertel H, Hillemanns P. Photodynamic therapy of cervical intraepithelial neoplasia with hexaminolevulinate. *Lasers Surg Med.* 2008;40(9):611-5. doi: 10.1002/lsm.20686.
13. Soergel P, Makowski L, Makowski E, Schippert C, Hertel H, Hillemanns P. Treatment of high grade cervical intraepithelial neoplasia by photodynamic therapy using hexylaminolevulinate may be costeffective compared to conisation procedures due to decreased pregnancy-related morbidity. *Lasers Surg Med.* 2011;43(7):713-20. doi: 10.1002/lsm.21072.
14. Soergel P, Dahl GF, Onsrud M, Hillemanns P. Photodynamic therapy of cervical intraepithelial neoplasia 1-3 and human papilloma virus (HMV) infection with methylaminolevulinate and hexaminolevulinate—a double-blind, dose-finding study. *Lasers Surg Med.* 2012;44(6):468-74. doi: 10.1002/lsm.22041. Epub 2012 Jun 12.
15. Juzeniene A, Nielsen KP, Zhao L, Ryzhikov GA, Biryulina MS, Stamnes JJ, et al. Changes in human skin after topical PDT with hexyl aminolevulinate. *Photodiagnosis Photodyn Ther.* 2008;5(3):176-81. Epub 2008 Aug 28.
16. Bader MJ, Stepp H, Beyer W, Pongratz T, Sroka R, Kriegmair M, et al. Photodynamic Therapy of Bladder Cancer - A Phase I Study Using Hexaminolevulinate (HAL). *Urol Oncol.* 2012;20:20.
17. Dognitz N, Salomon D, Zellweger M, Ballini JP, Gabrecht T, Lange N, et al. Comparison of ALA- and ALA hexyl-ester-induced PpIX depth distribution in human skin carcinoma. *J Photochem Photobiol B.* 2008;93(3):140-8. Epub 2008 Aug 17.
18. Rodriguez L, de Bruijn HS, Di Venosa G, Mamone L, Robinson DJ, Juarranz A, et al. Porphyrin synthesis from aminolevulinic acid esters in endothelial cells and its role in photodynamic therapy. *J Photochem Photobiol B.* 2009;96(3):249-54. Epub 2009 Jul 5.
19. Middelburg T, De Bruijn H, Tettero L, Van der Ploeg van den Heuvel A, Neumann H, De Haas E, et al. Topical Hexylaminolevulinate and Aminolevulinic Acid Photodynamic Therapy: Complete Arteriole Vasoconstriction Occurs Frequently and Depends on Protoporphyrin IX Concentration in Vessel Wall. *Journal of photochemistry and photobiology B: Biology.* 2013; Accepted for publication.
20. Langmack K, Mehta R, Twyman P, Norris P. Topical photodynamic therapy at low fluence rates—theory and practice. *J Photochem Photobiol B.* 2001;60(1):37-43.
21. Finlay JC, Mitra S, Patterson MS, Foster TH. Photobleaching kinetics of Photofrin in vivo and in multicell tumour spheroids indicate two simultaneous bleaching mechanisms. *Phys Med Biol.* 2004;49(21):4837-60.
22. Middelburg TA, Van Zaane F, De Bruijn HS, Van Der Ploeg-van den Heuvel A, Sterenberg HJ, Neumann HA, et al. Fractionated illumination at low fluence rate photodynamic therapy in mice. *Photochem Photobiol.* 2010;86(5):1140-6. doi: 10.1111/j.751-097.2010.00760.x.
23. de Bruijn HS, Casas AG, Di Venosa G, Gandara L, Sterenberg HJ, Batlle A, et al. Light fractionated ALA-PDT enhances therapeutic efficacy in vitro; the influence of PpIX concentration and illumination parameters. *Photochem Photobiol Sci.* 2013;12(2):241-5. doi: 10.1039/c2pp25287b. Epub 2012 Oct 29.

24. Marti A, Jichlinski P, Lange N, Ballini JP, Guillou L, Leisinger HJ, et al. Comparison of aminolevulinic acid and hexylester aminolevulinate induced protoporphyrin IX distribution in human bladder cancer. *J Urol*. 2003;170(2 Pt 1):428-32.
25. Endlicher E, Rummele P, Hausmann F, Krieg R, Knuchel R, Rath HC, et al. Protoporphyrin IX distribution following local application of 5-aminolevulinic acid and its esterified derivatives in the tissue layers of the normal rat colon. *Br J Cancer*. 2001;85(10):1572-6.
26. Casas A, Perotti C, Fukuda H, Rogers L, Butler AR, Batlle A. ALA and ALA hexyl ester-induced porphyrin synthesis in chemically induced skin tumours: the role of different vehicles on improving photosensitization. *Br J Cancer*. 2001;85(11):1794-800.
27. Rud E, Gederaas O, Hogset A, Berg K. 5-aminolevulinic acid, but not 5-aminolevulinic acid esters, is transported into adenocarcinoma cells by system BETA transporters. *Photochem Photobiol*. 2000;71(5):640-7.
28. Rodriguez L, Batlle A, Di Venosa G, Battah S, Dobbin P, MacRobert AJ, et al. Mechanisms of 5-aminolevulinic acid ester uptake in mammalian cells. *Br J Pharmacol*. 2006;147(7):825-33.
29. Rodriguez L, Batlle A, Di Venosa G, MacRobert AJ, Battah S, Daniel H, et al. Study of the mechanisms of uptake of 5-aminolevulinic acid derivatives by PEPT1 and PEPT2 transporters as a tool to improve photodynamic therapy of tumours. *Int J Biochem Cell Biol*. 2006;38(9):1530-9. Epub 2006 Mar 18.
30. Schulten R, Novak B, Schmitz B, Lubbert H. Comparison of the uptake of 5-aminolevulinic acid and its methyl ester in keratinocytes and skin. *Naunyn Schmiedebergs Arch Pharmacol*. 2012;385(10):969-79. doi: 10.1007/s00210-012-0777-4. Epub 2012 Jul 17.
31. Ascencio M, Estevez JP, Delemer M, Farine MO, Collinet P, Mordon S. Comparison of continuous and fractionated illumination during hexaminolaevulinate-photodynamic therapy. *Photodiagnosis Photodyn Ther*. 2008;5(3):210-6. Epub 2008 Oct 19.
32. Estevez JP, Ascencio M, Colin P, Farine MO, Collinet P, Mordon S. Continuous or fractionated photodynamic therapy? Comparison of three PDT schemes for ovarian peritoneal micrometastasis treatment in a rat model. *Photodiagnosis Photodyn Ther*. 2010;7(4):251-7. doi: 10.1016/j.pdpdt.2010.07.007. Epub Aug 14.
33. Mikolajewska P. Pain during topical photodynamic therapy [www document]. 2011;https://www.duo.uio.no/handle/10852/11075?locale-attribute=en [accessed on 12 March 2013].

7

Monitoring blood volume and saturation using superficial fibre optic reflectance spectroscopy during PDT of actinic keratosis.

Tom Middelburg
Chad Kanick
Ellen de Haas
Dick Sterenborg
Arjen Amelink
Martino Neumann
Dominic Robinson

J Biophotonics. 2011;4(10):721-30.

ABSTRACT

Optically monitoring the vascular physiology during photodynamic therapy (PDT) may help understand patient-specific treatment outcome. However, diffuse optical techniques have failed to observe changes herein, probably by optically sampling too deep. Therefore, we investigated using differential path-length spectroscopy (DPS) to obtain superficial measurements of vascular physiology in actinic keratosis (AK). The AK-specific DPS interrogation depth was chosen up to 400 microns in depth, based on the thickness of AK histology samples. During light fractionated aminolevulinic acid-PDT, reflectance spectra were analyzed to yield quantitative estimates of blood volume and saturation. Blood volume showed significant lesion-specific changes during PDT without a general trend for all lesions and saturation remained high during PDT. This study shows that DPS allows optically monitoring the superficial blood volume and saturation during skin PDT. The patient-specific variability supports the need for dosimetric measurements. In DPS, the lesion-specific optimal interrogation depth can be varied based on lesion thickness.

INTRODUCTION

In photodynamic therapy (PDT) a photosensitizer mediates the transfer of light energy to oxygen, which results in the formation of reactive oxygen species, notably singlet oxygen. This leads to cellular damage and to vascular and immunologic responses that can destroy dysplastic tissue. PDT has been applied in various organs including the skin, in which PDT using porphyrin precursors such as aminolevulinic acid (ALA) is being used worldwide. One of the indications for PDT is actinic keratosis (AK), an intraepithelial dysplasia that may progress into squamous cell carcinoma. PDT for AK is painful but usually effective, although recurrence rates are around 20%. In these recurrent lesions, there must be a reason why they respond insufficiently to PDT. The response of tissue to PDT is influenced by three important parameters: the concentrations of oxygen, of the photosensitizer, and the local light fluence. These vary significantly due to the use of different light treatment schedules and light sources and due to patient- and/or tumor-specific biological variations. These variations result in differences in effective PDT doses and therefore are likely to be responsible for incomplete responses. They may also be related to adverse events such as pain during treatment. To date, several studies have revealed the importance of using techniques that monitor these parameters during PDT to optimize individual patient dosimetry.^{1-7.}

As one of these techniques, reflectance spectroscopy is capable of measuring changes in tissue optical properties that provide information on the oxygen supply during PDT by measuring blood saturation and blood volume. Several different methods of reflectance spectroscopy exist that involve measuring reflectance over a broad range of wavelengths. The major differences between them are the optically interrogated volume and the uncertainty about the photon path length in tissue. To quantify the data of reflectance spectroscopy, mathematical models have been developed that incorporate Mie and Raleigh scattering mechanisms and the effects of main absorbing components of skin (i.e. hemoglobin, deoxyhemoglobin, melanin, and water)^{8-11.}

Although it is clearly important to measure blood oxygenation during PDT, two studies illustrate the complexity of using reflectance spectroscopy for this purpose. In one study diffuse reflectance spectroscopy (DRS) was used to measure reflectance spectra before and after PDT of mouse skin but no differences between the spectra were found^{12.} Also, in basal cell carcinoma Cottrell et al did not observe changes in spectra before and after PDT using DRS^{13.} In both studies DRS is likely to be not sensitive enough to detect changes in blood flow and oxygenation during PDT. This is because the oxygen that is involved in the PDT process is supplied by blood located in superficial dermal capillaries, while DRS measurements are strongly influenced by reflectance signals

from deeper blood vessels. It is however very unlikely that there are no true changes in blood volume and oxygenation because porphyrins have been known to have vascular effects, for which it is used in treating for example ocular neovascularization. As vascular endothelial cells accumulate PpIX also after topical ALA application, vascular effects are also expected in topical ALA-PDT.

To further study the tissue oxygenation effects during ALA-PDT while overcoming the problems occurring in DRS, we used a technique termed differential path-length spectroscopy (DPS) in this study and introduced its use in human skin. In principle, DPS allows for much more accurate reflectance measurements in the relevant superficial volume. DPS is based on two optical fibers that are in contact with the measured medium. One fiber is used for delivery and collection of light and one is used for collection only. The delivery-and-collection fiber measures superficially scattered light, while light that is scattered deeper in the tissue is collected by both fibers. Subtracting the two signals provides the DPS signal and by choosing different fiber diameters, the interrogation volume can be accurately determined. Additionally, model-based analysis of the DPS signals provides quantitative descriptions of vascular physiology that are independent of background tissue optical properties^{10, 14-16}.

In the present study we investigated the use of DPS in patients undergoing light fractionated ALA-PDT for AK. Since this is the first study using DPS to acquire reflectance spectra in human skin and in AK, its architecture had to be first considered in order to choose a probe with the correct optical interrogation volume. AK has a thicker epidermis than normal skin and since the relevant capillaries are situated directly under the epidermis we needed to measure the thickness of AK in skin biopsies and to design a probe based on these measurements.

Our goal was to investigate if DPS can be used to derive quantitative data of the superficial blood volume and oxygenation in human skin and if these would change during ALA-PDT for actinic keratosis. This will add to our understanding of PDT and support the attempts to optimize dosimetry aimed at improving the tolerability and/or efficacy of ALA-PDT.

MATERIALS AND METHODS

Patients and procedures

The epidermal thickness of AK excision biopsies from twenty patients was measured (see below). All lesions were located on the face and diagnosis was confirmed by a trained

pathologist. Nine other patients with a total of nine lesions received standard fractionated ALA-PDT for facial AK in which two illuminations (20 and 80 Jcm⁻² at 80 mW cm⁻² using an Omnilux[®] Waldmann LED device centered at 633 ± 20 nm) are delivered 4 and 6 hours after topical application of ALA cream (Fagron[®], Oud Beijerland, The Netherlands). The two illuminations were separated by a two-hour dark interval. In these nine patients DPS spectra were acquired by gently bringing the DPS probe into contact with the skin immediately before and after each illumination; these time points will be referred to as [Pre1, Post1, Pre2, Post2] throughout this manuscript. We took three repeated measurements, by removing and replacing the probe, from the centre and from the margin of the lesion and, as a control, from normal appearing skin from the contra-lateral side. A single measurement took approximately 3 seconds and all measurements were performed by one investigator (T.M.) to minimize inter-individual differences in pressure.

Epidermal thickness

In the paraffin-embedded and haematoxylin and eosin stained sections the epidermal thickness was measured from the granular to the basal layer, using a light microscope and a calibrated 2 mm long liner with intervals of 10 microns. Multiple sections of each lesion were scanned to locate the thickest and thinnest dysplastic area. In addition, a visual overall average thickness was estimated. Table 1 shows the findings of these measurements. The minimum thickness ranged from 30 to 360 microns (mean 120, median 100) and the maximum thickness ranged from 80 to 1000 microns (mean 510, median 550). The mean visually estimated thickness was 310 (SD 200). Patients mean age was 79 years (range 57-94) and maximum vessel diameter averaged 70 microns (range 30-100).

Table 1: Histologically measured thickness of twenty actinic keratosis sections.

	Thinnest dysplastic area	Thickest dysplastic area	Visual average	Age
Range	30 - 360	80 - 1000	60 - 720	57 - 94
Mean (SD)	122 (77)	514 (306)	313 (199)	79 (10)
Median (IQR)	95 (75-148)	550 (228-763)	280 (158-425)	81 (74-86)

The range, mean, standard deviation (SD), median and interquartile ranges (IQR) for the thinnest and thickest dysplastic area in each section are presented; as well as for the age and the visual average thickness.

DPS probe design

Based on these findings we chose to use an 800 microns diameter DPS probe that enabled us to obtain a DPS signal 400 microns deep¹⁶. This depth contains the whole epidermis (310 microns) and a fraction of papillary dermis (90 microns) where the blood vessels are located that oxygenate the dysplastic tissue during PDT. A DPS probe contains two optical fibers (Ocean Optics) of which one is used for delivery and collection

(dc) of light and the other adjacent fiber is used for light collection only (c), see Figure 1. Light from a tungsten halogen lamp (Avantes HL-2000) was coupled to one arm of an 800- μm bifurcated fiber (Ocean Optics). A second arm was connected to a dual-channel spectrograph with a notch filter inserted so that the system could be used for fluorescence measurements in other monitoring applications.

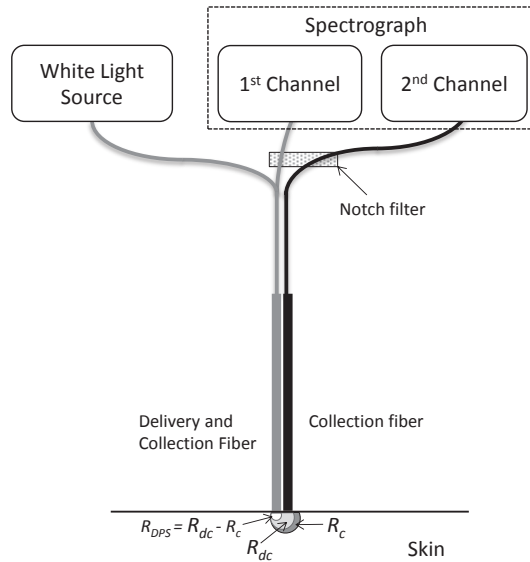


Figure 1. DPS experimental setup. During measurement light is delivered to the tissue by the dc-fiber and light remitted from the tissue is collected by both the delivery and collection (dc)-fiber and collection (c)-fiber and sent to a spectrograph. The dc-fiber collects both superficially and deeply scattered light, while the c-fiber collects only deeply scattered light. Subtraction of the two signals yields the superficially localized DPS signal.

Both the spectrograph and lamp were controlled by a custom made LabView program (National Instruments LabView 7.1) on a notebook computer. The other ends of the fibers, used for skin contact, were polished to an angle of 15° to minimize the collection of specularly reflected light at the probe-skin interface. Superficially scattered light was collected by the dc fiber, while light that was scattered deeper in the tissue was collected by both fibers. Subtracting these signals provides the superficial DPS signal.

To calibrate the setup we measured spectra from black and white Spectralon standards (Labsphere SRS-99 and SRS-02) in air and in a water-filled dark container. The difference in black and white measurement was used to correct for variations in lamp output and fiber-specific transmission properties while the air versus water measurement was used to correct for internal reflections¹⁷.

Data analysis

To derive quantitative information on amount and saturation of blood within the optically sampled tissue volume, all spectra were fitted using a Levenberg-Marquardt least squares fitting routine that uses the standard deviations of the binned data points calculated from 4 neighbouring pixels as weight factors. Background scattering and tissue absorption were incorporated using the models to calculate reflectance as first described by Amelink et al¹⁷ and later optimized by adding an extra Rayleigh scattering component^{18,19}. The absorption coefficient of skin μ_a was described by:

$$\mu_a = BVF \cdot (StO_2 \cdot \mu_a^{HbO_2}(\lambda) + (1 - StO_2) \cdot \mu_a^{Hb}(\lambda)) \cdot C_{corr}(\lambda) + Mel \cdot \mu_a^{Mel}$$

$$\text{where } \mu_a^{Mel} = p_1 \lambda_a^{p_2}$$

and where BVF is the blood volume fraction of the sampled tissue, StO_2 is the micro-vascular blood oxygen saturation, $\mu_a^{HbO_2}$ and μ_a^{Hb} are the absorption coefficients of fully oxygenated and deoxygenated blood respectively, and C_{corr} is a correction factor that depends on vessel diameter and accounts for the inhomogeneous distribution of blood in tissue²⁰. Mel is the concentration of melanin and the contribution of melanin to the tissue absorption is calculated by using the specific absorption coefficient μ_a^{Mel} , where p_1 and p_2 were estimated using the method described by Jacques²¹. The tissue reflectance (R_{DPS}) can be described by applying a Beer-Lambert description of absorption to the background scattering model, as:

$$R_{DPS} = a_1 \left[a_2 \frac{\lambda^{-b}}{\lambda_0} + (1 - a_2) \frac{\lambda^{-4}}{\lambda_0} \right] \exp(\mu_a \cdot \langle L \rangle)$$

The term in brackets represents a background scattering model composed of Mie and Rayleigh components. The fractional contributions of Mie and Rayleigh components are estimated by fitting the parameter a_2 (which occupied values in the range 0-1), and the respective wavelength dependencies of the components are given as λ^{-b} and λ^{-4} , where b is a fitted parameter. The fitted parameter a_1 corrects for changes in the absolute amplitude of the measured reflectance intensity; the value of a_1 is dependent on the distance between probe and Spectralon during calibration measurements and does not inform estimates of tissue scattering properties. The DPS photon path length -given as $\langle L \rangle$ - is insensitive to scattering effects in skin, as it is expected to fall within the range of 5-50 mm⁻¹. However, it can in part depend on the absorption coefficients, especially for the probe diameter d_{fiber} utilized in this study. We accounted for this dependence by using an empirical expression described previously by Kaspers et al¹⁴, given as;

$$\langle L \rangle = \frac{1.08 d_{fiber}}{1 + 1n(1 + 0.71 \mu_a d_{fiber})}$$

Statistics

Differences were statistically analysed using a paired Wilcoxon test, using $P < 0.05$ for significance.

RESULTS

Spectral fitting and a representative single lesion example

Figure 2a shows a representative example of the variations in measured BVF and StO_2 from one lesion during the course of light fractionated PDT. Each point represents the mean, weighted by the standard deviation of three measurements taken at the centre of a single lesion; there was little variation between these three measurements as is

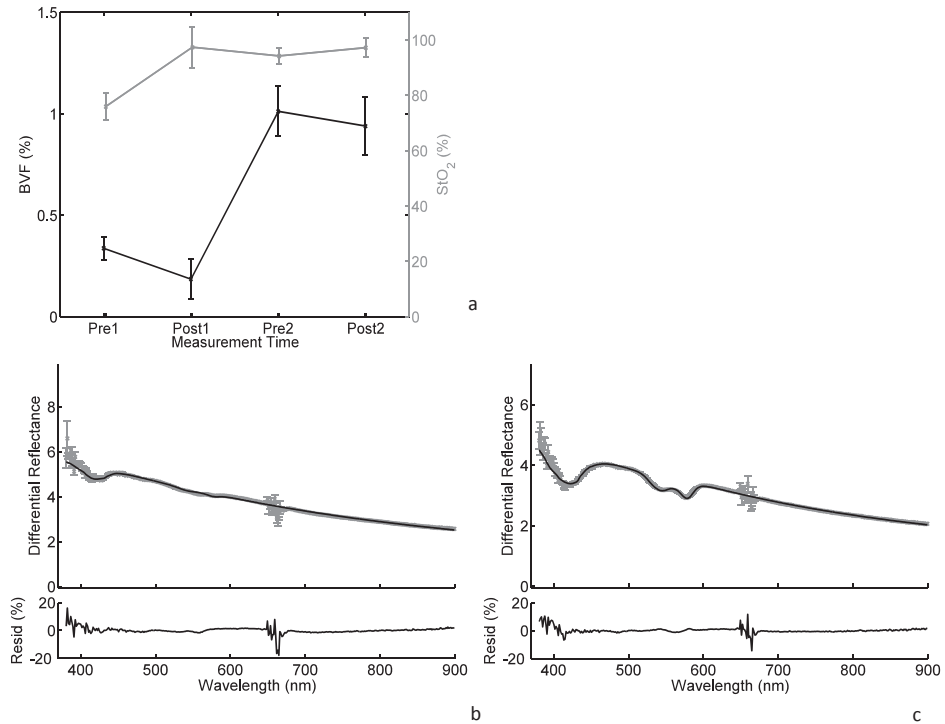


Figure 2. (a) Variations in BVF (black line) and StO_2 (grey line) from one representative lesion at different time points during the course of light fractionated PDT. Each data point represents the average value weighted by the standard deviations of three measurements taken from the centre of the lesion. (b) and (c) DPS reflectance spectra acquired before the first illumination (b, Pre1) and before the second illumination (c, Pre2) of the same lesion. Measured spectra are given as the grey data points and model fit is given as the black line. Model analysis yielded estimates of BVF and StO_2 . The residual line (given as Resid) below the spectra in both figures represents the percentage deviation between the model fit and the measured data.

illustrated by the relatively small 95% confidence intervals. During PDT of this lesion, the StO_2 increased after the first illumination and remained high before and after the second illumination; whereas the BVF decreased during the first illumination, increased considerably in the dark interval and decreased slightly during the second illumination. Note that the lines connecting the points are drawn only to illustrate the changes in the vascular physiology; they do not suggest linearity. Figures 2b and 2c show spectra corresponding to individual measurements acquired before the first and before the second illumination respectively. The model fit (solid line) of the blue data points illustrates the quality of the fitting procedure. The double dip in the 500-600 nm wavelength region in figure 2c indicates the characteristic presence of blood, in this case oxygenated haemoglobin, whereas in figure 2b the spectrum showed the presence of a much lower blood volume. Note the variability in the data points around 650 nm, which was caused by the notch filter but did not affect quality of the fit. High quality fitting was achieved in over 90% of measurements, also in the case of low blood volumes. Spectra that did not fit were excluded based on the presence of observable features in the residual between the model fit and the data ²². The poor quality of some individual measurements was due to probe and/or patient movement and incomplete contact between the probe and the skin surface.

Average saturation and blood volume fraction during light fractionated PDT

While the average StO_2 of individual lesions varied between 40-100%, the saturation was generally high and there was no consistent pattern in the StO_2 changes between patients. This is illustrated for the measurements obtained from the centres of the lesions in figure 3a. The BVF showed high variability between lesions, between the different time point measurements during PDT, but not between the three measurements of the same lesion as is illustrated for the centres of the lesions in figure 3b. There was no consistent pattern in BVF change during the course of light fractionated PDT for the group of lesions as a whole. However, for patients showing a low initial BVF (less than 0.5%), a trend was observed that the BVF relative to its starting value increased between time points Pre1 and Pre2 (bold lines in figure 3b). In figures 4a and 4b data points represent the mean relative BVF measured at each location (lesion centre, margin, and normal skin) at each sampled time point; each data point is relative to the value at the initial time point Pre1 (measured pre-treatment). For the subset of patients that had an initial BVF < 0.5% in the centre of the lesion, the median BVF increased by a factor of 2.9 ($P=0.06$), following the dark interval and prior to the second illumination (figure 4a). Interestingly, these patients show no such trend immediately after the 1st illumination; instead they showed increased variability immediately following treatment illumination as evidenced by the large interquartile ranges. The trend observed in Figure 4a was not observed at the margin or normal measurement locations. Moreover, patients that had

an initial BVF > 0.5% did not exhibit the trend shown in Figure 4a, instead showing an increasing inter-patient variability in BVF changes in response to treatment, illustrated by increasing inter-quartile ranges (Figure 4b).

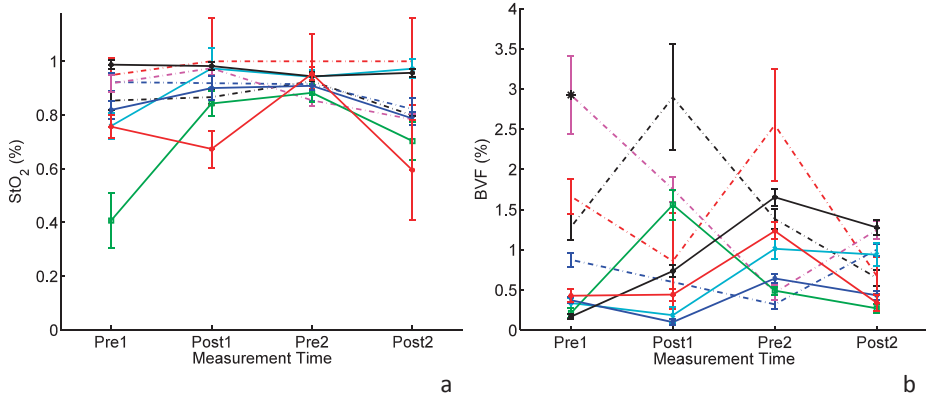


Figure 3. (a) StO_2 and (b) BVF measured in all lesions at each sampled time point during the course of light fractionated PDT. Each line represents one lesion and each data point represents the average StO_2 weighted by the standard deviation of three measurements taken from the center. On panel (b) the * mark indicates lesion 5; see text for details.

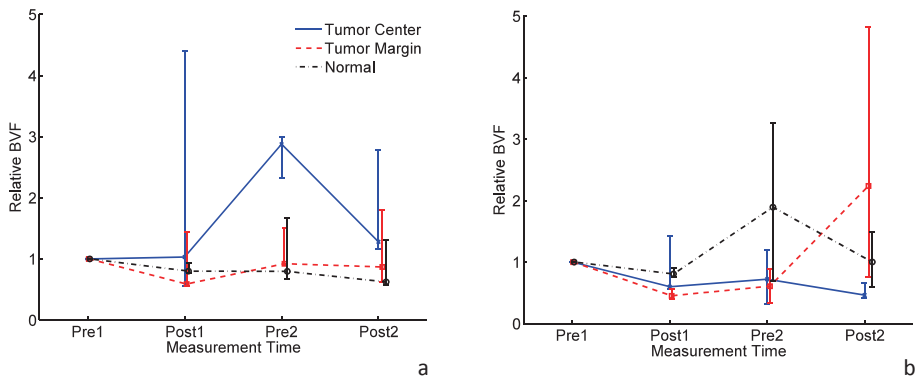


Figure 4. Relative BVF, expressed as a percentage of the measured value at time Pre1, at each sampled location (lesion center, lesion margin, and normal skin), and at each time point during the course of light fractionated PDT. Panel (a) shows relative BVF for patients with BVF < 0.5 % at the initial measurement (Pre1) in the center of the lesion. Panel (b) shows relative BVF for patients with BVF > 0.5 % at the initial measurement (Pre1) in the center of the lesion. Each data point represents the median relative BVF and the error bars represent interquartile ranges for all patients within the subgroup.

DISCUSSION

This study is the first to describe the use of DPS in human skin and it shows that DPS enables measurement of blood volume and saturation very superficially, and that it can be used to monitor changes herein during PDT for actinic keratosis. This is in contrast to what others have tried before when using other optical techniques such as DRS that are influenced by deeper signals. Our study also demonstrates the importance of choosing a probe diameter –and thus the interrogation depth- based on tissue properties, e.g. the histological thickness of AK. Ideally one would choose the fiber diameter based on a patient's individual histological thickness. We measured an average thickness that was 310 microns and showed a considerable variation (range 30 to 1000 microns). This is an important finding because in PDT the penetration of both drug and light is affected mainly by the epidermal thickness. In all our measurements we were able to measure the presence of blood, indicating that the diameter of our DPS probe of 800 microns was indeed appropriately chosen, measuring up to 400 microns in depth. The measurement of AK thickness was not only necessary for our probe design, but was also another relatively new feature to our study as this has not been studied well in the literature. One study found a mean maximum AK thickness of 110 ± 10 microns in 10 patients, which is included in our interrogation volume.²³

When considering the DPS spectra, our mathematical model resulted in good quality fits of the data, indicating that the results are reliable as is illustrated in figures 2b and 2c. Figure 2a also shows that single measurements were precise because they were repeatable with only small variations between them. The observed blood volume and saturation in this particular lesion is very interesting, because these changed considerably during PDT. For example: during the first illumination the saturation increased while the blood volume decreased. Since PDT consumes oxygen, this can only be explained by another factor such as increased blood flow, which we have not measured but a rapid increase in blood flow was recently demonstrated in a study on ALA-PDT for basal cell carcinoma²⁴. Another feature in this lesion is that during the dark interval the blood volume increased as much as fourfold. Apparently the blood vessels have dilated in that lesion after the first illumination. PDT is known to induce an inflammatory response and the increase could be explained by vasoactive cytokine release. Since ALA-PDT induces immediate vasoconstriction, another explanation might be a compensatory vasodilatation. It is reasonable to expect that the photodynamic process in this particular lesion is influenced by these changes, possibly influencing clinical outcome.

Not all lesions showed this pattern however. Especially for the blood volume there were large differences between lesions. In lesion five for example, represented by the dashed

purple line and marked with a * in figure 3b, the blood volume showed a completely different pattern. In that lesion the starting blood volume was much higher and it decreased during the first illumination and the dark interval to increase again during the second illumination. It is clear that these changes affect the PDT process in this lesion in a completely different way than the lesion illustrated in figure 1. These observations indicate that individual lesions and patients show changes that are important for the PDT effect, but that it is not possible to draw any general predictive conclusions. The clinical implication is that care should be taken when treatment schemes are applied to all patients or lesions while they may respond differently to treatment.

When considering the blood volume data of all patients, we noticed a pattern that in the center of lesions the blood volume increased during the dark interval in those lesions that had low initial starting values, whereas this was not the case in lesions that started with high blood volumes (figure 4). This increase in blood volume before the second illumination relative to the starting value was borderline statistically significant ($p=0.06$). This may be a real effect or it may be explained by regression to the mean or possibly because the blood vessels were already maximally stretched initially. It might mean however that these patients need an alternative approach, for which further study is needed.

Since this is the first time we used DPS in human skin, it is important to put our findings in perspective to other measurement techniques and to the PDT process in whole. Although we did not find a general trend or pattern for the blood volume and saturation, we did find different effects for different lesions. Other techniques previously also showed no overall changes but more importantly: they also showed no difference between lesions¹³. As explained in the introduction these techniques may not be sensitive for very superficial tissue volumes, where the PDT process takes place. Although we did not compare these techniques directly in this study, arguably DPS is more sensitive for superficial measurements. Using DPS, we have now shown that individual lesions respond differently to PDT with respect to blood volume and saturation. This highlights the fact that lesions need to be treated differently based on its individual properties. With respect to the PDT process as a whole it is immediately clear that we have not yet attempted to measure a critical parameter: the amount of PpIX within the lesion. It is very likely that the amount of PpIX within AK has a direct impact on the physiological responses that we observe. It is well known that local superficial quantitative measurements of tissue fluorescence are challenging and can be strongly influenced by the light delivery, tissue optical properties and collection geometries. The combination of superficial reflectance and photosensitizer fluorescence spectroscopy will be reported in a future study.

Before drawing conclusions from our study it is important to consider some limitations. First, to demonstrate the possible use of DPS in human skin we needed only a few patients, but to discover statistically significant changes in blood volume and saturation the power may have been too low. Second, we measured blood volume and microvascular saturation as a proxy measure for tissue oxygenation, not taking the time for oxygen to diffuse to the tissue into account. Related to this, the third limitation was the speed of measurements. Dynamic vascular effects such as a sudden increase in blood flow may not be detected during the ten seconds needed to perform the three measurements taken at each time-point. In general, the blood flow in capillaries is relatively slow however and we found no systematic difference in blood volume in time between these three measurements, indicating that neither speed of measurements nor pressure had a major impact. Time and speed of measurement remain important considerations though. It may be interesting to take a reflection spectrum during the second illumination at the time-point where 20 J cm⁻² was delivered, which is equal to the total dose during the first illumination. At the end of the second illumination only a small amount of PpIX remains that may not be sufficient to have a significant effect on the microvasculature. A fourth limitation is that lesion-specific variability in thickness may explain the starting variability of blood volume between patients. The variability in response in individual lesions however, cannot be caused by this. Also, possible changes in lesion thickness due to edema formation during the dark interval were not accounted for. The effect of this is expected to be small but it could be interesting to test this using small and large fibre diameter probes and compare the difference. Finally, we had to exclude about 10% of the spectra from our data analysis because of unsuccessful fits. Possible explanations for this are movement of the probe during the measurement, a bad contact with the skin or possible ambient light or the presence of other chromophores. For future use of this technique it would be useful to identify these failed measurements during the acquisition procedure.

In conclusion we showed that DPS can be used to measure blood volume and saturation in human skin. We also showed that individual lesions behave differently in ALA-PDT with respect to blood volume and saturation, which has not been shown using other techniques. This means that the current approach of treating all lesions with the same light dose may need to be reconsidered. It also means that DPS may be advantageous to other techniques such as diffuse reflectance spectroscopy to monitor blood volume and saturation in skin PDT. Our data show the need to monitor patient-specific vascular physiology during PDT. Moreover, incorporating fluorescence measurements using DPS would allow monitoring photosensitizer concentration; this will be incorporated in future studies.

REFERENCES

1. Yu G, Durduran T, Zhou C, Zhu TC, Finlay JC, Busch TM, et al. Real-time in situ monitoring of human prostate photodynamic therapy with diffuse light. *Photochem Photobiol.* 2006;82(5):1279-84.
2. Dysart JS, Patterson MS, Farrell TJ, Singh G. Relationship between mTHPC fluorescence photobleaching and cell viability during in vitro photodynamic treatment of DP16 cells. *Photochem Photobiol.* 2002;75(3):289-95.
3. Sitnik TM, Henderson BW. The effect of fluence rate on tumor and normal tissue responses to photodynamic therapy. *Photochem Photobiol.* 1998;67(4):462-6.
4. Wang HW, Putt ME, Emanuele MJ, Shin DB, Glatstein E, Yodh AG, et al. Treatment-induced changes in tumor oxygenation predict photodynamic therapy outcome. *Cancer Res.* 2004;64(20):7553-61.
5. Boere IA, Robinson DJ, de Bruijn HS, van den Boogert J, Tilanus HW, Sterenberg HJ, et al. Monitoring in situ dosimetry and protoporphyrin IX fluorescence photobleaching in the normal rat esophagus during 5-aminolevulinic acid photodynamic therapy. *Photochem Photobiol.* 2003;78(3):271-7.
6. Zeng H, Korbelik M, McLean DJ, MacAulay C, Lui H. Monitoring photoproduct formation and photobleaching by fluorescence spectroscopy has the potential to improve PDT dosimetry with a verteporfin-like photosensitizer. *Photochem Photobiol.* 2002;75(4):398-405.
7. Robinson DJ, de Bruijn HS, van der Veen N, Stringer MR, Brown SB, Star WM. Fluorescence photobleaching of ALA-induced protoporphyrin IX during photodynamic therapy of normal hairless mouse skin: the effect of light dose and irradiance and the resulting biological effect. *Photochem Photobiol.* 1998;67(1):140-9.
8. Tseng SH, Bargo P, Durkin A, Kollias N. Chromophore concentrations, absorption and scattering properties of human skin in-vivo. *Opt Express.* 2009;17(17):14599-617.
9. Amelink A, van der Ploeg van den Heuvel A, de Wolf WJ, Robinson DJ, Sterenberg HJ. Monitoring PDT by means of superficial reflectance spectroscopy. *J Photochem Photobiol B.* 2005;79(3):243-51. Epub 2005 Mar 23.
10. Kanick SC, Sterenberg HJ, Amelink A. Empirical model description of photon path length for differential path length spectroscopy: combined effect of scattering and absorption. *J Biomed Opt.* 2008;13(6):064042.
11. Kanick SC, Sterenberg HJ, Amelink A. Empirical model of the photon path length for a single fiber reflectance spectroscopy device. *Opt Express.* 2009;17(2):860-71.
12. Middelburg TA, Van Zaane F, De Bruijn HS, Van Der Ploeg-van den Heuvel A, Sterenberg HJ, Neumann HA, et al. Fractionated illumination at low fluence rate photodynamic therapy in mice. *Photochem Photobiol.* 2010;86(5):1140-6. doi: 10.111/j.751-097.2010.00760.x.
13. Cottrell WJ, Paquette AD, Keymel KR, Foster TH, Oseroff AR. Irradiance-dependent photobleaching and pain in delta-aminolevulinic acid-photodynamic therapy of superficial basal cell carcinomas. *Clin Cancer Res.* 2008;14(14):4475-83.
14. Kaspers OP, Sterenberg HJ, Amelink A. Controlling the optical path length in turbid media using differential path-length spectroscopy: fiber diameter dependence. *Appl Opt.* 2008;47(3):365-71.

15. Amelink A, Sterenberg HJ, Bard MP, Burgers SA. In vivo measurement of the local optical properties of tissue by use of differential path-length spectroscopy. *Opt Lett*. 2004;29(10):1087-9.
16. Amelink A, Sterenberg HJ. Measurement of the local optical properties of turbid media by differential path-length spectroscopy. *Appl Opt*. 2004;43(15):3048-54.
17. Amelink A, Bard MP, Burgers SA, Sterenberg HJ. Single-scattering spectroscopy for the endoscopic analysis of particle size in superficial layers of turbid media. *Appl Opt*. 2003;42(19):4095-101.
18. Saidi IS, Jacques SL, Tittel FK. Mie and Rayleigh modeling of visible-light scattering in neonatal skin. *Appl Opt*. 1995;34(31):7410-8. doi: 10.1364/AO.34.007410.
19. Kruijt B, de Bruijn HS, van der Ploeg-van den Heuvel A, de Bruin RW, Sterenberg HJ, Amelink A, et al. Monitoring ALA-induced PpIX photodynamic therapy in the rat esophagus using fluorescence and reflectance spectroscopy. *Photochem Photobiol*. 2008;84(6):1515-27. Epub 2008 Jun 13.
20. van Veen RL, Verkruysse W, Sterenberg HJ. Diffuse-reflectance spectroscopy from 500 to 1060 nm by correction for inhomogeneously distributed absorbers. *Opt Lett*. 2002;27(4):246-8.
21. Jacques SL. Melanosome absorption coefficient. <http://omlcogiedu/spectra/melanin/muahtml>. 1998.
22. Amelink A, Robinson DJ, Sterenberg HJ. Confidence intervals on fit parameters derived from optical reflectance spectroscopy measurements. *J Biomed Opt*. 2008;13(5):054044.
23. McLoone N, Donnelly RF, Walsh M, Dolan OM, McLoone S, McKenna K, et al. Aminolaevulinic acid diffusion characteristics in 'in vitro' normal human skin and actinic keratosis: implications for topical photodynamic therapy. *Photodermatol Photoimmunol Photomed*. 2008;24(4):183-90.
24. Becker TL, Paquette AD, Keymel KR, Henderson BW, Sunar U. Monitoring blood flow responses during topical ALA-PDT. *Biomed Opt Express*. 2010;2(1):123-30.

8

Correction for tissue optical properties enables quantitative skin fluorescence measurement using multi-diameter single fiber reflectance spectroscopy.

Tom Middelburg
Chris Hoy
Martino Neumann
Arjen Amelink
Dominic Robinson

Lasers Surg Med. 2013 (submitted).

ABSTRACT

Background and objective: Fluorescence measurements in the skin are very much affected by absorption and scattering but existing methods to correct for this are not applicable to superficial skin measurements.

Study design/materials and methods: The first use of multiple-diameter single fiber reflectance (MDSFR) and single fiber fluorescence (SFF) spectroscopy in human skin was investigated. MDSFR spectroscopy allows a quantification of the full optical properties in superficial skin (μ_a , μ_s' and γ), which can next be used to retrieve the corrected -intrinsic- fluorescence of a fluorophore $Q\mu_{ax}^f$. Our goal was to investigate the importance of such correction for individual patients. We studied this in 22 patients undergoing photodynamic therapy (PDT) for actinic keratosis.

Results: The magnitude of correction of fluorescence was around 4 (for both autofluorescence and protoporphyrin IX). Moreover, it was variable between patients, but also within patients over the course of fractionated aminolevulinic acid PDT (range 2.7-7.5). Patients also varied in the amount of protoporphyrin IX synthesis, photobleaching percentages and resynthesis (>100x difference between the lowest and highest PpIX synthesis). The autofluorescence was lower in actinic keratosis than contralateral normal skin (0.0032 versus 0.0052; $P < 0.0005$), and decreased further to 0.0021 after aminolevulinic acid application ($P = 0.01$).

Conclusions: Our results clearly demonstrate how important it is to correct fluorescence for optical properties, because these vary considerably between individual patients and also during PDT. The autofluorescence can be relevant for diagnostic use in the skin, but also for studies investigating its association with several internal diseases such as diabetes. Protoporphyrin IX synthesis and photobleaching kinetics allow monitoring clinical PDT which facilitates individual-based PDT dosing and improvement of clinical treatment protocols.

INTRODUCTION

Fluorescence spectroscopy can be used to measure the concentration of common fluorophores in the skin such as NAD(H), collagen, elastin, keratin, and advanced glycation end-products (1-4). The combined emission of these fluorophores constitutes the skin autofluorescence, which has gained considerable attention because higher autofluorescence intensities have been described to be correlated with cardiovascular events, diabetes mellitus, chronic pulmonary disease, renal disease, liver cirrhosis and inflammatory diseases (5-11). Fluorescence spectroscopy can also be used to measure for example the protoporphyrin IX (PpIX) concentration during photodynamic therapy (PDT). Such measurements are important because it is well documented that PpIX fluorescence kinetics can help predict PDT outcome (12-17). However, the problem with these fluorescence measurements is that the detected fluorescence signals are critically dependent on the tissue optical properties, but these are not taken into account (18-20).

When obtaining a fluorescence signal, both the excitation and emission light are absorbed and scattered and, as a result, raw fluorescence signals will underestimate the fluorophore concentration. It is obvious that individual lesions and patients will differ in their physical and biochemical properties and thus also in their optical properties. Furthermore, in the case of PDT, these optical properties may be changing in time during the course of treatment. Such variations in optical properties will result in differences in measured fluorescence intensity even if the fluorophore concentration is the same. Therefore, a crucial step to measure the intrinsic fluorescence in tissue is to correct it for the optical properties of that tissue. These must be quantified first to perform this correction accurately.

Measuring the optical properties in a superficial sampling volume such as in the human epidermis and upper dermis poses a significant challenge. Several techniques have been deployed that can be used, but these are either limited to a narrow wavelength range and/or are only valid for certain tissue optical properties (21-24). When using any optical instrument, knowledge of the photon path-length is necessary to quantify the optical properties of tissue. A solution therefore is to make use of an optical technique in which the path-length of light can be controlled. One such optical technique is single fibre reflectance (SFR) spectroscopy, which has recently been developed by our group (25-29). In SFR white light is emitted through a single fibre that is in contact with the skin. The same fiber also collects the reflected light and can be used to acquire a reflectance spectrum over a broad range of visible and near infrared wavelengths. This reflectance spectrum contains the combined information on how much light has been absorbed and scattered. From such a reflectance spectrum the tissue absorption coefficient, μ_a [mm^{-1}]

can be accurately quantified without prior knowledge of the scattering properties (28). Decomposition of μ_a into the constituent spectra of known tissue chromophores yields accurate measurements of the blood volume fraction, microvascular saturation, mean vessel diameter and of the melanin, bilirubin and beta-carotene content. To determine the tissue scattering properties however, a single SFR measurement does not suffice.

The geometry in SFR allows superficial measurements with relatively short photon path-lengths. As a result, the number of scattering events is also relatively small. This means that the angle in which the light is scattered becomes increasingly important for the amount of reflected light. This scattering angle follows a probability distribution that is described by the (unknown) tissue phase function. Because the reflectance in SFR is highly dependent on this phase function it is necessary to characterize it in order to measure the reduced scattering coefficient μ_s' [mm^{-1}]. We have recently demonstrated that successive SFR measurements using two or more carefully chosen fiber diameters in a single optical probe enables to solve this problem, allowing quantification of both the phase function parameter γ [-] and of μ_s' (30-32). This technique is termed multiple diameter single fiber reflectance (MDSFR) spectroscopy. The mathematical model to extract the optical properties from a measured spectrum has been validated using tissue-mimicking phantoms and in computer simulations that used a range of biologically possible optical properties (31, 32).

The optical properties that are measured using MDSFR can next be used to correct a subsequent fluorescence measurement (33). We have developed a model to accurately quantitate the fluorescence by correcting for the tissue absorption and scattering properties at both the excitation and emission wavelengths (34). This corrected -intrinsic- fluorescence is dependent on both the ability of the fluorophore to absorb the excitation light and its efficiency to emit light. Specifically, it is given as the product of the absorption coefficient of the fluorophore for the excitation wavelength $\mu_{a,\lambda}^f$ and the quantum efficiency of the fluorophore across the emission spectrum Q [-]. This method is termed single fiber fluorescence (SFF) spectroscopy and this has recently been applied for the measurement of intrinsic fluorescence in pre-clinical models (35).

In this study we describe for the first time the use of MDSFR and SFF spectroscopy in human skin. Our goal was to investigate the importance of correcting fluorescence signals for optical properties in individual patients. We studied this in patients undergoing fractionated aminolevulinic acid (ALA) PDT for actinic keratosis or Bowen's disease. This patient selection allowed us to measure both skin autofluorescence and ALA-induced PpIX fluorescence. Because optical properties are expected to change during PDT (36-39), we also studied the magnitude of the effect of variations in optical properties on

fluorescence signals. This was done by measuring protoporphyrin IX fluorescence at various time-points during PDT.

MATERIALS AND METHODS

MDSFR and SFF setup

To obtain a reflectance spectrum, light from a tungsten halogen lamp was directed on the skin through a probe containing 2 single fibers with diameters of 0.4 and 0.8 mm. This choice is related to the fact that the photon path length -and thus the sampling volume- is on the order of the fiber diameter (29, 40). This means that when using these fiber diameters, normally both the epidermis and superficial dermis will be sampled in normal skin and actinic keratosis lesions (37). Another rationale for our choice is that it was shown that the accuracy of the MDSFR technique works best for relatively large fiber diameters and that the diameters of the two fibers should be relatively close so that they are measuring the same optical properties (31). After these sequential reflectance measurements, a SSF fluorescence spectrum was taken using the 0.8 mm fiber by illuminating the skin with 405 nm laser light. The reflectance and fluorescence spectra were detected by three spectrometers, one for each fiber to measure reflectance and one to measure fluorescence with a filter blocking the laser light by a 435 nm long-pass filter (Figure 1). The spectrometers and light sources were controlled by a custom made

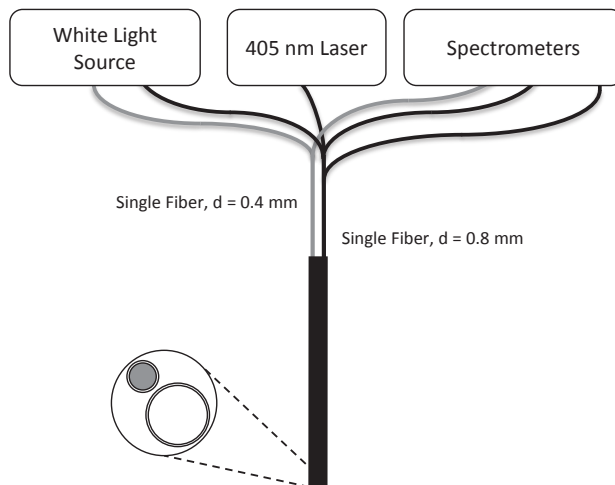


Figure 1. Schematic representation of the measurement setup. White light reflectance and fluorescence (405 nm laser excitation light) spectra were acquired using a single probe that contained two fibres of 0.4 and 0.8 mm. The 0.8 mm fiber was used for both fluorescence and reflectance spectroscopy while the 0.4 mm fiber performed reflectance spectroscopy only.

LabView program (National Instruments LabView 7.1) on a notebook computer. A single combined MDSFR/SFF measurement took approximately 3 seconds. The ends of the fibers, used for skin contact, were polished to an angle of 15° to minimize the collection of specularly reflected light at the probe-skin interface. Figure 2 shows an example of the MDSFR spectra acquired by the 0.4 and 0.8 mm fibers. In this figure the percentage of incident light collected by each optical fiber is plotted as a function of wavelength (grey dots and their standard deviations) with the MDSFR model fit to the data (black lines). For both fibers the overall shape of the SFR signal is characterized by a signal that decreases with wavelength (grey line) that is attributable to the background scattering. Note that the reflectance is higher for the 0.8 mm fiber diameter, because the collection area is larger.

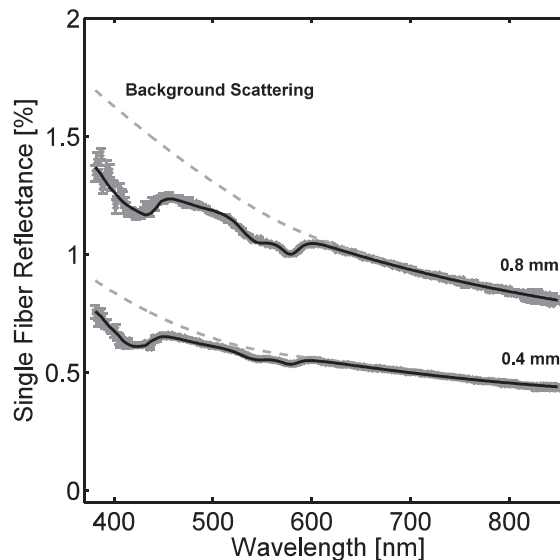


Figure 2. Example of an MDSFR spectrum for both the 0.4 and 0.8 mm fiber diameters. The characteristic wavelength-dependent features of haemoglobin are best seen in the 0.8 mm fiber in the 400 nm and 500 to 600 nm regions (“dips” in the black line).

Reflectance spectral analysis

To retrieve quantitative data on the tissue optical properties and the intrinsic fluorescence spectral analysis was performed using the same fitting model for the data described previously. For a detailed description of this model and the underlying mathematics, we refer to these articles (30-32, 35, 41). A simplified stepwise summary of our approach is described below.

First the tissue absorption properties are calculated, which are defined by the absorption coefficient μ_a [mm^{-1}]. For each wavelength this is the sum of the known absorption coefficients of (de)oxygenized hemoglobin, melanin, bilirubin and beta-carotene. These result in the following measured parameters of the sampled volume: the blood volume fraction, the average vessel diameter, the saturation, and the melanin, bilirubin and beta-carotene concentrations. Next, the absorption-corrected spectra from both fiber diameters are simultaneously fitted to extract μ_s' [mm^{-1}], and γ [-].

The melanin fitting routine is an important new addition to previous models, since this is the first study on human skin. Because the shape of the melanin absorption spectrum is similar to the scattering spectrum and the two properties have competing effects on the spectra, using melanin as an independent absorber can result in over-estimations of both melanin concentration and μ_s' . To address this, we assumed melanin to be confined predominantly to the basal membrane. This led us to model melanin as existing in a 20 μm layer (40 μm photon round trip path length) within the measurement volume. It was also assumed that the melanin concentration observed by each fiber in the 20 μm layer was the same, which allows simultaneous solution of the model equations for both fibers to produce an estimate of the melanin content. Another smaller addition to previous models was the inclusion of a new absorption spectrum for beta-carotene, based on a previous description of it in human skin (42).

Correction of fluorescence for absorption and scattering

To calculate the quantitative corrected intrinsic fluorescence, the raw fluorescence signals were corrected for the effects of absorption and scattering using the optical properties obtained from the MDSFR reflectance spectra. For a detailed mathematical description of the SFF model that was used we refer to earlier papers (33, 41). In short, the ratio of collected emission photons to delivered excitation photons at each wavelength is first corrected for the average of the absorption coefficient at the excitation and emission wavelengths. Next, the absorption-corrected fluorescence ratio is corrected for the effects of scattering using the reduced scattering coefficients at both excitation and emission wavelengths. This step results in a calibrated and corrected fluorescence spectrum expressed as the wavelength-dependent intrinsic fluorescence, $Q(\lambda)\mu_{a,x}^f$, where $Q(\cdot)$ is the quantum efficiency of the fluorophore at each emission wavelength. Lastly, the resulting wavelength-dependent intrinsic fluorescence is then integrated over the emission bandwidth of the fluorophore. This results in the intrinsic fluorescence of the fluorophore at the excitation wavelength, $Q\mu_{a,x}^f$, where Q is now the total fluorescence quantum yield of the fluorophore. For the purposes of this manuscript, we wish to illustrate the effect of correction for optical properties. Therefore, here we define the “uncorrected fluorescence” as fluorescence spectra which undergo the correction

process using μ_a and μ_s' values of zero. This ensures that the uncorrected and corrected fluorescence spectra have the same units.

Fluorescence spectral analysis

The fluorescence spectra, corrected for the influence of tissue optical properties, were then analyzed to determine the contribution from autofluorescence, PpIX and the PpIX fluorescent photoproducts. A skewed Gaussian was used to fit the autofluorescence while the basis spectra for PpIX and its photoproducts were isolated from spectra after subtraction of the autofluorescence (13)

Calibration of the MDSFR/SFF system

Before each set of measurements a careful calibration procedure was performed as described previously (30, 41) consisting of an integrating sphere calibration, a measurement of a calibrated light source, and measurements in water in a dark container and in a liquid phantom containing 6.6% Intralipid-20% with a known reduced scattering coefficient (μ_s' at 800 nm = 1.2 mm⁻¹). This procedure accounts for the output powers of the light sources and the spectral transmission and sensitivity of the system.

Lesion selection

Spectra were obtained in 22 patients undergoing fractionated ALA-PDT for actinic keratosis (n=20) or Bowen's disease (n=2). In fractionated PDT, which is the standard in our university hospital setting, two light fractions of 20 and 80 J cm⁻² are delivered 4 and 6 hours after ALA application, separated by a two-hour dark interval. All lesions were histologically confirmed. The study was performed within local written ethical guidelines and was in accordance with the declaration of Helsinki.

MDSFR/SFF measurements on skin

Both autofluorescence and PpIX fluorescence were measured in actinic keratosis or Bowen's disease lesions. Spectra were obtained from the centre of the lesion at various time-points. Normal skin measurements were taken from normal contralateral skin. The first set of measurements (before and after gentle curettage) were acquired before ALA application. During PDT 3 individual measurements were taken by removing and replacing the fiber probe at each of the following time-points: before and immediately after the first PDT illumination; and before and after the second illumination. All measurements were performed by the same investigator to minimize inter-individual variations in applied pressure.

Data analysis

For each reflectance measurement, containing spectra from both the 0.4 and 0.8 mm fibers, the goodness of the fit for the reflectance spectrum was calculated over the whole wavelength region using $\chi^2 = \sum (R_{model}(\lambda_i) - R_{measured}(\lambda_i))^2 / \sigma(\lambda_i)^2$ as an indicator of fit quality. Rejection criteria were: (1) a χ^2 value larger than $1.6(10)^5$ for either fiber diameter, which was set empirically from the fitted data, (2) a maximum residual between the fit and the data exceeding 25% at any part of the spectrum, (3) crossing of the 0.8 and 0.4 mm spectra, or (4) if an imaginary component resulted from the fit. The spectra failing any of these rejection criteria were not used for further analysis. This led to 418 of a total of 572 spectra being included. All successful reflectance and fluorescence spectra lead to values for corrected fluorescence that included a 95% confidence interval, based on the model fitting as described previously (43).

For each set of three measurements per time-point, averages of these measurements were calculated when it was clear that individual measurements of the same lesion showed very little variation. For the same reason of consistency in measurements at the same spot, lesional measurements before and after gentle curettage were also grouped together. Similarly, actinic keratosis and Bowen's disease were grouped as "lesional skin" and referred to as such throughout the rest of the manuscript.

The magnitude of correcting the autofluorescence and PpIX fluorescence signals for measured tissue optical properties was defined by dividing the average corrected by the average uncorrected values. This is referred to as "the correction factor" throughout the manuscript. We evaluated the effect of fluctuations in optical properties during PDT on the magnitude of the correction factor by comparing autofluorescence and PpIX fluorescence intensities over time during PDT. In addition, the variation between patients in corrected PpIX synthesis 4 hours after ALA application and PpIX photobleaching during PDT was investigated. Finally, differences in the corrected autofluorescence intensities between normal and lesional skin were compared, as well as the lesional autofluorescence signals before and 4 hours after ALA application.

RESULTS

The effect of correction for optical properties on individual spectra

Figure 3 illustrates how individual spectra were affected by correcting for the tissue optical properties. It shows a typical spectrum from an actinic keratosis lesion 4 hours after ALA application. The broad peak centered around 480 nm is due to the combined autofluorescence signal from a number of common fluorophores such as collagen, elas-

tin, keratin and NADH. The characteristic emission of PpIX is recognizable by its main peak around 635 nm. Note how the corrected fluorescence is about 4 times higher than the uncorrected (dashed line).

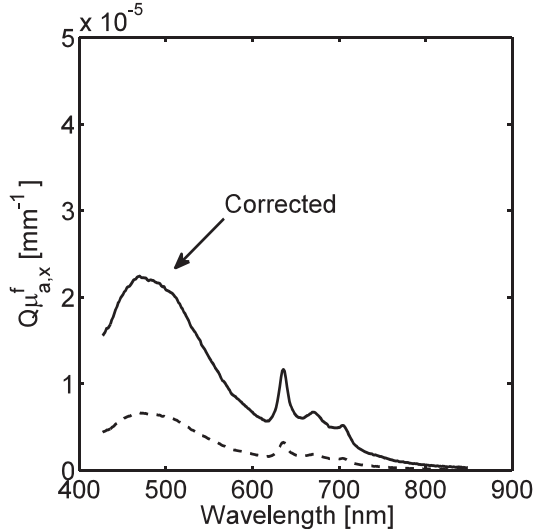


Figure 3. Example of corrected versus uncorrected (dashed line) spectra of actinic keratosis 4 hours after ALA application, showing the typical emission features of the skin autofluorescence below 600 nm and of PpIX fluorescence with a main peak at 635 nm. The corrected $Q\mu_{a,x}^f$ values are about 4 times higher than the uncorrected.

Magnitude of the correction factor on autofluorescence for individual patients

The autofluorescence was variable between patients for both normal and lesional skin (Fig. 4a and b respectively). Note the two scales of the Y-axis, showing that values for the corrected $Q\mu_{a,x}^f$ are always higher than the uncorrected. Taken in to account this different scale the corrected values are in some cases below and in some cases above the uncorrected values in this figure, indicating variability of their ratio. The magnitude of this correction factor was 3.7 on average (range = 2.4-6.3) for normal skin. For lesional skin the correction factor was higher with a wider range (mean = 4.9, range = 2.7 – 7.5).

TEMPORAL CHANGES IN OPTICAL PROPERTIES DURING PDT AND THEIR EFFECT ON THE AUTOFLUORESCENCE

Figure 5 illustrates the effect of temporal changes in optical properties on the autofluorescence of (a) normal and (b) lesional skin. For both normal and lesional skin the

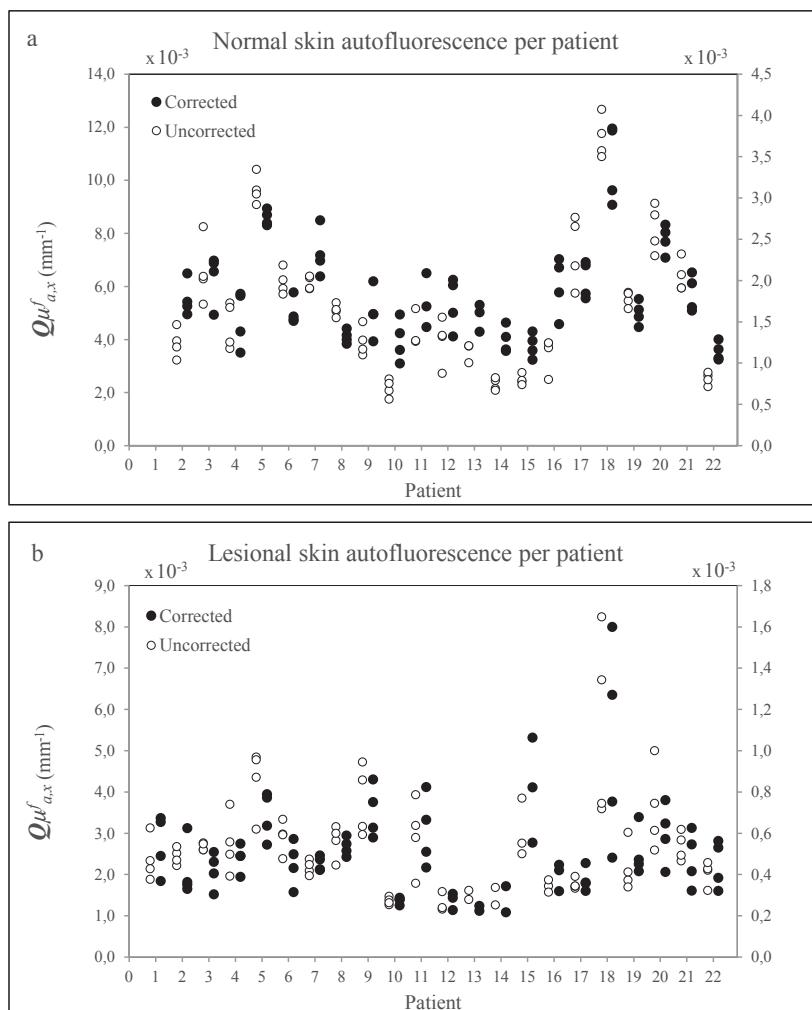


Figure 4. Corrected (●) and uncorrected (○) average values of individual measurements for the autofluorescence of (a) normal and (b) lesional skin. Shown are values at each of the four time-points before and after the first and second illumination for individual patients. The left y-axis is scaled to the corrected values and the right y-axis to the uncorrected.

corrected autofluorescence was variable for the four time-points during PDT (before and after the first and second illumination), but there was no systematic increase or decrease. For normal skin the correction factor remained fairly constant over time, which is illustrated by the same shape of the corrected and uncorrected lines that connect the four time-points in figure 5a. In contrast, this was not the case for lesional skin (Fig 5b), in which the correction factor, and thus the optical properties varied during the time-course of PDT. An example of a parameter that changed considerably during PDT is the

blood volume fraction. Compared to the initial value before PDT, the change in blood volume fraction ranged from a 7.7x decrease to a 4.9x increase. For individual patient the increase and decrease in blood volume fraction exhibited very variable patterns.

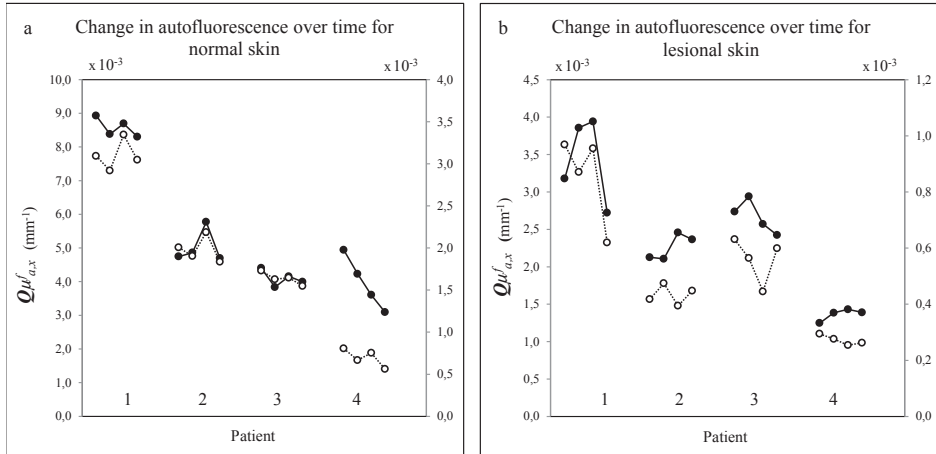


Figure 5. The average corrected (●) versus uncorrected (○) autofluorescence during the four time-points during PDT for (a) normal and (b) lesional skin. For graphical clarity only 4 patient are shown. The pattern of variability was the same for normal skin, but not for lesional skin, indicated by the different shapes of the lines connecting the time-points. The left y-axis is scaled to the corrected values and the right y-axis to the uncorrected.

The relation between optical properties and the magnitude of the correction factor

Figure 6 illustrates the effect of variations in (a) absorption and (b) scattering properties of the skin on the magnitude of the correction factor for the autofluorescence. In this figure the blood volume fraction and the scattering coefficient are used as illustrative examples for the effects of respectively absorption and scattering. Higher blood content showed a positive correlation with the correction factor (Pearson's correlation coefficient 0.68, $P < 0.0001$), and μ'_s showed a moderate negative correlation (correlation coefficient -0.44, $P < 0.0001$). The average value for μ'_s (at 800 nm) was 1.32 mm⁻¹ for lesional skin and 1.96 mm⁻¹ for normal skin.

PpIX synthesis and photobleaching for individual patients

Individual patients showed considerable variation in the amount of synthesized PpIX 4 hours after ALA application (figure 7). The corrected values were on average 4.4 times higher, but the magnitude of this correction factor was variable for individual patients, ranging from 3.3 – 5.9. This is graphically presented in figure 7 by the variable distance between corrected and uncorrected bars. Two patients synthesized minimal PpIX (8 and

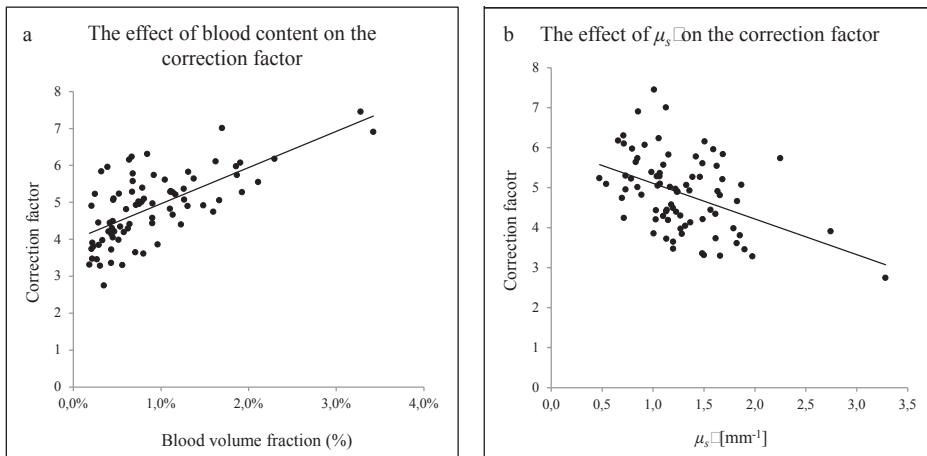


Figure 6. The effects of (a) absorption of blood and (b) the scattering coefficient μ_s' (at 800 nm) on the magnitude of the correction factor for autofluorescence. Shown are average lesional values of all time-points during PDT.

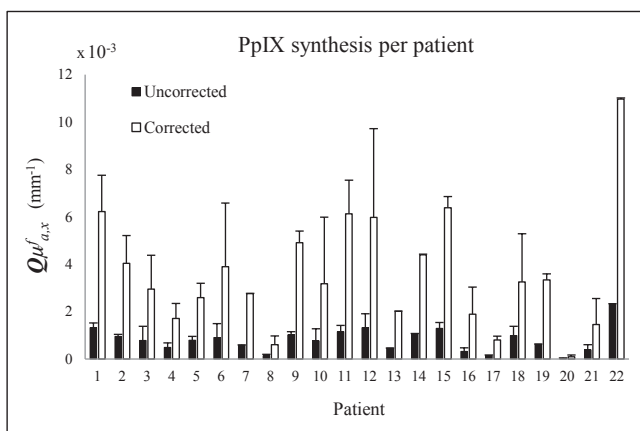


Figure 7. Average corrected and uncorrected PpIX fluorescence intensities 4 hours after ALA application per patient. There was a large variation between individual patients. The corrected values were on average 4.4 times higher than the uncorrected (range 3.3-5.9). Error bars represent 95% confidence intervals of the three repeated measurements, weighted by the confidence interval of their fit.

20). For these patients not only the uncorrected but also the corrected PpIX values were very low (for patient 20 this was a factor 113 times lower than the highest measured PpIX fluorescence in patient 22). Note that the confidence intervals in this figure appear much larger for the corrected values than the uncorrected. However, when these are normalized to the magnitude of the fluorescence they are on average 28% of the total for the corrected and 25% for the uncorrected values.

During PDT we observed PpIX photobleaching to 19% (SD 9%), followed by variable PpIX resynthesis during the two hour dark interval to 76% (SD 36%) and further photobleaching to 6% (SD 5%) remaining PpIX during the second illumination. These are averages of corrected PpIX fluorescence intensity values at these four time-points, normalized to the initial PpIX synthesis 4 hours after ALA application for all patients except patient 20 (who synthesized almost no PpIX at all).

Difference in autofluorescence between normal and lesional skin

The autofluorescence in lesional skin was significantly lower than in normal skin (Fig. 8; median = 0.0032 versus 0.0052; $P < 0.0005$, related samples Wilcoxon signed rank test). It was lower in 16 of the 18 patients in which we had successful sets of measurements for both normal and lesional skin. There was also an effect of ALA application on the autofluorescence in lesional skin. It decreased in 13/18 patients, which represented a statistical difference (median = 0.0032 versus 0.0021, $P = 0.01$, related samples Wilcoxon signed rank test).

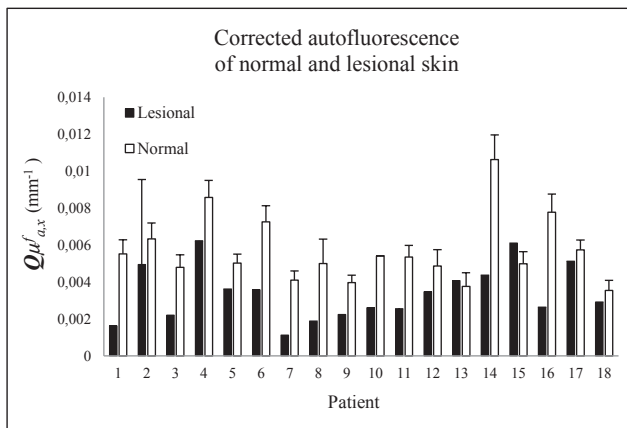


Figure 8. Significant lower average corrected autofluorescence in lesional compared with normal skin ($P < 0.0005$, related samples Wilcoxon signed rank test). Error bar represent the 95% confidence interval weighted by the goodness of the fit of individual measurements.

DISCUSSION

In this study we report on the first use of MDSFR and SFF spectroscopy to quantify the intrinsic fluorescence in the epidermis and superficial dermis of human skin. Our finding that the magnitude of the correction factor varied from 2.4 to 7.5 clearly illustrates how important it is to correct fluorescence signals for the tissue optical properties. This variability of the correction factor is a direct reflection of the heterogeneity in optical

properties of individual patients. Because of such heterogeneity it is crucial to first quantify the optical properties in individual patients and use these to correct the raw fluorescence signal of each measurement.

Effect of absorption and scattering on collected fluorescence

The way the fluorescence signal is affected by absorption and scattering is illustrated by the finding that the correction factor correlates with both the blood volume fraction and with μ'_s (figures 6a and b). Higher blood volumes will lead to higher absorption and thus to lower collected raw fluorescence signals. This explains why the correction factor increases with increasing blood volume fraction. However, to explaining the negative correlation between the correction factor and μ'_s necessitates a more detailed description of the empirical model used to correct fluorescence signals. This model is based on a recent publication on the underlying mechanisms associated with the influence of scattering and absorption properties on the fluorescence intensity collected by a single optical fiber (34). We have shown, based on Monte Carlo simulations, that for a single fiber the measured fluorescence is proportional to the fiber diameter. We have also shown that the collected fluorescence rapidly decreases from a constant value in the absence of scattering ($\mu'_s = 0$) to reach a minimum at μ'_s of around 0.5 mm^{-1} , and then increases with increasing scattering. This biphasic dependence is explained by two competing effects: superficially scattered photons tend to increase the collected fluorescence, whereas photons that are scattered deeper in the tissue are more likely to be scattered away from the fiber tip and thus decrease the collected fluorescence. At higher values for μ'_s more photons are scattered superficially (resulting in a relatively small sampling depth). The net effect is that the increase in collected fluorescence caused by superficial scattering starts to outweigh the decrease caused by deeper scattering. In our study the average value for μ'_s of lesional skin was 1.32 (range 0.48-3.28), which is of similar magnitude as previously reported (44). In this range of values for μ'_s (i.e. higher than around 0.5 mm^{-1}) increasing values for μ'_s lead to an increase in collected fluorescence. This explains the negative correlation between μ'_s and the correction factor.

Quantitative PpIX measurements during PDT: implications of our findings

When applying MDSFR with SFF measurements for the purpose of recovering the intrinsic PpIX fluorescence during PDT a few relevant findings can be highlighted. The first is that the optical properties in the sampled volume of lesional skin change during the course of PDT and these changes are different for individual patients. This is clear for example from the variable blood volume fraction over time during PDT, but can also be concluded from figures 5a and 5b. Figure 5a shows how the magnitude of the correction factor for the autofluorescence remained relatively constant over time for normal skin. In contrast, for lesional skin this correction factor varied over the time course of PDT

(figure 5b). This demonstrates that the optical properties in lesional skin change during PDT as a consequence of performing PDT. This again highlights the importance of correcting for these varying optical properties during PDT.

A second important implication for the purpose of PpIX fluorescence measurements in PDT, is that the intrinsic PpIX fluorescence –and thus the synthesized PpIX concentration – is very variable between patients (figure 7). Because of the quantitative nature of our measurement, PpIX fluorescence values close to zero (patients 8 and 20) really mean that very little PpIX is synthesized. Because lack of PpIX synthesis will be related to decreased treatment effect, a benefit of quantitative PpIX fluorescence measurements would be to better predict individual treatment effect. Without correcting for optical properties, this could previously have been attributed for example by a lot of blood present in the sampling volume or by scattering effects. How such an uncorrected measurement can be very misleading can again be concluded from the variability of the correction factor for PpIX fluorescence measurements (which varied from 2.8-5.9).

A third potentially relevant implication of our findings for PDT is that quantitative PpIX fluorescence measurements can be used to estimate the effective PDT dose. This can be very useful for the individual dosing of the first illumination in light fractionated PDT; an approach that we have successfully adopted in mice (45, 46). Because previously we had no way of quantifying the intrinsic fluorescence in human skin, changes in optical properties during PDT make it impossible to reliably measure PpIX photobleaching percentages and resynthesis in the dark interval. Now that we can, this opens up new possibilities for the clinic. The current clinical light treatment parameters (20 Jcm⁻² followed by 80 Jcm⁻² two hours later) were based on several preclinical studies. In these studies it was shown that the first light fraction needs to be small and larger first light fractions decrease efficacy (47). It was found that the optimal effective dose for the first illumination is to bleach circa 50% of PpIX. In our current study the PpIX photobleaching percentages during the first illumination were 81% on average. This suggests that the effective dose of the first illumination is too high. Possibly lower light doses will further increase efficacy. When we take a closer look at what our correction method may mean for an individual patient we see how use of a correction method changes the measured PpIX photobleaching kinetics. These are important because they have been related to PDT outcome in the past (48, 49). In patient 18 for example the uncorrected measured PpIX fluorescence at the four time-points during PDT is 100-15-73-8 %, whereas the corrected values are 100-3-106-11%. This difference illustrates how correcting for optical properties can be important for a personalized approach to PDT. While quantitative PpIX fluorescence measurements are important for PDT studies, our measurements of the intrinsic skin autofluorescence can also be relevant for very different purposes.

Quantitative skin autofluorescence measurements: implications of our findings

First, the different autofluorescence of normal and lesional skin (figure 9) points towards a diagnostic potential of intrinsic autofluorescence measurements. Again, it must be stressed that this is impossible unless a proper correction method is available. Several studies using different fluorescence spectroscopy techniques have described the potential value of the autofluorescence to differentiate between normal and neoplastic skin (50-52). To further explain why the autofluorescence is different for neoplastic skin it will be helpful to distinguish between the individual fluorophores that constitute the combined autofluorescence signal, but our method currently does not allow this. Therefore a lower autofluorescence signal in lesional skin could simply reflect sampling less fluorescent collagen in the dermis due to thicker epidermis of lesional skin, although one study reported that the epidermal thickness was not related to the autofluorescence (19). Another explanation may be that in lesional skin the mitochondrial function or redox state is somehow altered, which has been reported to affect the autofluorescence (4, 53). Future research that focuses on separating out the individual components in the autofluorescence signals are needed such as use of different excitation light (54) or phasor analysis of multiphoton spectral imaging (2).

A second potential benefit of quantifying the skin autofluorescence is that the autofluorescence is considered a risk factor for a range of conditions that are related to increased cumulative metabolic stress. Currently a spectroscopic device called the AGE reader is commonly used to perform autofluorescence measurements (1, 5-8, 55), which are related to reference values for different age categories of normal Caucasian skin (56). Although these measurements are used for example to assess the risk for cardiovascular complications in diabetes patients, they do not involve any correction for optical properties and thus may be off by a factor of around 6. This value may actually be even higher. This is because our measurements were also preceded by a careful calibration procedure. This way both the uncorrected and corrected outcomes were already corrected for the variable output powers of the light sources and the spectral transmission and sensitivity of the system. Apart from this comparison with the AGE-reader it is interesting to also compare our method with other methods that have attempted to correct raw fluorescence for optical properties.

Comparison with other methods to retrieve intrinsic fluorescence

A range of investigators have developed methods to correct fluorescence for optical properties in various biological tissues and tissue mimicking phantoms. However, these are often based on diffuse measurements with large source-detector separations (21, 57). The correction methods associated with these measurements are often based on diffusion theory, which is useful for the measurements of larger volumes but not for

superficial measurements in the skin. Equally a number of groups have developed specific probe geometries for superficial fluorescence measurements (21, 24, 58-60) and combined these with more complicated models of light transport in tissue. Many of these approaches lead to substantial errors in recovered intrinsic fluorescence (61), or are restricted by specific ranges of optical properties over which the recovery of intrinsic fluorescence is valid (24). Some have also used single optical fiber fluorescence spectroscopy (62, 63), but they have had to make assumptions about the scattering properties. Because we are using multiple fibers we can measure them (both $\mu s'$ and γ) to correct fluorescence for each individual measurement. This is an important difference because the phase function has been shown to have a great impact on the collected reflectance (64-66) and thus also on the corrected fluorescence signal (33).

From PpIX fluorescence to PpIX concentration

Given that we have measured $Q\mu_{a,x}^f$ of PpIX in actinic keratosis and Bowen's disease it is interesting to consider if we can use this to estimate the concentration of PpIX. Clearly such an estimation requires some assumptions that are difficult to verify in-vivo without a thorough investigation of the relationship between the intrinsic fluorescence and the concentration of PpIX determined by chemical extraction. However, we can use a representative extinction spectrum of PpIX (67) to assume the extinction of PpIX at 405 nm in vivo to be $14000 \text{ L} \cdot \text{M}^{-1}\text{mm}^{-1}$. Next we can adopt a fluorescence quantum yield of 0.5%, which is recently reported using diffuse optical tomography (57, 68). Under these assumptions the average PpIX concentration before PDT in actinic keratosis and Bowen's disease is $2.25 \text{ nmol ml}^{-1}$ [range 0.38 – 6.81]. These values are comparable with values reported in the literature using chemical extraction of PpIX from biopsies of basal cell carcinoma (69) and actinic keratosis (70).

It is also interesting to consider the detection limit of our technique. Using the integration times utilized in the present study we were able to accurately fit (i.e. with a 95% confidence interval <10% of the measured value) the very low PpIX fluorescence after the therapeutic illumination, which corresponded to a PpIX concentration of $0.06 \text{ nmol ml}^{-1}$.

A way to further investigate if the assumed value of Q for PpIX in tissue is correct, would be to measure PpIX fluorescence in tissue with known pH. The decrease in autofluorescence after ALA application that we found is an example of how the pH can affect the quantum efficiency of a fluorophore. This is likely due to the acidity of ALA, decreasing the pH. This also indicates that the moment during PDT at which autofluorescence is measured is critical, which can be relevant for example when the skin autofluorescence is measured to perform a crude correction for the PpIX fluorescence.

Limitations

Some limitations of this study must also be addressed. The main limitation of our method is that the model is based on the assumption that the two optical fibers measure the same optical properties. This may not necessarily be the case because they are seeing different volumes due to different diameters and due to the side-by-side placement of the fibers within the probe. In this study this problem is partly solved by our strict rejection criteria. As described in the methods section spectra were excluded for a number of reasons, including crossing of the spectra of the two fibers. This is an indication that the scattering properties are not truly consistent between the two fiber diameters due to differences in sampled volume. Apart from using this rejection of spectra we have been working on improvements of the technique to overcome this problem. One option has been to use a single fiber with variable diameter using a coherent bundle and a series of pinholes to control the effective fiber diameter (71). This has recently been updated to a 19-core fiber bundle that is quicker and that simulates a variable-diameter solid-core fiber while there is no disturbance by free-space optical components (41). A solid-core fiber with variable diameters may be the optimal solution for the future, but is challenging to construct. An additional benefit of these improvements is also that measurements can be tailored to the desired sampling depth, which greatly increases the applicability of the system for various research questions.

The number of spectra that were rejected can also be considered a limitation of this study. As described above, some were attributable to either crossing of spectra. A small number of spectra were also rejected because the nonlinear regression routine could not fit the spectra without generating imaginary components to the fit parameters. Most rejected spectra were however attributable to experimental errors such as movement artifacts and cream remnants that contained unknown chromophores. These errors can be largely avoided in future MDSFR/SFF use by instructing the patients to keep still during the measurement and by more thorough cleaning of the sampled skin.

A further but minor limitation is that $Q\mu_{a,x}^f$ is still not a direct measure of the concentration. To calculate this the extinction coefficient of PpIX is also needed, but this is unknown. This coefficient will depend on the pH, which is assumed to be fairly constant at the inside of the mitochondrial membrane even in the presence of ALA.

Summary

In summary, in this study the optical properties of the epidermis and superficial dermis in human skin were successfully quantified and used to correct fluorescence measurements. For both the autofluorescence and the PpIX fluorescence we demonstrated how important such corrections are to obtain quantitative results. We showed that optical

properties change during PDT and that for this reason fluorescence measurements at different time-points are needed to correct for these temporal changes. The resulting PpIX fluorescence kinetics can be useful to predict efficacy and optimize clinical PDT illumination protocols. A quantitative measurement of the skin autofluorescence on the other hand has the potential to differentiate between neoplastic and normal skin. It can also provide important information on the concentration of advanced glycation end products, which are related to several internal diseases and are considered important risk factors for cardiovascular complications. This study illustrates how a combination of MDSFR and SFF spectroscopy opens up new possibilities for future research that involve measurements of intrinsic fluorescence in the skin.

REFERENCES

1. Meerwaldt R, Links T, Graaff R, Thorpe SR, Baynes JW, Hartog J, et al. Simple noninvasive measurement of skin autofluorescence. *Ann N Y Acad Sci.* 2005;1043:290-8.
2. Fereidouni F, Bader AN, Colonna A, Gerritsen HC. Phasor analysis of multiphoton spectral images distinguishes autofluorescence components of in vivo human skin. *J Biophotonics.* 2013;11(10):201200244.
3. Na R, Stender IM, Ma L, Wulf HC. Autofluorescence spectrum of skin: component bands and body site variations. *Skin Res Technol.* 2000;6(3):112-7.
4. Mayevsky A, Rogatsky GG. Mitochondrial function in vivo evaluated by NADH fluorescence: from animal models to human studies. *Am J Physiol Cell Physiol.* 2007;292(2):C615-40. Epub 2006 Aug 30.
5. Mulder DJ, van Haelst PL, Graaff R, Gans RO, Zijlstra F, Smit AJ. Skin autofluorescence is elevated in acute myocardial infarction and is associated with the one-year incidence of major adverse cardiac events. *Neth Heart J.* 2009;17(4):162-8.
6. Genevieve M, Vivot A, Gonzalez C, Raffaitin C, Barberger-Gateau P, Gin H, et al. Skin autofluorescence is associated with past glycaemic control and complications in type 1 diabetes mellitus. *Diabetes Metab.* 2013;2(13):00051-7.
7. Gopal P, Reynaert NL, Scheijen JL, Engelen L, Schalkwijk CG, Franssen FM, et al. Plasma AGEs and skin autofluorescence are increased in COPD. *Eur Respir J.* 2013;3:3.
8. Smit AJ, Smit JM, Botterblom GJ, Mulder DJ. Skin autofluorescence based decision tree in detection of impaired glucose tolerance and diabetes. *PLoS One.* 2013;8(6):e65592. doi: 10.1371/journal.pone.0065592. Print 2013.
9. Arsov S, Graaff R, van Oeveren W, Stegmayr B, Sikole A, Rakhorst G, et al. Advanced glycation end-products and skin autofluorescence in end-stage renal disease: a review. *Clin Chem Lab Med.* 2013;4:1-10.
10. Maury E, Vergniol J, Ledinghen V, Rigalleau V. Skin autofluorescence is high in patients with cirrhosis - further arguing for the implication of Advanced Glycation End products. *J Hepatol.* 2011;54(5):1079-80. doi: 10.16/j.jhep.2010.10.012. Epub Nov 10.
11. de Groot L, Hinkema H, Westra J, Smit AJ, Kallenberg CG, Bijl M, et al. Advanced glycation end-products are increased in rheumatoid arthritis patients with controlled disease. *Arthritis Res Ther.* 2011;13(6):R205. doi: 10.1186/ar3538. Epub 2011 Dec 14.
12. Boere IA, Robinson DJ, de Bruijn HS, Kluin J, Tilanus HW, Sterenberg HJ, et al. Protoporphyrin IX fluorescence photobleaching and the response of rat Barrett's esophagus following 5-aminolevulinic acid photodynamic therapy. *Photochem Photobiol.* 2006;82(6):1638-44.
13. Robinson DJ, de Bruijn HS, van der Veen N, Stringer MR, Brown SB, Star WM. Fluorescence photobleaching of ALA-induced protoporphyrin IX during photodynamic therapy of normal hairless mouse skin: the effect of light dose and irradiance and the resulting biological effect. *Photochem Photobiol.* 1998;67(1):140-9.

14. Ascencio M, Collinet P, Farine MO, Mordon S. Protoporphyrin IX fluorescence photobleaching is a useful tool to predict the response of rat ovarian cancer following hexaminolevulinate photodynamic therapy. *Lasers Surg Med.* 2008;40(5):332-41.
15. Tyrrell JS, Campbell SM, Curnow A. The relationship between protoporphyrin IX photobleaching during real-time dermatological methyl-aminolevulinate photodynamic therapy (MAL-PDT) and subsequent clinical outcome. *Lasers Surg Med.* 2010;42(7):613-9.
16. Wang Y, Gu Y, Liao X, Chen R, Ding H. Fluorescence monitoring of a photosensitizer and prediction of the therapeutic effect of photodynamic therapy for port wine stains. *Exp Biol Med (Maywood).* 2010;235(2):175-80. doi: 10.1258/ebm.2009.009294.
17. Sheng C, Hoopes PJ, Hasan T, Pogue BW. Photobleaching-based dosimetry predicts deposited dose in ALA-PpIX PDT of rodent esophagus. *Photochem Photobiol.* 2007;83(3):738-48.
18. Jongen AJ, Sterenberg HJ. Mathematical description of photobleaching in vivo describing the influence of tissue optics on measured fluorescence signals. *Phys Med Biol.* 1997;42(9):1701-16.
19. Sandby-Moller J, Poulsen T, Wulf HC. Influence of epidermal thickness, pigmentation and redness on skin autofluorescence. *Photochem Photobiol.* 2003;77(6):616-20.
20. Na R, Stender IM, Henriksen M, Wulf HC. Autofluorescence of human skin is age-related after correction for skin pigmentation and redness. *J Invest Dermatol.* 2001;116(4):536-40.
21. Saager RB, Cuccia DJ, Saggese S, Kelly KM, Durkin AJ. Quantitative fluorescence imaging of protoporphyrin IX through determination of tissue optical properties in the spatial frequency domain. *J Biomed Opt.* 2011;16(12):126013.
22. Lin AJ, Ponticorvo A, Konecky SD, Cui H, Rice TB, Choi B, et al. Visible spatial frequency domain imaging with a digital light microprojector. *J Biomed Opt.* 2013;18(9):096007. doi: 10.1117/1.JBO.18.9..
23. Kim A, Roy M, Dadani F, Wilson BC. A fiberoptic reflectance probe with multiple source-collector separations to increase the dynamic range of derived tissue optical absorption and scattering coefficients. *Opt Express.* 2010;18(6):5580-94. doi: 10.1364/OE.18.005580.
24. Kim A, Khurana M, Moriyama Y, Wilson BC. Quantification of in vivo fluorescence decoupled from the effects of tissue optical properties using fiber-optic spectroscopy measurements. *J Biomed Opt.* 2010;15(6):067006. doi: 10.1117/1.3523616.
25. Amelink A, van der Ploeg van den Heuvel A, de Wolf WJ, Robinson DJ, Sterenberg HJ. Monitoring PDT by means of superficial reflectance spectroscopy. *J Photochem Photobiol B.* 2005;79(3):243-51. Epub 2005 Mar 23.
26. Amelink A, Bard MP, Burgers SA, Sterenberg HJ. Single-scattering spectroscopy for the endoscopic analysis of particle size in superficial layers of turbid media. *Appl Opt.* 2003;42(19):4095-101.
27. Kanick SC, Gamm UA, Schouten M, Sterenberg HJ, Robinson DJ, Amelink A. Measurement of the reduced scattering coefficient of turbid media using single fiber reflectance spectroscopy: fiber diameter and phase function dependence. *Biomed Opt Express.* 2011;2(6):1687-702. doi: 10.364/BOE.2.001687. Epub 2011 May 25.

28. Kanick SC, Robinson DJ, Sterenborg HJ, Amelink A. Method to quantitate absorption coefficients from single fiber reflectance spectra without knowledge of the scattering properties. *Opt Lett*. 2011;36(15):2791-3. doi: 10.1364/OL.36.002791.
29. Kanick SC, Sterenborg HJ, Amelink A. Empirical model of the photon path length for a single fiber reflectance spectroscopy device. *Opt Express*. 2009;17(2):860-71.
30. Gamm UA, Kanick SC, Sterenborg HJ, Robinson DJ, Amelink A. Quantification of the reduced scattering coefficient and phase-function-dependent parameter gamma of turbid media using multidiameter single fiber reflectance spectroscopy: experimental validation. *Opt Lett*. 2012;37(11):1838-40. doi: 10.364/OL.37.001838.
31. Gamm UA, Kanick SC, Sterenborg HJ, Robinson DJ, Amelink A. Measurement of tissue scattering properties using multi-diameter single fiber reflectance spectroscopy: in silico sensitivity analysis. *Biomed Opt Express*. 2011;2(11):3150-66. doi: 10.1364/BOE.2.003150. Epub 2011 Oct 26.
32. Kanick SC, Gamm UA, Sterenborg HJ, Robinson DJ, Amelink A. Method to quantitatively estimate wavelength-dependent scattering properties from multidiameter single fiber reflectance spectra measured in a turbid medium. *Opt Lett*. 2011;36(15):2997-9. doi: 10.1364/OL.36.002997.
33. Kanick SC, Robinson DJ, Sterenborg HJ, Amelink A. Extraction of intrinsic fluorescence from single fiber fluorescence measurements on a turbid medium. *Opt Lett*. 2012;37(5):948-50. doi: 10.1364/OL.37.000948.
34. Kanick SC, Robinson DJ, Sterenborg HJ, Amelink A. Semi-empirical model of the effect of scattering on single fiber fluorescence intensity measured on a turbid medium. *Biomed Opt Express*. 2012;3(1):137-52. doi: 10.1364/BOE.3.000137. Epub 2011 Dec 14.
35. van Leeuwen-van Zaane F, Gamm UA, van Driel PB, Snoeks TJ, de Bruijn HS, van der Ploeg-van den Heuvel A, et al. In vivo quantification of the scattering properties of tissue using multidiameter single fiber reflectance spectroscopy. *Biomed Opt Express*. 2013;4(5):696-708. doi: 10.1364/BOE.4.000696. Print 2013 May 1.
36. Tyrrell J, Thorn C, Shore A, Campbell S, Curnow A. Oxygen saturation and perfusion changes during dermatological methylaminolaevulinate photodynamic therapy. *Br J Dermatol*. 2011;165(6):1323-31. doi: 10.1111/j.165-2133.011.10554.x. Epub 2011 Nov 17.
37. Middelburg TA, Kanick SC, de Haas ER, Sterenborg HJ, Amelink A, Neumann MH, et al. Monitoring blood volume and saturation using superficial fibre optic reflectance spectroscopy during PDT of actinic keratosis. *J Biophotonics*. 2011;4(10):721-30. doi: 10.1002/jbio.201100053. Epub 2011 Aug 15.
38. Wang KK, Cottrell WJ, Mitra S, Oseroff AR, Foster TH. Simulations of measured photobleaching kinetics in human basal cell carcinomas suggest blood flow reductions during ALA-PDT. *Lasers Surg Med*. 2009;41(9):686-96. doi: 10.1002/lsm.20847.
39. Wang Y, Liao XH, Gu Y, Chen R, Zeng J. [The change of reflection spectra and fluorescence spectra of port wine stains during PDT]. *Guang Pu Xue Yu Guang Pu Fen Xi*. 2011;31(11):2969-72.
40. Kanick SC, Robinson DJ, Sterenborg HJ, Amelink A. Monte Carlo analysis of single fiber reflectance spectroscopy: photon path length and sampling depth. *Phys Med Biol*. 2009;54(22):6991-7008. doi: 10.1088/0031-9155/54/22/016. Epub 2009 Nov 4.

41. Hoy CL, Gamm UA, Sterenborg HJ, Robinson DJ, Amelink A. Method for rapid multidiameter single-fiber reflectance and fluorescence spectroscopy through a fiber bundle. *J Biomed Opt.* 2013;18(10):107005.
42. Prince MR, Frisoli JK. Beta-carotene accumulation in serum and skin. *Am J Clin Nutr.* 1993;57(2):175-81.
43. Amelink A, Robinson DJ, Sterenborg HJ. Confidence intervals on fit parameters derived from optical reflectance spectroscopy measurements. *J Biomed Opt.* 2008;13(5):054044.
44. Tseng SH, Bargo P, Durkin A, Kollias N. Chromophore concentrations, absorption and scattering properties of human skin in-vivo. *Opt Express.* 2009;17(17):14599-617.
45. Middelburg TA, Van Zaane F, De Bruijn HS, Van Der Ploeg-van den Heuvel A, Sterenborg HJ, Neumann HA, et al. Fractionated illumination at low fluence rate photodynamic therapy in mice. *Photochem Photobiol.* 2010;86(5):1140-6. doi: 10.1111/j.751-097.2010.00760.x.
46. Middelburg T, De Bruijn H, Van der Ploeg van den Heuvel A, Neumann H, Robinson D. The effect of light fractionation with a two-hour dark interval on the efficacy of topical hexyl-aminolevulinate photodynamic therapy in normal mouse skin. Submitted to *Photodiagnosis and Photodynamic Therapy.* 2013.
47. Robinson DJ, de Bruijn HS, Star WM, Sterenborg HJ. Dose and timing of the first light fraction in two-fold illumination schemes for topical ALA-mediated photodynamic therapy of hairless mouse skin. *Photochem Photobiol.* 2003;77(3):319-23.
48. Zeng H, Korbelik M, McLean DI, MacAulay C, Lui H. Monitoring photoproduct formation and photobleaching by fluorescence spectroscopy has the potential to improve PDT dosimetry with a verteporfin-like photosensitizer. *Photochem Photobiol.* 2002;75(4):398-405.
49. Dysart JS, Patterson MS. Photobleaching kinetics, photoproduct formation, and dose estimation during ALA induced PpIX PDT of MLL cells under well oxygenated and hypoxic conditions. *Photochem Photobiol Sci.* 2006;5(1):73-81. Epub 2005 Nov 15.
50. Drakaki E, Kaselouris E, Makropoulou M, Serafetinides AA, Tsenga A, Stratigos AJ, et al. Laser-induced fluorescence and reflectance spectroscopy for the discrimination of basal cell carcinoma from the surrounding normal skin tissue. *Skin Pharmacol Physiol.* 2009;22(3):158-65. doi: 10.1159/000211912. Epub 2009 Apr 8.
51. Galletly NP, McGinty J, Dunsby C, Teixeira F, Requejo-Isidro J, Munro I, et al. Fluorescence lifetime imaging distinguishes basal cell carcinoma from surrounding uninvolved skin. *Br J Dermatol.* 2008;159(1):152-61. doi: 10.1111/j.365-2133.008.08577.x. Epub 2008 Jul 1.
52. Na R, Stender IM, Wulf HC. Can autofluorescence demarcate basal cell carcinoma from normal skin? A comparison with protoporphyrin IX fluorescence. *Acta Derm Venereol.* 2001;81(4):246-9.
53. Sanchez WY, Obispo C, Ryan E, Grice JE, Roberts MS. Changes in the redox state and endogenous fluorescence of in vivo human skin due to intrinsic and photo-aging, measured by multiphoton tomography with fluorescence lifetime imaging. *J Biomed Opt.* 2013;18(6):061217. doi: 10.1117/1.JBO.18.6..
54. Beisswenger PJ, Howell S, Mackenzie T, Corstjens H, Muizzuddin N, Matsui MS. Two fluorescent wavelengths, 440(ex)/520(em) nm and 370(ex)/440(em) nm, reflect advanced glycation and oxi-

- dation end products in human skin without diabetes. *Diabetes Technol Ther.* 2012;14(3):285-92. doi: 10.1089/dia.2011.0108. Epub 2011 Oct 24.
55. Koetsier M, Lutgers H, Smit AJ, Links TP, Vries RD, Gans RO, et al. Skin autofluorescence for the risk assessment of chronic complications in diabetes: a broad excitation range is sufficient. *Opt Express.* 2009;17(2):509-19.
 56. Koetsier M, Lutgers HL, de Jonge C, Links TP, Smit AJ, Graaff R. Reference values of skin autofluorescence. *Diabetes Technol Ther.* 2010;12(5):399-403. doi: 10.1089/dia.2009.0113.
 57. Keshpore DS, Gibbs-Strauss SL, O'Hara JA, Hutchins M, Mincun N, Leblond F, et al. Imaging of glioma tumor with endogenous fluorescence tomography. *J Biomed Opt.* 2009;14(3):030501. doi: 10.1117/1.3127202.
 58. Finlay JC, Foster TH. Recovery of hemoglobin oxygen saturation and intrinsic fluorescence with a forward-adjoint model. *Appl Opt.* 2005;44(10):1917-33.
 59. Palmer GM, Viola RJ, Schroeder T, Yarmolenko PS, Dewhirst MW, Ramanujam N. Quantitative diffuse reflectance and fluorescence spectroscopy: tool to monitor tumor physiology in vivo. *J Biomed Opt.* 2009;14(2):024010. doi: 10.1117/1.3103586.
 60. Wilson RH, Chandra M, Scheiman J, Simeone D, McKenna B, Purdy J, et al. Optical spectroscopy detects histological hallmarks of pancreatic cancer. *Opt Express.* 2009;17(20):17502-16. doi: 10.1364/OE.17.017502.
 61. Baran TM, Foster TH. Recovery of intrinsic fluorescence from single-point interstitial measurements for quantification of doxorubicin concentration. *Lasers Surg Med.* 2013;45(8):542-50. doi: 10.1002/lsm.22166. Epub 2013 Aug 23.
 62. Finlay JC, Zhu TC, Dimofte A, Stripp D, Malkowicz SB, Busch TM, et al. Interstitial fluorescence spectroscopy in the human prostate during motexafin lutetium-mediated photodynamic therapy. *Photochem Photobiol.* 2006;82(5):1270-8.
 63. Diamond KR, Patterson MS, Farrell TJ. Quantification of fluorophore concentration in tissue-simulating media by fluorescence measurements with a single optical fiber. *Appl Opt.* 2003;42(13):2436-42.
 64. Cihan C, Arifler D. Influence of phase function on modeled optical response of nanoparticle-labeled epithelial tissues. *J Biomed Opt.* 2011;16(8):085002. doi: 10.1117/1.3608999.
 65. Yaroslavsky AN, Yaroslavsky IV, Goldbach T, Schwarzmaier HJ. Influence of the scattering phase function approximation on the optical properties of blood determined from the integrating sphere measurements. *J Biomed Opt.* 1999;4(1):47-53.
 66. Mourant JR, Boyer J, Hielscher AH, Bigio IJ. Influence of the scattering phase function on light transport measurements in turbid media performed with small source-detector separations. *Opt Lett.* 1996;21(7):546-8.
 67. Van den Bergh H, Ballini JP. In: Gragoudas ES, Miller JW, Zografos L, editors. *Principles of PDT, in PDT of Ocular Diseases* Lippincott Williams & Wilkins; 2004. p. 11-42.

68. Davis SC, Pogue BW, Springett R, Leussler C, Mazurkewitz P, Tuttle SB, et al. Magnetic resonance-coupled fluorescence tomography scanner for molecular imaging of tissue. *Rev Sci Instrum.* 2008;79(6):064302. doi: 10.1063/1.2919131.
69. Fritsch C, Lehmann P, Stahl W, Schulte KW, Blohm E, Lang K, et al. Optimum porphyrin accumulation in epithelial skin tumours and psoriatic lesions after topical application of delta-aminolaevulinic acid. *Br J Cancer.* 1999;79(9-10):1603-8.
70. Smits T, van Laarhoven AI, Staassen A, van de Kerkhof PC, van Erp PE, Gerritsen MJ. Induction of protoporphyrin IX by aminolaevulinic acid in actinic keratosis, psoriasis and normal skin: preferential porphyrin enrichment in differentiated cells. *Br J Dermatol.* 2009;160(4):849-57. doi: 10.1111/j.1365-2133.008.09012.x. Epub 2009 Jan 27.
71. Hoy CL, Gamm UA, Sterenborg HJ, Robinson DJ, Amelink A. Use of a coherent fiber bundle for multi-diameter single fiber reflectance spectroscopy. *Biomed Opt Express.* 2012;3(10):2452-64. doi: 10.1364/BOE.3.002452. Epub 2012 Sep 12.

9

Discussion

DISCUSSION

This thesis is focused on three main topics that are closely related to a more fundamental understanding of PDT in the skin:

- 1) The distribution of PpIX in the skin and how this relates to vascular effects during PDT.
- 2) The measurement of PpIX fluorescence during PDT. This enables monitoring PpIX synthesis and photobleaching and it provides information on oxygen consumption and singlet oxygen formation.
- 3) The use of optical techniques that allow superficial measurements of optical properties in the skin. These measurements provide information on the blood supply during PDT and presence of other chromophores, while they can also be used to measure scattering properties and correct detected fluorescence signals.

These topics are critically important for the optimization of current treatment protocols, and show how approaches to personalize PDT could be applied in future studies. The importance of the need to improve PDT is illustrated by lack of long term complete responses in some patients¹⁻⁴ and by the considerable pain associated with PDT using porphyrin pre-cursors^{5,6}.

Distribution of PpIX in the skin and vascular effects

The results presented in chapters 4-6 clearly illustrate the magnitude of the vascular effects associated with topical HAL and ALA-PDT. These effects include arteriole vasoconstriction during and after PDT, and damage to the endothelial membrane of dermal blood vessels. It is demonstrated how vascular effects are related to PpIX concentration in the vasculature. The consistent trend is that HAL is more potent than ALA, which is more potent than MAL in photosensitizing the superficial vasculature. This leads to most extensive vascular constriction and vascular damage during PDT for HAL, then ALA, then MAL. It is important to realize that it is not immediately clear whether such vascular effects are beneficial to PDT outcome or not. Since PDT requires oxygen, vasoconstriction of the superficial vessels that supply this oxygen can lead to insufficient oxygen availability during PDT. This in turn can harm the efficiency and the effectiveness of PDT. When the vasoconstriction is long-lasting or if the vasculature is damaged, this can lead to ischemia post-PDT. When such ischemia is extensive, too many normal cells may die too. This can lead to an inferior cosmetic or functional outcome. However, some ischemia may be beneficial because it can give a final blow to already damaged tumour cells, increasing effectiveness of PDT.

While the clinical relevance of this delicate balance between inducing too extensive or too little vascular effects needs to be further investigated, its importance can be il-

illustrated by the response to light fractionated PDT. The idea behind the increased effect of light fractionation is that a small first light fraction makes cells sensitive to a larger second light fraction. It has been shown that light fractionation works best for lower concentrations of PpIX⁷, and that it is critical that the effective dose of the first light fraction is low⁸. Because in topical PDT endothelial cells synthesize low concentrations of PpIX (compared with keratinocytes) these are considered the target of light fractionation⁹, leading to vascular damage after PDT and increased PDT efficacy. The fractionated illumination protocol used in this thesis has been developed and optimized for ALA-PDT. When these same illumination parameters are used for MAL-PDT however, it appears that the vascular PpIX concentrations are too low to lead to biologically relevant effects. Similarly, for HAL-PDT the vascular PpIX concentrations may be a little too high, leading to too much damage in the first illumination. This explains why light fractionation works best for ALA, appears to work for HAL but does not work for MAL-PDT¹⁰. Potential solutions are to lengthen the first illumination for MAL or to shorten it for light fractionated HAL-PDT. This illustrates how future fractionated illumination protocols for different porphyrin precursors (*e.g.* HAL or MAL) may need to be optimized based on their ability to photosensitize the vasculature and the resulting vascular effects.

Importantly, this ability may be different in human skin than in mouse skin due to potentially lower penetration of porphyrin precursors. It is commonly believed that ALA is too hydrophilic to penetrate the human epidermis well. However, the physiological changes that we measured with DPS and MDSFR during light fractionated ALA-PDT (chapters 7 and 8) indicate otherwise. Since we have shown that the vascular response in mice is strongly dependent on the PpIX concentration in the vessel wall, it is logical to assume that this will be true also in human skin. This in turn means that the superficial vessels in human skin also synthesize biologically relevant amount of PpIX in ALA-PDT. This is important because then a logical conclusion is that ALA does penetrate well through the epidermis and that its hydrophilic nature is not a limitation. How the vascular distribution of ALA compares to that of HAL and MAL after topical application in human skin is unknown, but may provide useful information that can be related to vascular effects in human skin.

PpIX fluorescence measurements

Monitoring PpIX fluorescence during PDT has the potential to be a powerful tool because it provides a wealth of relevant information about the PDT process. This includes the PpIX synthesis and resynthesis (which is important in light fractionated PDT), the kinetics of PpIX photobleaching, the availability of oxygen and the rate of singlet oxygen formation. It thus also informs on the effective deposited PDT dose. Another way in which PpIX fluorescence can be used to help understand fundamental processes involved in

PDT, is illustrated by its measurement in histological sections and in the mouse skin fold chamber model (chapters 4 and 5). These measurements are hardly affected by scattering and absorption because of the minimal volume of the examined tissue, but they are invasive methods. A surface measurement (using imaging or spectroscopy) has the advantage that it is a non-invasive method that can be applied during PDT illumination. However, as we have shown, the accuracy of such measurements is critically dependent on the effects of both light absorption and light scattering within the measured tissue. It is only when fluorescence is corrected for these optical properties that the power of measuring PpIX fluorescence can be used to its full extent in PDT. This is why throughout this thesis particular attention has been paid to try and optimize optical measurements on human skin.

Optical measurements on human skin

The first crucial consideration when optically sampling skin is the realisation that the epidermis and superficial part of the dermis are the volume of interest. This is where most PpIX is located and where the blood vessels are that directly supply oxygen during PDT. Furthermore, this is where many skin diseases will differ most in their optical properties. The second crucial consideration is that for spectroscopic techniques it is only possible to say something sensible about the collected light if you know what happens to the light in the tissue. This is why it is important to apply appropriate theories about light propagation in biological tissue to such spectroscopic measurements. It must be stressed that diffusion theory, widely employed for large volumes of tissue, is not valid for superficial spectroscopic measurements of μ_s' or fluorescence in skin. The reason for this is that light propagation is not diffuse at short source-detector separations that are necessary for superficial measurements¹¹. In such superficial measurements the proportion of wide-angle backscattering effects significantly affects the amount of light collected in a reflectance measurement^{12,13}. DPS is already a step forward because it samples from a superficial volume (chapter 7). However, it can only be used to measure the absorption but not the scattering properties. Because of this, it has been essential to develop a new model on light scattering that incorporates theory about the tissue phase function, which describes the distribution of the angle in which the light is scattered. This theoretical model was developed and the technique validated in computer simulations and in tissue-mimicking phantoms¹⁴⁻¹⁶. This has led to the development of MDSFR and SFF spectroscopy¹⁷⁻²³, which is being applied for the first time on human tissue in this thesis. This is an important step forward in biomedical optics. These types of measurements are not only valuable for PDT, but potentially also for applications that are beyond PDT and/or beyond the skin.

Potential value of MDSFR and SFF spectroscopy for PDT

For PDT the primary value of MDSFR and SFF spectroscopy is that it can be used to quantify PpIX fluorescence in human skin. The synthesis and photobleaching kinetics of PpIX in turn can be related to patient-specific PDT outcome in clinical studies. Furthermore, as we have shown to be possible in mice, MDSFR/SFF spectroscopy has the potential to control the effective deposited PDT dose in human skin. An example of this potential is to measure PpIX photobleaching and resynthesis during the dark interval in light fractionated PDT to optimize clinical treatment protocols. Again it is important to stress that this is not possible unless changes in optical properties during PDT are corrected for. While MDSFR/SFF spectroscopy enables to measure these changes in order to adequately correct PpIX fluorescence, it also allows to monitor changes in the vascular physiology during PDT of human skin. While such changes are likely to affect PDT outcome, clinical follow-up studies investigating this are needed.

Potential value of MDSFR and SFF spectroscopy for diagnostics (in the skin)

A closely related subject is the potential for using MDSFR and SFF spectroscopy to differentiate between skin diseases. Although this is not directly related to PDT it is worth paying particular attention to, because this diagnostic potential may be an important additional asset of MDSFR/SFF spectroscopy. As we have shown, the skin autofluorescence is significantly lower in actinic keratosis than in normal skin, for reasons that are however not immediately clear. This may be related to the thicker epidermis in actinic keratosis but possibly also to differences in the redox state between dysplastic and normal keratinocytes^{24, 25}. In addition to the autofluorescence measured with MDSFR/SFF, it is interesting to also consider the potential diagnostic value of the reflectance measurements. After all, with this approach it is possible to quantify the optical properties in a superficial volume of the skin. Importantly, this is the region in which most skin diseases will differ most in their histological and thus also in their optical characteristics. These different characteristics can be picked up by our innate optimal instruments –the eye– to distinguish between different skin diseases. Our eyes are however very limited optical instruments that are easily fooled by variable optical properties, which is why we perceive for example melanin and blood as blue when they are located deeper in the skin. Because MDSFR is an optical technique that is able to quantify the optical properties in the skin, it is conceivable that such an approach may improve the differentiation between skin diseases. The optical properties that can be quantitated with MDSFR and SFF spectroscopy can be divided into the: (1) scattering, (2) absorption and (3) autofluorescence. Each of these may have diagnostic value, and it is important to make a distinction between them and their separate diagnostic potential.

Scattering

When we consider the scattering properties of skin, it needs to be realized that these can be altered by nanoscale morphological changes that occur during early carcinogenesis in cells²⁶⁻²⁹. Because earlier cancer detection increases cure rates, scattering spectroscopy is a potentially valuable non-invasive diagnostic tool. With MDSFR spectroscopy it is now possible to quantify μ_s' in a superficial sampling volume that includes only the epidermis or the epidermis and a part of the dermis (depending on the choice of fiber diameters). The values of μ_s' have not yet been systematically investigated, because it has not been possible to quantify these in a superficial volume. Previous attempts to measure μ_s' have been based on diffuse, deep measurements that basically inform on an average of the scattering properties over a large sampling volume. Obviously, scattering properties are not homogeneously distributed throughout the thickness of the skin. This makes diffuse measurements insensitive to detection of superficial scattering changes that may be important in diagnostics. In addition to quantifying μ_s' , MDSFR spectroscopy also enables a measurement of the scattering power a_2 . This is considered an indicator of the relative size of scattering particles and has yet unclear potential value for diagnostics. Moreover, MDSFR allows the measurement of the phase function parameter γ . Gamma is believed to be related to the tissue ultrastructure³⁰. Differences in tissue ultrastructure such as cytoskeleton alterations in early cancer may be reflected by changes in γ . It is important to note that the diagnostic potential of phase function parameters such as γ are at the forefront of research in biomedical optics and their potential value are therefore still largely unexplored.

Absorption

The quantification of the absorption coefficient μ_a with MDSFR spectroscopy yields information on the vascular parameters (*i.e.* blood volume fraction, mean vessel diameter and saturation). These may be diagnostically valuable because cancer tissue is known for its alterations in the local microvasculature. From μ_a it is also possible to calculate the local concentration of other chromophores, such as melanin, bilirubin and beta-carotene. These parameters may also be different for different skin conditions, but their measurement needs further validation in the skin.

Autofluorescence

Finally, the quantification of the intrinsic autofluorescence may also be diagnostically valuable. Several studies using different fluorescence spectroscopic techniques have described the potential value of the autofluorescence to differentiate between normal and neoplastic skin³¹⁻³³. Obviously, it is necessary to correct the fluorescence for the optical properties of the sampled volume to obtain quantitative results. It is also important to improve our ability to differentiate between the individual fluorophores that constitute

the combined autofluorescence signal. Finally, *in-vivo* spectroscopic measurements need to be validated for example by comparing the fluorescence with chemical extraction of the fluorophores in skin biopsies.

While the potential diagnostic value of MDSFR and SFF spectroscopy will be further investigated in the near future, it is nevertheless interesting to take a closer look at our measurements of chapter 8. When we compare our MDSFR measurements of actinic keratosis before ALA application with those acquired from contralateral normal skin during PDT (chapter 8) we see some interesting differences between them. It is important to again stress that these measurements need to be validated. Table 1 gives an overview of the absorption, scattering and autofluorescence parameters that were measured with MDSFR spectroscopy. Even though these data are based on relatively few patients, three parameters were significantly different after correction for multiple comparisons: the blood volume fraction, the bilirubin content, and the autofluorescence.

Table 1. Overview of the absorption and scattering parameters measured with MDSFR and SFF spectroscopy in normal and lesional skin (actinic keratosis or Bowen's disease).

Measured parameter (unit)	Lesional skin median (¼ - ¾ IQR)	Normal skin median (¼ - ¾ IQR)	Magnitude of median difference (lesional/normal)	P-value (paired Wilcoxon signed rank test)
Saturation (%)	60 (38-75)	48 (32-65)	1.2	0.27
Blood volume fraction (%)	<i>0.61 (0.34-0.75)</i>	<i>0.33 (0.18-0.42)</i>	1.9	<i><0.005</i>
Mean vessel diameter (mm)	0.013 (0.008-0.022)	0.014 (0.010-0.020)	0.89	0.85
Melanin (µM)	15 (2.3-38)	27 (16-50)	0.54	0.16
Beta carotene (µM)	0.047 (0.011-0.082)	0.022 (0.013-0.041)	2.1	0.03
Bilirubin (a.u.)	<i>3.4 (2.5-5.4)</i>	<i>0.92 (0.52-2.36)</i>	3.7	<i><0.0005</i>
γ at 800nm (-)	1.6 (1.5-1.7)	1.6 (1.5-1.7)	1.0	0.81
μ _s ' 800nm (mm ⁻¹)	1.4 (1.2-1.6)	1.6 (1.1-2.6)	0.85	0.08
a ₂ 800nm (mm ⁻¹ nm ⁻¹)	1.0 (0.9-1.3)	1.4 (1.1-1.7)	0.71	0.09
Autofluorescence (mm ⁻¹)	<i>0.003 (0.002-0.004)</i>	<i>0.005 (0.005-0.006)</i>	0.61	<i><0.0005</i>

In italic are the parameters that were significantly different after correction for multiple comparisons (*i.e.* P-value < 0.005). IQR=interquartile range.

While the higher blood volume is in accordance with the clinical reddish appearance of actinic keratosis, our eyes cannot see the difference between vasodilation in inflammation and neovascularisation in (pre)malignant change. In our MDSFR measurements the blood volume fraction was higher for actinic keratosis than normal skin but the vessel diameter was not, which indicates that neovascularisation (and not inflammatory vasodilation is primarily responsible for the red appearance of actinic keratosis. Such information can be useful for diagnostics in the skin and other organs.

The higher bilirubin content in lesional skin is interesting but without a full validation is difficult to explain. Bilirubin is a breakdown product of haemoglobin, and this breakdown process occurs in macrophages. Since actinic keratosis is accompanied by a macrophage containing infiltrate, the higher bilirubin content in actinic keratosis may be a reflection of increased local breakdown of haemoglobin. Note that bilirubin is also absorbed in the same spectral regions in which melanin and haemoglobin are well absorbed, making bilirubin measurements less precise. However, this may not be problematic because the magnitude of the difference was large (3.7x) and this finding was very consistent between patients (in 89% of patients the bilirubin was higher in lesional than in normal skin).

Although the scattering properties were not significantly different in this studied example, it can be expected that morphological changes of neoplastic cells will result in differences in scattering properties as explained above. The magnitude of the difference in μ_s' and a_2 suggest that MDSFR may allow the detection of such differences. Obviously our dataset was small and not powered to detect any statistical difference properly. A larger follow up study is needed that is better powered and thus also allows for multivariate regression analysis to detect combinations of measured parameters that can be considered predictors of disease. Upon histology, actinic keratosis exhibits a more or less characteristic combination of visible features and here a single histologic feature (e.g. acanthosis) is not disease-specific and thus not a good predictor for the diagnosis. Likewise, individual optical parameters may also be not a good predictor on their own, but specific combinations for actinic keratosis may exist that are good predictors for a diagnosis. The combination of blood volume fraction and vessel diameter is an example of such a combination. In conclusion, the full potential of the predictive value of MDSFR spectroscopy for diagnostics in the skin needs further study. It is promising however that we can already detect statistical differences in optical properties between actinic keratosis and normal skin in a small sample of patients.

Potential value of MDSFR and SFF spectroscopy beyond PDT and beyond the skin

It is interesting to also consider the potential applications of MDSFR/SFF spectroscopy other than for PDT or diagnostics in the skin. First, MDSFR/SFF is not limited to being applied solely in the skin. In principle, it can also aid the diagnosis of diseases in various organs in which superficial changes in optical properties are likely to be characteristic of disease. As such it may be used in the epithelia of the oral cavity, the gastrointestinal tract, the bladder, the cervix or the lung. The small diameters of the probes may even allow them to be incorporated in fine-needle aspiration which may also aid the diagnostic process. Because MDSFR/SFF spectroscopy enables measurements of local

fluorophore or chromophore concentrations, it may also be helpful to detect certain internal diseases. These can be liver diseases accompanied with high bilirubin levels, porphyrias accompanied by porphyrin accumulation in the blood, or metabolic storage diseases in which several molecules can accumulate in tissue such as the skin. Further, the quantification of the autofluorescence from advanced glycation end products using MDSFR and SFF spectroscopy can be very valuable for risk assessment in a range of diseases associated with cumulative metabolic stress. The list of associations with high skin autofluorescence is long: cardiovascular complications, glucose intolerance in diabetes, chronic obstructive pulmonary disease, postsurgical complications, renal insufficiency, liver cirrhosis, leg ulceration, advanced age and more^{25, 34-43}. It cannot be stressed strongly enough that it is crucial to correct any skin fluorescence measurement for the tissue optical properties. In the studies investigating these associations a diffuse, deep optical measurement was taken and this was not corrected for absorption, scattering or variability in for example lamp output or light transmission within the system. This can result in a patient being treated for assumed high cardiovascular risk based on high skin autofluorescence that does not represent high fluorescence from advanced glycation end-products at all, but simply increased backscattering or reduced absorption that has no relation to the risk of cardiovascular events. This illustrates that studies relating skin autofluorescence to any of the mentioned conditions can benefit enormously from MDSFR and SFF spectroscopy. This is especially true when the aim is to derive meaningful information about an autofluorescence measurement in a single patient. When fluorescence is measured in a large number of patients, correlations (if present) will be found also with non-quantitative measurements. However, the likelihood of a single measurement in a single patient to be a good predictor (for example for cardiovascular events) is a lot better for accurate than for inaccurate measurements. In other words: accurate, quantitative autofluorescence measurements can provide useful information on risk assessment on a personalized level, while non-quantitative and inaccurate measurements cannot.

This thesis and personalized PDT

It is now time to consider how this thesis contributes to an improved and more personalized approach to PDT. One important contribution is related to the potential of PpIX photobleaching kinetics to monitor and control the effective deposited PDT dose for individual mice (chapters 3 and 6). Now that we have the ability to quantitate PpIX fluorescence in human skin using MDSFR and SFF spectroscopy, this kind of approach can also be applied to human PDT. It can be used to control the effective PDT dose of the illuminations in light fractionated PDT. PpIX fluorescence measurements can be performed on an individual basis to optimize PDT on a personalized level. Moreover, monitoring PDT with MDSFR/SFF spectroscopy will allow for pain-free and effective

PDT. This can be achieved by applying low fluence rate, light fractionated PDT. During illumination, the effective PDT dose for each individual patient can be monitored based on the PpIX photobleaching kinetics to ensure effectiveness.

Another potential contribution to personalize PDT is that when the PpIX concentration before the (first) PDT illumination turns out to be too low, it may be best to not perform PDT at that time for that particular patient. Potentially the peak in PpIX synthesis in some patients requires a longer application time of the porphyrin precursor. The optimal time-point for illumination can be based on such individual differences, because the PpIX fluorescence can now be quantified with MDSFR/SFF spectroscopy. This can help to improve PDT effectiveness on a personal basis.

Finally, it is now possible to accurately monitor changes in the physiology of the superficial vasculature in individual patients. Such changes can influence the oxygen supply that is required for PDT. Therefore, extensive vasoconstriction during PDT can decrease its efficiency and effectiveness. In this respect, it is interesting that lowering the fluence rate will likely result in less vasoconstriction. This can be explained by the apparent threshold for arteriole vasoconstriction which is related to the PpIX concentration in the arteriole wall (chapter 3). It can be assumed that this threshold is not in fact directly and causally related to this PpIX concentration. Instead, it makes biologically more sense that it is related to the rate of singlet oxygen formation, which is higher for higher PpIX concentrations. As a result, the threshold for vasoconstriction will be reached quicker at high PpIX concentration and at high photobleaching rates. A solution would therefore be to use a lower fluence rate, which leads to lower photobleaching and singlet oxygen formation rates. It may be that at low fluence rate PDT, the rate of singlet oxygen production will be lower than the threshold that leads to vasoconstriction.

Future perspectives

When using MDSFR and SFF spectroscopy to monitor PDT, this is ideally performed continuously during illumination while providing immediate feedback during illumination. Currently this is limited due to the computation time of analysing the spectra. Advances in computation speed can be combined with the development of software that automatically generates graphical or other types of feedback on measured parameters. However, when continuous measurements are taken, then the MDSFR/SFF probe would be in the way of the PDT illumination light, which is an obvious problem. A way to overcome this problem would be to adapt the system so that it uses red (~635 nm) light to excite PpIX while emitted PpIX fluorescence is detected at longer wavelengths (PpIX has another emission peak centred at 705 nm). This ensures that the probed area will receive the same amount of excitation light as the rest of the treated area.

Another important future perspective that is however not related to PDT is the use of MDSFR spectroscopy for diagnostics in the skin. A significant improvement of the MS-DFR/SFF system used in this thesis is the recent development of a 19-fiber optical probe²⁰. This allows tailoring the sampling volume to the desired depth, which will increase sensitivity for depth-dependent parameters that have diagnostic value. Skin diseases are expected to have more or less characteristic combinations of optical properties, similar to them having more or less characteristics histological features under light microscopy. By now, many books have been written about which patterns of histological features fit best with a particular diagnosis. In a similar fashion it may be advantageous to build a database that contains the typical pattern of optical properties of skin diseases for a range of optical sampling depths. It will then be theoretically possible to construct an algorithm that automatically generates an optical differential diagnosis of a single MDSFR measurement which would significantly aid the clinical and histological diagnostic process.

Conclusion

This thesis is focused on the identification and measurement of parameters that contribute to an improved understanding of fundamental PDT processes. It is shown how this type of approach can improve and personalize PDT, and control side effects. I'd like to conclude with two expressions of Lord Kelvin from the 19th century that seem particularly applicable to this thesis and to science in general: "When you can measure what you are speaking about, and express it in numbers, you know something about it , and "If you cannot measure it, you cannot improve it".

REFERENCES

1. Rhodes LE, de Rie MA, Leifsdottir R, Yu RC, Bachmann I, Goulden V, et al. Five-year follow-up of a randomized, prospective trial of topical methyl aminolevulinate photodynamic therapy vs surgery for nodular basal cell carcinoma. *Arch Dermatol*. 2007;143(9):1131-6.
2. Roozeboom MH, Arits AH, Nelemans PJ, Kelleners-Smeets NW. Overall treatment success after treatment of primary superficial basal cell carcinoma: a systematic review and meta-analysis of randomized and nonrandomized trials. *Br J Dermatol*. 2012;167(4):733-56. doi: 10.1111/j.365-2133.012.11061.x. Epub 2012 Sep 7.
3. Roozeboom MH, Aardoom MA, Nelemans PJ, Thissen MR, Kelleners-Smeets NW, Kuijpers DI, et al. Fractionated 5-aminolevulinic acid photodynamic therapy after partial debulking versus surgical excision for nodular basal cell carcinoma: a randomized controlled trial with at least 5-year follow-up. *J Am Acad Dermatol*. 2013;69(2):280-7. doi: 10.1016/j.jaad.2013.02.014. Epub Apr 6.
4. Nashan D, Meiss F, Muller M. Therapeutic strategies for actinic keratoses—a systematic review. *Eur J Dermatol*. 2013;23(1):14-32. doi: 10.1684/ejd.2013.1923.
5. Ibbotson SH. Adverse effects of topical photodynamic therapy. *Photodermatol Photoimmunol Photomed*. 2011;27(3):116-30. doi: 10.1111/j.600-0781.2010.00560.x.
6. Mikolajewska P. Pain during topical photodynamic therapy [www document]. 2011; <https://www.duo.uio.no/handle/10852/11075?locale-attribute=en> [accessed on 12 March 2013].
7. de Bruijn HS, Casas AG, Di Venosa G, Gandara L, Sterenberg HJ, Batlle A, et al. Light fractionated ALA-PDT enhances therapeutic efficacy in vitro; the influence of PpIX concentration and illumination parameters. *Photochem Photobiol Sci*. 2013;12(2):241-5. doi: 10.1039/c2pp25287b. Epub 2012 Oct 29.
8. Robinson DJ, de Bruijn HS, Star WM, Sterenberg HJ. Dose and timing of the first light fraction in two-fold illumination schemes for topical ALA-mediated photodynamic therapy of hairless mouse skin. *Photochem Photobiol*. 2003;77(3):319-23.
9. de Bruijn HS, Meijers C, van der Ploeg-van den Heuvel A, Sterenberg HJ, Robinson DJ. Microscopic localisation of protoporphyrin IX in normal mouse skin after topical application of 5-aminolevulinic acid or methyl 5-aminolevulinate. *J Photochem Photobiol B*. 2008;92(2):91-7. doi: 10.1016/j.jphotobiol.2008.05.005. Epub May 15.
10. de Bruijn HS, de Haas ER, Hebeda KM, van der Ploeg-van den Heuvel A, Sterenberg HJ, Neumann HA, et al. Light fractionation does not enhance the efficacy of methyl 5-aminolevulinate mediated photodynamic therapy in normal mouse skin. *Photochem Photobiol Sci*. 2007;6(12):1325-31. Epub 2007 Aug 28.
11. Jacques SL, Pogue BW. Tutorial on diffuse light transport. *J Biomed Opt*. 2008;13(4):041302. doi: 10.1117/1.2967535.
12. Cihan C, Arifler D. Influence of phase function on modeled optical response of nanoparticle-labeled epithelial tissues. *J Biomed Opt*. 2011;16(8):085002. doi: 10.1117/1.3608999.

13. Mourant JR, Boyer J, Hielscher AH, Bigio IJ. Influence of the scattering phase function on light transport measurements in turbid media performed with small source-detector separations. *Opt Lett*. 1996;21(7):546-8.
14. Kanick SC, Robinson DJ, Sterenborg HJ, Amelink A. Monte Carlo analysis of single fiber reflectance spectroscopy: photon path length and sampling depth. *Phys Med Biol*. 2009;54(22):6991-7008. doi: 10.1088/0031-9155/54/22/016. Epub 2009 Nov 4.
15. Kanick SC, Gamm UA, Schouten M, Sterenborg HJ, Robinson DJ, Amelink A. Measurement of the reduced scattering coefficient of turbid media using single fiber reflectance spectroscopy: fiber diameter and phase function dependence. *Biomed Opt Express*. 2011;2(6):1687-702. doi: 10.364/BOE.2.001687. Epub 2011 May 25.
16. Kanick SC, Sterenborg HJ, Amelink A. Empirical model of the photon path length for a single fiber reflectance spectroscopy device. *Opt Express*. 2009;17(2):860-71.
17. Gamm UA, Kanick SC, Sterenborg HJ, Robinson DJ, Amelink A. Measurement of tissue scattering properties using multi-diameter single fiber reflectance spectroscopy: in silico sensitivity analysis. *Biomed Opt Express*. 2011;2(11):3150-66. doi: 10.1364/BOE.2.003150. Epub 2011 Oct 26.
18. Gamm UA, Kanick SC, Sterenborg HJ, Robinson DJ, Amelink A. Quantification of the reduced scattering coefficient and phase-function-dependent parameter gamma of turbid media using multidiameter single fiber reflectance spectroscopy: experimental validation. *Opt Lett*. 2012;37(11):1838-40. doi: 10.364/OL.37.001838.
19. Hoy CL, Gamm UA, Sterenborg HJ, Robinson DJ, Amelink A. Use of a coherent fiber bundle for multi-diameter single fiber reflectance spectroscopy. *Biomed Opt Express*. 2012;3(10):2452-64. doi: 10.1364/BOE.3.002452. Epub 2012 Sep 12.
20. Hoy CL, Gamm UA, Sterenborg HJ, Robinson DJ, Amelink A. Method for rapid multidiameter single-fiber reflectance and fluorescence spectroscopy through a fiber bundle. *J Biomed Opt*. 2013;18(10):107005.
21. Kanick SC, Gamm UA, Sterenborg HJ, Robinson DJ, Amelink A. Method to quantitatively estimate wavelength-dependent scattering properties from multidiameter single fiber reflectance spectra measured in a turbid medium. *Opt Lett*. 2011;36(15):2997-9. doi: 10.1364/OL.36.002997.
22. Kanick SC, Robinson DJ, Sterenborg HJ, Amelink A. Semi-empirical model of the effect of scattering on single fiber fluorescence intensity measured on a turbid medium. *Biomed Opt Express*. 2012;3(1):137-52. doi: 10.1364/BOE.3.000137. Epub 2011 Dec 14.
23. Kanick SC, Robinson DJ, Sterenborg HJ, Amelink A. Extraction of intrinsic fluorescence from single fiber fluorescence measurements on a turbid medium. *Opt Lett*. 2012;37(5):948-50. doi: 10.1364/OL.37.000948.
24. Mayevsky A, Rogatsky GG. Mitochondrial function in vivo evaluated by NADH fluorescence: from animal models to human studies. *Am J Physiol Cell Physiol*. 2007;292(2):C615-40. Epub 2006 Aug 30.
25. Sanchez WY, Obispo C, Ryan E, Grice JE, Roberts MS. Changes in the redox state and endogenous fluorescence of in vivo human skin due to intrinsic and photo-aging, measured by multiphoton

- tomography with fluorescence lifetime imaging. *J Biomed Opt.* 2013;18(6):061217. doi: 10.1117/1.JBO.18.6..
26. Roy HK, Subramanian H, Damania D, Hensing TA, Rom WN, Pass HI, et al. Optical detection of buccal epithelial nanoarchitectural alterations in patients harboring lung cancer: implications for screening. *Cancer Res.* 2010;70(20):7748-54. doi: 10.1158/0008-5472.CAN-10-1686. Epub 2010 Oct 5.
 27. Roy HK, Turzhitsky V, Kim Y, Goldberg MJ, Watson P, Rogers JD, et al. Association between rectal optical signatures and colonic neoplasia: potential applications for screening. *Cancer Res.* 2009;69(10):4476-83. doi: 10.1158/0008-5472.CAN-08-4780. Epub 2009 May 5.
 28. Subramanian H, Pradhan P, Liu Y, Capoglu IR, Li X, Rogers JD, et al. Optical methodology for detecting histologically unapparent nanoscale consequences of genetic alterations in biological cells. *Proc Natl Acad Sci U S A.* 2008;105(51):20118-23. doi: 10.1073/pnas.0804723105. Epub 2008 Dec 10.
 29. Pradhan P, Damania D, Joshi HM, Turzhitsky V, Subramanian H, Roy HK, et al. Quantification of nanoscale density fluctuations by electron microscopy: probing cellular alterations in early carcinogenesis. *Phys Biol.* 2011;8(2):026012. doi: 10.1088/1478-3975/8/2/. Epub 2011 Mar 25.
 30. Thueler P, Charvet I, Bevilacqua F, St Ghislain M, Ory G, Marquet P, et al. In vivo endoscopic tissue diagnostics based on spectroscopic absorption, scattering, and phase function properties. *J Biomed Opt.* 2003;8(3):495-503.
 31. Drakaki E, Kaselouris E, Makropoulou M, Serafetinides AA, Tsenga A, Stratigos AJ, et al. Laser-induced fluorescence and reflectance spectroscopy for the discrimination of basal cell carcinoma from the surrounding normal skin tissue. *Skin Pharmacol Physiol.* 2009;22(3):158-65. doi: 10.1159/000211912. Epub 2009 Apr 8.
 32. Galletly NP, McGinty J, Dunsby C, Teixeira F, Requejo-Isidro J, Munro I, et al. Fluorescence lifetime imaging distinguishes basal cell carcinoma from surrounding uninvolved skin. *Br J Dermatol.* 2008;159(1):152-61. doi: 10.1111/j.1365-2133.008.08577.x. Epub 2008 Jul 1.
 33. Na R, Stender IM, Wulf HC. Can autofluorescence demarcate basal cell carcinoma from normal skin? A comparison with protoporphyrin IX fluorescence. *Acta Derm Venereol.* 2001;81(4):246-9.
 34. Arsov S, Graaff R, van Oeveren W, Stegmayr B, Sikole A, Rakhorst G, et al. Advanced glycation end-products and skin autofluorescence in end-stage renal disease: a review. *Clin Chem Lab Med.* 2013;4:1-10.
 35. Bos DC, de Ranitz-Greven WL, de Valk HW. Advanced glycation end products, measured as skin autofluorescence and diabetes complications: a systematic review. *Diabetes Technol Ther.* 2011;13(7):773-9. doi: 10.1089/dia.2011.0034. Epub 2011 Apr 21.
 36. de Groot L, Hinkema H, Westra J, Smit AJ, Kallenberg CG, Bijl M, et al. Advanced glycation end-products are increased in rheumatoid arthritis patients with controlled disease. *Arthritis Res Ther.* 2011;13(6):R205. doi: 10.1186/ar3538. Epub 2011 Dec 14.
 37. de Vos LC, Noordzij MJ, Mulder DJ, Smit AJ, Lutgers HL, Dullaart RP, et al. Skin autofluorescence as a measure of advanced glycation end products deposition is elevated in peripheral artery dis-

- ease. *Arterioscler Thromb Vasc Biol.* 2013;33(1):131-8. doi: 10.1161/ATVBAHA.112.300016. Epub 2012 Nov 8.
38. Genevieve M, Vivot A, Gonzalez C, Raffaitin C, Barberger-Gateau P, Gin H, et al. Skin autofluorescence is associated with past glycaemic control and complications in type 1 diabetes mellitus. *Diabetes Metab.* 2013;2(13):00051-7.
 39. Gopal P, Reynaert NL, Scheijen JL, Engelen L, Schalkwijk CG, Franssen FM, et al. Plasma AGEs and skin autofluorescence are increased in COPD. *Eur Respir J.* 2013;3:3.
 40. Hartog JW, Gross S, Oterdoom LH, van Ree RM, de Vries AP, Smit AJ, et al. Skin-autofluorescence is an independent predictor of graft loss in renal transplant recipients. *Transplantation.* 2009;87(7):1069-77. doi: 10.97/TP.0b013e31819d3173.
 41. Mulder DJ, Bieze M, Graaff R, Smit AJ, Hooymans JM. Skin autofluorescence is elevated in neovascular age-related macular degeneration. *Br J Ophthalmol.* 2010;94(5):622-5. doi: 10.1136/bjo.2009.162990. Epub 2009 Sep 1.
 42. Ohnuki Y, Nagano R, Takizawa S, Takagi S, Miyata T. Advanced glycation end products in patients with cerebral infarction. *Intern Med.* 2009;48(8):587-91. Epub 2009 Apr 15.
 43. Pol HW, Sibma E, Zeebregts CJ, Pierik EG, Meerwaldt R. Increased skin autofluorescence after colorectal operation reflects surgical stress and postoperative outcome. *Am J Surg.* 2011;202(5):583-9. doi: 10.1016/j.amjsurg.2010.10.019. Epub 1 Sep 3.

10

Summary

Chapter 1 is the introduction of this thesis. The quantum mechanics and general applications of PDT are introduced, followed by the specific use of PDT in the skin using porphyrin precursors. It is described how the combination of light, oxygen and PpIX leads to a range of biological effects that include cellular, immunological and vascular responses leading to cell death. Limitations of PDT in the skin are discussed and it is highlighted how an individual approach may benefit our understanding of treatment failures and side effects. Potentially relevant measurable parameters that may contribute to such an approach are discussed while some are considered more relevant than others. The importance of the distribution of PpIX in tissue is emphasized, as well as monitoring its fluorescence during PDT, which provides information on the concentration of PpIX photosensitizer, the rate of its photobleaching process and the related oxygen consumption. It is explained how fluorescence measurements are affected by tissue optical properties which are determined by absorption and scattering of light in the tissue. Several techniques that attempt to measure these optical properties are described and the limitations explained. New techniques that are more suitable for superficial skin measurements are introduced. These techniques may be used for diagnostic purposes, to measure physiological parameters such as oxygenation during PDT and to quantify skin fluorescence measurements by correcting for the measured optical properties. The chapter concludes with the outline of this thesis.

Chapter 2 describes a study on one of the main limitations of PDT: pain. Many risk factors for pain have already been described in the literature but the clinical relevance is often hard to interpret. Severe pain was scored as a clinically relevant outcome in a patient group treated with PDT for an area of actinic field cancerisation of at least 25 cm². In addition, patient satisfaction was scored using a validated questionnaire. Severe, sometimes intolerable, pain was a frequently reported outcome (in 28 of 48 patients), necessitating infiltrative or nerve block anaesthesia. When identifying predictors for patients to experience severe pain only the size of the treated area size was statistically significant, and it was associated with patient dissatisfaction. The patients included in the study are in principle ideal candidates for PDT field treatment. However, because of the high risk for severe pain the applicability of PDT is limited for this patient group. The study illustrates that there is need for methods to control pain during PDT other than using infiltrative anaesthesia.

In **Chapter 3** an approach to decrease pain during PDT is studied: the use of low fluence rate. A lower fluence rate will also lead to more efficient PDT due to more efficient use of available oxygen. PpIX fluorescence measurements were used to optically monitor PDT efficiency and control the deposited effective PDT dose in mice. Several single and fractionated illumination protocols were studied, in which a total dose of 50 or 100 J

cm^{-2} was delivered at fluence rates of either 20 mW cm^{-2} ("low") or at 50 mW cm^{-2} ("high") fluence rate. Outcome was cumulative daily visual skin damage 7 days after PDT. The fractionated delivery of 100 J cm^{-2} was equally effective at low and high fluence rates. At low fluence rate PDT was more efficient, but the average total treatment time was considerably longer (80 versus 33 minutes). Possibly the most promising light delivery protocol for clinical purposes was the one in which initially low fluence rate light was delivered, followed by a high fluence rate. An important consideration for this illumination scheme is that increasing the fluence rate when there is little PpIX remaining has been documented not to cause pain. In this group efficacy was maintained but the total illumination time was reduced to 58 minutes. This type of illumination scheme is therefore expected to lead to effective, more efficient PDT with less pain at acceptable illumination times. It is concluded that low fluence rate is an interesting option for clinical investigation, stressing the importance of PpIX fluorescence measurements to monitor PDT dose and ensure effectiveness.

In **chapters 4, 5 and 6** three papers are presented that share a central theme: the spatial distribution of PpIX and the related vascular effects of PDT with a focus on the use of HAL, the hexyl ester of ALA. Vascular responses to PDT may influence the availability of oxygen during PDT and the extent of tumor destruction after PDT. In **chapter 4** the vascular constrictive response of HAL and ALA-PDT and the relationship with PpIX distribution in the vessel walls were studied in a mouse skin fold chamber model. This geometry allows to directly visualize the subcutaneous blood vessels underlying the treated area and measure PpIX fluorescence intensity without being disturbed by absorption and scattering effects of overlying tissue. Vessel diameters were measured before and after PDT. The results were similar between HAL and ALA. Most (>60%) arterioles were completely constricted immediately after PDT and many remained constricted 20 minutes later. Venules generally did not respond. The extend of arteriole vasoconstriction was strongly correlated with the PpIX fluorescence intensity in the arteriole wall. It is concluded that such vasoconstrictive effects during topical HAL and ALA- PDT may have important effects on the oxygen supply necessary for PDT, and that prolonged vasoconstriction after PDT could result in increased cell death of both normal and malignant cells. In **chapter 5** the microscopic distribution of PpIX in dermal blood vessels of mouse skin after topical application of HAL, MAL (the methyl ester of ALA) or ALA is investigated first, followed by a study of the potential of topical PDT to induce vascular damage to these vessels. Fluorescent-labeled CD31 antibodies were used to visualize the vessels in microscopic sections of skin biopsies. To measure the vascular distribution of PpIX the colocalisation of CD31 and PpIX fluorescence was calculated using confocal microscopy imaging. The vascular damage after PDT was scored by visual interpretation of fluorescent CD31 and CD144 confocal images. Vascular damage results in a loss of normal CD144 staining

along the plasma membrane, while CD31 staining is unaffected. The PpIX concentration within the vessel wall was highest in the HAL group, followed by the ALA and then the MAL group. Similarly, vascular damage was highest for HAL, then ALA and then MAL. It is concluded that the dermal vasculature synthesizes biologically relevant concentrations of PpIX and that topical PDT can lead to vascular damage. These effects appear to be causally related and are therefore most pronounced for HAL. The study shows that the vasculature can be a potential target of PDT and it supports the hypothesis that vascular responses are important for the increased effect of light fractionation. **In chapter 6** this idea is utilized to study the effect of light fractionation for HAL-PDT in a mouse model. Visual skin damage was scored after PDT and PpIX photobleaching kinetics were measured during PDT. A single illumination and two light fractionation schemes were studied for both HAL and ALA. For both precursors light fractionation increased visual skin damage, but the effect was not statistically significant for HAL. Photobleaching rates were similar for HAL and ALA and PpIX fluorescence intensity was higher for ALA than for HAL. This PpIX fluorescence intensity is mainly dependent on the epidermal PpIX synthesis. Because it was not correlated with efficacy, this indicates that other factors such as superficial vascular responses may play an important role. The potential use of light fractionation HAL-PDT is discussed as well as methods to potentially further improve fractionated HAL-PDT.

In chapter 7 the use of a newly developed technique termed DPS (differential path-length spectroscopy) is described. DPS allows optical monitoring of the vascular physiology during PDT in human skin and this was studied in 9 patients undergoing PDT for actinic keratosis. DPS is a spectroscopic technique that combines the reflectance signals from two optical fibers to determine the absorption characteristics of a superficial collection volume. This is opposed to diffuse measurements in which signals from deeper in the skin greatly influence the measured reflectance. The sampling depth was tailored to the average epidermal thickness of actinic keratosis, which was first measured in histologic sections. The vascular response to PDT was highly variable for individual patients, especially the blood volume fraction and to a lesser extent the saturation. This could not be demonstrated before using diffuse measurement techniques, stressing the importance of using optical monitoring techniques that allow superficial measurements. It is concluded that the patient-specific variability of the vascular physiological changes during PDT can be relevant for the oxygen supply during PDT for individual patients.

In Chapter 8 a study is presented in which another reflectance spectroscopic technique is introduced: multi-diameter single fiber reflectance (MDSFR) spectroscopy. This technique enables a complete determination of the optical properties, defined by the absorption and reduced scattering coefficient, in a superficially sampled volume

of skin. It has been recently developed and validated in computer simulations and tissue-mimicking phantoms and this is the first use in human skin. In this study MDSFR is specifically applied in combination with single fiber fluorescence (SFF) spectroscopy. This combination enables to quantify the fluorescence by correcting for the measured optical properties. To illustrate the importance of performing such correction, uncorrected and corrected values for PpIX and autofluorescence were compared. This was done at various time-points in 22 patients undergoing light fractionated ALA-PDT. Measurements were taken immediately before and after the two PDT illuminations. We found that the corrected values were higher than the uncorrected, varying from 2.4-7.5 times higher. This variability reflects the heterogeneity in individual patients' or lesions' optical properties. Also, the optical properties changed during the course of PDT, and in a different way for different patients. Both the variability in optical properties between patients and the varying optical properties during PDT illustrate the importance of individually correcting for optical properties to obtain quantitative results. This is the first time quantitative fluorescence has been successfully measured in a superficial volume of skin. Our values are of the same magnitude as those obtained using chemical extraction of PpIX from tissue biopsies. This is a big step in biomedical optics, not only for PDT but also for applications beyond PDT and beyond the skin. With MDSFR/SFF it is now possible to correlate the intrinsic PpIX fluorescence with PDT outcome, and to use PpIX photobleaching kinetics as a method to individually dose PDT. In addition to the usefulness of quantifying PpIX fluorescence, the skin autofluorescence may also be valuable but for different purposes. First, it can be used as a diagnostic tool, as we have shown that the autofluorescence of actinic keratosis is significantly lower than of normal skin. It will also be interesting to include a comparison of the absorption and scattering properties measured with MDSFR between lesions, because these may also have diagnostic value. In many studies high autofluorescence has also been related to an increased risk for several internal diseases associated with cumulative metabolic stress. Quantitative MDSFR/SFF measurements in which the sampled volume can be tailored to the desired depth will greatly benefit such research.

Chapter 9 is the discussion of the thesis. It focuses on the distribution of PpIX and how this relates to vascular effects, on the importance of measuring PpIX fluorescence during PDT, and on optical techniques that allow superficial measurements in skin. It is described how these topics are interrelated because of the complex interactions between light, oxygen, PpIX and the effects they have on the tissue and vice versa. For example: it may seem advantageous to have a lot of PpIX and light available, but this combination can lead to vascular constriction that limits the oxygen supply required for PDT. It is discussed how individual monitoring of relevant parameters can aid the optimization process of PDT, for which accurate measurements are necessary. The improvements in

optical measurement techniques contribute significantly to the potential of research on PDT in human skin. The translational step is made from our findings in mice and humans and how these can be combined to optimize clinical PDT protocols. The potential for personalized PDT is discussed as well as future perspectives of PDT and how optical monitoring can be incorporated to improve PDT with the aim to increase its efficacy while minimizing associated pain.

11

Samenvatting

Hoofdstuk 1 is de algemene introductie van dit proefschrift. Eerst wordt de quantum mechanica waarop PDT is gebaseerd uitgelegd en daarna het gebruik van PDT in het algemeen en specifiek voor de huid waarbij porfyrine precursors gebruikt worden. Er wordt beschreven hoe de combinatie van licht, zuurstof en PpIX leidt tot diverse biologische effecten, waaronder cellulaire, immunologische en vasculaire responsen die resulteren in celdood. De beperkingen van PDT worden besproken en de nadruk wordt gelegd op het belang van een patiënt-specifieke aanpak om beter te begrijpen waarom PDT faalt of waarom bijwerkingen optreden bij individuele patiënten. Enkele parameters die tijdens PDT gemeten of gecontroleerd kunnen worden en die belangrijk zouden kunnen zijn voor het beter begrijpen van PDT worden geïntroduceerd. Er wordt benadrukt hoe belangrijk het meten van de distributie van PpIX is en hoe belangrijk het monitoren van de PpIX fluorescentie tijdens PDT is, omdat dit informatie verschaft over de PpIX concentratie, de mate van bleiking en het hieraan gerelateerde zuurstofverbruik. Uitgelegd wordt hoe fluorescentiemetingen worden beïnvloed door de optische eigenschappen van het weefsel zoals absorptie en verstrooiing van licht. Verschillende technieken om deze optische eigenschappen te meten worden besproken, inclusief hun beperkingen. De nadruk ligt op het bespreken van nieuwe technieken die het mogelijk maken om nauwkeurige metingen te doen van oppervlakkige delen van de huid. Deze kunnen waardevol zijn als diagnostische toepassing, om bijvoorbeeld de bloetoevoer en saturatie tijdens PDT te meten. Tevens maken ze het mogelijk om fluorescentie metingen te corrigeren voor de optische eigenschappen van het gemeten deel van de huid. De introductie sluit af met een beschrijving van de verschillende onderdelen van dit proefschrift.

Hoofdstuk 2 beschrijft een studie waarin een van de belangrijkste beperkingen van PDT wordt onderzocht: pijn. In de literatuur zijn al diverse risicofactoren voor pijn tijdens PDT beschreven, maar de klinische relevantie hiervan is vaak moeilijk te interpreteren. In deze studie werd ernstige pijn als klinisch relevante uitkomstmaat onderzocht bij patiënten die behandeld werden met PDT voor actinische keratosen op een gebied van 25 cm² of meer. Tevens werd de patiënttevredenheid onderzocht met een gevalideerde vragenlijst. Het bleek dat ernstige pijn, waarvoor infiltratieve anesthesie noodzakelijk was, vaak voorkwam (in 28 van de 48 patiënten). Alleen de grootte van het behandelde gebied was een statistisch significante voorspeller van ernstige pijn en dit was tevens geassocieerd met ontevredenheid van patiënten over de behandeling. PDT is in principe een ideale behandeling om een groot gebied met actinische keratose te behandelen, maar de toepasbaarheid in de praktijk wordt dus beperkt door de pijn. De studie demonstreert dat pijn een relevant probleem is en dat er behoefte is aan andere methoden naast lokale anesthesie om de pijn te verminderen.

In **hoofdstuk 3** wordt een mogelijke oplossing voor het pijnprobleem tijdens PDT onderzocht: het gebruik van licht met een laag vermogen. Dit leidt tevens tot een efficiënter gebruik van zuurstof en dus tot efficiëntere PDT. PpIX fluorescentie metingen werden gebruikt om de efficiëntie te monitoren en om de geleverde effectieve PDT dosis te controleren in een muizenstudie. Diverse enkele en gefractioneerde belichtingsschema's werden onderzocht, waarin een totale dosis van 50 of 100 Jcm⁻² werd gegeven bij een vermogen van ofwel 20 ("laag") ofwel 50 ("hoog") mW cm⁻². De cumulatieve visuele huidschade gedurende 7 dagen na PDT werd gemeten als effectiviteitsmaat voor PDT. Een dosis van 100 Jcm⁻² was even effectief voor laag als hoog vermogen belichting. Bij laag vermogen was PDT efficiënter, maar was de totale belichtingstijd aanzienlijk langer (80 versus 33 minuten). Het meest veelbelovend voor de kliniek is het geven van eerst laag, en later hoog vermogen belichting binnen een gefractioneerd schema. Het is beschreven dat wanneer er nog maar weinig PpIX over is, ook hoog vermogen PDT geen pijn doet bij mensen. In deze groep muizen die behandeld werden met dit schema was PDT effectief en de totale belichtingstijd was verkort naar 58 minuten. Het kan verwacht worden dat een dergelijk schema klinisch gebruikt kan worden voor effectieve, efficiëntere PDT met minimale pijn. Geconcludeerd wordt dat laag vermogen PDT een veelbelovende behandeloptie is waarbij het belangrijk is om de PpIX fluorescentie tijdens PDT te meten om de geleverde dosis en daarmee de effectiviteit individueel te kunnen controleren.

In **hoofdstukken 4, 5 en 6** worden drie studies gepresenteerd die een gezamenlijk thema hebben: de distributie van PpIX en de daaraan gerelateerde vasculaire effecten van PDT, met een focus op HAL, de hexyl ester van ALA. Vasculaire effecten kunnen de zuurstofvoorziening tijdens PDT belemmeren, maar ook de mate van tumor destructie na PDT beïnvloeden. In **hoofdstuk 4** worden de resultaten van onderzoek in een kamertjesmodel op muizenhuid naar vasoconstrictie en de relatie met de hoeveelheid PpIX in de vaatwand beschreven. Dit kamertjesmodel maakt het mogelijk om de vaten die onder het behandelde gebied liggen direct te visualiseren en om fluorescentiemetingen te doen zonder last te hebben van absorptie of verstrooiing van het licht door tussenliggend weefsel. Vaatdiameters werden gemeten voor en na PDT. De resultaten waren vergelijkbaar tussen HAL en ALA. De meerderheid (>60%) van de arteriolen waren volledig vernauwd direct na PDT en dit bleef vaak zo wanneer er na 20 minuten opnieuw gemeten werd. De venules reageerden niet of nauwelijks. De mate van constrictie van arteriolen was sterk gecorreleerd met de PpIX concentratie in de vaatwand. Er wordt geconcludeerd dat de sterk vasoconstrictieve effecten van topicale HAL en ALA-PDT belangrijke gevolgen kunnen hebben voor de zuurstofvoorziening die nodig is voor PDT, en dat langdurige vasoconstrictie kan leiden tot ischemie en tot toegenomen celdood van zowel normale cellen als tumorcellen. In **hoofdstuk 5** wordt eerst de microscopi-

sche distributie van PpIX in dermaal gelegen vaten na topicale applicatie van HAL, MAL (de methyl ester van ALA) of ALA onderzocht, gevolgd door een studie naar de eventuele schade aan deze vaten na PDT. Fluorescerende antilichamen tegen CD31 werden gebruikt om de vaten te visualiseren. Om de PpIX distributie in de vaten te meten, werd de colocalisatie tussen CD31 en PpIX fluorescentie berekend met behulp van confocale microscopie. De vaatschade na PDT werd gescoord door visuele interpretatie van CD31 en CD144 confocale opnamen. Vaatschade leidt tot verlies van normale kleuring van CD144 langs de plasma membraan, terwijl CD31 onveranderd zichtbaar blijft. De PpIX concentratie in de vaatwand was het hoogst voor HAL, daarna kwam ALA en MAL had de laagste concentratie. De vaatschade na PDT had hetzelfde patroon met de meeste vaatschade na HAL, daarna ALA en daarna MAL-PDT. Geconcludeerd wordt dat dermale vaten biologisch relevante hoeveelheden PpIX synthetiseren en dat dit resulteert in vaatschade na PDT. Deze effecten lijken met elkaar samen te hangen en zijn daarom het meest uitgesproken voor HAL. Deze studie illustreert dat de oppervlakkige vaten beschouwd kunnen worden als mogelijk target (primaïr of secundair) van PDT, en het ondersteunt de hypothese dat de vasculaire respons belangrijk is voor het toegenomen effect van gefractioneerde belichting. In **hoofdstuk 6** wordt dit idee verder gebruikt om het effect van gefractioneerde belichting te onderzoeken voor HAL-PDT in een muizenmodel. Visuele huidschade na PDT en PpIX fluorescentie tijdens PDT werden gemeten. Drie belichtingsschema's (één enkele belichting en twee gefractioneerde schema's) werden vergeleken voor zowel HAL als ALA-PDT. Voor beide leidde fractioneren tot meer huidschade, hoewel dit effect niet statistisch significant was voor HAL. De snelheid van PpIX bleking was vergelijkbaar voor HAL en ALA, maar de initiële PpIX fluorescentie was hoger voor ALA dan voor HAL. De intensiteit van deze fluorescentiemeting wordt vooral wordt bepaald door de epidermale PpIX concentratie. Aangezien er geen relatie was tussen gemeten PpIX synthese en huidschade, lijken andere zaken zoals de vasculaire respons een belangrijke rol te spelen. Het potentieel van klinische HAL-PDT voor gynaecologische en urologische toepassingen wordt besproken alsmede methoden om fractionele HAL-PDT verder te verbeteren.

In **hoofdstuk 7** wordt een nieuw ontworpen techniek genaamd DPS (differential path-length spectroscopy) besproken. Met DPS is het mogelijk om de vasculaire fysiologie tijdens PDT in menselijke huid te meten, en dit werd gedaan in 9 patiënten die behandeld werden met PDT voor actinische keratose. DPS is een spectroscopische techniek waarbij reflectiesignalen van twee optische fibers worden gecombineerd om de absorptie karakteristieken te kunnen meten in een oppervlakkig deel van de huid. Dit is in contrast met algemeen gebruikte diffuse metingen, waarbij signalen van dieper in de huid de gemeten reflectie sterk beïnvloeden. De diepte van de metingen werd afgestemd op de gemiddelde dikte van actinische keratose, hetgeen eerst onderzocht

werd in histologische coupes. De vasculaire respons tijdens PDT bleek sterk te verschillen voor individuele patiënten, met name de bloed volume fractie en in mindere mate de saturatie. Eerder kon dit niet worden aangetoond met de diffuse metingen, wat illustreert hoe belangrijk het is om optische technieken te gebruiken die betrouwbare oppervlakkige metingen toelaten. Er wordt geconcludeerd dat de patiënt-specifieke variabiliteit in veranderingen in de vasculaire fysiologie tijdens PDT belangrijk kan zijn voor de zuurstofvoorziening tijdens PDT voor individuele patiënten.

In **hoofdstuk 8** wordt een studie gepresenteerd waarin een andere spectroscopische techniek wordt geïntroduceerd: multi-diameter single fiber reflectance (MDSFR) spectroscopie. Met deze techniek is het mogelijk om de volledige optische eigenschappen van een oppervlakkige meting in de huid te kwantificeren. Deze optische eigenschappen worden bepaald door de absorptiecoëfficiënt en de afgeleide verstrooiingscoëfficiënt. MDSFR spectroscopie is recent ontwikkeld en gevalideerd in computer simulaties en modellen waarin weefsel wordt nagebootst. In deze studie wordt MDSFR voor het eerst toegepast in mensenhuid en wordt specifiek gebruikt in combinatie met single fiber fluorescentie (SFF) spectroscopie. Deze combinatie maakt het mogelijk om oppervlakkige fluorescentiemetingen in de huid te kwantificeren door ze te corrigeren voor de optische eigenschappen van datzelfde oppervlakkige deel van de huid. Om het belang van een dergelijke correctie te illustreren werden gecorrigeerde en niet-gecorrigeerde waarden voor PpIX en autofluorescentie met elkaar vergeleken. Dit werd gedaan in 22 patiënten die werden behandeld voor actinische keratose of de ziekte van Bowen met gefractioneerde ALA-PDT. Metingen werden genomen direct voor en direct na de eerste en tweede PDT belichting. Het bleek dat de gecorrigeerde waarden hoger waren dan de ongecorrigeerde en dat dit verschil varieerde van een factor 2,4 tot 7,5. Deze variabiliteit geeft de heterogeniteit van optische eigenschappen tussen individuele patiënten/laesies weer. Ook waren de optische eigenschappen van de huid onderhevig aan veranderingen tijdens PDT, en dit was weer verschillend voor individuele patiënten. Zowel de variabiliteit in optische eigenschappen tussen laesies als de veranderingen tijdens PDT illustreren het belang van de correctie hiervoor om kwantitatieve resultaten te verkrijgen. Dit is de eerste keer dat succesvolle kwantitatieve fluorescentie metingen werden verricht in een oppervlakkig deel van de huid, en onze waarden komen overeen met waarden die worden verkregen met chemische extractie van PpIX uit biopsieën. Dit is een grote stap voorwaarts in de biomedische toepassing van optische metingen. Niet alleen voor PDT, maar ook voor applicaties buiten PDT en ook buiten de huid. Met MDSFR/SFF is het nu mogelijk om de intrinsieke PpIX fluorescentie te correleren aan PDT uitkomst, en de PDT dosis individueel af te stemmen aan de hand van PpIX bleking tijdens PDT. Naast dit belang van PpIX fluorescentie, is ook de autofluorescentie mogelijk belangrijk voor diverse toepassingen. Ten eerste kan het als diagnostisch hulpmiddel

worden toegepast, aangezien de autofluorescentie van actinische keratose significant lager is dan die van normale huid. Een andere interessante toepassing van MDSFR/SFF is om de absorptie en verstrooiingseigenschappen tussen laesies te vergelijken aangezien deze ook mogelijk diagnostische waarde hebben. Ten tweede is de autofluorescentie in veel studies gerelateerd aan een verhoogd risico op verscheidene interne ziekten die geassocieerd zijn met cumulatieve metabole stress. Kwantitatieve MDSFR/SFF metingen waarbij het gesampelde volume nauwkeurig afgestemd kan worden naar de gewenste diepte kunnen van groot nut zijn voor dergelijk onderzoek.

Hoofdstuk 9 is de discussie van het proefschrift. Er wordt gefocust op de distributie van PpIX en de relatie met vasculaire effecten, op het belang van het meten van PpIX fluorescentie tijdens PDT, en op optische technieken die oppervlakkige metingen mogelijk maken. Er wordt beschreven hoe deze onderwerpen nauw met elkaar samenhangen en elkaar beïnvloeden vanwege de complexe relatie tussen licht, zuurstof, PpIX en de effecten die zij hebben op het weefsel en andersom. Als voorbeeld: het lijkt op het eerste gezicht nuttig om veel PpIX en veel licht te hebben, maar dit leidt o.a. tot vasoconstrictie waardoor er misschien niet genoeg zuurstof beschikbaar is voor PDT. Er wordt besproken hoe het individueel monitoren van relevante parameters tijdens PDT kan bijdragen aan de optimalisering van PDT, en dat hiervoor accurate metingen nodig zijn. De recente verbeteringen in optische meettechnieken leveren een significante bijdrage aan de mogelijkheden om PDT in mensenhuid verder te onderzoeken. De translationele stap tussen onze bevindingen in muizenhuid en die in mensenhuid wordt gemaakt en besproken wordt hoe deze kunnen worden gecombineerd om klinische behandelprotocollen te verbeteren. Het potentieel voor gepersonaliseerde PDT wordt besproken, alsmede de toekomstperspectieven van PDT en hoe het optisch monitoren kan bijdragen om de effectiviteit van PDT te verhogen en de pijn te verminderen.

12

Addendum

Dankwoord

List of publications

Curriculum Vitae

PhD portfolio

List of abbreviations

DANKWOORD

Promoveren doe je niet alleen. Ook ik heb dankbaar gebruik mogen maken van de hulp van velen die mij op diverse manieren hebben geholpen bij het tot stand komen van dit proefschrift. Van sommigen heb ik veel geleerd, anderen hebben mij geïnspireerd om nog meer mijn best te doen of hebben mij gemotiveerd om door te zetten. Weer anderen hebben me fysiek geholpen met het uitvoeren van de onderzoeken, of met de logistiek die ook komt kijken bij het doen van onderzoek. Tot slot zijn er nog diegenen die mij op enigerlei andere wijze hebben ondersteund. Ik wil bij deze iedereen van harte bedanken voor zijn of haar hulp. Een aantal mensen wil ik in het bijzonder bedanken.

Professor Neumann. Het is een eer om u als promotor en als opleider te hebben gehad. In beide functies hebt u altijd in mij geloofd en mij altijd in woord en daad gesteund, geïnspireerd en gemotiveerd. U bent degene die mijn promotie van begin tot eind mogelijk heeft gemaakt waarvoor ik u zeer dankbaar ben.

Dominic Robinson. Als co-promotor ben jij het nauwst betrokken geweest bij alles wat bij mijn promotie kwam kijken. Je hebt me altijd onvoorwaardelijk geholpen met de opzet van de studies, de uitvoering, het nadenken over de betekenis van de resultaten en met het uiteindelijke opschrijven en publiceren van de artikelen. Ik heb genoten van de geestdrift en het enthousiasme waarmee je mij keer op keer wilde uitleggen hoe het ook alweer zat met die quantummechanica of andere voor mij ingewikkelde natuurkundige fenomenen. Dank je voor je niet aflatende inzet gedurende al die jaren.

Riëtte de Bruijn en Angelique van der Ploeg-van den Heuvel. Zonder jullie toewijding en bekwaamheid in het uitvoeren van de dierexperimenten zou ik geen betrouwbare data hebben kunnen verkrijgen. Het is me altijd een genoegen geweest te mogen en kunnen vertrouwen in jullie kunde en kennis. Om nog maar te zwijgen van de extra vrije tijd in weekenden en vrije dagen die jullie hebben opgeofferd om bijvoorbeeld huidscores te verrichten. Allebei ontzettend bedankt voor alle hulp en steun.

Tamar Nijsten. Achter de schermen heb jij veel bijgedragen aan mijn wetenschappelijke inzicht, het nadenken over methoden en statistiek en het efficiënt schrijven. Je nam altijd de tijd voor een vraag van mij waarna jij in een periode van een half uur de essentie niet alleen begrepen had, maar ook de valkuilen had gezien en tevens oplossingen hiervoor had bedacht plus nog wat overige verbeterpunten. Erg fijn dat je je op die manier belangeloos met mijn onderzoek hebt willen bemoeien.

Loes Hollestein. Met meerdere artikelen heb jij me geholpen antwoord te vinden waar niemand anders antwoord op had: hoe de juiste statistiek op de juiste manier toe te passen. Dank je wel voor je bereidheid om me te willen helpen waarbij je altijd even enthousiast bent geweest om naar een oplossing te zoeken.

Ellen de Haas. Jij staat aan de basis van de samenwerking tussen de afdeling dermatologie en het Centrum voor Optische Diagnostiek en Therapie. Dankzij jouw inzet hiervoor heb ik de mogelijkheid gehad om deze samenwerking verder op te pakken en te continueren waardoor dit proefschrift mogelijk is geworden.

Alle overige co-auteurs van de artikelen wil ik bij deze nogmaals bedanken voor jullie bijdrage in de totstandkoming hiervan.

Alle mensen die hebben bijgedragen aan de inclusie van patiënten zowel in het Erasmus MC als in het Amphia ziekenhuis te Breda bedankt. En natuurlijk de patiënten zelf enorm bedankt dat jullie hebben willen meewerken.

Van degenen die in praktische zin hebben bijgedragen aan het behandelen/plannen van patiënten wil ik Jolanda, Jeanette, Elsbeth, Franka en Hilly uit Rotterdam en Ans uit Breda bedanken hiervoor.

Alle(oud-)collega AIOS, dermatologen en onderzoekers van de afdeling dermatologie in het Erasmus, bedankt voor de gezellige tijd die ik met jullie heb gehad tijdens mijn opleiding waarin ik ook het grootste deel van mijn onderzoek heb gedaan. In het bijzonder gaat mijn dank uit naar Willemijn, Renate, Petra, Rick, Ewout, Hanke, Suzan, Marlies, Anke, Michelle, Manon, Annette, Esmee, Hessel, Hilde, Enes, Lisette, Armanda, Eموke, Wendy, Gijs, Simone, Femke, Bing, Errol, Eric, Annik, Michael, Kai, Annieke, Tannja, Barbera, Ria, Mimi en Rennie.

Mijn familie en dan vooral mijn ouders die aan de basis hebben gestaan van mijn leergierigheid en onderzoekende aard en mij daarin altijd hebben gestimuleerd. Dank jullie wel hiervoor.

Lieve Marijke, jij beweert dat je me vrijwel niet hebt geholpen met mijn onderzoek. Je hebt het mis. Je hebt me geleerd om te gaan met de tegenslagen die horen bij het promoveren. Zonder jou zou ik wellicht niet het vertrouwen hebben gehad om door te gaan. Je hebt altijd voor me klaargestaan en altijd een luisterend oor gehad. Je hebt het meest in mij geloofd van iedereen. Daarom.

LIST OF PUBLICATIONS

Brouwer AM, **Middelburg T**, Smeets JB, Brenner E. Hitting moving targets: a dissociation between the use of target's speed and direction of motion. *Exp Brain Res* 2003;152:368-75.

Middelburg TA, van Praag MCG. A rare complication of BCG vaccination. *Int J Dermatol*. 2009 May;48(5):546-8.

Reeder SWI, **Middelburg TA**, Neumann HAM. An extremely painful ulcer on the lower leg: Martorell arteriosclerotic ulcer. *Ned Tijdschr Geneeskd*. 2009;153:B421 Dutch.

de Vijlder HC, **Middelburg TA**, de Bruijn HS, Neumann HA, Sterenborg HC, Robinson DJ, de Haas ER. Optimizing ALA-PDT in the management of non-melanoma skin cancer by fractionated illumination. *G Ital Dermatol Venereol*. 2009 Aug;144(4):433-9. Review.

de Vijlder, HC, **Middelburg TA**, de Bruijn, HS, Robinson DJ, Neumann, HAM, de Haas, ERM. De Rotterdamse benadering van fotodynamische therapie van oppervlakkige huidmaligniteiten, gefractioneerd met 5-aminolevulinezuur. *Ned Tijdschr Dermatol Venereol* Dec 2009, 19;10,589-92.

Middelburg TA, van Zaane F, de Bruijn HS, van der Ploeg-van den Heuvel A, Sterenborg HJCM, Neumann HAM, de Haas ERM, Robinson DJ. Fractionated illumination at low fluence rate photodynamic therapy in mice. *Photochem Photobiol*. 2010 Sep-Oct;86(5):1140-6.

de Vos FY, **Middelburg TA**, Seynaeve C, de Jonge MJ. Ecthyma gangrenosum caused by *Pseudomonas Aeruginosa* in a patient with astrocytoma treated with chemotherapy. *J Infect Chemother*. 2010 Feb;16(1):59-61.

Middelburg TA. History of Photodynamic therapy. Chapter in Canon of dermatology book in Dutch. 2011 March: 96-97.

Middelburg TA, Kanick SC, de Haas ERM, Sterenborg HJCM, Amelink A, Neumann HAM, Robinson DJ . Monitoring blood volume and saturation using superficial fibre optic reflectance spectroscopy during PDT of actinic keratosis. *J Biophotonics*. 2011 Oct;4(10):721-30.

Van den Bos RR, **Middelburg TA**, van Biezen P, van der Eijk AA, Pas HH, Diercks GF. Orf-induced pemphogoid with anti-laminin-332 antibodies. *Br J Dermatol.* 2012 Oct;167(4):956-8.

P.K. Dikrama, **T. Middelburg**, V. Noordhoek Hegt. Dermatopathologie kennistest Casus 1: Lichen Planus. *Ned Tijdschr Derm Venereol.* 2012;22:4:256,257,277,278.

P.K. Dikrama, **T. Middelburg**, V. Noordhoek Hegt. Dermatopathologie kennistest Casus 2: acrovesiculeus eczeem. *Ned Tijdschr Derm Venereol.* 2012;22:5 310,318,319.

P.K. Dikrama, **T. Middelburg**, V. Noordhoek Hegt. Dermatopathologie kennistest Casus 3: Psoriasis vulgaris. *Ned Tijdschr Derm Venereol.* 2012;22:7: 442,443,457,458.

P.K. Dikrama, **T. Middelburg**, V. Noordhoek Hegt. Dermatopathologie kennistest Casus 4: Sarcoidose. *Ned Tijdschr Derm Venereol.* 2012;22:08: 478,491,492.

P.K. Dikrama, **T. Middelburg**, V. Noordhoek Hegt. Dermatopathologie kennistest Casus 5: Morfea. *Ned Tijdschr Derm Venereol.* 2012;22:10: 616,617,628,629.

P.K. Dikrama, T. Middelburg, V. Noordhoek Hegt. Dermatopathologie kennistest Casus 6: Hailey-Hailey. *Ned Tijdschr Derm Venereol.* 2013;23:10: 16,17,30,31.

P.K. Dikrama, **T. Middelburg**, V. Noordhoek Hegt. Dermatopathologie kennistest Casus 7: Cutane Discoïde Lupus Erythematosus. *Ned Tijdschr Derm Venereol.* 2013;23:02: 86,87,116,117.

P.K. Dikrama, **T. Middelburg**, V. Noordhoek Hegt. Dermatopathologie kennistest Casus 8: Lues. *Ned Tijdschr Derm Venereol.* 2013;23:05:284,285,301,302.

P.K. Dikrama, **T. Middelburg**, V. Noordhoek Hegt. Dermatopathologie kennistest Casus 9: Leucocytoclastische Vasculitis. *Ned Tijdschr Derm Venereol.* 2013;23:6: 333-334, 346.

P.K. Dikrama, **T. Middelburg**, V. Noordhoek Hegt. Dermatopathologie kennistest Casus 10: Herpes Simplex. *Ned Tijdschr Derm Venereol.* 2013;23:7: 400,401, 418-419.

A.M.R. Schrader, P.K. Dikrama, **T. Middelburg**, V. Noordhoek Hegt. Dermatopathologie kennistest Casus 11: Dermatofibroom. *Ned Tijdschr Derm Venereol.* 2013;23:10: 612,613,628,629.

A.M.R. Schrader, **T. Middelburg**, P.K. Dikrama, V. Noordhoek Hegt. Dermatopathologie kennistest Casus 12: Verruca vulgaris. Ned Tijdschr Derm Venereol. 2013;23:11: 664,665, 684,685.

Middelburg TA, Nijsten T, Neumann HAM, de Haas ERM, Robinson DJ. Red light ALA-PDT for large areas of actinic keratosis is limited by severe pain and patient dissatisfaction. Photodermatol Photoimmunol Photomed. 2013 Oct;29(5):276-8.

Middelburg TA, de Bruijn H, Tettero L, van der Ploeg-van den Heuvel A, Neumann H, de Haas, Robinson D. Topical hexylaminolevulinate and aminolevulinic acid photodynamic therapy: complete arteriole vasoconstriction occurs frequently and depends on protoporphyrin IX concentration on vessel wall. J Photochem and Photobiol B: Biology. 2013 Sep 5;126:26-32.

Robinson D, **Middelburg T**, Hoy C, de Haas E, Nijsten T, Amelink A. Quantitative optical spectroscopy in the skin. Ned Tijdschr Derm Venereol. 2013.

Middelburg TA, de Bruijn HS, van der Ploeg-van den Heuvel A, Neumann HAM, Robinson DJ. The effect of light fractionation with a two-hour dark interval on the efficacy of topical hexyl-aminolevulinate photodynamic therapy in normal mouse skin. Photodiagn and Photodyn ther. 2013(10);703-709.

Middelburg TA, de Vijlder HC, de Bruijn HS, van der Ploeg-van den Heuvel A, Neumann HAM, de Haas ERM, Robinson DJ. Topical photodynamic therapy using different porphyrin precursors leads to differences in vascular photosensitization and vascular damage in normal mouse skin. Photochem Photobiol. Accepted for publication.

Middelburg T, Hoy C, Neumann H, Amelink A, Robinson D. Correction for tissue optical properties enables quantitative skin fluorescence measurement using multi-diameter single fiber reflectance spectroscopy. Lasers Surg Med. 2013 (submitted).

CURRICULUM VITAE

Tom Alexander Middelburg werd op 13 augustus 1980 geboren te Rotterdam. In 1997 behaalde hij zijn gymnasium diploma aan het Rotterdams Montessori Lyceum. Het daarop volgende jaar behaalde hij cum laude zijn propedeuse diploma biologie aan de Universiteit Leiden behaald alvorens te starten met de opleiding geneeskunde aan de Erasmus Universiteit Rotterdam. Na het behalen van het doctoraal diploma in 2002, de Internationaal Meestertitel in schaken in 2004, en het artsdiploma in 2005, heeft hij in het Ruwaard van Putten ziekenhuis te Spijkenisse ervaring opgedaan op de spoedeisende hulp. Nadien heeft hij nog gewerkt als arts-niet-in-opleiding op de afdeling dermatologie van het Sint Franciscus Gasthuis te Rotterdam totdat hij in 2006 begon aan de opleiding tot dermatoloog. Tijdens deze opleiding aan het Erasmus MC te Rotterdam startte tevens zijn promotieonderzoek onder leiding van copromotor dr. D. Robinson en promotor prof. dr. H.A.M. Neumann. Het promotieonderzoek vond plaats in het kader van een samenwerking tussen de afdelingen dermatologie en het Centrum voor Optische Diagnostiek en Therapie van het Erasmus MC. Aandachtsgebieden tijdens de opleiding hebben met name bestaan uit de dermatopathologie, de Mohs micrografische chirurgie en natuurlijk de fotodynamische therapie. Nadat hij de opleiding tot dermatoloog had afgerond in 2011, ging het promotieonderzoek een jaar de ijskast in vanwege een reis om de wereld. Bij terugkomst in Nederland heeft Tom in de jaren 2012 en 2013 het promotieonderzoek volledig opgepakt en gecombineerd met werkzaamheden als dermatoloog in het Sint Franciscus Gasthuis. De toekomst na de promotie ligt nog grotendeels open.

PHD PORTFOLIO

General academic skills

DOO course samenwerking	2009	8 hours
Journal Club	2009-10	1 ECTS
DOO course communicatie	2010	8 hours
Biomedical English Writing and communication	2010	4 ECTS
Supervised and unsupervised intervision	2010-11	1 ECTS

Workshops and seminars

NVED meeting	2008	1 ECTS
DIS PDT symposium Amsterdam	2009	16 hours
Discussiepunten in de praktijk Rotterdam	2008	8 hours
NVED meeting	2009	1 ECTS
PhD weekend Maastricht	2012	2 ECTS
PDT symposium Ankeveen Bopharma	2013	8 hours

Presentations

National Huidfonds symposium Rotterdam Nederland "fotodynamische therapy"	2008	1 ECTS
National Huidfonds symposium Rotterdam Nederland "fotodynamische therapy update"	2009	1 ECTS
SFG wetenschapsdag "BCG granuloma"	2009	1 ECTS
40 th European Society of Dermatological research annual meeting Helsinki Finland "low fluence rate PDT" (poster)	2009	1 ECTS
13 th European Society for Photobiology Congress Wroclaw Poland	2009	1 ECTS
refereeravond Erasmus MC "nieuwe inzichten in PDT"	2009	1 ECTS
13 th International Photodynamic Therapy Association annual meeting Seattle USA "Optimizing ALA-PDT" (poster)	2010	1 ECTS
13 th International Photodynamic Therapy Association annual meeting Innsbruck Austria "Differential Path length spectroscopy in PDT"	2011	1 ECTS

Conferences

Introductory Course on the Biology of the Skin Cambridge United Kingdom	2007	1 ECTS
Euro-PDT Barcelona Spain	2009	1 ECTS
13 th European Society for Photobiology Congress Wroclaw Poland	2009	1 ECTS
40 th European Society of Dermatological research annual meeting Helsinki Finland	2010	1 ECTS
13 th International Photodynamic Therapy Association annual meeting Innsbruck Austria	2011	1 ECTS
69 th American Academy of Dermatology annual meeting	2011	1 ECTS
9 th Summer academy of dermatopathology Graz Austria	2011	1 ECTS

Teaching activities

referaat internisten Erasmus MC	2010	1 ECTS
refereeravond Erasmus MC voorzitter	2010	0.5 ECTS
ICK onderwijs locale therapie	2009-11	1 ECTS

Other

Organisatie skintermezzo	2009-10	1 ECTS
Expertise training in dermatopathology Rotterdam Nederland	2009-12	2 ECTS
Occasional reviewer for NTVG	2009-10	8 hours
Introduction to confocal microscopy Rotterdam	2013	16 hours

LIST OF ABBREVIATIONS

ALA, aminolevulinic acid

AK, actinic keratosis

AUC, area under the curve

BVF, blood volume fraction

CI, confidence interval

DRS, diffuse reflectance spectroscopy

DPS, differential path-length spectroscopy

HAL, hexylaminolevulinate

IQR, interquartile range

MAL, methylaminolevulinate

MDSFR, multi-diameter single fiber reflectance

OR, odds ratio

PDT, photodynamic therapy

PpIX, protoporphyrin IX

ROI, region of interest

SD, standard deviation


SFF, single fiber fluorescence

SFR, single fiber reflectance

StO₂, microvascular saturation

TSQM, treatment satisfaction questionnaire for medication

VAS, visual analogue scale



Bij het bekijken van de cover van dit boekje denkt u misschien: "wat ziet die foto er gek uit". Het klopt dat er iets ongewoons aan de hand is. Wat u ziet is niet gewoon een foto van kiezelsteentjes, maar er zit een patroon in verborgen in de vorm van een autostereogram. Dit kunt u zichtbaar maken door als het ware "door de foto heen te kijken". Zoek op de voorkant van het boekje naar een wat grotere steen in het midden van de foto. U zult zien dat ongeveer 3 cm naar links en rechts deze steen opnieuw te vinden is in een zichzelf repeterend patroon. Wanneer u focust op iets dat achter de foto ligt, kunt u twee stenen laten "samenvallen" zodat uw linkeroog de linker steen ziet en uw rechteroog de rechter. Dan verschijnt plotseling in 3-D het woord "EUREKA". Dit autostereogram staat symbool voor de wetenschap. Eerst is er het gevoel dat er meer aan de hand is met de foto. Deze verwondering prikkelt ons om te onderzoeken en ontdekken wat dat dan precies is. Dankzij ons menselijk vermogen om patronen te herkennen kunnen we uiteindelijk de ruis van de informatie scheiden. Wanneer dit lukt zouden we het zogenaamde "EUREKA moment" kunnen ervaren. Archimedes heeft dit naar verluidt geroepen terwijl hij naakt door de straten van Syracuse rende, nadat hij in bad de naar hem vernoemde wet bedacht had. In het geval van dit proefschrift is het vooral bedoeld als een ironische verwijzing naar stelling 10 die luidt: *The most exciting phrase to hear in science, the one that heralds new discoveries, is not 'Eureka!' but 'That's funny...'* van Isaac Asimov. Tevens vormen de eerste letters EUR de afkorting van de Erasmus Universiteit Rotterdam. EKA kan van alles betekenen volgens Google. Overigens is de originele foto gemaakt aan het prachtige Lake Wakatipu in Queenstown op het Zuidereiland van Nieuw Zeeland. Tussen de vele steentjes kan men daar ook op zoek naar kiezels van het waardevolle gesteente nefriet jade. Hiervoor is trouwens wel weer een heel andere zoekstrategie nodig.